

# NOUS TERMOESTABLES EPOXÍDICS MODIFICATS AMB GAMMA-LACTONES I BIS-GAMMA-LACTONES CONDENSADAES

**TESI DOCTORAL**

**M<sup>a</sup> Mercè Arasa Bertomeu**

Dpt. Química Analítica i Química Orgànica

---



Universitat Rovira i Virgili  
Tarragona, Febrer 2009

M<sup>a</sup> Mercè Arasa Bertomeu

NOUS TERMOESTABLES EPOXÍDICS  
MODIFICATS AMB GAMMA-  
LACTONES I BIS-GAMMA-LACTONES  
CONDENSADAES

Tesi doctoral

dirigida per la Dra. Ana Maria Mantecón Arranz  
i la Dra. Àngels Serra Albet

Departament de Química Analítica  
i Química Orgànica



Tarragona 2009



UNIVERSITAT  
ROVIRA I VIRGILI

DEPARTAMENT DE QUÍMICA ANALÍTICA  
I QUÍMICA ORGÀNICA

Campus Sescelades  
Marcel·lí Domingo, s/n  
43007 Tarragona  
Tel. +34 977 55 97 69  
Fax +34 977 55 84 46  
www.quimica.urv.es/qaqo

Ana Maria Mantecón Arranz i Àngels Serra Albet, Catedràtiques  
d'Universitat, del Departament de Química Analítica i Química  
Orgànica de la Facultat de Química de la Universitat Rovira i  
Virgili de Tarragona,

CERTIFIQUEN:

Que el treball “**Nous termoestables epoxídics modificats amb gamma-lactones i bis-gamma-lactones condensades**” que ha dut a terme i que presenta M<sup>a</sup> Mercè Arasa Bertomeu per l'obtenció del Grau de Doctor en Química amb menció europea, ha estat desenvolupat sota la nostra supervisió i direcció en els laboratoris d'aquest mateix departament, i que tots els resultats obtinguts, són fruit de les diferents experiències realitzades per la mencionada doctora.

Tarragona, 5 de Febrer 2009

## *AGRAÏMENTS*

*No m'agradaria acabar aquest projecte sense deixar de donar tots els meus agraïments a totes aquelles persones que m'han ajudat, ensenyat, comprès i acompanyat durant aquests últims quatre anys.*

*Gràcies als professors del grup per haver-me donat l'oportunitat de poder dur a terme el doctorat amb ells, en especial a les meves directores de tesi, Àngels Serra i Ana Mantecón. Gràcies al temps i esforç que m'han dedicat avui puc tenir aquesta tesi a les meves mans. I també als seus col·laboradors per les seves opinions, correccions i propostes, especialment al Dr. Xavier Ramis qui ha participat amb molt d'interès des del inici fins a la fi d'aquesta tesi.*

*Thank you to Richard Pethrick to give me the opportunity of being some month in his group and thank you my laboratory mates to be so kind with me during my stay.*

*També voldria donar les gràcies a tots els companys que he anat coneixent durant tots aquests anys i dels quals m'enduc un bon record. Gràcies als meus companys de grup i laboratori, als sucrets, i a les químiomètriques. Gràcies a tots pels riures, la companyia i l'ajuda que m'heu donat. Gràcies a la Roser, per saber compartir tots els seus coneixements, a la Clara per tants kilòmetres i converses compartides, a la Silvana per tants bons moments, a la Marisa, la Marta i tots en general simplement per l'amistat compartida.*

*I ja per acabar, aprofito aquestes últimes paraules que tanquen un període de quatre anys de la meva vida, que són el fi d'una etapa, en la qual molts de tots els que he nombrat seguirem camins diversos per donar els meus agraïments més especials als meus pares i germans per haver contribuït en el meu projecte, per haver-m'ho fet més fàcil, per tots els instants que m'heu dedicat en els meus desplaçaments, per la vostra paciència, sens dubte, és gràcies a tots ells que avui sóc aquí.*

# Índex

---

1. Introducció i objectius	1
2. Polimerització catiònica del diglicidilèter del bisfenol A (DGEBA) amb la $\gamma$ -valerolactona ( $\gamma$ -VL) i la $\alpha$ -metil- $\gamma$ -butirolactona ( $\gamma$ -MBL)	21
2.1 Introducció	21
2.2 FTIR/ATR study of the copolymerization of diglycidylether of bisphenol A with methyl-substituted $\gamma$ -lactones catalyzed by rare earth triflate initiators	23
2.3 A study of the degradation of ester modified epoxy resins obtained by cationic copolymerization of DGEBA with $\gamma$ -lactones initiated by rare earth triflates	37
2.4 Kinetic study by FTIR and DSC on the cationic curing of a DGEBA/ $\gamma$ -valerolactone mixture with ytterbium triflate as initiator	51
2.5 Study on the effect of rare earth metal triflates as initiators in the cationic curing of the DGEBA/ $\gamma$ -valerolactone mixtures and characterization of the thermosets obtained	67
3. Preparació de <i>nanocomposites</i> per copolimerització catiònica de mescles DGEBA/ $\gamma$ -VL/argila iniciades amb triflats de terres rares	84
3.1 Introducció	84
3.2 New nanocomposites prepared from diglycidyl ether of bisphenol A and $\gamma$ -valerolactone initiated by rare earth metal triflate initiators	93
4. Copolimerització aniònica i catiònica del diglicidilèter del bisfenol A (DGEBA) amb bis( $\gamma$ -lactones) condensades	107
4.1 Introducció	107

4.2 Anionic copolymerization of DGEBA with two derivatives of bis( $\gamma$ -lactone)s using tertiary amines as initiators	110
4.3 Cationic copolymerization of DGEBA with two bicyclic bis( $\gamma$ -lactone) derivatives using rare earth metal triflates as initiators	126
4.4 Study of the copolymerization of DGEBA and two bicyclic bis( $\gamma$ -lactone)s using rare earth metal triflates as initiators by infrared spectroscopy	
5. Conclusions	155
6. Annex i acrònims	157
7. Contribucions científiques	160

# Í. Introducció i

---

## Objectius

UNIVERSITAT ROVIRA I VIRGILI  
NOUS TERMOESTABLES EPOXÍDICS MODIFICATS AMB GAMMA-LACTONES I BIS-GAMMA-LACTONES CONDENSADES  
M<sup>a</sup> Mercè Arasa Bertomeu  
ISBN:978-84-692-4157-8/DL:T-1171-2009

## 1.1 INTRODUCCIÓ

La primera síntesi d'una reïna epoxi basada en bisfenol A va ser descrita pel suís P. Castan i el nord-americà S.O. Greenlee el 1936<sup>1</sup>. El diglicidilèter de bisfenol A (DGEBA) va esdevenir la primera reïna epoxi comercial (1940)<sup>2</sup> i des de llavors ha estat una de les més emprades en el món industrial. La seva principal via de síntesi pràcticament no ha variat i es tracta de fer reaccionar bisfenol A amb epiclorohidrina en medi bàsic fort<sup>3</sup>. Variant la relació epiclorohidrina/bisfenol A emprada permet obtenir pre-polímers amb diferents pesos moleculars.

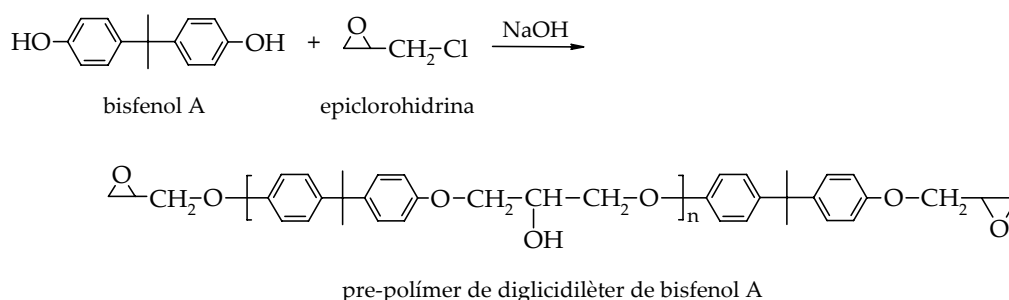


**Figura 1.1.** Obtenció de la reïna de diglicidilèter de bisfenol A (DGEBA)

Les reïnes epoxi tenen múltiples aplicacions en recobriments, adhesius i en la fabricació de composites (mescles de reïnes epoxi amb fibres, generalment de vidre o de carboni). La química dels epòxids i el ampli ventall de reïnes disponibles comercialment permet obtenir materials amb una gran varietat de propietats. En general, les reïnes epoxi són conegudes per la seva excel·lent adhesió, resistència química i tèrmica, bones propietats mecàniques i bones propietats com a aïllants elèctrics<sup>4</sup>. A més, hi ha centenars de maneres en que poden ser modificades com per addició de càrregues minerals (talc, sílica, alumina, etc), de flexibilitzants, colorants, acceleradors, reductors de la viscositat, etc., per tal de reduir-ne el cost, obtenir unes propietats determinades o simplement facilitar-ne el seu processat. Com a resultat es pot obtenir milers de possibles formulacions, cadascuna preparada per tal d'aconseguir les propietats requerides en el mercat.

En el camp de la microelectrònica es requereixen materials que siguin capaços de recobrir o encapsular els components electrònics, protegint-los així d'agents atmosfèrics externs com la pols o la humitat. El fet que es produeixi una contracció durant el procés de curat (que té lloc normalment en qualsevol tipus de polimerització) influeix negativament sobre les propietats finals i la durabilitat del material obtingut, ja que durant aquest procés es formen microesclerxes, microporus i tensions mecàniques que amb el temps poden evolucionar cap a una fatiga mecànica del material i a una possible pèrdua d'adherència. Tot això pot portar a la penetració d'humitat, a l'aparició de problemes de corrosió en els components metàl·lics i finalment a la destrucció del material electrònic<sup>5</sup>. A més, el fet que el material sigui un termoestable fa que el material recobert no pugui ser reutilitzat.

A pesar de les bones propietats que presenten, segons l'ús que se'n vol fer (com per exemple el recobriments de xips), les reïnes de DGEBA es veuen limitades degut a certs inconvenients com són: la seva fragilitat, la contracció que experimenten durant el procés de curat i la falta de reciclabilitat/degradabilitat impeding així una possible reutilització del material recobert. S'ha de tenir en compte que l'eliminació de recobriments termoestables és difícil degut a que són materials infusibles i insolubles. Es parla de termoestables reciclables quan aquests es poden eliminar i recuperar el material recobert. La introducció de grups tèrmica o químicament làbils és la manera més utilitzada per obtenir termoestables reciclables (degradables). Per exemple, la presència de grups ester en la xarxa polimèrica fa possible que aquests materials puguin ser degradats de forma controlada tèrmicament o per hidròlisi alcalina, tenint en compte que també siguin el suficientment estables per evitar la seva degradació durant el procés de curat i durant el temps de servei. El desenvolupament de mètodes de reciclatge per materials polimèrics és un tema de gran importància en el camp de la ciència dels polímers i la seva tecnologia<sup>6</sup>. En concret, la degradació tèrmica és un dels mètodes més emprats en aquests tipus de materials ja que ens ofereix la possibilitat d'un procés ràpid i net.

Entre els diferents treballs que s'han trobat a la literatura i que parlen sobre degradació tèrmica de materials termoestables trobem els realitzats per Wang i Wong<sup>7</sup>. Aquests autors van proposar la introducció de grups tèrmicament làbils, tipus carbonat, dintre l'estructura de la reïna de partida. Això els portava a obtenir materials que podien ser degradats a temperatures inferiors a 350 °C. A més, aquesta temperatura disminuïa al augmentar el grau de substitució del carbonat.

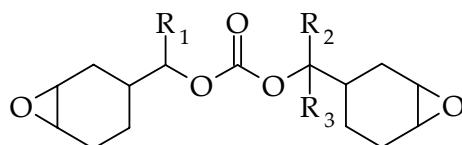


**Figura 1.2.** Reïna epoxi emprada en l'obtenció de termoestables degradables

Chen i col.<sup>8</sup> també han treballat en aquest camp introduint grups ester en la reïna de partida (figura 1.3).

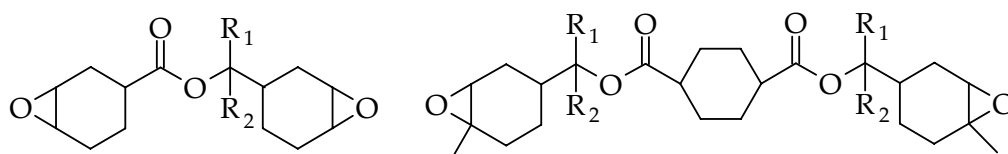


**Figura 1.3.** Reïnes epoxi emprades en l'obtenció de termoestables degradables

Aquests grups ester també són tèrmicament làbils permetent obtenir materials que podien ser degradats a temperatures entre 200 i 250°C. Aquesta temperatura disminuïa a mesura que augmentava la substitució en el C<sub>β</sub> degut a que un major nombre de hidrògens en γ afavoreix l'eliminació pirolítica (figura 1.4).

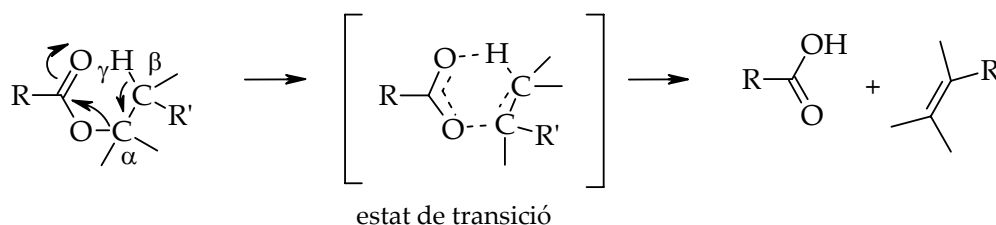


**Figura 1.4.** Mecanisme d'eliminació pirolítica d'esters (β-eliminació)

Més recentment, Okamura i col.<sup>9</sup> van sintetitzar noves reïnes epoxi difuncionals i trifuncionals amb unions ester terciari. Aquestes reïnes eren aplicades com agent de curat en un sistema amb propietats fotocurables per tal de degradar el material mitjançant un posterior tractament tèrmic que porta al trencament dels enllaços ester.

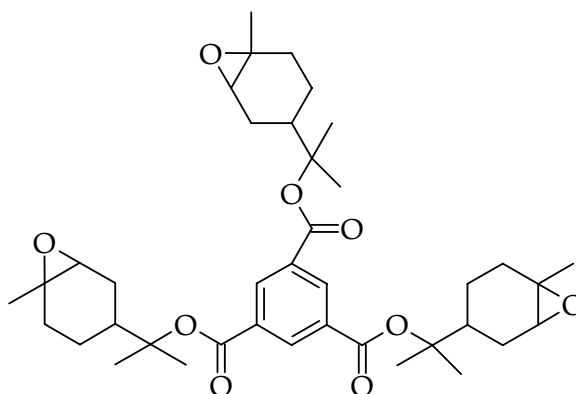


**Figura 1.5.** Reïnes cicloalifàtiques proposades per Okamura i col.

A part d'aquests autors n'hi ha d'altres que introdueixen altres grups làbils a la xarxa polimèrica. Entre ells trobem Shirai i col.<sup>8(c),10</sup>, que introdueix grups sulfonat, Malik i col.<sup>11</sup>, que introdueixen grups urea, Tesoro i col.<sup>12</sup>, que introdueixen enllaços disulfur o Buchwalter i col.<sup>13</sup>, que introdueixen enllaços cetal i acetal.

Una altra estratègia per aconseguir termoestables degradables és la formació *in situ* de grups làbils per copolimerització per obertura d'anell de reïnes epoxi amb carbonats cíclics o lactones en presència d'un iniciador. S'ha pogut observar com, en presència d'un àcid de Lewis, un epòxid reacciona amb un carbonat cíclic o una lactona per donar lloc a la formació d'un espiroortocarbonat (SOC) o un espiroortoester (SOE) i per polimerització

d'aquests composts es formen grups carbonat o ester en la matriu polimèrica final. A més, s'ha observat com la copolimerització d'aquest tipus de compostos porta a materials amb un menor grau d'encongiment<sup>14</sup>.

Bodenbenner<sup>15</sup> va ser el primer en sintetitzar un espiroortoester per reacció de l'òxid d'etilè amb  $\gamma$ -butirolactona en presència de trifluorur de bor ( $\text{BF}_3$ ) obtenint un 33 % de rendiment. Bailey va estudiar la homopolimerització d'aquest compost en un dilatòmetre a temperatura ambient utilitzant  $\text{BF}_3$  com a iniciador i va observar un lleuger increment de volum del 0,1 % al finalitzar la polimerització<sup>16</sup>.

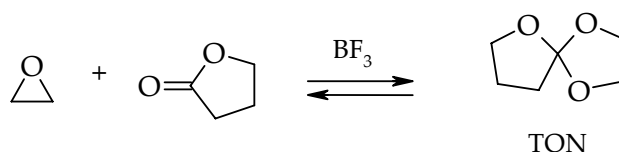


**Figura 1.6.** Síntesi del 1,4,6-trioxaspiro[4.4]nonà (TON)

Bailey<sup>17</sup> va ser el primer en definir el que ell va anomenar “expanding monomers”, monòmers que al polimeritzar no experimentaven cap encongiment o que fins i tot podien experimentar una lleugera expansió. Això es va atribuir al mode de polimerització que és una obertura d'anell on per cada distància de Van der Waals (3) que passa a una distància covalent (3a) almenys hi ha dues distàncies covalents (1, 2) que passen a distàncies properes a la de Van der Waals (1a, 2a) i un enllaç covalent senzill (4) que passa a un doble (4a), segons es representa a la figura 1.7.

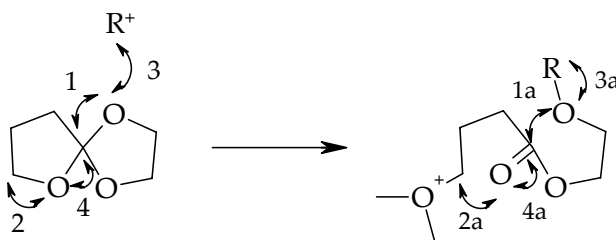


**Figura 1.7.** Canvis d'enllaços durant la homopolimerització d'un SOE

Alguns exemples de compostos que compleixen els requeriments establerts per Bailey per ser considerats monòmers expandibles són els espiroortoesters (SOEs)<sup>17</sup>, espiroorto-carbonats (SOCs)<sup>18</sup> i els bicicloortoesters (BOEs)<sup>19</sup> entre d'altres<sup>20</sup>.

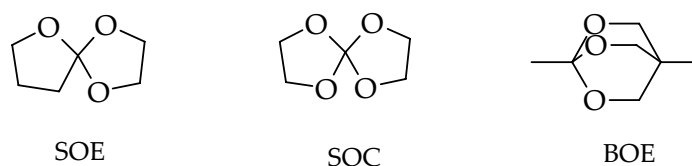


**Figura 1.8.** Estructura de diferents monòmers expandibles

Bailey va proposar un possible mecanisme per descriure com tenia lloc la doble obertura d'un SOE (figura 1.9). Segons ell, la reacció s'inicia per un atac electròfil a l'oxigen. En el cas de que el grup epoxi tingui substituents l'atac es dona preferentment en l'oxigen de l'anell eteri i si no n'hi ha l'atac es produeix en qualsevol dels oxígens. En qualsevol cas es forma un catió oxoni que s'isomeritza a un carbocatió estabilitzat pels oxígens adjacents. La propagació es dona per l'atac d'un altre monòmer que genera un altre catió oxoni seguit de la isomerització del grup cetàlic a grup ester<sup>15,17,20,21</sup>. Estudis posteriors, realitzats per Nishida i col.<sup>22</sup>, van confirmar el mecanisme i que la reactivitat del SOE podia dependre d'altres factors com la grandària de l'anell o del tipus de substituent en el C\* (figura 1.9).

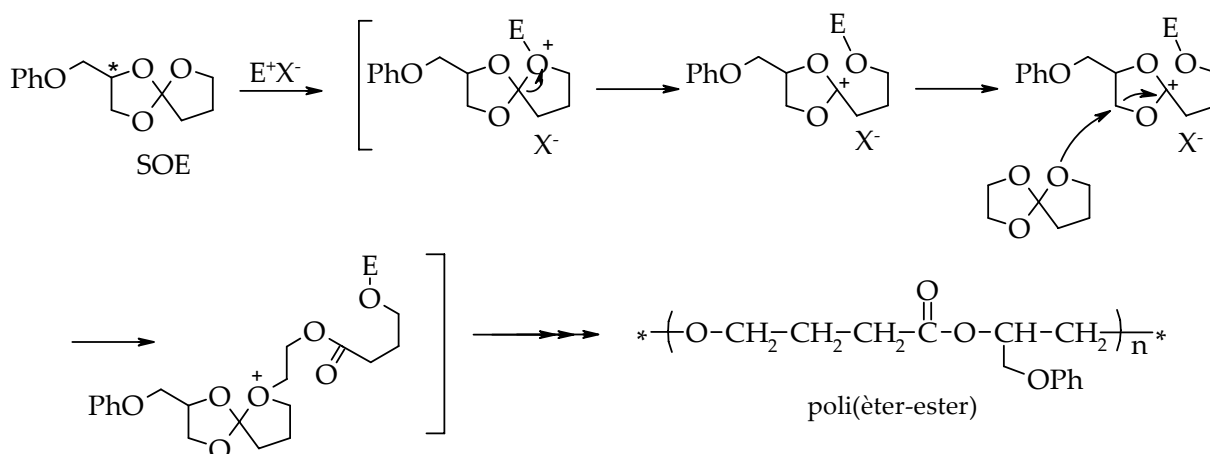


**Figura 1.9.** Mecanisme proposat per la doble obertura d'un SOE

Matyjaszewski<sup>23</sup> va proposar un segon mecanisme pel qual podia tenir lloc l'obertura d'aquest tipus de compostos. Segons ell, el mecanisme tenia lloc amb dues etapes, una primera ràpida on es produeix l'obertura d'un dels anells seguida d'una isomerització lenta per donar lloc al poli(èter-ester) (figura 1.10).

Estudis posteriors van permetre observar com depenent de la temperatura de polimerització es podia obtenir dos tipus de polímers<sup>24</sup>. Mentre que a temperatures superiors a 100 °C es produïa la doble obertura de l'anell, donant lloc al corresponent poli(èter-ester), a temperatures per sota dels 40 °C el SOE només experimentava l'obertura

d'un sol anell, donant lloc a la formació d'un poli(cicloortoester). Malgrat tot, aquest últim procés només tenia lloc amb SOEs amb un anell d'èter de 7 baules ( $n=5$ ), segurament degut a la falta de homopolimeritzabilitat dels anells de 5 i 6 baules. Com que aquesta reacció és d'equilibri, es pot recuperar fàcilment el monòmer de partida, obtenint així una via de reciclatge químic<sup>25</sup>. L'obtenció del poli(cicloortoester) no té interès en el camp dels termoestables, ja que la baixa temperatura emprada porta a la vitrificació del material.

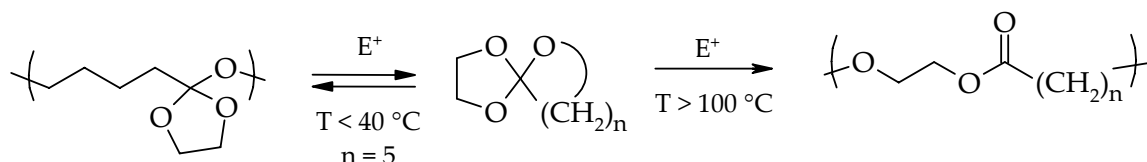
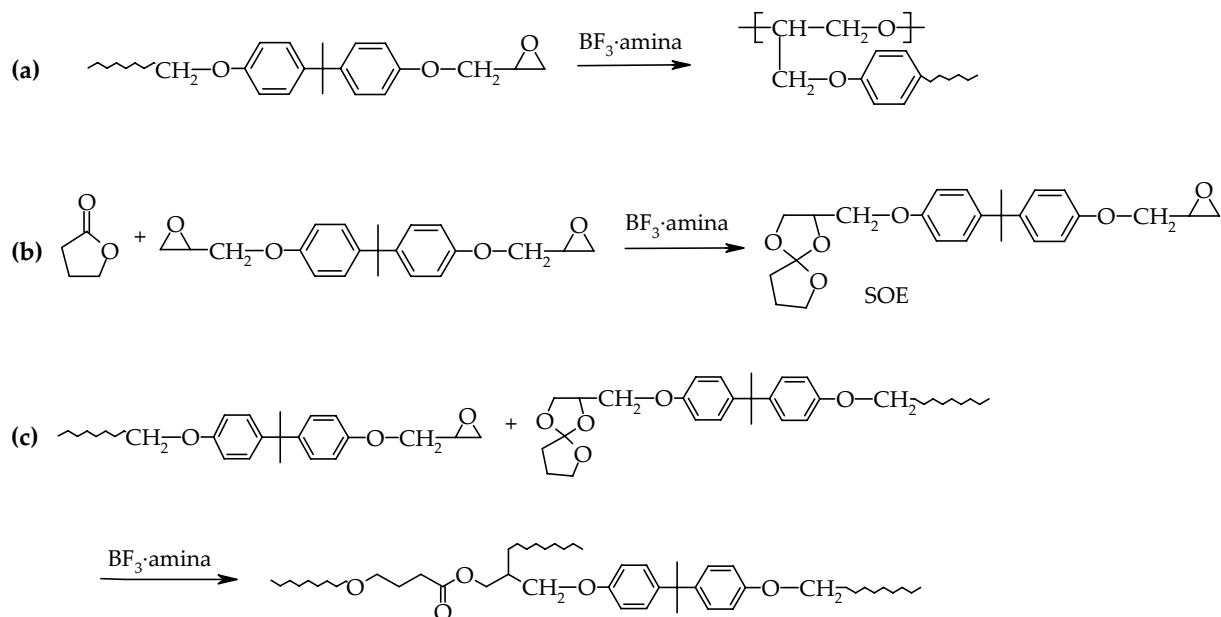


Figura 1.10. Evolució del SOE en funció de la temperatura

Chabanne i col.<sup>26</sup> van estudiar la reacció de polimerització del fenilglicidilèter (PEG) i el diglicidilèter de bisfenol A en presència de complexos de  $\text{BF}_3$ -amina solubilitzats en una petita quantitat de  $\gamma$ -butirolactona ( $\gamma$ -BL). El complex  $\text{BF}_3$ -amina presentava l'inconvenient de ser sòlid a temperatura ambient i no es dissolia bé en la reïna. Així doncs, per tal d'obtenir mescles més homogènies van substituir el poliòxid d'etilè (PEO), el primer dissolvent estudiat amb detall<sup>27</sup>, per la  $\gamma$ -BL, que era millor dissolvent per aquest tipus d'iniciadors a més de ser menys viscosa, el que facilitava la homogeneïtzació de la mescla. Malgrat no homopolimeritzar per raons termodinàmiques<sup>28</sup>, la  $\gamma$ -BL s'incorporava a la xarxa polimèrica per formació d'un SOE intermedi, degut a la presència de l'àcid de Lewis<sup>14</sup>. A més van veure un increment en la reactivitat del sistema<sup>29</sup>. Fedtke i col.<sup>30</sup> també van investigar la formació de xarxes polimèriques a partir de sistemes epoxídics com el fenilglicidilèter (PGE) o el diglicidilèter de bisfenol A en presència de  $\gamma$ -BL en medi catiònic. Tots dos grups van comprovar que es donaven simultàniament diverses reaccions, entre elles la homopolimerització de l'epòxid (a), la formació *in situ* del SOE (b) i la seva copolimerització amb l'epòxid (c) (figura 1.11).

Així doncs, en el nostre grup de recerca es va plantejar la idea de millorar algunes de les propietats que presenten els termoestables epoxídics per copolimerització directa de reïnes epoxi amb lactones<sup>31</sup> i carbonats<sup>32</sup>. Les propietats que es pretenien millorar eren la reducció de l'encongiment al curat, les propietats mecàniques i augmentar la degradabilitat.

Dels diferents agents de curat catiònics aplicables a les reïnes epoxi<sup>33</sup>, el nostre grup de recerca ha desenvolupat uns agents de curat nous com són els triflats de terres rares. Els triflats de metalls de terres rares són àcids de Lewis, estables en medis aquosos, freqüentment usats en reaccions orgàniques<sup>34</sup> i que han estat considerats com mediambientalment favorables. L'estabilitat i l'activitat catalítica dels triflats de terres rares en aigua es deguda principalment al seu gran radi iònic i a l'equilibri que es forma



**Figura 1.11.** Reaccions que tenen lloc durant el curat catiònic del DGEBA amb  $\gamma$ -BL en presència de  $\text{BF}_3 \cdot \text{amina}$

entre els àcids de Lewis i l'aigua<sup>34(e)</sup>. Aquest tipus de catalitzadors són àcids de Lewis molt forts<sup>35</sup> degut a l'acidesa del catió, la qual es veu potenciada pel caràcter electroattractor que presenta el grup trifluorometansulfonil ( $\text{TfO}$ )<sup>36</sup>. Aquests cations tenen una gran afinitat cap a l'oxigen del grup epòxid afeblint l'enllaç C-O de l'anell i afavorint la seva obertura<sup>37</sup>. L'acidesa del catió ve determinada per factors com l'electronegativitat, l'oxofília i el radi iònic del metall<sup>38</sup>. A la figura 1.12 es mostren com es veuen afectades aquestes propietats en funció del tipus de lantànid<sup>35</sup>. A més, els cations lantànids ( $\text{Ln(III)}$ ) són durs segons la terminologia de Pearson<sup>39</sup> i presenten una elevada capacitat de coordinació<sup>40</sup>. Dels diferents triflats de terres rares que s'han utilitzat en el present treball, l'acidesa de Lewis i la duresa de Pearson disminueix en el següent ordre:  $\text{Sc}(\text{OTf})_3 > \text{Yb}(\text{OTf})_3 > \text{La}(\text{OTf})_3$ <sup>34(d)</sup>.

També és important destacar que degut a la baixa basicitat, pobra nucleofília i baixa capacitat coordinativa de l'anió triflat cal esperar una baixa proporció de processos de finalització de cadena quan s'utilitzen com iniciadors de polimerització<sup>41</sup>.

Els triflats lantànid i altres metalls també han estat utilitzats en la polimerització d'altres monòmers com l'anhídrid succínic/tetrahidrofurà<sup>42</sup> i lactones<sup>43</sup> permeten aconseguir inclús polimeritzacions tipus "living"<sup>44</sup>.

Finalment, podem dir de manera general que aquests nous iniciadors presenten uns certs avantatges respecte a d'altres àcids de Lewis com el  $\text{AlCl}_3$ ,  $\text{BF}_3$  i  $\text{TiCl}_4$ , ja que<sup>37</sup>:

- Són tolerants a l'aigua. Els àcids de Lewis, en presència d'aigua, reaccionen i es desacti-

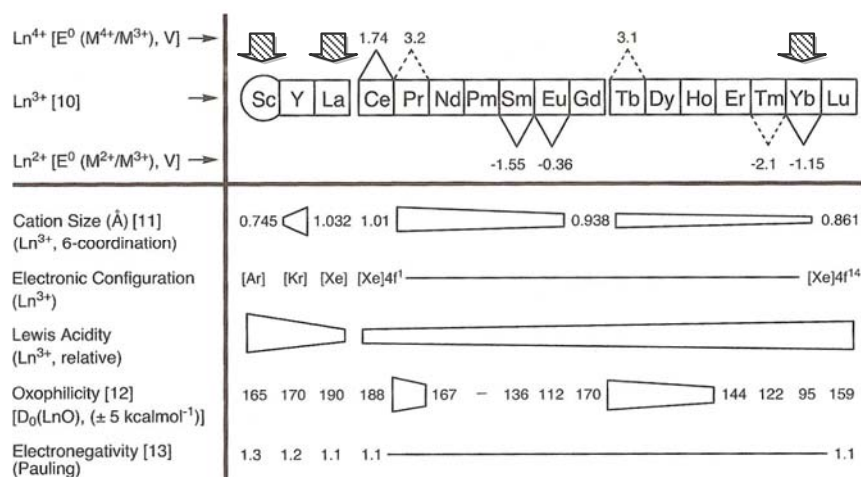


Figura 1.12. Tendència de les propietats intrínseques dels lantànids

ven, mentre que els triflats de lantànid poden utilitzar-se en medis aquosos<sup>38,45</sup>.

- Són estables a l'aire i per tant no cal emmagatzemar-los en atmosfera inert.
- Són bastant solubles en compostos orgànics, la qual cosa ens permet obtenir mescles més homogènies.
- Pel que fa a la toxicitat, la dels lantànids és menor que la dels metalls de transició i similar a la dels metalls alcalins.

Aquests avantatges fan possible que els triflats de lantànid i terres rares puguin tenir una aplicació tecnològica, ja que les mescles de reacció són estables a l'aire i no és precís emmagatzemar-les ni treballar en unes condicions especials.

En treballs anteriors del nostre grup es va realitzar un estudi de l'activitat de diferents triflats de lantànid en la polimerització del diglicidelèter de bisfenol A (DGEBA)<sup>46</sup> i una reïna epoxi cicloalifàtica<sup>46(b)</sup> i es va observar com el procés de curat esdevenia molt més eficaç que en el cas d'utilitzar el BF<sub>3</sub>/monoetilamina (iniciador convencional utilitzat en el curat catiònic de reïnes epoxi). Es va observar, al igual que descriu Nomura<sup>44(b)</sup>, com la presència de grups hidroxílics conduïa a una acceleració del procés de curat de les reïnes epoxi. Aquest fet va ser atribuït a la coexistència de dos mecanismes de propagació<sup>47</sup>: (a) el mecanisme de monòmer activat (AM), el qual requereix de la presència de grups hidroxílics i (b) el mecanisme de final de cadena activat (ACE) (figura 1.13).

Després es va estudiar la copolimerització de reïnes epoxi amb  $\gamma$ -lactones. L'estudi es va realitzar amb aquest tipus de lactones ja que presenten l'avantatge que no poden homopolimeritzar<sup>28</sup> en les condicions estudiades i per tant la seva reacció amb epòxids només pot tenir lloc prèvia formació del espiroortoester (SOE).

Els primers estudis realitzats amb  $\gamma$ -butirolactona ( $\gamma$ -BL) i reïnes epoxi de baix pes molecular utilitzant diversos triflats com iniciadors van donar lloc a materials més flexibles

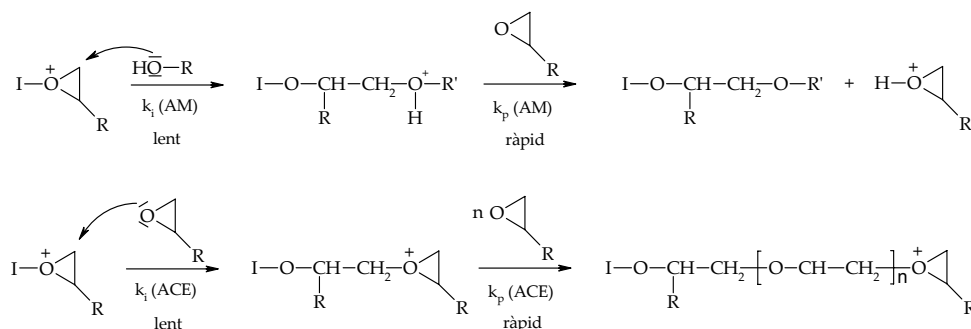


**Figura 1.13.** Mecanisme de monòmer activat (AM) i mecanisme de final de cadena activat (ACE)

degut a que augmenta la distància entre punts d'entrecruament i s'incorporen restes alifàtiques<sup>48</sup>. Això podria ajudar-nos a disminuir la fragilitat dels materials obtinguts sense haver d'afegir cap tipus d'additiu, el que evitaria processos posteriors de mesclat i elimina els inconvenients de la migració dels additius<sup>49</sup>. També es va observar, al igual que Chabanne<sup>29</sup>, com l'addició de  $\gamma$ -BL i/o l'acidesa de Lewis del iniciador utilitzat produïa una acceleració del procés de curat<sup>50</sup>. Mitjançant FTIR es va confirmar com la coordinació del catió iterbi tenia lloc principalment al oxigen oxirànic mentre que el catió lantà es coordinava preferentment al oxigen de la lactona<sup>31(a)</sup>. Això es podria explicar per la teoria de Pearson<sup>39</sup> ja que la lactona es una base tova i per tant reacciona millor amb àcids tous, com el catió lantà, mentre que l'epòxid és una base dura i es coordina millor amb cations més durs com l'iterbi. Per FTIR-ATR es van poder seguir les diferents reaccions que podien tenir lloc durant la copolimerització les quals van coincidir amb les descrites per Chabanne<sup>26</sup> i Fedtke<sup>30</sup>, però en el nostre cas es va observar un altra reacció, que encara no havia estat descrita, la homopolimerització del SOE, que tenia lloc al final del curat quan ja no quedava epoxi en el medi de reacció<sup>51</sup>.

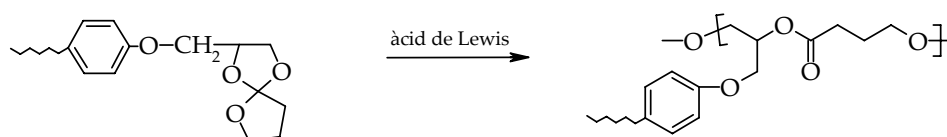


**Figura 1.14.** Homopolimerització del espiroortoester (SOE)

Pel que fa a l'encongiment global, es va observar com abans de la gelificació l'encongiment era bastant elevat degut a la formació del SOE i la homopolimerització dels grups epòxid. En canvi, després de la gelificació l'encongiment era molt petit. L'encongiment abans del punt de gelificació no dona cap problema ja que té lloc quan el material és un fluid mentre que després de la gelificació, quan el moviment es veu restringit, sí que l'encongiment porta a l'aparició de tensions internes en el material i possibles formacions d'esclatxes i pèrdua d'adhesió. A temps de curat llargs, després de la gelificació, els principals processos que tenien lloc estaven relacionats amb la

polimerització del SOE, portant tan sols a un lleuger encongiment<sup>31(a)</sup>. El fet que tingues lloc un petit encongiment i no una expansió després de la gelificació podria ser degut a que la proporció de grups SOE polimeritzats no era capaç de compensar l'encongiment produït per la polimerització dels epòxids. La copolimerització amb un altre tipus de lactones, com són les bislactones derivades de l'àcid de Meldrum (figura 1.15), sí van donar lloc a la reducció global de l'encongiment durant el curat<sup>31(b)</sup>. Això es va reflectir en millor resistència al impacte o en les propietats anticorrosives dels recobriments<sup>52</sup>.

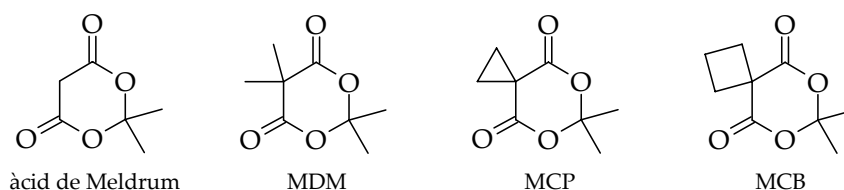


**Figura 1.15.** Estructura del 2,2-dimetil-1,3-dioxà-4,6-diona (àcid de Meldrum) i derivats: 2,2,5,5-tetrametil-4,6-dioxo-1,3-dioxà (MDM), 6,6-dimetil-5,7-dioxaspiro[2.5]octan-4,8-diona (MCP) i 7,7-dimetil-6,8-dioxaspiro[3.5]nonan-5,9-diona (MCB)

Pel que fa a l'estabilitat tèrmica de tots els materials derivats de reïnes epoxi i lactona, es va observar com un augment del contingut de lactona en la mescla conduïa a materials més degradables, especialment quan els esters introduïts en la xarxa eren terciaris. A més, es va comprovar com l'acidesa del iniciador emprat afectava la degradabilitat del material; quan major era l'acidesa de Lewis del iniciador, més degradable esdevenia el material<sup>53</sup>.

Brady i col.<sup>54</sup> van observar com l'addició de lactones espirobicícliques al curat aniónic de reïnes epoxi amb poli(amido-amines) portava a un menor grau d'encongiment. En les seves investigacions van observar una lleugera expansió que tenia lloc al principi del curat però que amb el temps anava desapareixent, segurament a causa de la contracció causada per la reacció dels epòxids amb la amina. L'expansió inicial revelava com els compostos espirànics eren considerablement més reactius que els anells oxirànics envers la nucleofília de l'amina. Així doncs, els inicis de la reacció tenien lloc principalment per la reacció dels espiro monòmers mentre que la reacció dels oxirans no esdevenia important fins la desaparició dels espiro compostos. A més el grau d'encongiment variava segons la quantitat de espirobislactona utilitzada.

S'ha estudiat la copolimerització de reïnes epoxi amb diferents bis( $\gamma$ -lactones)<sup>55</sup> (figura 1.16) utilitzant alcòxids com iniciadors. A diferència de les mono( $\gamma$ -lactones), les bis( $\gamma$ -lactones) copolimeritzen amb epòxids amb iniciadors aniónics, el que permet el desenvolupament de nous materials funcionals que podrien exhibir noves propietats.

Endo i col.<sup>56</sup> van estudiar la copolimerització de les bis( $\gamma$ -lactones) amb fenilglicidilèter i DGEBA i van observar que aquest tipus de lactones no homopolimeritzaven, però sí copo-

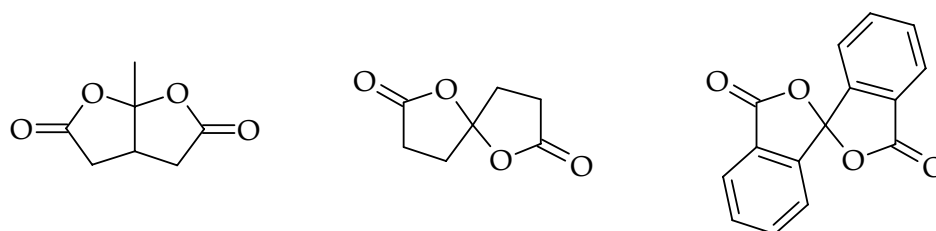


**Figura 1.16.** Estructura de diverses bis( $\gamma$ -lactones) bicíclics estudiades en la copolimerització aniónica amb epòxids

limeritzaven aniónicament de forma alternada per obertura d'anell amb epòxids. El mecanisme proposat es representa a la figura 1.17 i implica un atac nucleòfil del iniciador ( $t\text{-BuO}^-$ ) al carbonil de l'anell de  $\gamma$ -lactona per donar lloc a un carboxilat per doble obertura d'anell amb isomerització. Aquest carboxilat ataca selectivament un anell oxirànic, ja que la lactona no té possibilitat d'homopolimeritzar. L'alcòxid resultant ataca preferentment l'anell de lactona ja que el carboni carbonílic és molt més electròfil que el carboni oxirànic. Finalment, s'arriba a l'obtenció d'un copolímer alternat que conté un grup cetona en la unitat repetitiva.

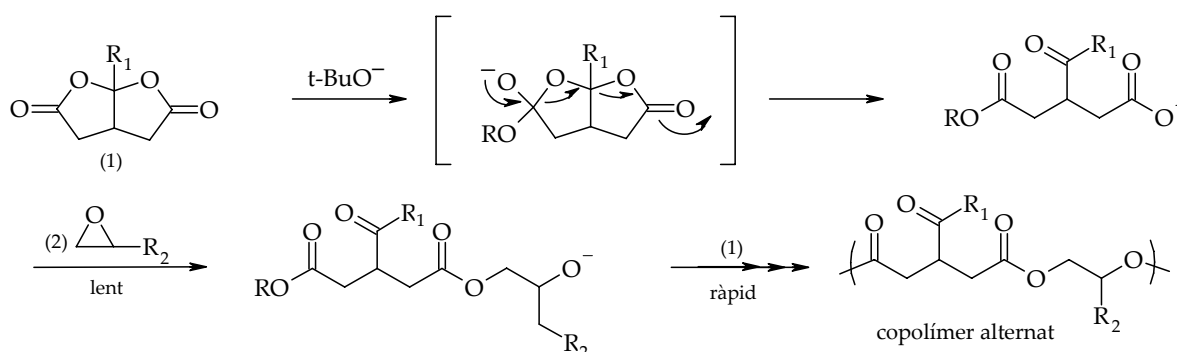


**Figura 1.17.** Mecanisme de copolimerització aniónica entre una  $\gamma$ -lactona bicíclica i un grup epòxid

Aquest tipus de mecanisme explicaria perquè Brady i col. obtenien una reducció del encongiment al principi de la polimerització quan afegien petites quantitats de espirobis( $\gamma$ -lactones). L'encongiment estava directament relacionat amb la proporció de bislactona afegida. L'encongiment era mínim al utilitzar quantitats equimoleculares de bis(lactones) i grups epòxid<sup>57</sup>.

Zhang i col.<sup>58</sup> van realitzar un estudi sobre les possibles reaccions laterals que podien tenir lloc en aquest tipus de polimeritzacions, com el "back-biting" i les reaccions de transferència de cadena (figura 1.18). Van observar com un augment de lactona accelerava la reacció i com aquestes reaccions laterals tenien lloc quan la mescla de reacció contenia un excés d'epòxid mentre que eren pràcticament eliminades a mesura que augmentava el contingut de bis( $\gamma$ -lactona). El procés de back-biting consisteix en l'atac d'un alcòxid final

de cadena a un grup ester de la pròpia cadena per originar cicles, mentre que els processos de transferència de cadena tenen lloc per atac d'un alcòxid final de cadena a un grup ester d'una altra cadena. Ambdós processos donen lloc a un augment de la polidispersitat. En el cas de materials termoestables aquests dos processos porten a canvis estructurals a la xarxa.

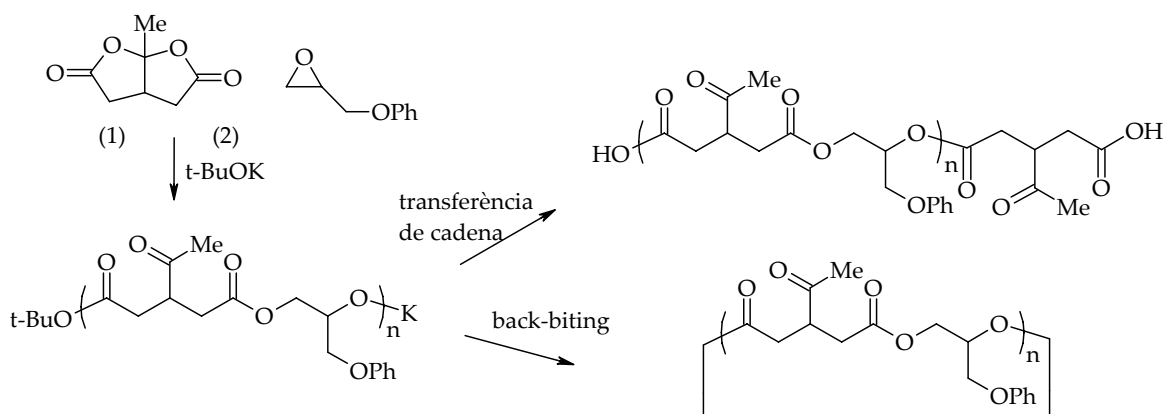


**Figura 1.18.** Reaccions laterals que tenen lloc en la copolimerització de (1) i (2) amb *t*-BuOK

S'ha utilitzat una estratègia similar per disminuir l'encongiment en el curat aniónic de polímers vinílics amb grups epoxi laterals afegint a la mescla de reacció bis( $\gamma$ -lactones)<sup>55</sup> (figura 1.19).

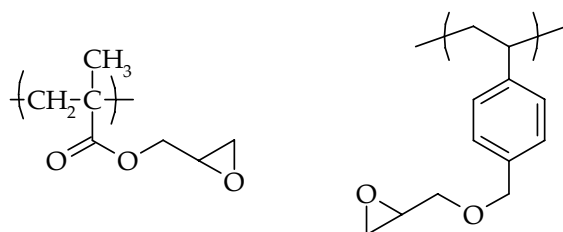


**Figura 1.19.** Polímers vinílics amb grups glicidil laterals copolimeritzats amb bis( $\gamma$ -lactones) en condicions anióniques

En estudis realitzats per Uenishi i col.<sup>59</sup> en copolimerització d'epòxids amb 3,4-dihidrocumarina ( $\delta$ -lactona) es va utilitzar imidazole com a iniciador. També es va observar en aquests casos una copolimerització alternada en la qual les espècies actives eren alcòxids i fenòxids. Els imidazoles s'han utilitzat àmpliament en el curat d'epòxids<sup>60</sup> per diverses aplicacions i en la fabricació de nanocomposites<sup>61</sup>.

En el nostre grup de recerca es va utilitzar per primer cop la 4-(*N,N*-dimetilamino)piridina (DMAP) com a agent de curat de reïnes epoxi<sup>62</sup> i es va demostrar la seva eficàcia com iniciador aniónic. Dell'Erba i Williams<sup>63</sup> van realitzar un estudi sobre la

homopolimerització de monòmers epoxídics com el DGEBA i el PGE iniciada per DMAP i van observar que la DMAP era més activa que d'altres amines terciàries i que el valor de la  $T_g$  dels materials obtinguts era superior. Tot i així, la homopolimerització aniònica de grups epoxi iniciada per amines terciàries i imidazoles N-substituïdes és una reacció complexa i presenta dos inconvenients: (a) velocitat de reacció baixes i (b) formació de cadenes principals curtes degut a l'elevada velocitat de les reaccions de transferència de cadena<sup>64</sup>.

Estudis més recents, realitzats per Fernández-Francos i col.<sup>65</sup> han demostrat que la copolimerització aniònica del DGEBA amb una espirobislactona ( $s(\gamma\text{-BL})$ ) amb DMAP i imidazole porta a: (a) una copolimerització inicial entre la  $s(\gamma\text{-BL})$  i el DGEBA i una posterior homopolimerització del DGEBA un cop exhaurida la lactona, (b) la existència de reaccions de transferència, terminació i regeneració associades amb la homopolimerització del DGEBA, (c) un efecte acceleratiu del sistema degut a l'addició de la  $s(\gamma\text{-BL})$ , el qual permet un curat complet amb una menor quantitat d'iniciador i (d) l'ús de la DMAP va resultar ser el iniciador més efectiu.

Seguint les tendències actuals aplicades a la millora de les propietats mecàniques dels materials, en els últims anys s'ha estudiat l'efecte que produeix la introducció de nanopartícules en matrius epoxídiques, ja que els materials resultants són fàcils d'obtenir, aplicables en un ampli ventall d'àrees, només es requereix de petites quantitats de nanopartícules i permet obtenir millores notables en el material final. Els nanocomposites polímer/silicat han estat estudiats des de fa aproximadament 60 anys<sup>66</sup> però no va ser fins després de la publicació dels bons resultants obtinguts pels investigadors de Toyota<sup>67</sup> que els filossilicats laminars nanomètrics van adquirir importància en la millora de materials. Des de llavors s'han estudiant diversos mètodes per obtenir nanocomposites basats en reïnes epoxi<sup>68</sup>, poliestirè<sup>69</sup>, poliamida<sup>70</sup>, polipropilè<sup>71</sup>, poliuretans<sup>72</sup>, etc. Per aconseguir aquestes millores cal destruir les interaccions entre làmines d'argila i aconseguir una completa dispersió de l'argila dintre la matriu polimèrica, ja que s'ha vist que només en aquest cas s'aconsegueix una millora substancial en les propietats del material final. Malgrat tot, la dispersió de l'argila no resulta gens fàcil degut al caràcter inorgànic de l'argila i el caràcter orgànic de la matriu polimèrica, per la qual cosa es requereix d'un tractament previ de l'argila amb la finalitat d'augmentar la comptabilitat argila/matriu.

Una gran part dels treballs realitzats en el camp dels nanocomposites epoxídics tracten sobre l'efecte que produeix l'addició de fil·losilicats laminars nanomètrics a la matriu epoxídica a les propietats mecàniques<sup>73</sup>, òptiques<sup>74</sup>, d'estabilitat tèrmica i resistència a la flama<sup>75</sup>, d'absorció i permeabilitat de gas<sup>76</sup>, etc. S'ha observat com el mètode de preparació de la mescla<sup>77</sup>, el pre-acondicionament d'aquesta<sup>78</sup>, la natura i el tipus d'agent modificant de l'argila<sup>79</sup>, el tipus d'agent de curat i la seva concentració<sup>79(b),80</sup> són factors que poden afectar al grau de deslaminació de l'argila i per tant a la morfologia i a les propietats dels materials obtinguts. Alguns exemples de millores que s'han aconseguit, els trobem en els estudis realitzats per Messersmith i col.<sup>68(a)</sup> que amb només l'addició d'un 4 % d'argila van

augmentar en un 58 % el mòdul en l'estat vitri i en més d'un 450 % el mòdul en la l'estat gomós; Massam i col.<sup>81</sup> van aconseguir reduir el coeficient d'expansió tèrmica en un 27 % en l'estat vitri mitjançant la introducció d'un 5 % d'argila; Mohan i col.<sup>82</sup> van incrementar la temperatura d'inici de degradació tèrmica en un 16 % i Gensler i col.<sup>83</sup> van reduir la permeabilitat al vapor d'aigua fins a un 80-90 %.

## Referències

- [1] Lee, H.; Neville, K.; "Handboobk of Epoxy Resins" McGraw-Hill, New York (1967).
- [2] Castan, P.; Swiss Pat. 211, 116 (1940).
- [3] Potter, WG.; "Epoxy Resins" Plastic Institute, New York (1970).
- [4] May, CA.; "Epoxy Resins: Chemistry and Technology" Marcel Dekker, New York (1988).
- [5] Chung, K.; Takata, T.; Endo, T.; *Macromolecules*, 28, 3048-3054 (1995).
- [6] Huang, SJ.; "Environmentally Degradable Polymers" Elsevier, Oxford, 1994.
- [7] (a) Wang, L.; Li, H.; Wong, CP.; *J. Polym. Sci., Part A: Polym. Chem.*, 37, 2991-3001 (1999); (b) Wang, L.; Li, H.; Wong, CP.; *J. Polym. Sci., Part A: Polym. Chem.*, 38, 3771-3782 (2000); (c) Li, H.; Wong, CP.; *IEEE Trans. Adv. Packag.*, 27, 165-172 (2004).
- [8] (a) Yang, S.; Chen, J.; Körner, H.; Breiner, T.; Ober, CK.; *Chem. Mater.*, 10, 1475-1482 (1998); (b) Chen, JS.; Ober, CK.; Poliks, MD.; *Polymer*, 43, 131-139 (2002); (c) Shirai, M.; Kawano, A.; Okamura, H.; Tsunooka, M.; *Chem. Mater.*, 15, 4075-4081 (2003); (d) Chen, JS.; Ober, CK.; Poliks, MD.; Zhang, Y.; Wiesner, U.; Cohen, C.; *Polymer*, 45, 1939-1950 (2004).
- [9] Okamura, H.; Shin, K.; Tsunooka, M.; Shirai, M.; *J. Polym. Sci., Part A: Polym. Chem.*, 42, 3685-3696 (2004).
- [10] Shin, Y.; Kawaue, A.; Okamura, H.; Shirai, M.; *Reac. Funct. Polym.*, 61, 293-302 (2004).
- [11] Malik, J.; Clarson, SJ.; *Polymer*, 43, 2561-2567 (2002).
- [12] (a) Tesoro, GC.; Sastri, VR.; *J. Appl. Polym. Sci.*, 39, 1439-1457 (1990); (b) Sastri, VR.; Tesoro, GC.; *J. Appl. Polym. Sci.*, 39, 1425-1437 (1990).
- [13] (a) Buchwalter, SL.; Kosbar, LL.; *J. Polym. Sci., Part A: Polym. Chem.*, 34, 249-260 (1996); (b) Buchwalter, SL.; Kosbar, LL.; *J. Polym. Sci., Part A: Polym. Chem.*, 34, 1439-1441 (1996).
- [14] Sadhir, RK.; Luck, MR., (Eds.), *Expanding Monomers: Synthesis, Characterization and Applications*; CRC Press: Boca Raton, FL (1992).
- [15] Bodenbenner, K.; *Ann. Chim.*, 623, 183-191 (1959).
- [16] Bailey, WJ.; Sun, RLJ.; Katsuki, H.; Endo T.; Iwama, H.; Tsushima, R.; Saigou, K.; Bittrito, MM.; "Ring-opening Polymerization with Expansion in Volume", in "Ring-opening Polymerization", ACS Symp. Ser., No.59, Saegusa, T.; Goethals, E.; Eds., Am. Chem. Soc., Washington D.C. (1977).
- [17] Bailey, WJ.; *J. Elastoplast*, 5, 142-152 (1973).
- [18] Bailey, WJ.; Katsuki, H.; Endo T.; *J. Am. Chem. Soc., Div. Polym. Prepr.*, 155, 445-450 (1974).

- [19] Bailey, WJ.; Saigo, K.; J. Am. Chem. Soc., Div. Polym. Prepr., 21, 4-5 (1980).
- [20] Bailey, WJ.; J. Macromol. Sci., Chem., A9(5), 849-865 (1975).
- [21] Tagoshi, H.; Endo, T.; J. Polym. Sci., Polym. Lett., 28, 77-81 (1988).
- [22] Nishida, H.; Sanda, F.; Endo, T.; Nakahara, T.; Ogata, T.; J. Polym. Sci., Part A: Polym. Chem., 37, 4502-4509 (1999).
- [23] Matyjaszewski, K.; J. Polym. Sci., Part A: Polym. Chem., 22, 29-40 (1984).
- [24] (a) Chikaoka, S.; Takata, T.; Endo, T.; Macromolecules, 25, 625-628 (1992); (b) Endo, T.; Suzuki, T.; Sanda, F.; Takata, T.; Macromolecules, 29, 4819 (1996).
- [25] (a) Chikaoka, S.; Takata, T.; Endo, T.; Macromolecules, 24, 331-332 (1991); (b) Hitomi, M.; Sanda, F.; Endo, T.; J. Polym. Sci., Part A: Polym. Chem., 36, 2823-2825 (1998); (c) Hitomi, M.; Sanda, F.; Endo, T.; Macromol. Chem. Phys., 200, 1268-1273 (1999); (d) Endo, T.; Sansa, F.; Macromol. Symp., 153, 227-321 (2000).
- [26] Chabanne, P.; Tighzert, L.; Pascault, JP.; J. Appl. Polym. Sci., 53, 787-806 (1994).
- [27] (a) Bouillon, N.; Pascault, JP.; Tighzert, L.; Makromol. Chem, 191, 1403-1416 (1990); (b) Bouillon, N.; Pascault, JP.; Tighzert, L.; Makromol. Chem, 191, 1417-1433 (1990); (c) Bouillon, N.; Pascault, JP.; Tighzert, L.; Makromol. Chem, 191, 1435-1449 (1990).
- [28] (a) Cherdron, H.; Oshe, H.; Korte, F.; Makromol. Chem., 56, 187-194 (1962); (b) Houk, KN.; Jabbari, A.; Hall, HK.; Alemán, C.; J. Org. Chem., 73, 2674-2678 (2008).
- [29] Chabanne, P.; Pascault, JP.; Tighzert, L.; French Pat. 90.06608 (1991).
- [30] Fedtke, M.; Haufe, J.; Kahler, E.; Müller, G.; Angew. Makromol. Chem., 255, 53-59 (1998).
- [31] (a) Mas, C.; Ramis, X.; Salla, JM.; Mantecón, A.; Serra, A.; J. Polym. Sci., Part A: Polym. Chem., 41, 2794-2808 (2003); (b) González, L.; Ramis, X.; Salla, JM.; Mantecón, A.; Serra, A.; J. Polym. Sci., Part A: Polym. Chem., 44, 6869-6879 (2006); (c) González, S.; Fernandez-Francos, X.; Salla, JM.; Serra, A.; Mantecón, A.; Ramis, X.; J. Appl. Polym. Sci., 104, 3406-3416 (2007); (d) Canadell, J.; Mantecón, A.; Cádiz, V.; J. Polym. Sci., Part A: Polym. Chem., 44, 4722-4730 (2006).
- [32] Cervellera, R.; Ramis, X.; Salla, JM.; Mantecón, A.; Serra, A.; J. Polym. Sci., Part A: Polym. Chem., 44, 2873-2882 (2006).
- [33] (a) Park, SJ.; Seo, MK.; Lee, JR.; Lee, DR.; J. Polym. Sci., Part A: Polym. Chem., 39, 187-195 (2001); (b) Grazulevicius, JV.; Kublickas, R.; Kavaliunas, R.; J. Macromol. Sci. Part A Pure Appl. Chem., 31, 1303-1313 (1994); (c) Morio, K.; Murase, H.; Tsuchiya, H.; J. Appl. Polym. Sci., 32, 5727-5732 (1986); (d) Lin, RH.; Chen, CL.; Kao, LH.; Yang, PR.; J. Appl. Polym. Sci., 82, 3539-3551 (2001) (e) Endo, T.; Sanda, F.; Macromol. Symp., 107, 237-242 (1996).
- [34] (a) Kobayashi, S.; Synlett, 9, 689-701 (1994); (b) Kobayashi, S.; Hachiya, I.; Araki, M.; Ishitani, H.; Tetrahedron Lett., 34, 3755-3758 (1993); (c) De Nino A., Maiuolo, L.; Nardi, M., Procopio, A., Tagarelli, A.; Synthesis, 4, 496-498 (2004); (d) Tsuruta, H.; Yamaguchi, K.; Imamoto, T.; Chem. Commun., 1703-1704 (1999); (e) Kobayashi, S.; Nagayama, S.; Busujima, T.; J. Am. Chem. Soc., 120, 8287-8288 (1998).
- [35] Kobayashi, S.; "Lanthanides: Chemistry and Use in Organic Synthesis", Springer, Berlin (1999).
- [36] Aggarwal, VK.; Vennall, GP.; Tetrahedron Lett., 37, 3745-3746 (1996).

- [37] Imamoto, T.; "Lanthanides in Organic Synthesis" Academic Press, London (1994).
- [38] Satoh, K.; Kamigaito, M.; Sawamoto, M.; *Macromolecules*, 33, 4660-4666 (2000).
- [39] Pearson, R.G.; *J. Am. Chem. Soc.* 85, 3533-3539 (1963).
- [40] (a) Kobayashi, S.; Hachiya, I.; *J. Org. Chem.*, 59, 3590-3596 (1994); (b) Iranpoor, N.; Shekarriz, M.; Shiriny, F.; *Synth. Commun.* 28, 347-366 (1998).
- [41] Aspinall, H.C.; Dwyer, J.L.; Greeves, N.; McIver, E.G.; Woolley, J.C.; *Organometallics*, 17, 1884-1888 (1998).
- [42] Wang, Y.; Kunioka, M.; *Macromol. Symp.*, 224, 193-205 (2005).
- [43] (a) Dunsing, R.; Kricheldorf, H.R.; *Eur. Polym. J.*, 24, 145-150 (1988); (b) Wang, Y.; Onozawa, S.; Kunioka, M.; *Green. Chem.*, 5, 571-574 (2003).
- [44] (a) Nomura, N.; Taira, A.; Tomioka, T.; Okada, M.; *Macromolecules*, 33, 1497-1499 (2000); (b) Nomura, N.; Taira, A.; Nakase, A.; Tomioka, T.; Okada, M.; *Tetrahedron*, 63, 8478-8484 (2007).
- [45] (a) Satoh, K.; Kamigaito, M.; Sawamoto, M.; *Macromolecules*, 32, 3827-3832 (1999); (b) Kobayashi, S.; Wakabayashi, T.; Nagayama, S.; Oyamada, H.; *Tetrahedron Lett.*, 38, 4559-4562 (1997).
- [46] (a) Castell, P.; Galià, M.; Serra, A.; Salla, J.M.; Ramis, X.; *Polymer*, 41, 8465-8474 (2000); (b) Mas, C.; Serra, A.; Mantecón, A.; Salla, J.M.; Ramis, X.; *Macromol. Chem. Phys.*, 202, 2554-2564 (2001); (c) García, S.J.; Ramis, X.; Serra, A.; Suay, J.; *Thermochim. Acta*, 441, 45-52 (2006); (d) García, S.J.; Ramis, X.; Serra, A.; Suay, J.; *J. Therm. Anal. Calorim.*, 83, 429-438 (2006).
- [47] (a) Kubisa, P.; Matyjaszewski, K.; in "Cationic Polymerization. Mechanism, Synthesis, and Applications", Marcel Dekker, New York (1996); (b) Matejka, L.; Chabanne, L.; Tighzert, L.; Pascault, J.P.; *J. Polym. Sci., Part A: Polym. Chem.*, 32, 1447-1458 (1994).
- [48] Mas, C.; Ramis, X.; Salla, J.M.; Mantecón, A.; Serra, A.; *J. Polym. Sci., Part A: Polym. Chem.*, 44, 1711-1721 (2006).
- [49] Constantin, F.; Fenouillot, F.; Guillaume, J.M.; Koenig, R.; Pascault, J.P.; *Macromol. Symp.*, 198, 335-344 (2003).
- [50] (a) Mas, C.; Ramis, X.; Salla, J.M.; Mantecón, A.; Serra, A.; *J. Polym. Sci., Part A: Polym. Chem.*, 42, 3782-3791 (2004); (b) Mas, C.; Ramis, X.; Salla, J.M.; Mantecón, A.; Serra, A.; *J. Polym. Sci., Part A: Polym. Chem.*, 43, 2337-2347 (2005).
- [51] Mas, C.; Ramis, X.; Salla, J.M.; Mantecón, A.; Serra, A.; *J. Appl. Polym. Sci.*, 92, 381-393 (2004).
- [52] García, S.J.; Suay, J.; *Prog. Org. Coat.*, 57, 319-331 (2007).
- [53] Gonzalez, L.; Ramis, X.; Salla, J.M.; Mantecón, A.; Serra, A.; *Polym. Degrad. Stab.*, 92, 596-607 (2007).
- [54] (a) Brady, R.F.; Simon, F.E.; *J. Polym. Sci., Part A: Polym. Chem.*, 25, 231-239 (1987); (b) Sikes, A.; Brady, R.F.; *J. Polym. Sci., Part A: Polym. Chem.*, 28, 2533-2546 (1990).
- [55] Chung, K.; Takata, T.; Endo, T.; *Macromolecules*, 30, 2532-2538 (1997).
- [56] (a) Takata, T.; Tadokoro, A.; Endo, T.; *Macromolecules*, 25, 2782-2783 (1992); (b) Tadokoro, A.; Takata, T.; Endo, T.; *Macromolecules*, 26, 4400-4406 (1993); (c) Takata, T.; Tadokoro, A.; Chung, K.; Endo, T.; *Macromolecules*, 28, 1340-1345 (1995).

- [57] (a) Tadokoro, A.; Takata, T.; Endo, T.; *Macromolecules*, 26, 6686-6687 (1993); (b) Chung, K.; Takata, T.; Endo, T.; *Macromolecules*, 28, 3048-3054 (1995); (c) Chung, K.; Takata, T.; Endo, T.; *Macromolecules*, 28, 1711-1713 (1995).
- [58] Zhang, C.; Ochiai, B.; Endo, T.; *J. Polym. Sci., Part A: Polym. Chem.*, 43, 2643-2649 (2005).
- [59] (a) Uenishi, K.; Sudo, A.; Endo, T.; *Macromolecules*, 40, 6535-6539 (2007); (b) Uenishi, K.; Sudo, A.; Endo, T.; *J. Polym. Sci., Part A: Polym. Chem.*, 46, 3447-3451 (2008); (c) Uenishi, K.; Sudo, A.; Endo, T.; *J. Polym. Sci., Part A: Polym. Chem.*, 46, 4092-4102 (2008).
- [60] (a) Ricciardi, F.; Romanchick, WA.; Joullié, MM.; *J. Polym. Sci., Polym. Chem. Ed.*, 21, 1475-1490 (1983); (b) Heise, MS.; Martin, GC.; *Macromolecules*, 22, 99-104 (1989); (c) Heise, MS.; Martin, GC.; *J. Appl. Polym. Sci.*, 39, 721-738 (1990); (d) Barton, JM.; Hamerton, I.; Howlin, BJ.; Jones, JR.; Liu, S.; *Polym. Int.*, 41, 159-168 (1996).
- [61] Chen, D.; He, P.; *Compos. Sci. Technol.*, 64, 2501-2507 (2004).
- [62] (a) Galià, M.; Serra, A.; Mantecón, A.; Cádiz, V.; *J. Appl. Polym. Sci.*, 56, 193-200 (1995); (b) Ribera, D.; Mantecón, A.; Serra, A.; *J. Polym. Sci., Part A: Polym. Chem.*, 40, 3916-3929 (2007).
- [63] Dell'Erba, IE.; Williams, RJJ.; *Polym. Eng. Sci.*, 46, 351-359 (2006).
- [64] (a) Mika, T.; Bauer, RS.; "Curing Agents and Modifiers" in "Epoxy Resins Chemistry and Technology", May, CA.; Ed., 2nd ed., Marcel Dekker, New York (1988); (b) Pascault, JP.; Sautereau, H.; Verdu, J.; Williams, RJJ.; "Thermosetting Polymers", Marcel Dekker, New York (2002).
- [65] Fernández-Francos, X.; Salla, JM.; Mantecón, A.; Serra, A.; Ramis, X.; *J. Appl. Polym. Sci.*, 109, 2304-2315 (2008).
- [66] Carter, LW.; Hendricks, JG.; Bolley, DS.; *US Pat.* 2, 531, 396 (1950).
- [67] (a) Okada, A.; Kawasumi, M.; Kurauchi, T.; Kamigaito, O.; *Polym. Prepr. (Am. Chem. Soc., Div. Polym. Chem.)*, 28, 447-448 (1987); (b) Usuki, A.; Kojima, Y.; Kawasumi, M.; Okada, A.; Fukushima, Y.; Kurauchi, T.; Kamigaito, O.; *J. Mater. Res.*, 8, 1179-1184 (1993).
- [68] (a) Messersmith, PB.; Giannelis, EP.; *Chem. Mater.*, 6, 1719-1725 (1994); (b) Kelly, P.; Akelah, A.; Qutubuddin, S.; Moet, A.; *J. Mater. Sci.*, 29, 2274-2280 (1994).
- [69] Vaia, RA.; Jandt, KD.; Giannelis, EP.; *Macromolecules*, 28, 8080-8085 (1995).
- [70] Yano, K.; Usuki, A.; Okada, A.; Kurauchi, T.; Kamigaito, O.; *J. Polym. Sci., Part A: Polym. Chem.*, 31, 2493-2398 (1993).
- [71] Hasegawa, N.; Kawasumi, M.; Kato, M.; Usuki, A.; Okada, A.; *J. Appl. Polym. Sci.*, 63, 137-138 (1997).
- [72] Wang, Z.; Pinnavaia, T.; *Chem. Mater.*, 10, 3769-3771 (1998).
- [73] (a) Triantafillidis, CS.; LeBaron, PC.; Pinnavaia, TJ.; *J. Solid State Chem.*, 167, 354-362 (2002); (b) Xue, S.; Pinnavaia, TJ.; *Microporous Mesoporous Mater.*, 107, 134-140 (2008); (c) Kowalczyk, K.; Spychaj, T.; *Prog. Org. Coat.*, 62, 425-429 (2008).
- [74] (a) Deng, Y.; Gu, A.; Fang, Z.; *Polym. Int.*, 53, 85-91 (2004); (b) Kaya, E.; Tanoglu, M.; Okur, S.; *J. Appl. Polym. Sci.*, 109, 834-840 (2008).
- [75] (a) Liang, G.; *Polym. Degrad. Stab.*, 80, 383-391 (2003); (b) Lakshimi, MS.; Narmadha, B.; Reddy, BSR.; *Polym. Degrad. Stab.*, 93, 201-213 (2008).

- [76] (a) Osman, MA.; Mittal, V.; Morbidelli, M.; Suter, UW.; *Macromolecules*, 37, 7250-7257 (2004); (b) Sun, L.; Boo, WJ.; Clearfield, A.; Sue, HJ.; Pham, HQ.; *J. Membr. Sci.*, 318, 129-136 (2008).
- [77] (a) Wang, K.; Wang, L.; Wu, J.; Chen, L.; He, C.; *Langmuir*, 21, 3613-3618 (2005); (b) Ma, J.; Yu, ZZ.; Zhang, QX.; Kie, XL.; Mai, YW, Luck, I.; *Chem. Mater.*, 16, 756-759 (2004); (c) McIntyre, S.; Kaltzakorta, I.; Liggat, JJ.; Pethrick, RA.; Rhoney, I.; *Ind. Eng. Chem. Res.*, 44, 8573-8579 (2005); (d) Hutchinson, JM.; Montserrat, S.; Román, F.; Cortés, P.; Campos, L.; *J. Appl. Polym. Sci.*, 102, 3751-3763 (2006); (e) Wang, J.; Qin, S.; *Mater. Lett.*, 61, 4222-4224 (2000).
- [78] Tolle, TB.; Anderson, DP.; *J Appl. Polym. Sci.*, 91, 89-100 (2004).
- [79] Lan, T.; Kaviratna, PD.; Pinnavaia, TJ.; *Chem. Mater.*, 7, 2144-2150 (1995); (b) Lü, JK.; Ke, YC.; Qi, ZN.; Yi, XS.; *J. Polym. Sci. Part B: Polym. Phys.*, 39, 115-120 (2001); (c) Kornmann, X.; Lindberg, H.; Berlung, LA.; *Polymer*, 42, 1303-1310 (2001); (d) Kornmann, X.; Thomann, R.; Mülhaupt, R.; Finter, J.; Berlung, L.; *J. Appl. Polym. Sci.*, 86, 2643-2652 (2002); (e) Chen, C.; Curliss, D.; *J. Appl. Polym. Sci.*, 90, 2276-2287 (2003).
- [80] (a) Kornmann, X.; Lindberg, H.; Berlung, LA.; *Polymer*, 42, 4493-4499 (2001); (b) Chin, IJ.; Thurn-Albrecht, T.; Kim, HC.; Russell, TP.; Wang, J.; *Polymer*, 42, 5947-5952 (2001).
- [81] Massam, J.; Pinnavaia, TJ.; *Mater. Res. Soc. Symp. Proc.*, 520, 223-232 (1998).
- [82] Mohan, TP.; Ramesh-Kumar, M.; Velmurugan, R.; *J. Mater. Sci.*, 41, 5915-5925 (2006).
- [83] Gensler, R.; Gröppel, P.; Muhrer, V.; Müllen, N.; *Part. Syst. Charact.*, 19, 293-299 (2002).

## 1.2 OBJECTIUS I METODOLOGIA

L'objectiu d'aquest treball és l'obtenció i l'estudi de nous materials termoestables preparats per copolimerització del diglicidilèter de bisfenol A (DGEBA) amb monolactones com la  $\gamma$ -valerolactona ( $\gamma$ -VL) i la  $\alpha$ -metil- $\gamma$ -butirolactona ( $\gamma$ -MBL) i bis( $\gamma$ -lactones) com la 1-metil-2,8-dioxabicyclo[3.3.0]octan-3,7-diona (bisMe) i la 1-fenil-2,8-dioxabicyclo[3.3.0]octan-3,7-diona (bisPhe) utilitzant diversos triflats de terres rares com iniciadors catiónics i varies amines terciàries com iniciadors aniònics. A més, com a iniciador catiònic s'ha estudiat el  $\text{BF}_3 \cdot \text{MEA}$ , que és el més utilitzat a nivell industrial, per tal de comprovar els avantatges que suposen el triflats de terres rares, tant des del punt de vista cinètic com estructural. En el cas d'utilitzar  $\gamma$ -monolactones la copolimerització només pot tenir lloc en condicions catióniques mentre que en el cas d'utilitzar bis( $\gamma$ -lactones) aquestes poden copolimeritzar catiònica i aniònicament mitjançant un procés tàndem de doble obertura d'anell. També es pretén realitzar una comparació dels materials obtinguts segons el tipus d'iniciador emprat.

El present estudi pot ésser considerat una continuació de la Tesi Doctoral "Modificació de reïnes epoxi amb lactones" presentada per Cristina Mas en el nostre departament. En aquesta tesi es va utilitzar  $\gamma$ -butirolactona i s'ha ampliat l'estudi a lactones substituïdes i a bislactones condensades. Aquesta estratègia de copolimerització és molt versàtil, donat que es pot jugar amb les diferents condicions de reacció, com la proporció de comonòmers, el tipus de iniciador i la seva proporció, el que permet l'obtenció de materials amb característiques molt variades. Amb les noves lactones s'ha volgut explorar la validesa de l'estratègia utilitzada prèviament amb èxit en la millora de materials epoxídics, basada en la copolimerització de reïnes epoxi amb lactones. A més, s'ha utilitzat el triflat d'escandi, degut a que presenta una major acidesa de Lewis que els triflats de lantànid, i que no havia estat assajat a l'esmentada tesi.

A més, s'ha estudiat la viabilitat de la preparació de *nanocomposites* a partir de filossilicats laminars nanomètrics en els sistemes catiónics basats en DGEBA i  $\gamma$ -valerolactona, donat que presentaven una baixa viscositat abans del curat, la qual cosa podia preveure una bona dispersió de l'argila en la matriu polimèrica. L'obtenció de *nanocomposites* amb base epoxídica mitjançant curat tèrmic amb iniciadors catiónics no ha estat pràcticament estudiada fins a l'actualitat i per tant constitueix per si sol un repte.


La metodologia emprada en el desenvolupament del treball ha estat:

- Estudi dels processos de curat emprant calorimetria diferencial d'escombrat (DSC) i espectroscòpia infraroja (FTIR/ATR).
- Estudi de la cinètica de curat a partir de dades calorimètriques i d'infraroig.
- Caracterització fenomenològica dels processos de curat i establiment dels diagrames temps-temperatura-transformació.

- Avaluació de la conversió a la gelificació ( $\alpha_{gel}$ ) mitjançant anàlisi termomecànica (TMA) i DSC.
- Estudi del procés de curat en els *nanocomposites* per diferents tècniques.
- Estudi de la dispersió de l'argila en el termoestable per microscòpia de transmissió electrònica (TEM).
- Estudi de la degradabilitat tèrmica dels materials obtinguts per anàlisi termogravimètrica (TGA).
- Estudi de les característiques termomecàniques: avaluació dels mòduls i de les transicions tèrmiques per anàlisi termodinamomecànica (DMTA).
- Determinació de la microduresa i del mòdul de Young.
- Determinació dels coeficients d'expansió tèrmica per TMA.
- Observació de la superfície de trencament dels materials obtinguts per microscòpia electrònica d'escombrat (SEM).

La tesi està estructurada en set capítols:

1. Introducció i objectius.
2. Polimerització catiònica del diglicidileter del bisfenol A (DGEBA) amb  $\gamma$ -valerolactona i  $\alpha$ -metil- $\gamma$ -butirolactona.
3. Preparació de *nanocomposites* per copolimerització catiònica del DGEBA amb  $\gamma$ -VL iniciada amb triflats de terres rares amb esmectites.
4. Copolimerització aniònica i catiònica del diglicidileter del bisfenol A (DGEBA) amb bis( $\gamma$ -lactones) condensades.
5. Conclusions.
6. Annex i acrònims.
7. Llistat de contribucions científiques.

Polimerització catiónica del  
2.  diglicidilèter de bisfenol A  
(DGEBA) amb la  $\gamma$ -valerolactona  
( $\gamma$ -VL) i la  $\alpha$ -metil- $\gamma$ -butirolactona  
( $\gamma$ -MBL)

UNIVERSITAT ROVIRA I VIRGILI  
NOUS TERMOESTABLES EPOXÍDICS MODIFICATS AMB GAMMA-LACTONES I BIS-GAMMA-LACTONES CONDENSADES  
M<sup>a</sup> Mercè Arasa Bertomeu  
ISBN:978-84-692-4157-8/DL:T-1171-2009

## 2.1 INTRODUCCIÓ

Com s'ha comentat anteriorment, Chabanne i col.<sup>1</sup> van estudiar la influència de l'addició de petites quantitats de  $\gamma$ -butirolactona ( $\gamma$ -BL) en la polimerització catiónica del fenilglicidilèter (PGE) amb  $\text{BF}_3$ :amina, ja que en estudis anteriors s'havia observat com aquesta lactona en presència d'un àcid de Lewis podia ser incorporada en la xarxa polimèrica malgrat la seva falta de polimeritzabilitat<sup>2</sup>. Així doncs, van concloure que en la reacció de polimerització de l'epòxid en presència de la  $\gamma$ -BL no només tenia lloc la homopolimerització de l'epòxid sinó que a més s'incorporava la lactona prèvia formació del corresponent espiroortoester.

En una de les tesis doctorals realitzades en el nostre grup de recerca anomenada "Modificació química de reïnes epoxi amb lactones"<sup>3</sup> es va realitzar l'estudi de la copolimerització de reïnes epoxi i  $\gamma$ -BL emprant diversos triflats de lantànid com iniciadors. En aquest estudi, mitjançant FTIR, es van observar les diferents reaccions que tenien lloc durant la copolimerització i mitjançant calorimetria l'acceleració del procés de curat el que permetia disminuir la temperatura i/o el temps de curat. Els materials obtinguts presentaven una millora en la degradabilitat respecte els termoestables obtinguts a partir de reïnes epoxi curades amb  $\text{BF}_3$ :amina.

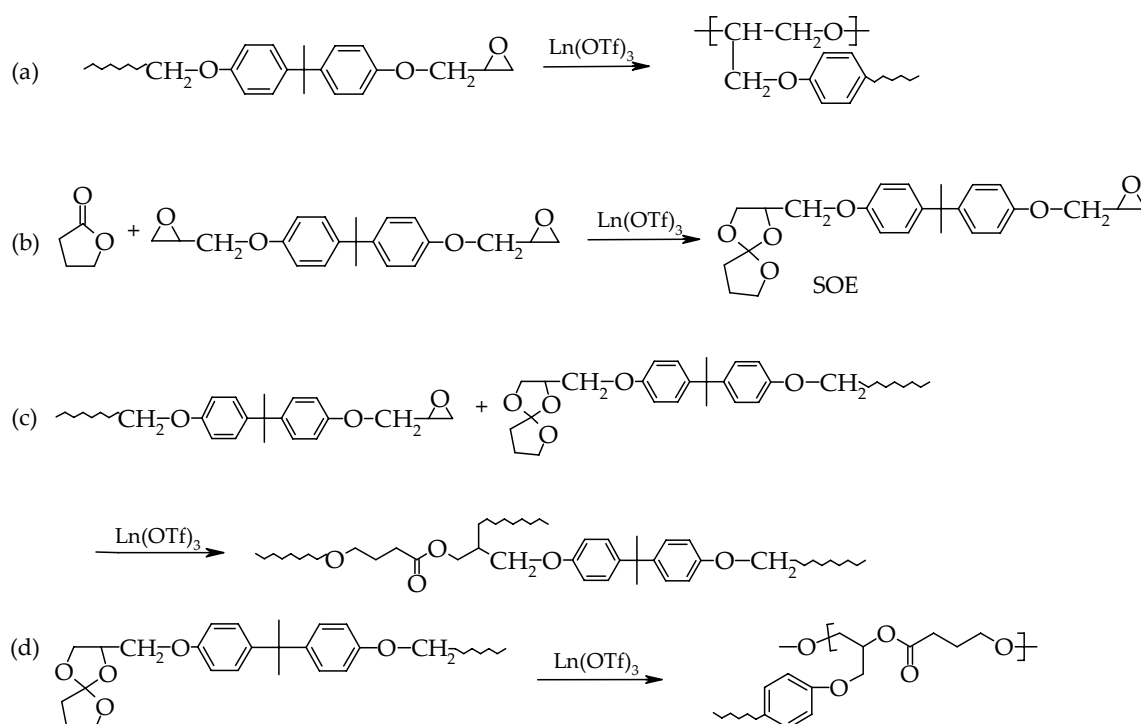


**Figura 2.1.** Reaccions que tenen lloc durant el curat catiónic del DGEBA amb  $\gamma$ -BL: (a) homopolimerització del epòxid, (b) formació del SOE, (c) copolimerització de l'epòxid amb SOE i (d) homopolimerització del SOE

El present capítol tracta de l'obtenció de nous materials termoestables per copolimerització catiònica del diglicidilèter del bisfenol A (DGEBA) amb  $\gamma$ -valerolactona ( $\gamma$ -VL) i  $\alpha$ -metil- $\gamma$ -butirolactona ( $\gamma$ -MBL) emprant triflats de terres rares com iniciadors.

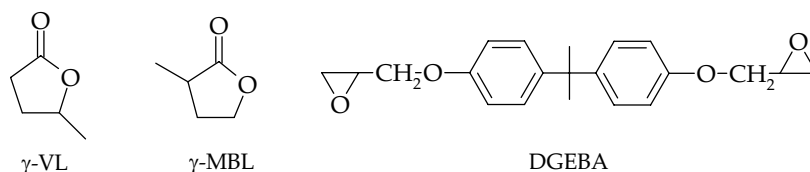


**Figura 2.2.** Estructura de les diferents monòmers utilitzats en l'estudi

Ja que les estructures de les lactones són similars a la de la  $\gamma$ -BL, seria d'esperar que seguissin el mateix mecanisme de curat i s'arribés a una xarxa de poli(èter-ester). En aquest treball s'ha estudiat l'efecte dels substituents en la lactona tant en la formació del espiroortoester com en la seva polimerització i l'efecte que produeix la quantitat de lactona introduïda i el tipus o la quantitat d'iniciador en els materials finals.

El curat catiònic s'han dut a terme amb  $\text{La}(\text{OTf})_3$  i  $\text{Yb}(\text{OTf})_3$  i s'ha inclòs el  $\text{Sc}(\text{OTf})_3$  el qual no s'havia utilitzat anteriorment en  $\gamma$ -lactones. Aquests iniciadors es diferencien en la seva acidesa de Lewis i duresa de Pearson. En alguns sistemes també s'ha utilitzat el  $\text{BF}_3 \cdot \text{MEA}$ , iniciador catiònic convencionalment utilitzat, per tal de comparar-lo amb els triflats de terres rares.

Els resultats d'aquest treball es reflecteixen en les següents treballs:

- FTIR/ATR study of the copolymerization of DGEBA with methyl-substituted  $\gamma$ -lactones catalyzed by rare earth triflates
- Study on the degradation of ester-modified epoxy resins obtained by cationic copolymerization of DGEBA with  $\gamma$ -lactones initiated by rare earth triflates
- Kinetic study by FTIR and DSC on the cationic curing of a DGEBA/ $\gamma$ -valerolactone mixture with ytterbium triflate as initiator
- Study on the effect of rare earth metal triflates as initiators in the cationic curing of the DGEBA/ $\gamma$ -valerolactone mixtures and characterization of the thermosets obtained

## Referències

- [1] Chabanne, P.; Tighzert, L.; Pascault, P.; J. Appl. Polym. Sci., 53, 787-806 (1994).
- [2] Bailey, WJ.; J. Elastoplast, 5, 142 (1973).
- [3] Cristina Mas Quílez, "Modificació química de reïnes epoxi amb lactones", Universitat Rovira i Virgili, setembre 2004.

2.2 FTIR-ATR STUDY OF THE COPOLYMERIZATION OF  
DIGLYCIDYL ETHER OF BISPHENOL A WITH  $\gamma$ -METHYL-  
SUBSTITUTED  $\gamma$ -LACTONES CATALYZED BY RARE  
EARTH TRIFLATE INITIATORS

---

*Mercè Arasa, Xavier Ramis, Josep Maria Salla, Ana Mantecón, Àngels Serra; Journal of Polymer Science: Part A: Polymer Chemistry 45 (2007) 2129-2141*

UNIVERSITAT ROVIRA I VIRGILI  
NOUS TERMOESTABLES EPOXÍDICS MODIFICATS AMB GAMMA-LACTONES I BIS-GAMMA-LACTONES CONDENSADES  
M<sup>a</sup> Mercè Arasa Bertomeu  
ISBN:978-84-692-4157-8/DL:T-1171-2009



# FTIR/ATR STUDY OF THE COPOLYMERIZATION OF DIGLYCIDYL ETHER OF BISPHENOL A WITH METHYL-SUBSTITUTED $\gamma$ - LACTONES CATALYZED BY RARE EARTH TRIFLATE INITIATORS

Mercè Arasa,<sup>1</sup> Xavier Ramis,<sup>2</sup> Josep Maria Salla,<sup>2</sup> Ana Mantecón,<sup>1</sup> Àngels Serra<sup>1</sup>

<sup>1</sup>Dpt. Q. Analítica i Q. Orgànica, URV. C/Marcel·lí Domingo s/n, 43007 Tarragona, Spain

<sup>2</sup> Lab. Termodinàmica, ETSEIB. UPC, Av. Diagonal 647, 08028 Barcelona, Spain

## Abstract

Mixtures of DGEBA with  $\gamma$ -valerolactone ( $\gamma$ -VL) or  $\alpha$ -methyl- $\gamma$ -butyrolactone ( $\gamma$ -MBL) 2:1 (mol/mol) were cationically copolymerized in the presence of scandium, ytterbium or lanthanum triflates as initiators. The evolution of the different reactive groups was followed by means of FTIR/ATR spectroscopy. From these experiments, we could detect the coexistence of two unexpected processes: a reversion of the intermediate spiroorthoester formed to the initial products and a depolymerization process, which only takes place in samples with  $\gamma$ -VL, when scandium triflate was used as initiator or when the proportion of ytterbium triflate was increased from 1 to 3 phr. When  $\gamma$ -MBL was used as comonomer no depolymerization occurs which supports the proposed mechanism.

*Keywords:* Cationic polymerization, copolymerization, crosslinking, epoxy resin, FT-IR, lactones, lanthanide triflates, shrinkage, thermoset.

## Introduction

Epoxy resins are widely applied in microelectronics as coatings or encapsulants. However, the curing is generally accompanied by shrinkage because van der Waals distances are converted into covalent bonds, thus increasing the density of the materials. This shrinkage produced during curing is a big problem because it leads to the formation of microvoids and microcracks, which reduces the durability of the material and worsens the properties. Moreover, it

produces the loss of adhesion and reduces their protection capability.<sup>1,2</sup> The use of expanding monomers is a possible way to solve these problems. Spiroorthoesters (SOEs) are bicyclic compounds that were defined by Bailey et. al.<sup>1,3</sup> as expanding monomers because they experiment cationic ring-opening polymerization<sup>4</sup> without shrinkage or even with expansion. They can be synthesized from lactones and epoxides in the presence of a Lewis acid as a catalyst.<sup>5,6</sup> However, the use of expanding monomers in industrial applications is still

limited because of the problems arising from their synthesis and polymerizability.<sup>7</sup>

A possible way to overcome the previous synthesis of SOE monomers is to generate them "*in situ*" from epoxy resins and lactones. We demonstrated that, in these systems, the shrinkage after gelation is very low and that SOE polymerizes at the end of the curing.<sup>8</sup> Moreover, there is another mechanism to reduce the shrinkage after gelation which is associated with the degree of conversion at the gelation point that increases on adding lactone to the epoxy resin, due to the functionality of lactone, which is two, whereas epoxy resin has a functionality of four in the cationic ring-opening copolymerization.<sup>9</sup> The reduction of the contraction after gelation is the main goal because after this point the mobility of the polymeric chains is strongly reduced and the internal stresses appear.

The polymerization of SOE groups leads to poly(ether-ester) structures. The presence of ester groups in the three-dimensional network has another beneficial consequence: that is the increase in the degradability of the thermosets. The introduction of ester groups in the cross-linked epoxy resins was previously proposed by Ober and coworkers<sup>10,11</sup> and Wang et. al.,<sup>12,13</sup> to increase the reworkability of the electronic materials. They proposed the use of modified cycloaliphatic epoxy resins containing ester groups in their structure. However, the use of cycloaliphatic epoxy resins has some limitations in their curing and mechanical properties. To overcome these

limitations increasing the versatility of the thermosets we propose the copolymerization strategy aforementioned.

Because the formation of SOE requires the presence of a Lewis acid and these compounds can act as cationic initiators in the copolymerization process, we used several rare earth triflates in the present work. In preceding studies, we used lanthanide triflates as initiators in the curing of similar systems and we could observe a relation between the curing rate and the Lewis acidity.<sup>14</sup> However, there is no clear tendency in the degree of chemical incorporation of the lactone into the three-dimensional structure.<sup>14</sup> Moreover, we described in a preceding article<sup>9</sup> that the reaction of diglycidylether of bisphenol A (DGEBA) with  $\gamma$ -caprolactone ( $\gamma$ -CL) initiated by 3 phr of ytterbium triflate is accompanied by a partial depolymerization of the material in the last stages of the curing to give small proportions of free  $\gamma$ -CL.

In the present work, we studied the influence of the acidity and the effect of methylic substituents in the  $\gamma$ -lactone ring on the depolymerization process. We tested ytterbium, lanthanum, and scandium triflate, which are Lewis acids with different strength but all of them stable in water.<sup>15,16</sup> As lactones we tested  $\gamma$ -valerolactone ( $\gamma$ -VL) and  $\alpha$ -methyl- $\gamma$ -butyrolactone ( $\gamma$ -MBL) for copolymerizing with DGEBA because  $\gamma$ -lactones cannot cationically homopolymerize because of thermodynamical reasons, and therefore its incorporation should take place through the formation of an intermediate SOE. The presence of methyl groups can change the charac-

teristics of the materials, among them the degradability, and the reaction evolution.

## Experimental Part

### Materials

Diglycidylether of bisphenol A (DGEBA) EPIKOTE RESIN 827 from Shell Chemicals (Epoxy Equiv. = 182.08 g/equiv.),  $\gamma$ -valerolactone ( $\gamma$ -VL; Aldrich), and  $\alpha$ -methyl- $\gamma$ -butyrolactone ( $\gamma$ -MBL; Aldrich) were used as received.

Lanthanum (III), ytterbium (III), and scandium (III) trifluoromethanesulfonates (Aldrich) were used without previous purification.

### Preparation of the curing mixtures

The samples were prepared by mixing the selected initiator in the corresponding amount of lactone and the addition of the required proportion of DGEBA with manual stirring. All the mixtures contained 1 phr of metal triflate (1 part per 100 parts of lactone/resin mixture, w/w). The prepared mixtures were kept at -18 °C before use.

### Characterization and measurements

The isothermal curing process, at 160 °C, was monitored with a Fourier transform infrared spectrophotometer (FTIR) 680 Plus from Jasco with resolution of 4 cm<sup>-1</sup> in the absorbance mode. An attenuated total reflection accessory (ATR) with thermal control and a diamond crystal (a Golden Gate heated single-reflection diamond ATR from Specac-Teknokroma) was used to determine FTIR spectra. The disappearance of the absorbance peak at 910 cm<sup>-1</sup>

(epoxy bending) was used to monitor the epoxy conversion. The consumption of the reactive carbonyl group in the lactone was evaluated by measuring the changes in absorbance at 1775 cm<sup>-1</sup> (carbonyl C=O stretching of cyclic ester). The appearance of the peak at 1737 cm<sup>-1</sup> (carbonyl C=O stretching of aliphatic linear ester), which does not exist in the sample before curing, indicates that ring-opening polymerization has occurred in SOE. So, the latter was used to evaluate the linear ester formation. The peak at 1605 cm<sup>-1</sup> (phenyl group) was chosen as an internal standard. Conversions of the different reactive groups, epoxide, lactone, and linear ester, were determined by the Lambert-Beer law from the normalized changes of absorbance at 910, 1775, and 1737 cm<sup>-1</sup>

$$\alpha_{\text{epoxy}} = 1 - \left( \frac{\overline{A}_{910}^t}{\overline{A}_{910}^0} \right) \quad \alpha_{\text{lactone}} = 1 - \left( \frac{\overline{A}_{1775}^t}{\overline{A}_{1775}^0} \right)$$
$$\alpha_{\text{linear ester}} = 1 - \left( \frac{\overline{A}_{1737}^t}{\overline{A}_{1737}^\infty} \right)$$

where  $\overline{A}^0$ ,  $\overline{A}^t$ , and  $\overline{A}^\infty$  are the normalized absorbance of the reactive group before curing, after reaction time  $t$ , and after complete curing.

## Results and discussion

In a previous article,<sup>14</sup> we described the crosslinking process of several DGEBA/ $\gamma$ -BL mixtures using different lanthanide triflates as initiators. We demonstrated that four competitive processes took place and that their extension was affected by the lanthanide used as initiator. When we used  $\gamma$ -caprolactone ( $\gamma$ -CL) we also detected the

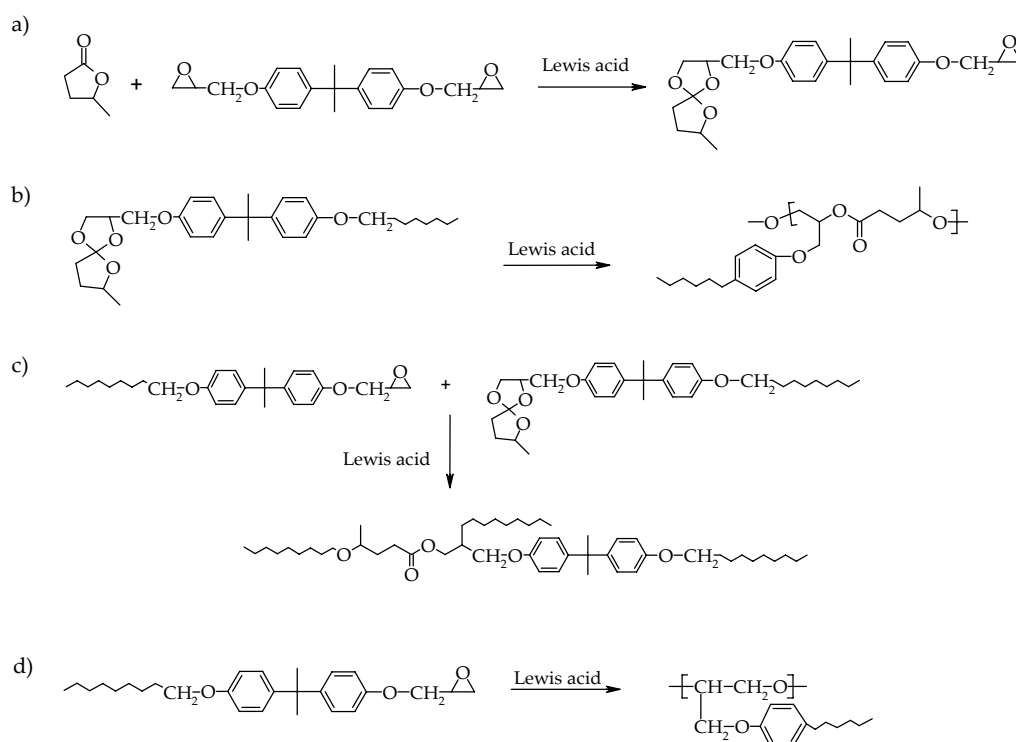
formation of free lactone at the end of the curing by a depolymerization process.

In **Scheme 1** are represented the four main reactions for DGEBA/ $\gamma$ -VL copolymerizations, which are usually expected. The reaction (a) shows the formation of SOE, (b) is its homopolymerization, (c) is the copolymerization of SOE and epoxide, and (d) is the homopolymerization of epoxide. The extent to which these four processes occur should depend on the type of initiator. It must be said that, in this type of copolymerization, the DGEBA resin acts as a tetrafunctional monomer and the lactone and the intermediate SOE act as bifunctional ones. Therefore, a higher chemical incorporation of lactone leads to a higher molecular weight between crosslinks. Processes (b) and (c) are responsible for

the formation of ester groups in the three-dimensional network, which in turn influences the degradability of the thermoset and decreases the shrinkage in the last steps of the curing. In the present study, we followed the individual reactions by means of FTIR-ATR.

**Figure 1** shows the FTIR spectra of the mixture DGEBA/ $\gamma$ -VL 2:1 (mol/mol) with 1 phr of  $\text{Yb}(\text{OTf})_3$  obtained before and after curing (150 min) and at intermediate time of 7.5 min at 160 °C. During the curing process there are changes mainly in three typical bands:

1. The carbonyl stretching band of  $\gamma$ -VL at 1775  $\text{cm}^{-1}$ , which decreases because  $\gamma$ -VL reacts with the epoxide groups of DGEBA to form SOE groups and at the end of the curing slightly increases again.



**Scheme 1**

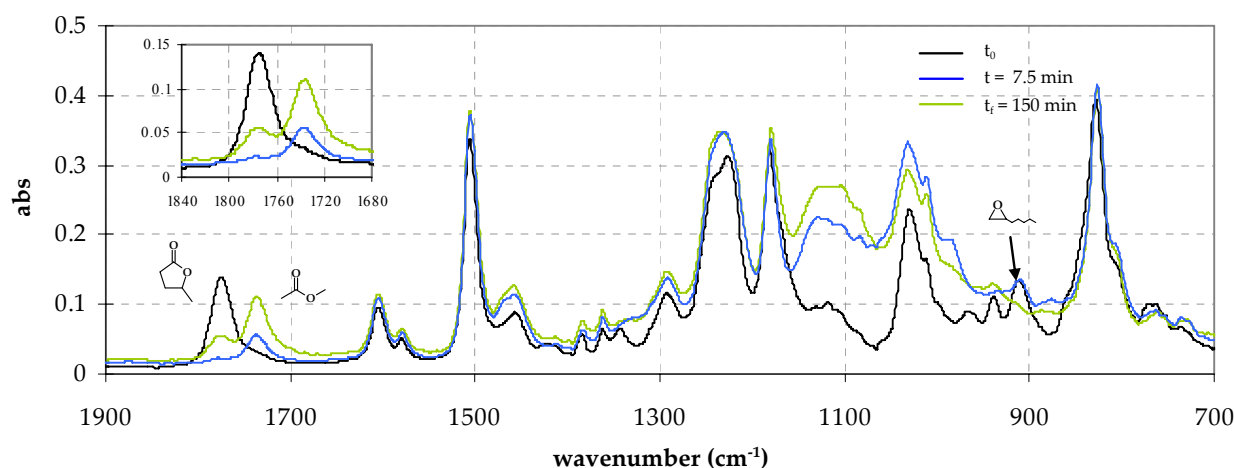


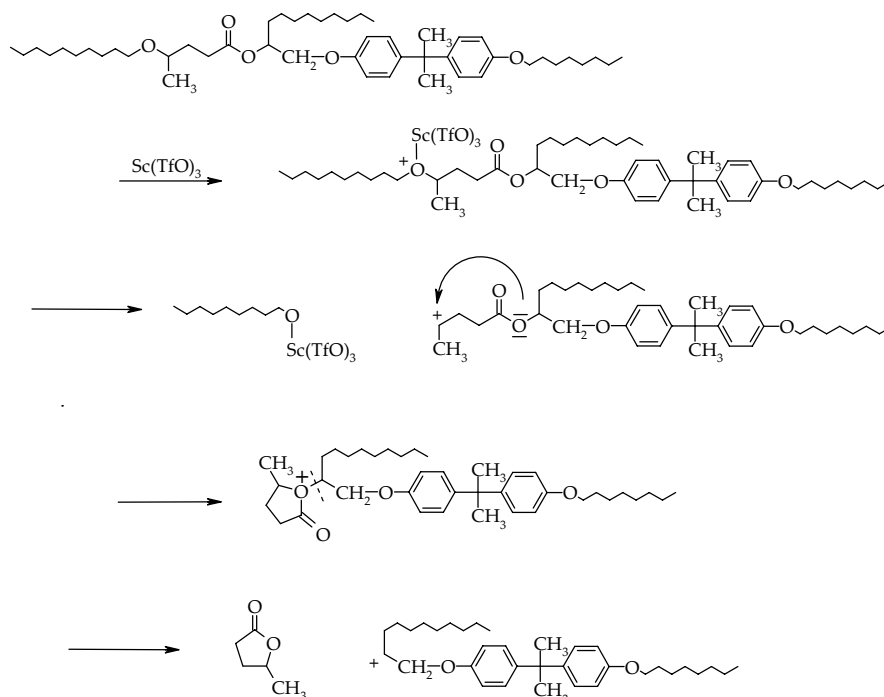
**Figure 1.** FTIR-ATR spectra taken at different times of curing of a mixture of DGEBA/ $\gamma$ -VL in a molar ratio of 2:1 with 1 phr of Yb(OTf)<sub>3</sub> at 160 °C.

2. The peak at 1737 cm<sup>-1</sup> is attributable to the linear aliphatic ester, increases steadily and confirms that the ring-opening polymerization of SOE occurs, by homo- or copolymerization with epoxide.

3. The band at 910 cm<sup>-1</sup> associated with the oxirane ring disappears indicating that the epoxide completely polymerizes.

The changes in the carbonylic band at 1775 cm<sup>-1</sup> indicates that  $\gamma$ -VL firstly completely reacts to form the SOE group and then the lactone is newly formed. An explanation to this fact could be the reversion of SOE groups formed to the lactone and epoxide, that is, the reaction (a) in **Scheme 1** must be reversible. In this way, the epoxide absorption should increase in a similar proportion than lactone band, but the homopolymerization of epoxide can reduce the proportion of free epoxide in the sample as it is formed. The reversibility in the formation of SOE was previously reported by Booth.<sup>17</sup> Another possibility could be a depolymerization process, such as is represented in **Scheme 2**, which forms  $\gamma$ -VL and diminishes the

proportion of linear ester groups. This diminution is not observable in our spectra, but it could be explained because at the same time the polymerization of SOE occurs, which could increase the linear ester carbonylic band in a similar proportion. When we used lanthanum triflate the behaviour is more or less the same. However, when we used scandium triflate some differences were observed (see **Figure 2**). Initially, the bands at 1775 and 910 cm<sup>-1</sup> diminished during the curing time but the former does not disappear completely and at longer reaction times it slightly raises again. In this case the band of linear ester at 1737 cm<sup>-1</sup> initially increases, indicating that SOE polymerizes until reaching a maximum and then newly decreases. This fact confirms that the depolymerization process depicted in **Scheme 2** occurs. Moreover, the reversion of SOE also coexists because of at 70 min both the bands at 1775 and 1737 cm<sup>-1</sup> increase. In fact, the reversion process should be more important for scandium than for the other initiators because there is always free lactone in the reaction mixture.



Scheme 2

We proposed in **Scheme 2** that the coordination of the scandium salt to an ether group favors the rupture of the polymeric chain with the formation of a cation, which is stabilized by the presence of the methyl group. The rupture of ether groups catalyzed by Lewis acids such as  $\text{BF}_3$ ,  $\text{BBr}_3$  or  $\text{AlCl}_3$  is well documented in the literature.<sup>18,19</sup>

To confirm the proposed mechanism we studied by FTIR the copolymerization of DGEBA/ $\gamma$ -MBL 2:1 (mol/mol) mixture initiated by 1 phr of  $\text{Sc}(\text{TfO})_3$ , because this lactone should not lead to a secondary cation but to a primary one, which is less favoured. As can be seen in the spectra of **Figure 3**, no decrease in the carbonylic band of the linear ester occurs indicating that no depolymerization takes place. However, the absorption band at  $1775\text{ cm}^{-1}$  does not disappear completely and this absorption increases after more or less 10 min of curing con-

firming the reversibility of the reaction (a) in **Scheme 1**.

In previous papers,<sup>8,14</sup> we reported the copolymerization of DGEBA/ $\gamma$ -butyrolactone mixtures and we saw the complete disappearance of the lactone, which does not appear again at the end of the curing. Thus, it seems that the presence of substituents makes difficult the SOE formation and also its polymerization. In this way, the reversion of SOE to the initial products becomes more important. The hindrance caused in the polymerization of spiroorthocarbonates<sup>20</sup> by the substituents was previously reported, but no references of it could be found in spiroorthocarbonate.

**Figure 4** shows the evolution of epoxide,  $\gamma$ -VL, and linear ester against time for the DGEBA/ $\gamma$ -VL 2:1 (mol/mol) formulations initiated by 1 phr of the different rare earth triflates calculated

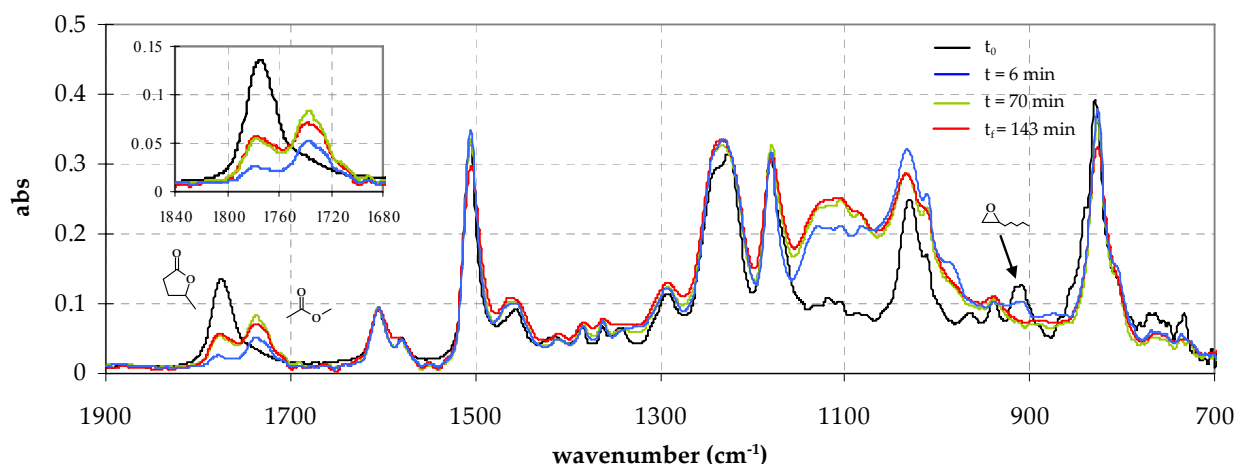


**Figure 2.** FTIR-ATR spectra taken at different times of curing of a mixture of DGEBA/ $\gamma$ -VL in a molar ratio of 2:1 with 1 phr of Sc(OTf)<sub>3</sub> at 160 °C.

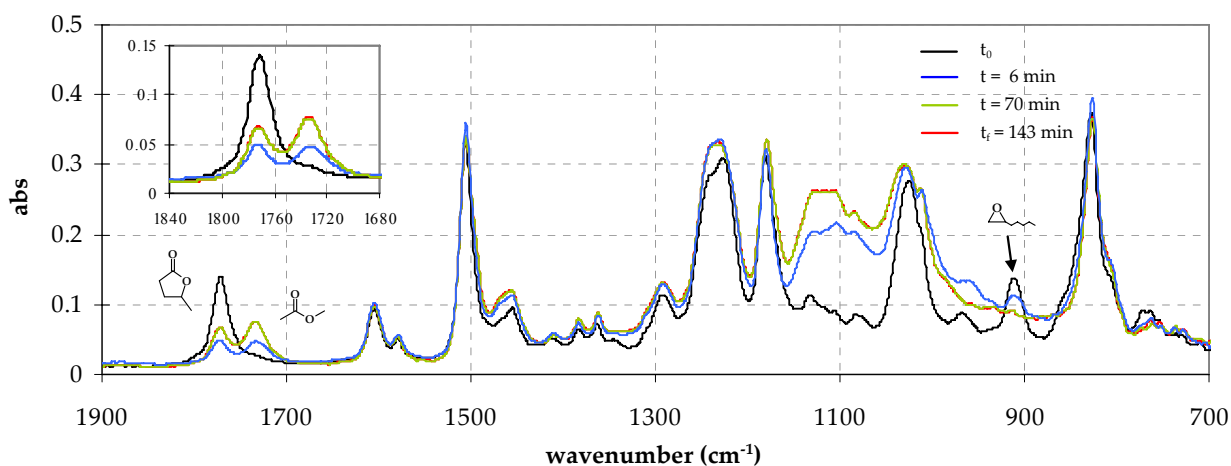


**Figure 3.** FTIR-ATR spectra taken at different times of curing of a mixture of DGEBA/ $\gamma$ -MBL in a molar ratio of 2:1 with 1 phr of Sc(OTf)<sub>3</sub> at 160 °C.

from the FTIR spectra. The conversions have been normalized to the maximum reached for each functional group regardless of the initiator used. Thus, scandium leads to the maximum proportion of carbonyl linear ester band, although not all the lactone has reacted to form the SOE group. If we look at the epoxy conversion we can see the complete incorporation of epoxy to the network. Moreover, the rate of incorporation follows the Lewis acidity trend. So, scandium triflate leads to the fastest reaction and lanthanum salt to the slowest. However, the evolution of  $\gamma$ -VL presents some differences. Although

using the three initiators the reaction is fast, especially with scandium and ytterbium triflates, there is no total reaction of lactone with epoxide when we used the scandium salt. Moreover, all the initiators tested caused, after some time of curing, that the  $\gamma$ -VL appears again. The formation of lactone goes faster and the proportion of the free lactone remaining entrapped in the network follows the trend Sc > Yb > La. Kinetics of the reactions can be related to the Lewis acidity of the catalysts. However, there is no direct relation between Lewis acidity and the extension reached in an equilibrium process. The

fact that a higher proportion of lactone is released in the order of  $Sc > Yb > La$  could be related with the Pearson's HSBA theory,<sup>21</sup> which explains that the hardness increases from La to Sc, because of the size. In a previous article,<sup>14</sup> we related the Pearson hardness with the coordination to the epoxide or lactone. The harder the metal is the higher the coordination to the epoxide and there-

fore the higher its homopolymerization. Thus, a higher homopolymerization of epoxide leads to a higher proportion of free lactone, because the reversion equilibrium of SOE is shifted by the consumption of the epoxide. On the contrary, lanthanum salt is the softer acid and it coordinates more effectively with lactone, which reduces the proportion of initiator coordinated to the epoxide and therefore the homopolymerization is reduced.

Finally, the plot of the formation of linear ester in the network by homo- and copolymerization of SOE groups against time shows the concordance, from the kinetic point of view, with the Lewis acidity of the initiator. However, in the curing of the sample with scandium triflate, although at short curing time the proportion of the linear ester reaches the maximum value, we can observe a decrease after 80 min at 160 °C, related to the depolymerization mechanism depicted in **Scheme 2**. Thus, at the final of the process, the maximum incorporation of linear ester in the material is achieved with the ytterbium salt as initiator and the lowest with the scandium.

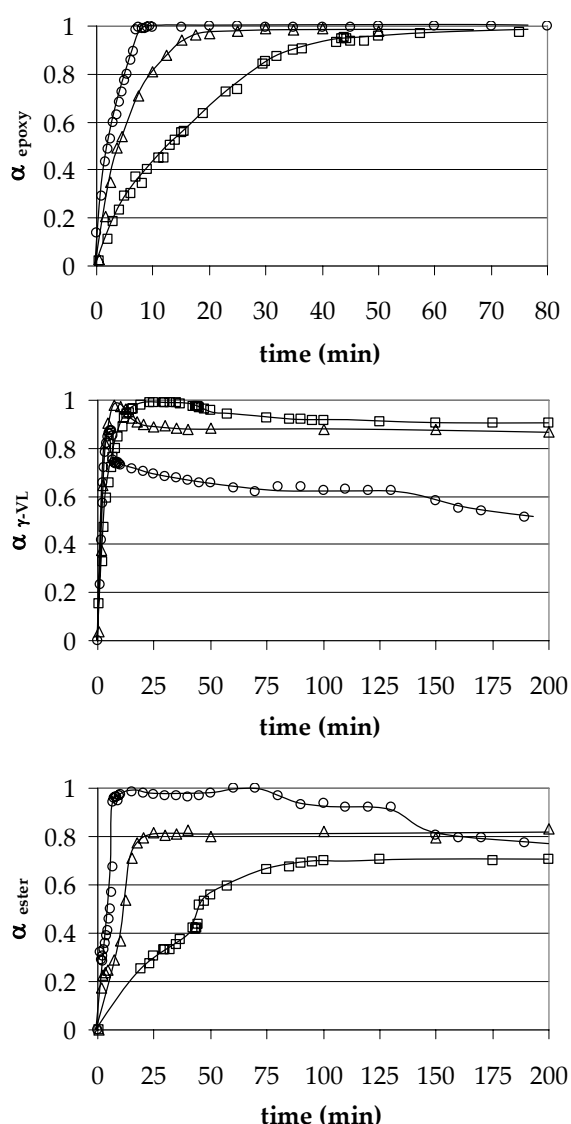


**Figure 4.** Epoxy,  $\gamma$ -VL and linear ester conversion degrees vs. time for the DGEBA/ $\gamma$ -VL 2:1 (mol/mol) formulation with the three rare earth triflates (La  $\square$ , Yb  $\Delta$  and Sc  $\circ$ ) during curing at 160 °C determined by FTIR-ATR.

The  $\alpha_{\text{epoxy}} - \alpha_{\gamma\text{-VL}}$  curves are represented in **Figure 5** for the same formulation and the three initiators tested. Because of the formation of SOE groups that takes place from 1 mol of DGEBA and 2 mols of lactone, and the ratio of the sample is DGEBA/ $\gamma$ -VL 2:1 (mol/mol) a consumption of a 20 % of lactone should lead to a conversion of a 5 % of the initial epoxide. From the figure we can observe that with all the initiators the  $\alpha_{\text{epoxy}}$  is higher than 0.05. Thus, the homopolymerization of

epoxide occurs since the beginning of the reaction. We can clearly see that this homopolymerization is more important when the harder is the metal triflate. In contrast, the incorporation of the lactone is higher when the softer is the initiator. With all the initiators tested we can see a partial recovery of the initial lactone, by reversion in the SOE formation or by the depolymerization process. This recovery is much higher for scandium, which leads to the appearance of a 50 % of the initial lactone. Thus, scandium triflate should produce free  $\gamma$ -VL by both the reversion of SOE and the depolymerization mechanisms, which takes place in a little proportion, such as is observed in **Figure 4**.

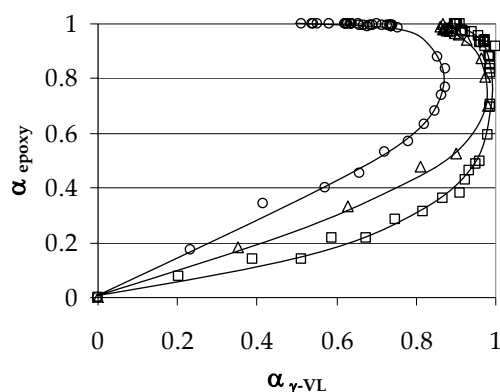


**Figure 5.** Conversion of epoxy vs. conversion of  $\gamma$ -VL for the curing at 160 °C of a mixture DGEBA/ $\gamma$ -VL 2:1 (mol/mol) formulation with 1 phr of the different rare earth triflates tested (La  $\square$ , Yb  $\triangle$  and Sc  $\circ$ ).

**Figure 6** represents the evolution of the epoxide,  $\gamma$ -MBL, and linear esters against time for the DGEBA/ $\gamma$ -MBL 2:1 (mol/mol) formulation initiated by 1 phr of the different rare earth triflates during 100 min. Longer reaction times did not lead to any difference. Scandium and ytterbium triflates does not lead to differences in the kinetics of epoxy

consumption but the lanthanum salt leads to a slower incorporation. If we look at the  $\alpha_{\gamma\text{-MBL}}$  representation, we can see that both the ytterbium and the scandium salt react faster but a notable reversion of SOE occurs, more important for the scandium triflate. However, in the sample initiated by lanthanum triflate the reaction of  $\gamma$ -MBL goes more slowly, as epoxide does, but the reversion is very slight. If we compare the proportions of linear ester and free lactone, we can deduce that a notable proportion of lactone remains as unreacted SOE groups. It should be said that the linear ester conversion has been normalized to the maximum reached. The different kinetic behaviour in the chemical incorporation of  $\gamma$ -VL and  $\gamma$ -MBL to the material could be related to the steric hindrance caused by the methyl group neighbouring to the spiranic carbon in the  $\gamma$ -MBL. Thus the biggest cation, the lanthanum, experiments the higher steric hindrance which retards the formation of SOE. However, when it forms polymerizes or copolymerizes with epoxide slowly without depolymerization, as we can see in the plot of linear ester formation against time. In the same plot, we can see that scandium triflate leads to the faster formation of linear ester and no diminution occurs. Although the proportion of SOE formation is higher for the lanthanum triflate, the proportion of linear ester groups is the lowest, which could be explained by the difficulty in the homo or copolymerization of SOE groups, which should remain unreacted in the material. The lowest reactivity of SOE groups when initiated by lanthanum triflate could also be explained by the steric hindrance of the methyl group

which difficult the coordination of the metal to the oxygen.

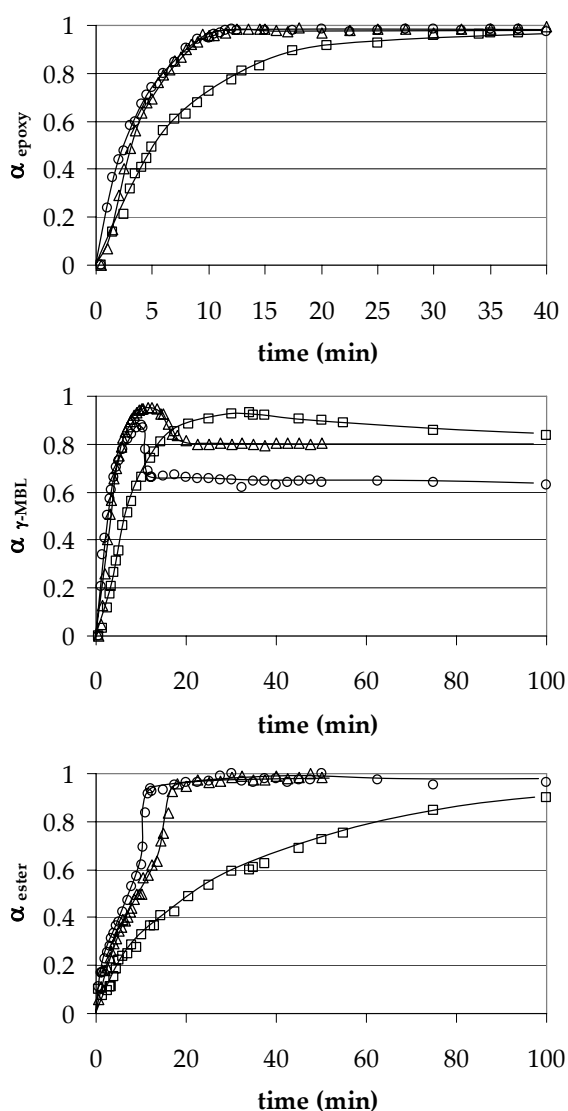


**Figure 6.** Epoxy,  $\gamma$ -MBL and linear ester conversion degrees vs. time for the DGEBA/ $\gamma$ -MBL 2:1 (mol/mol) formulation with the three rare earth triflates (La  $\square$ , Yb  $\Delta$  and Sc  $\circ$ ) during curing at 160 °C determined by FTIR-ATR.

**Figure 7** shows the representation of  $\alpha_{\text{epoxy}} - \alpha_{\gamma\text{-MBL}}$  for the same formulation and the three initiators tested. If we compare **Figures 5** and **7**, the biggest difference is the evolution of the samples initiated by lanthanum triflate. Thus, whereas in samples with  $\gamma$ -VL the

disappearance of epoxide follows the Pearson's hardness order, in the samples with  $\gamma$ -MBL lanthanum triflate leads to a much higher homopolymerization of epoxide in front of the other initiators. This fact could be related to the difficulty in the coordination to the lactone, which favours the homopolymerization of epoxide. **Figure 7** clearly shows the reversion of SOE, which produces  $\gamma$ -MBL, which is higher for the scandium salt, reaching a value of about 35 % of reversion, lower than in case of  $\gamma$ -VL for the same initiator. It should be taken into account that  $\gamma$ -VL is produced by both reversion and depolymerization processes, whereas  $\gamma$ -MBL is produced only by reversion of the SOE to the initial products. The presence of methyl groups in the  $\gamma$ -MBL makes it difficult for the formation of SOE, because any initiator leads to the complete disappearance of the lactone during the curing.

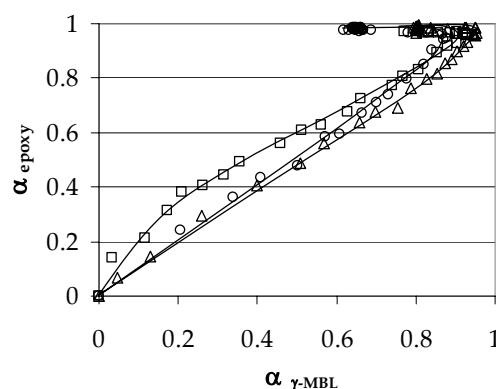


**Figure 7.** Conversion of epoxide vs. conversion of  $\gamma$ -MBL for the curing at 160 °C of a mixture DGEBA/ $\gamma$ -MBL 2:1 (mol/mol) formulation with 1 phr of the different rare earth triflates tested (La  $\square$ , Yb  $\Delta$  and Sc  $\circ$ ).

If we compare the reaction of both DGEBA/lactone mixtures using ytterbium triflate as initiator (**Figure 8**) we can see that in the epoxide conversions

there are not big differences, but the reversion of SOE takes place at lower rate but with a higher extension for  $\gamma$ -MBL and this lactone is which produces a lower incorporation of linear ester in the final material. The fact that the reversion seems to be higher for  $\gamma$ -MBL with the ytterbium salt, on the contrary that we saw for the scandium initiator, is a consequence of the depolymerization process, which only occurs with  $\text{Sc}(\text{OTf})_3$  in  $\gamma$ -VL mixtures. It should be mentioned that the incorporation of lactone as linear ester for  $\gamma$ -MBL is much lower than with  $\gamma$ -VL, however, there is no as big difference in the reversion of both lactones. The explanation to this fact seems to indicate that a higher proportion of  $\gamma$ -MBL remains in the material as unreacted SOE, because of methyl groups hinder its polymerization.

Finally, we considered the influence of the proportion of initiator in the incorporation of  $\gamma$ -VL to the material and we selected ytterbium triflate, because of the better results achieved in the incorporation of linear ester to the polymeric network. **Figure 9** represents the evolution of all the reactive groups for proportions of 0.5, 1, and 3 phr of this initiator. As we can see, the highest the proportion of the ytterbium salt the faster the reactions are, as expected. We can see bigger differences in the reactivity of the epoxide than in the reactivity of the  $\gamma$ -VL, which can be attributed to the hard character of the ytterbium salt, which preferentially favours the epoxide reactions. It can be also observed, that the highest the proportion of initiator the more important the reversion becomes. However, the most significant fact can be

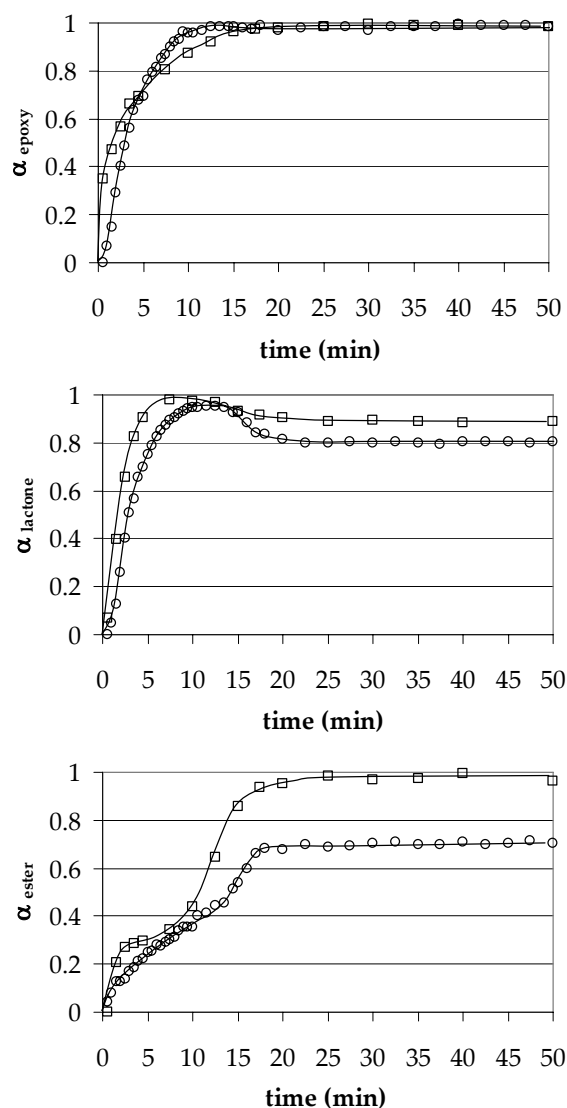


**Figure 8.** Epoxy,  $\gamma$ -lactone and linear ester conversion degrees vs. time for samples DGEBA/ $\gamma$ -VL ( $\square$ ) and DGEBA/ $\gamma$ -MBL ( $\circ$ ) 2:1 (mol/mol) formulation with 1 phr of  $\text{Yb}(\text{OTf})_3$  during curing at 160 °C determined by FTIR-ATR.

observed in the evolution of linear ester groups, because at proportions of 3 phr a depolymerization process is clearly detected. Moreover, the proportion of ester linkages in the polymeric chain is much lower when the proportion of the initiator is reduced until 0.5 phr, which can indicate that some proportion of SOE remains unreacted in the material. The decrease in the proportion of linear ester groups in the material when 3 phr of

$\text{Yb}(\text{OTf})_3$  were added is in accordance to the mechanism of depolymerization depicted in **Scheme 2** in which a higher proportion of Lewis acid or a higher acidity of the rare earth triflate leads to a higher extension of the breakage of ether groups and to the subsequent formation of free lactone. From these results we can conclude that 1 phr of ytterbium triflate is the most adequate proportion to reach a higher modification of DGEBA with  $\gamma$ -VL.

**Table 1** collects the relative proportions of linear ester groups in the final crosslinked material. The absorptions are referred to the phenyl absorptions band of the DGEBA at  $1605\text{ cm}^{-1}$ , which should not react during curing. As we can see, the maximum ester modification is achieved for DGEBA/ $\gamma$ -VL mixtures, when 1 phr of ytterbium triflate was used as initiator. The scandium salt leads to the maximum value of linear ester during curing, but at the end decreases because the depolymerization process is produced. In the same table we have also collected the proportion of free lactone, which remains entrapped in the materials. As we can see, the highest proportion of free lactone in the thermoset is achieved when we used scandium triflate as initiator.

## Conclusions

The copolymerization of DGEBA with  $\gamma$ -VL or  $\gamma$ -MBL in the presence of rare earth triflates led to the incorporation of ester groups in the network. In addition to the expected reactions: formation of intermediate SOE, its homopolymerization, its copolymerization with epoxide

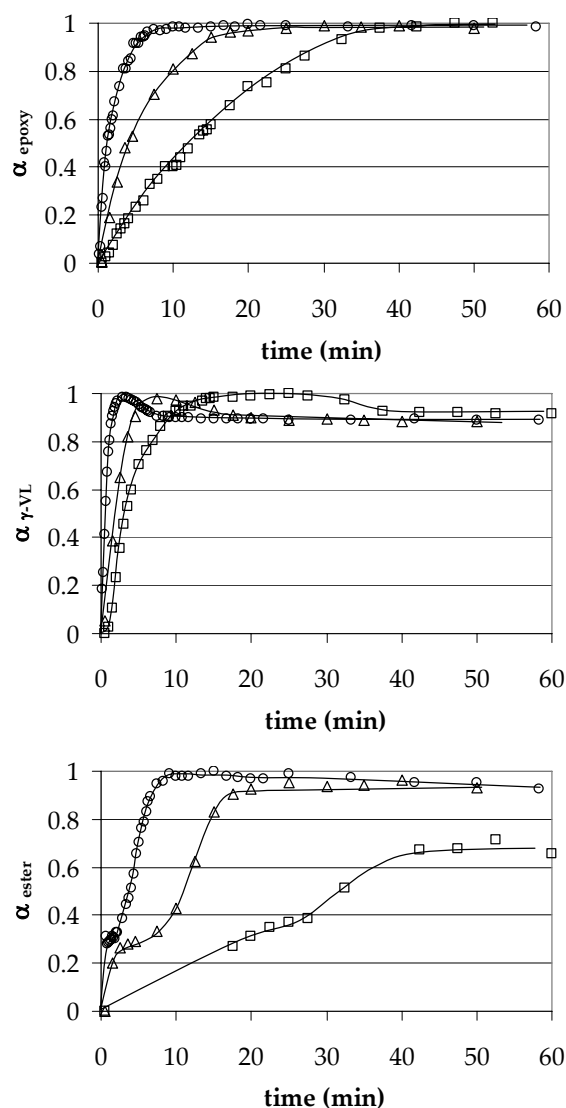


**Figure 9.** Epoxy,  $\gamma$ -VL and linear ester conversion degrees vs. time for the DGEBA/ $\gamma$ -VL 2:1 (mol/mol) formulation initiated by 0.5 ( $\square$ ), 1 ( $\Delta$ ) and 3 ( $\circ$ ) phr of  $\text{Yb}(\text{OTf})_3$  during curing at  $160\text{ }^\circ\text{C}$  determined by FTIR-ATR.

and polyetherification, the reversion of SOE has also been observed, which leads to different proportions of free lactone which remains entrapped in the thermoset.

When we used 1 phr of scandium triflate or 3 phr of ytterbium triflate as initiator a depolymerization process is observed, but only with  $\gamma$ -valerolactone. This fact was explained by a mechanism

**Table 1.** Composition of the initial curing mixture and relative quantifications by FTIR of linear ester and lacton groups after curing at 160 °C in the ATR

Lactone	Initiator	Proportion initiator (phr)	Abs <sub>ester</sub> /Abs <sub>1605</sub> <sup>a</sup>	Free lactone (%) <sup>b</sup>
γ-VL	La(OTf) <sub>3</sub>	1	1.867	10
		0.5	1.663	10
	Yb(OTf) <sub>3</sub> →	1	2.207	13
		3 →	2.381 <sup>c</sup>	14
	Sc(OTf) <sub>3</sub>	1 →	1.811 <sup>d</sup>	14
				2.657 <sup>c</sup>
γ-MBL	La(OTf) <sub>3</sub>	1	1.495	16
	Yb(OTf) <sub>3</sub>	1	1.580	20
	Sc(OTf) <sub>3</sub>	1	1.749	37

<sup>a</sup> absorbance of ester band in reference to the absorbance of the band of phenyl group

<sup>b</sup> in reference to the initial lactone in the mixture

<sup>c</sup> maximum of ester absorbance reached during curing

<sup>d</sup> final ester absorbance reached after complete curing

initiated by the coordination of the Lewis acid to ethereal oxygen, which broke the polymeric chain and formed a stabilized secondary cation. This mechanism also explains the formation of free lactone. The depolymerization process was related to the highest Lewis acidity of the catalyst.

The most adequate conditions to reach a higher chemical modification of DGEBA with γ-VL were the use of 1 phr of ytterbium triflate.

The homopolymerization of epoxide was favoured for DGEBA/γ-VL mixtures in the order of Sc > Yb > La, which is in accordance to the Pearson's hardness, or when a higher proportions of Yb(OTf)<sub>3</sub> was used.

In the curing of DGEBA/γ-MBL mixtures the presence of the methyl group neighbour to the spiranic carbon in the intermediate SOE sterically made

difficult both the formation of SOE and its polymerization and therefore the reversion to the initial products became higher. Homopolymerization of epoxides was favoured when we used the lanthanum cation, which has the biggest size. γ-VL was chemically incorporated into the network in much proportion than γ-MBL, because of the steric hindrance produced by the α-methyl substituent.

#### Acknowledgements

The authors from the Universitat Politècnica de Catalunya would like to thank CICYT and FEDER (MAT2004-04165-C02-02) for their financial support. The authors from the Universitat Rovira i Virgili would like to thank the CICYT (Comisión Interministerial de Ciencia y Tecnología), FEDER (Fondo Europeo de Desarrollo Regional) (MAT2005-01806).

## References

- [1] Expanding Monomers: Synthesis, Characterization and Applications; Sadhir, RK.; Luck, MR., Eds; CRC Press: Boca Raton, FL, 1992.
- [2] Eom, Y.; Boogh, L.; Michaud, V.; Sunderland, P.; Manson, JA. Polym Eng Sci 2001, 41, 492-503.
- [3] Bailey, WJ. J Elastoplast 1973, 5, 142-152.
- [4] Bailey, WJ.; Sun, RLJ.; Katsuki, T.; Endo, T.; Iwama, H.; Tsushima, R.; Saigou, K.; Bittrito, M.; Ring-opening polymerization with expansion in volume, in Ring Opening Polymerization, ACS Symp. Ser. No. 59 Saegusa, T.; Goethals, E., Eds; American Chemical Society, Washington, DC, 1977, 55.
- [5] Bodenbenner, K. Justus Liebigs Ann Chem 1956, 625, 183-191.
- [6] Fedtke, M.; Haufe, J.; Kahlert, E.; Müller, G. Angew Makromol Chem 1998, 255, 53-59.
- [7] Takata, T.; Endo, T. Prog Polym Sci 1993, 18, 839-870.
- [8] Mas, C.; Ramis, X.; Salla, JM. ; Mantecón, A.; Serra, A. J Polym Sci Part A: Polym Chem 2003, 41, 2794-2808.
- [9] González, S.; Fernández-Francos, X.; Salla JM.; Serra A.; Mantecón A.; Ramis X. J Polym Sci Part A: Polym Chem 2007, 45, 1968-1979.
- [10] Chen, JS.; Ober, CK.; Poliks, MD. Polymer 2002, 43, 131-139.
- [11] Chen, JS.; Ober, C.; Poliks, MD.; Zhang, Y.; Wiesner, U.; Cohen, C. Polymer 2004, 45, 1939-1950.
- [12] Wang, L.; Lee, H.; Wong, CP. J Polym Sci Part A: Polym Chem 2000, 38, 3771-3782.
- [13] Wang, Z.; Xie, M.; Zhao, Y.; Yu Y.; Fang, S. Polymer 2003, 444, 923-929.
- [14] Mas, C.; Mantecón, A.; Serra, A.; Ramis, X.; Salla, JM. J Polym Sci Part A: Polym Chem 2004, 42, 3782-3791.
- [15] Kobayashi, S. Eur J Org Chem 1999, 15-27.
- [16] Kobayashi, S.; Sugiura, M.; Kitagawa, H.; Lam, WWL. Chem Rev 2002, 102, 2227-2302.
- [17] Booth, HJ. in Expanding Monomers: Synthesis, Characterization and Applications; Sadhir, RK.; Luck, MR., Eds.; CRC Press: Boca Raton, FL, 1992, p. 208.
- [18] Guindon, Y.; Yoakim, C.; Morton, HE. Tetrahedron Lett 1983, 24, 2969-2972.
- [19] Niwa, H.; Hida, T.; Yamada, K. Tetrahedron Lett 1981, 22, 4239-4240.
- [20] Fujinami, T.; Tsuji, H.; Sakai, S. Polym J 1977, 7, 553-560.
- [21] Pearson, RG. J Am Chem Soc 1963, 85, 3533-3539.

2.3  
A STUDY OF THE DEGRADATION OF ESTER-  
MODIFIED EPOXY RESINS OBTAINED BY CATIONIC  
COPOLYMERIZATION OF DGEBA WITH  $\gamma$ -LACTONES  
INITIATED BY RARE EARTH TRIFLATE

---

*Mercè Arasa, Xavier Ramis, Josep Maria Salla, Ana Mantecón, Àngels Serra; Polymer Degradation and Stability 92 (2007) 2214-2222*

UNIVERSITAT ROVIRA I VIRGILI  
NOUS TERMOESTABLES EPOXÍDICS MODIFICATS AMB GAMMA-LACTONES I BIS-GAMMA-LACTONES CONDENSADAS  
M<sup>a</sup> Mercè Arasa Bertomeu  
ISBN:978-84-692-4157-8/DL:T-1171-2009



# A STUDY OF THE DEGRADATION OF ESTER-MODIFIED EPOXY RESINS OBTAINED BY CATIONIC COPOLYMERIZATION OF DGEBA WITH $\gamma$ -LACTONES INITIATED BY RARE EARTH TRIFLATES

Mercè Arasa,<sup>1</sup> Xavier Ramis,<sup>2</sup> Josep Maria Salla,<sup>2</sup> Ana Mantecón,<sup>1</sup> Àngels Serra<sup>1</sup>

<sup>1</sup>Dpt. Q. Analítica i Q. Orgànica, URV. C/Marcel·lí Domingo s/n, 43007 Tarragona, Spain

<sup>2</sup> Lab. Termodinàmica, ETSEIB. UPC, Av. Diagonal 647, 08028 Barcelona, Spain

## Abstract

The thermal degradation of new thermosetting materials prepared by cationic copolymerization of mixtures with different proportions of diglycidylether of bisphenol A (DGEBA) with  $\gamma$ -valerolactone ( $\gamma$ -VL) or  $\alpha$ -methyl- $\gamma$ -butyrolactone ( $\gamma$ -MBL) initiated by scandium, ytterbium or lanthanum triflate and a complex of boron trifluoride was investigated. To study the thermal degradation thermogravimetry (TGA) was used. The materials are more degradable than conventional epoxy resins due to the presence of ester groups in the polymeric chain, which are broken at the beginning of degradation. The degradability increased with the proportion of linear ester groups and the Lewis acidity of the initiator used in the polymerization and when the proportion of lactone in the initial mixture increased. The kinetic parameters of the degradation were calculated from TGA data by applying isoconversional procedures.

*Keywords:* Epoxy resins, degradation, thermoset, cationic polymerization, kinetics.

## Introduction

Rare earth triflates have been demonstrated to be excellent Lewis acids stable in oxygen and humid environments.<sup>1,2</sup> Until now, lanthanide triflates have been used by us to obtain thermosets from epoxy resins alone<sup>3</sup> or from their mixtures with lactones,<sup>4</sup> showing satisfactory results. Because scandium triflate is the most acidic compound of the series of rare earth triflates and is

commercially available, in a previous paper we reported its ability to copolymerize DGEBA with  $\gamma$ -valerolactone ( $\gamma$ -VL) or  $\alpha$ -methyl- $\gamma$ -butyrolactone ( $\gamma$ -MBL) in addition to ytterbium and lanthanum triflates.<sup>5</sup>

The interest of this kind of copolymerizations lies in the introduction of ester linkages into network structures, which leads to thermosetting materials



with improved degradability. These materials can be used as coatings, underfills or encapsulants in microelectronic applications and therefore, the increase in the thermal degradability is important to recover the electronic components.

Some research groups introduce thermally labile secondary and tertiary ester groups into the network to induce reworkability to the thermosets.<sup>6-10</sup> However, most of this work is based on cycloaliphatic structures which contain ester groups, which show low versatility.

Our strategy to introduce ester groups into the epoxy network is based on a copolymerization procedure. Epoxides react with lactones in cationic conditions to form spiroorthoester compounds (SOEs), which have been described as expandable monomers. They can homopolymerize or copolymerize with epoxides to yield poly(ether-ester) chains.<sup>11</sup> The polyetherification of epoxides can also occur. Because  $\gamma$ -lactones cannot homopolymerize for thermodynamic reasons, the incorporation of ester groups in the epoxy network is due only to the formation and polymerization of SOE groups, which in addition reduces the shrinkage after gelation.<sup>4</sup> The reduction of the shrinkage after gelation is a very important achievement because it leads to a reduction of the internal stresses in the material and increases the adhesion to the substrate, which is important for coatings' applications.

In previous studies,<sup>5</sup> we proved that the different Lewis acidity and the different Pearson's hardness of the rare

earth cations led to differences in the curing rate and in the chemical structure of the final thermosets. The evolution of the reactive groups involved in the curing was followed by FTIR/ATR. This technique allowed us to observe that the use of 1 phr of scandium triflate or 3 phr of the ytterbium salt as initiators produced a partial depolymerization, leading to the reappearance of free  $\gamma$ -VL, which remained entrapped in the three-dimensional structure. Moreover, all the rare earth triflates tested led to a partial reversion of the SOE group to the initial  $\gamma$ -lactone and epoxide, which polymerizes to form polyether structures.<sup>5</sup>

We also reported that the copolymerization of DGEBA and 6,6-dimethyl(4,8-dioxaspiro[2.5]octane-5,7-dione) (MCP)<sup>12</sup> in the presence of ytterbium and lanthanum triflates increased the thermal degradability of epoxy resins through the cleavage of ester groups introduced into the polymer chain. The higher the proportion of MCP in the reactive mixture the more degradable the materials were. Moreover, lanthanide triflates led to more degradable materials than the conventional  $\text{BF}_3\cdot\text{MEA}$  cationic initiator, even for pure DGEBA homopolymer, which indicates that lanthanide triflates play an important role in the degradation mechanism.

With these proceedings, in the present study we aimed to know the influence of the Lewis acidity of the rare earth triflates and the proportion of ester groups in the modified network on the degradability of the thermosets obtained and compare them with those produced with  $\text{BF}_3\cdot\text{MEA}$  as initiator.



In the present study, thermogravimetric analysis was used to assess the thermal stability of the DGEBA/lactone systems studied. The kinetic of thermal degradation was determined using non-isothermal experiments. A kinetic analysis was performed with an integral isoconversional procedure (model free), and the kinetic model was chosen by the Coats-Redfern method as the model with an activation energy similar to that obtained isoconversionally and through the integral and differential master plots method.

## Experimental Part

### Materials

Diglycidylether of bisphenol A (DGEBA) EPIKOTE RESIN 827 from Shell Chemicals (Epoxy Equiv. = 182.08 g/eq) was used as received.

$\gamma$ -Valerolactone ( $\gamma$ -VL) and  $\alpha$ -methyl- $\gamma$ -butyrolactone ( $\gamma$ -MBL) (Aldrich) were used as received.

Lanthanum (III), ytterbium (III) and scandium (III) trifluoromethanesulfonates and borontrifluoride monoethylamine ( $\text{BF}_3 \cdot \text{MEA}$ ) (Aldrich) were used without purification.

### Preparation of the materials

The samples were prepared as previously described.<sup>5</sup>

The mixtures were cross-linked by pouring into a silanized glass mould and then cured in an oven at 150 °C for 1 h, followed by a post curing at 160 °C for 5 h. For lanthanum triflate and boron trifluoride an additional post-curing for

2 h at 180 °C was made. The samples were then allowed to cool at room temperature. It was confirmed by DSC that they were completely cured.

### Characterization and measurements

Calorimetric studies were carried out on a Mettler DSC-821e thermal analyzer in covered Al pans under  $\text{N}_2$  at 10 °C/min to confirm the complete curing of the samples. The calorimeter was calibrated using an indium standard (heat flow calibration) and an indium-lead-zinc standard (temperature calibration). The samples weighed approximately 7 mg.

Thermogravimetric analyses (TGAs) were carried out with a Mettler TGA/SDTA 851e thermobalance. Cured samples with an approximate mass of 7 mg were degraded between 30 and 600 °C at a heating rate of 10 °C/min in  $\text{N}_2$  (100 ml/min) measured at normal conditions. Non-isothermal thermogravimetric tests were carried out at rates of 5, 10, 20 and 40 °C/min to evaluate the kinetic parameters. Isothermal studies at selected temperatures were also carried out.

### Kinetic analysis

Integral non-isothermal kinetic analysis was used to determine the kinetic triplet (pre-exponential factor  $A$ , activation energy  $E$  and integral function of degree of conversion  $g(\alpha)$ ).

The degree of conversion as the mass loss is defined as:

$$\alpha = \frac{m_0 - m}{m_0 - m_\infty} \quad (1)$$



where  $m$  is the mass corresponding to a temperature  $T$ ,  $m_0$  is the initial mass and  $m_\infty$  is the mass of the substance at the end of the experiment.

In non-isothermal kinetics of heterogeneous condensed phase reactions, it is usually accepted that the reaction rate is given by:<sup>13</sup>

$$\frac{d\alpha}{dt} = \beta \frac{d\alpha}{dT} = A \exp\left(-\frac{E}{RT}\right) f(\alpha) \quad (2)$$

where  $\alpha$  is the degree of conversion,  $T$  temperature,  $t$  time,  $f(\alpha)$  the differential conversion function,  $R$  the gas constant,  $\beta = dT/dt$  the linear constant heating rate, and  $A$  and  $E$  the pre-exponential factor and the activation energy given by the Arrhenius equation.

By integrating eq. (2), the integral rate equation, so-called temperature integral, may be expressed as:

$$\begin{aligned} g(\alpha) &= \int_0^\alpha \frac{d\alpha}{f(\alpha)} = \frac{A}{\beta} \int_0^T e^{-E/RT} dT = \\ &= \frac{AE}{\beta R} \int_x^\infty \frac{e^{-x}}{x^2} dx = \frac{AE}{\beta R} p(x) \quad (3) \end{aligned}$$

where  $g(\alpha)$  is the integral conversion function,  $x = E/RT$  and  $p(x)$  is the exponential integral, which has no analytic solution.<sup>14</sup> However, there are many approximations that make it possible to obtain the kinetic parameters through the linearization of the experimental data.<sup>15-17</sup> There are more complex variations of  $p(x)$ , such as those put forward by Senum and Yang<sup>18</sup> and Agrawal<sup>19</sup> whose approximations of the temperature integral at an interval of  $x$  offer far higher accuracy and lower error.

Isoconversional methodology in non-isothermal experiments assumes that for a given degree of conversion, the reaction mechanism does not depend on the heating rate.

By using the Coats-Redfern<sup>15</sup> approximation to solve eq. (3) and considering that  $2RT/E$  is much lower than 1, the Kissinger-Akahira-Sunose (KAS) equation may be written:<sup>20,21</sup>

$$\ln\left(\frac{\beta}{T^2}\right) = \ln\left[\frac{AR}{g(\alpha)E}\right] - \frac{E}{RT} \quad (4)$$

For each conversion degree, the linear plot of  $\ln(\beta/T^2)$  versus  $T^{-1}$  enables  $E$  and  $\ln[AR/g(\alpha)E]$  to be determined from the slope and the intercept. If the reaction model,  $g(\alpha)$ , is known, the corresponding pre-exponential factor can be calculated for each conversion. The Flynn-Wall-Ozawa integral<sup>17,22</sup> method based on Doyle's approach<sup>16</sup> was not used because it gives similar results to the KAS method.

By reordering eq. (4), we can write the Coats-Redfern equation:<sup>15</sup>

$$\ln\frac{g(\alpha)}{T^2} = \ln\left[\frac{AR}{\beta E}\right] - \frac{E}{RT} \quad (5)$$

For a given kinetic model, the linear representation of  $\ln[g(\alpha)/T^2]$  against  $T^{-1}$  makes it possible to determine  $E$  and  $A$  from the slope and the ordinate at the origin. In this work, we selected the kinetic model that had a good linear correlation in the Coats-Redfern equation and an activation energy similar to that obtained isoconversionally (considered to be the effective  $E$ ).



Using as a reference point at  $\alpha = 0.5$ , the following differential master equation is easily derived from eq. (2):

$$\frac{f(\alpha)}{f(0.5)} = \frac{d\alpha/dt}{(d\alpha/dt)_{0.5}} \frac{\exp(E/RT)}{\exp(E/RT_{0.5})} \quad (6)$$

where  $(d\alpha/dt)_{0.5}$ ,  $T_{0.5}$  and  $f(0.5)$  are, respectively, the reaction rate, the temperature of reaction and the differential conversion function at  $\alpha = 0.5$ .

The left side of eq. (6) is a reduced theoretical curve which is characteristic of each kinetic function. The right side of the equation is associated with the reduced rate and can be obtained from experimental data if the activation energy is known and remains constant throughout the reaction. Comparison of both sides of eq. (6) tells us which kinetic model describes an experimental reaction process.

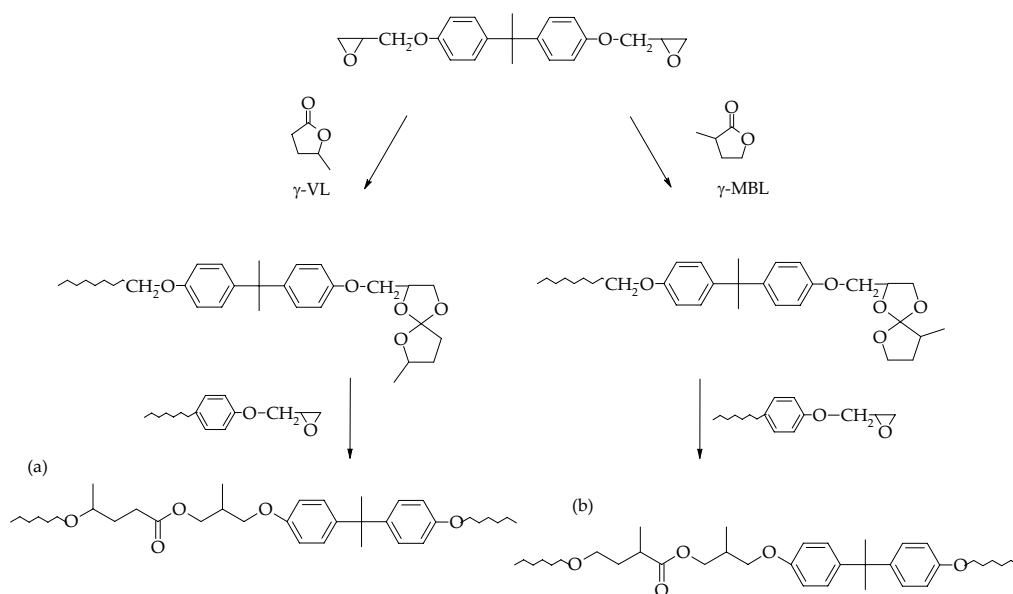
The kinetic model was also chosen by the integral master plot method<sup>23,24</sup> using the fourth rational approximation of

Senum and Yang.<sup>18</sup>

In order to determine the kinetic model, it is necessary to include the conversion function,  $f(\alpha)$ , characteristic of the process studied, in the set of functions analysed. Different kinetic models were studied: diffusion ( $D_1$ ,  $D_2$ ,  $D_3$  and  $D_4$ ), Avrami-Erofeev ( $A_{3/2}$ ,  $A_2$ ,  $A_3$  and  $A_4$ ), power law ( $P_2$ ), phase-boundary-controlled reaction ( $R_2$  and  $R_3$ ), reaction-order  $n$  ( $n = 4, 3, 2, 1.5$  and  $1$  denominated  $F_1$ ) and autocatalytic ( $n + m = 2$  and  $3$  with different values of  $n$  and  $m$ ).<sup>25</sup> Although there is no reason for some of these models to have any physicochemical meaning in the degradation processes, they can still be used to aid description of the DTG curve.

## Results and discussion

The reaction of DGEBA and  $\gamma$ -lactones in cationic conditions leads to the formation of cross-linked poly(ether-ester) structures through the formation of intermediate spiroorthoesters (SOEs).



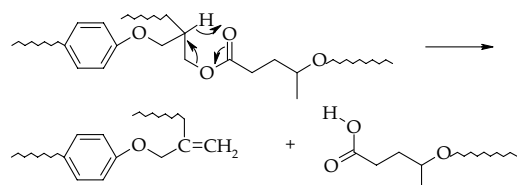
Scheme 1



**Scheme 1** shows the simplified chemical structures of the networks formed by copolymerization of DGEBA with  $\gamma$ -VL and  $\gamma$ -MBL.

In previous work,<sup>5</sup> we determined that the use of 1 phr of ytterbium triflate leads to the highest proportion of ester linkages in the final network. We also detected that some proportion of SOE did not react and that free lactone remained trapped in the network, because of the partial reversion of SOE groups and the partial depolymerization produced when 1 phr of scandium triflate or 3 phr of ytterbium triflate were added as initiator.<sup>5</sup> Previous tests allowed us to conclude that the boron complex led to the lowest ester group content.

Ester groups are thermally cleavable by a  $\beta$ -elimination mechanism,<sup>26,27</sup> which leads to the formation of acid and vinyl ether groups as chain ends such is represented in **Scheme 2** for  $\gamma$ -VL containing materials. Each time that an ester group is cleaved, the local crosslink density decreases and therefore, the higher the proportion of esters is the more degradable character of the modified epoxy resin should be.



**Scheme 2**

**Figure 1** shows the TGA and DTG curves of the materials obtained from DGEBA/ $\gamma$ -VL 2:1 (mol/mol) mixtures

using the corresponding amount of the four initiators tested. As we can see,  $\text{BF}_3\cdot\text{MEA}$  initiated materials lead to a degradation curve at higher temperatures than when we used rare earth triflates, which could be attributed to the lower ester content or to the lower effect of this initiator on the degradation. Moreover, the shape of the DTG curve is sharp and practically unimodal, which seems to indicate that a single degradation mechanism takes place, whereas the other curves are broader and suggest a more complex degradation.

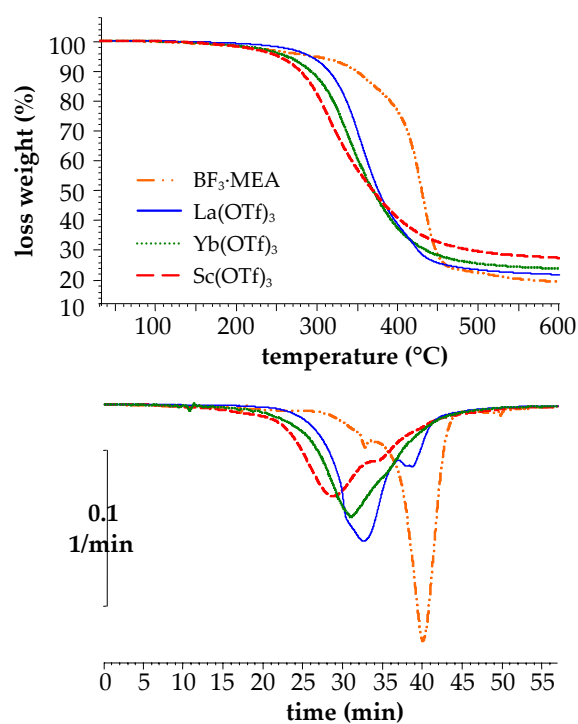


**Figure 1.** Thermogravimetric and DTG curves under  $\text{N}_2$  atmosphere at  $10^\circ\text{C}/\text{min}$  of the materials obtained from DGEBA/ $\gamma$ -VL formulations varying the type of initiator used in the curing.

The degradability of the materials obtained is much higher as the Lewis acidity of the rare earth triflates increases ( $\text{La} < \text{Yb} < \text{Sc}$ ) because these compounds participate in the degradation mechanism, as we demonstrated in a previous



**Table 1.** Thermogravimetric data under N<sub>2</sub> atmosphere of the materials obtained from DGEBA/ $\gamma$ -VL and DGEBA/ $\gamma$ -MBL formulations varying the type of initiator used in the curing

Formulation (mol/mol)	Initiator	mol init./ eq. epoxy	T <sub>5%</sub> <sup>a</sup> (°C)	T <sub>max</sub> <sup>b</sup> (°C)	Char yield <sup>c</sup> (%)
DGEBA/ $\gamma$ -VL 2:1	BF <sub>3</sub> ·MEA	0.018216	286	430	15.1
DGEBA/ $\gamma$ -VL 2:1	La(OTf) <sub>3</sub>	0.003539	294	356	18.0
DGEBA/ $\gamma$ -VL 2:1	Yb(OTf) <sub>3</sub>	0.003344	258	340	19.6
DGEBA/ $\gamma$ -VL 2:1	Sc(OTf) <sub>3</sub>	0.004214	248	311	23.5
DGEBA/ $\gamma$ -MBL 2:1	La(OTf) <sub>3</sub>	0.003539	294	354	16.3
DGEBA/ $\gamma$ -MBL 2:1	Yb(OTf) <sub>3</sub>	0.003344	266	337	17.4
DGEBA/ $\gamma$ -MBL 2:1	Sc(OTf) <sub>3</sub>	0.004214	251	318	20.1

<sup>a</sup> temperature of a 5 % of weight loss

<sup>b</sup> temperature of the maximum degradation rate

<sup>c</sup> char yield at 600 °C

publication.<sup>12</sup> It should be said that the degradability of the reworkable materials is associated with the temperature at which a low percentage of weight is loss (for example 5 %) because the loss of mechanical characteristics takes place at this low percentage, independently of the temperature at which the maximum weight loss occurs. **Table 1** shows the thermal parameters calculated from the TGA curves. It is noticeable that although BF<sub>3</sub>·MEA initiated materials have the curve shifted to higher temperatures, the T<sub>5%</sub> is lower for this initiator than for lanthanum triflate, which can be attributed to the higher proportion of unreacted lactone trapped in the network which is eliminated on heating and not to the breakage of the polymer chain. Among the several rare earth triflates both the T<sub>5%</sub> and T<sub>max</sub> follow the Lewis acidity as expected. Thus, as mentioned previously, the material with the highest content of linear ester groups is that obtained with the ytterbium salt but it is not the most degradable, confirming the importance of the Lewis acidity of the

metal as reported by us.<sup>12</sup> It is noticeable that the char yield at 600 °C increases when the Lewis acidity of the initiator used also increases. Thus, materials obtained from scandium triflate as initiator lead to the highest proportion of char and lanthanum to the lowest.

Isothermal experiments at 250 °C were also performed and are represented in **Figure 2**. As we can see, the material obtained with the boron trifluoride initially experiences a slight decrease of weight and then it remains practically constant. A different behaviour is shown by the other materials, because a progressive weight loss is observed during the whole experiment, which is higher as the acidity of the metal triflate is higher.

Similar experiments were performed with materials obtained from  $\gamma$ -MBL as lactone. In previous work<sup>5</sup> we could prove that this lactone led to a lower incorporation of linear ester groups in the network than  $\gamma$ -VL but no depolymerization occurred when scandium

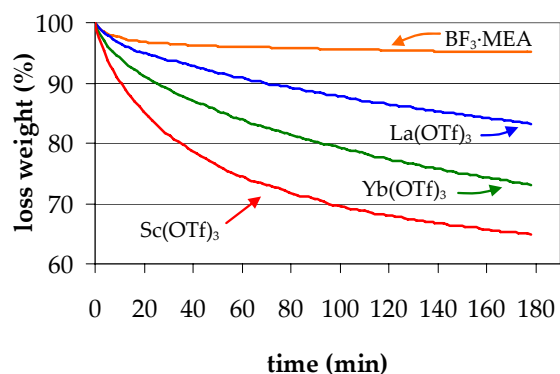


**Figure 2.** Isothermal thermogravimetric curves under N<sub>2</sub> atmosphere at 250 °C of the materials obtained from DGEBA/ $\gamma$ -VL formulations varying the type of initiator used in the curing.

triflate acted as initiator. In this case boron trifluoride was not tested because this initiator leads to very low chemical incorporation of the lactone to the network. **Table 1** shows the thermogravimetric results obtained for these materials. We can see that again the higher the Lewis acidity is the lower the T<sub>5%</sub> and the T<sub>max</sub> and the higher the char yield. Because of the similarity in the degradation behaviour of the materials obtained from both lactones,  $\gamma$ -VL was selected to follow the study.

When the proportion of initiator was changed in the preparation of the thermosets the thermal behaviour also changed. **Figure 3** shows the thermogravimetric and DTG curves for the materials obtained from a DGEBA/ $\gamma$ -VL 2:1 (mol/mol) formulation initiated by 0.5, 1 and 3 phr of Yb(OTf)<sub>3</sub>. As we can see, on increasing the proportion of initiator the degradation begins at lower temperatures (see **Table 2**) and T<sub>max</sub> decreases. Thus, this is another experimental confirmation that the Lewis acid acts in the degradative rupture of the network. However, in a previous study<sup>28</sup>

we proved that the proportion of ytterbium triflate influences the network morphology because the coexistence of the AM and ACE mechanisms, the former becoming more important as the proportion of initiator increases which in turn produce a decrease of the T<sub>g</sub> of the material. This change in the network morphology could influence the thermal degradation in an unpredictable way. As we observed with the Lewis acidity, the char yield increases with the proportion of initiator.

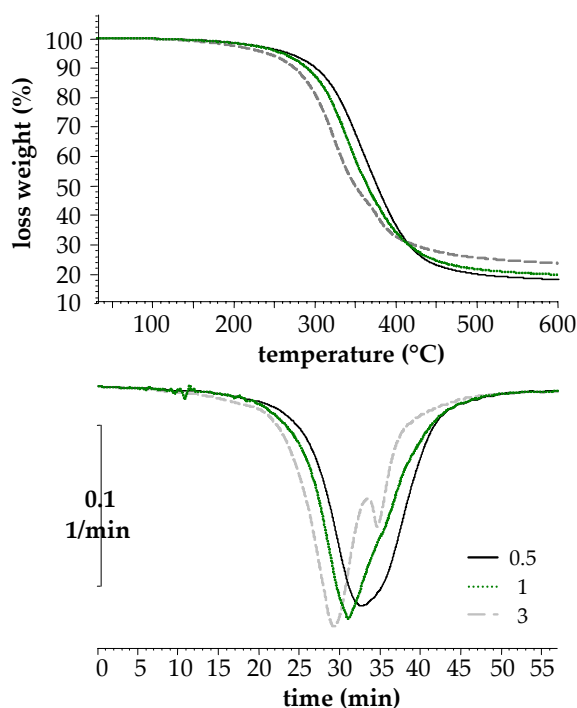


**Figure 3.** Thermogravimetric and DTG curves under N<sub>2</sub> atmosphere at 10 °C/min of the materials obtained from DGEBA/ $\gamma$ -VL formulations varying the proportion of Yb(OTf)<sub>3</sub> used as initiator in the curing.

The DTG curves have different shapes depending on the amount of initiator in the material. Thus, the highest proportion of initiator splits the broad degradation curve into two peaks, the most important at 322 °C and the smallest at 376 °C. When 1 phr of initia-



**Table 2.** Thermogravimetric data under N<sub>2</sub> atmosphere of the materials obtained from DGEBA and DGEBA/ $\gamma$ -VL formulations varying the proportion of Yb(OTf)<sub>3</sub> used as initiator in the curing

Formulation (mol/mol)	Proportion of initiator (phr)	mol init./eq. epoxy	T <sub>5%</sub> <sup>a</sup> (°C)	T <sub>max</sub> <sup>b</sup> (°C)	Char yield <sup>c</sup> (%)
DGEBA	1	0.002935	299	345	21.7
DGEBA/ $\gamma$ -VL 3:1	1	0.003207	275	342	19.7
DGEBA/ $\gamma$ -VL 2:1	0.5	0.001672	266	356	17.9
DGEBA/ $\gamma$ -VL 2:1	1	0.003344	258	340	19.6
DGEBA/ $\gamma$ -VL 2:1	3	0.010032	240	322	23.6
DGEBA/ $\gamma$ -VL 1:1	1	0.003751	243	331	19.3

<sup>a</sup> temperature of a 5 % of weight loss

<sup>b</sup> temperature of the maximum degradation rate

<sup>c</sup> char yield at 600 °C

tor was used, only a shoulder appears at the temperature of the smallest peak. This fact could be attributed to the catalytic effect of the Lewis acid on the degradation of ester moieties.

As expected, there is also an increase in the degradability of the materials on increasing the proportion of  $\gamma$ -VL in the reactive mixture. **Figure 4** shows the thermogravimetric curves and their derivatives for materials initiated with 1 phr of ytterbium triflate. On increasing the proportion of ester groups in the network, the degradation begins at lower temperatures (see **Table 2**), however, there are not big differences among the materials in the residues after heating until 600 °C but the proportion of char is slightly lower for the samples with lactone, which can be attributed to their more aliphatic character. On increasing the proportion of ester groups the DTG curve becomes slightly broader and in the case of DGEBA/ $\gamma$ -VL 1:1 (mol/mol) mixtures a shoulder appears.

Thermogravimetric analysis has been

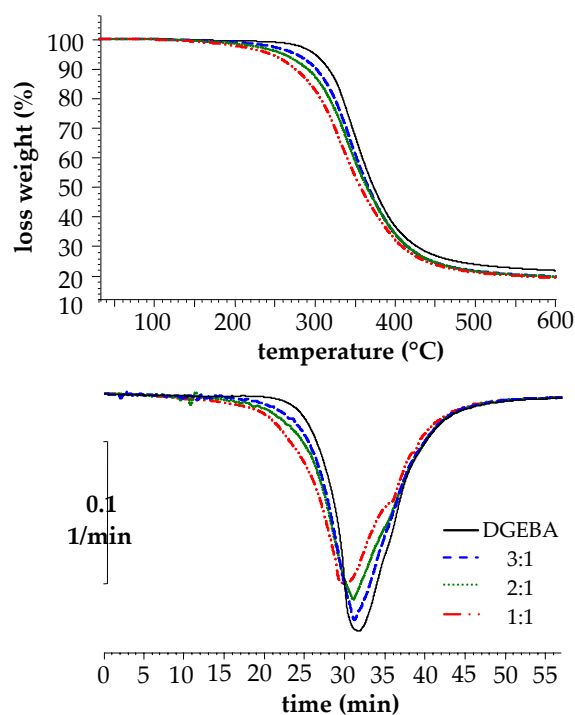


**Figure 4.** Thermogravimetric and DTG curves under N<sub>2</sub> atmosphere at 10 °C/min of the materials obtained from different DGEBA/ $\gamma$ -VL mol/mol formulations with 1 phr of Yb(OTf)<sub>3</sub>.

widely used to estimate the kinetic parameters of degradation processes such as activation energies ( $E_a$ ), kinetic model, Arrhenius pre-exponential factor ( $A$ ), rate constant ( $k$ ) and degradation rate ( $v$ ).<sup>29,30</sup>



The dependence of the activation energy on the degree of conversion using the isoconversional method (eq. 4) is represented in **Figure 5** for the degradation of the samples containing  $\gamma$ -VL with the different initiators. As we can see, the higher activation energy corresponds to the initiated boron trifluoride material. Rare earth triflates lead to degradation with a practically constant energy value between 20 and 80 % of conversion. At the end of the reaction the activation energy increases especially for the lanthanum salt.

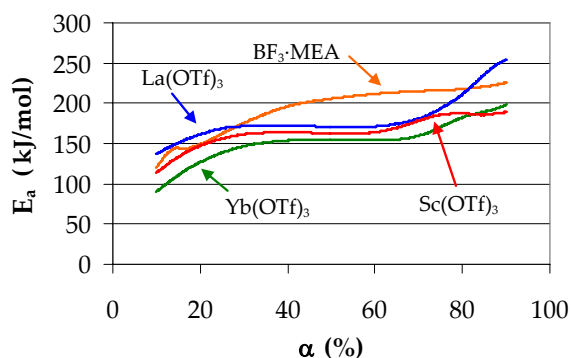


**Figure 5.** Dependence of the activation energy on the degree of conversion for the degradation under  $N_2$  atmosphere of the materials obtained from DGEBA/ $\gamma$ -VL formulations varying the type of initiator used in the curing.

To find the kinetic parameters associated with the set of thermogravimetric curves obtained for the different materials, we applied the isoconversional KAS equation (eq. 4) at a conversion of 0.5. The kinetic model was chosen by the Coats-Redfern method and confirmed by the integral and differential master plots. All three methods gave the same model. **Table 3** collects the activation energies, the Arrhenius pre-exponential factor and the regression for the models considered calculated using Coats-Redfern method for the degradation of

DGEBA/ $\gamma$ -VL 2:1 initiated by 1 phr of  $La(OTf)_3$ . We choose as the kinetic model the  $n = 3$  because of the good regression and its calculated value of  $E_a$  is the nearest to the experimental value 170.7 kJ/mol. As an example **Figures 6** and **7** show, respectively, the theoretical and experimental integral and differential master curves calculated using a constant value of  $E_a$  (154.6 kJ/mol) for the material DGEBA/ $\gamma$ -VL 2:1 initiated by 1 phr of  $Yb(OTf)_3$ . The best fitting is performed by the  $n = 3$  model for both methodologies.

The thermal degradation of the materials studied follows the  $n = 3$  kinetic model, with the exception of the materials obtained with 1 phr of  $Sc(OTf)_3$  and the formulation DGEBA/ $\gamma$ -VL 1:1 (mol/mol) initiated by 1 phr of  $Yb(OTf)_3$ , which follows the  $n = 4$  model. The materials obtained with 3 phr of  $BF_3 \cdot MEA$  follow a completely different model, the  $D_2$ , because the material is densely cross-linked with a low content of linear ester groups and therefore the diffusional factors of the degradation are more important than the strictly reactive processes.

Once the model has been established by the processes described the kinetic parameters were calculated. **Tables 4** and **5** show the experimental activation energies, the calculated Arrhenius pre-exponential factors, the constant rate values and the degradation rates. The values in **Table 4** show for the materials obtained from  $\gamma$ -VL and  $\gamma$ -MBL no dependence of the  $E_a$  and  $\ln A$  values with the Lewis acidity of the rare earth triflates. However, both the constant and the degrada-



**Table 3.** Calculated kinetic data of the thermal degradation of materials obtained from DGEBA/ $\gamma$ -VL 2:1 (mol/mol) formulation initiated by 1 phr of  $\text{La}(\text{OTf})_3$  for different kinetic models and their regression calculated by using the Coats-Redfern method

Model	$E_a$ (kJ/mol)	$\ln A$ ( $\text{min}^{-1}$ )	R
$A_{3/2}$	49.79	7.234	0.9900
$A_2$	34.71	4.089	0.9882
$A_3$	19.64	0.735	0.9830
$A_4$	12.10	-1.141	0.9742
$R_2$	65.67	9.463	0.9801
$R_3$	70.14	10.041	0.9845
$D_1$	118.23	19.667	0.9694
$D_2$	142.93	25.786	0.9815
$D_3$	150.81	24.407	0.9868
$D_4$	138.59	21.821	0.9815
$F_1$	79.94	13.275	0.9915
Power	21.67	0.942	0.9428
$n = 1.9; m = 0.1$	103.43	18.597	0.9989
$n = 1.5$	96.79	16.903	0.9973
$n = 3$	160.89	30.436	0.9951
$n = 4$	211.57	40.988	0.9890

tion rate increase with the acidity of the metal. When the proportion of  $\text{Yb}(\text{OTf})_3$  increases there are no big differences in  $E_a$  and  $\ln A$  but, by the compensation effect,<sup>31</sup> both the constant and the degradation rate increase with the amount of initiator (**Table 5**). A similar trend is observed when the proportion of  $\gamma$ -VL increases in the initial mixture (**Table 5**). From all the degradation experiments performed we can conclude that the higher degradation rate at 350 °C is reached for materials obtained from DGEBA/ $\gamma$ -VL 2:1 (mol/mol) mixtures initiated by 3 phr of  $\text{Yb}(\text{OTf})_3$ . It should be said that the use of 1 phr of  $\text{Sc}(\text{OTf})_3$  or 3 phr of  $\text{Yb}(\text{OTf})_3$  led to the depolymerization of the polymer chain

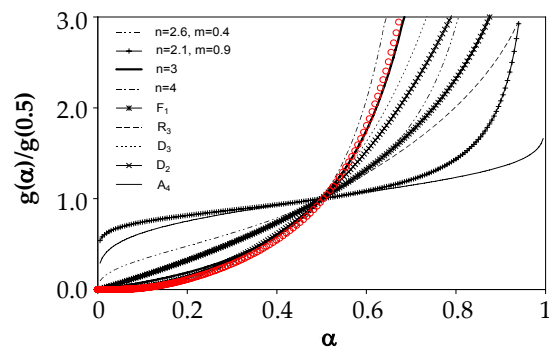


**Figure 6.** Comparison of the theoretical integral master plots of  $g(\alpha)/g(0.5)$  versus  $\alpha$  with the experimental master curve. The empty symbols correspond to experimental data determined for the degradation of the material obtained from a DGEBA/ $\gamma$ -VL 2:1 (mol/mol) formulation with 1 phr of  $\text{Yb}(\text{OTf})_3$  as initiator.

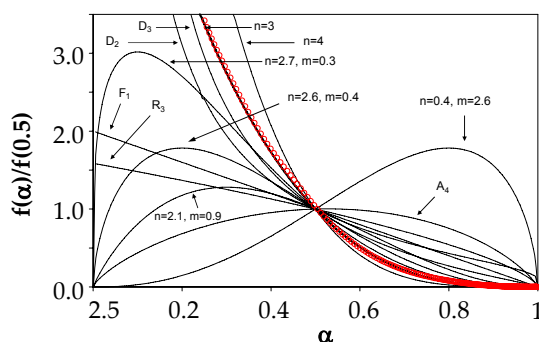


**Figure 7.** Comparison of the theoretical differential master plots of  $f(\alpha)/f(0.5)$  versus  $\alpha$  with the experimental master curve. The empty symbols correspond to experimental data determined for the degradation of the material obtained from a DGEBA/ $\gamma$ -VL 2:1 (mol/mol) formulation with 1 phr of  $\text{Yb}(\text{OTf})_3$  as initiator.

forming free lactone, as reported in a previous paper.<sup>5</sup> Thus, this process could also occur in the thermal degradation of the materials in addition to ester  $\beta$ -elimination and ether rupture catalyzed by the Lewis acid.<sup>12</sup> On comparing the thermal degradation of the samples obtained from higher proportions of lactone (DGEBA/ $\gamma$ -VL 1:1) with materials with a lower proportion of lactone but a higher proportion of rare earth triflate (3 phr of



**Table 4.** Kinetic data of the thermal degradation of materials obtained from DGEBA/ $\gamma$ -VL and DGEBA/ $\gamma$ -MBL formulations varying the type of initiator used in the curing

Formulation (mol/mol)	Initiator	mol init./eq. epoxy	$E_a^a$ (kJ/mol)	ln A (s <sup>-1</sup> )	$k_{350^\circ\text{C}} \cdot 10^2$ (s <sup>-1</sup> )	$v_{350^\circ\text{C}} \cdot 10^2$ (s <sup>-1</sup> )
DGEBA/ $\gamma$ -VL 2:1	BF <sub>3</sub> .MEA	0.018216	205.9	31.66 <sup>b</sup>	0.007	0.01
DGEBA/ $\gamma$ -VL 2:1	La(OTf) <sub>3</sub>	0.003539	170.7	28.35 <sup>c</sup>	0.99	0.12
DGEBA/ $\gamma$ -VL 2:1	Yb(OTf) <sub>3</sub>	0.003344	154.6	26.00 <sup>c</sup>	2.12	0.26
DGEBA/ $\gamma$ -VL 2:1	Sc(OTf) <sub>3</sub>	0.004214	162.4	28.63 <sup>d</sup>	6.59	0.41
DGEBA/ $\gamma$ -MBL 2:1	La(OTf) <sub>3</sub>	0.003539	191.8	32.59 <sup>c</sup>	1.19	0.15
DGEBA/ $\gamma$ -MBL 2:1	Yb(OTf) <sub>3</sub>	0.003344	169.6	28.92 <sup>c</sup>	2.19	0.27
DGEBA/ $\gamma$ -MBL 2:1	Sc(OTf) <sub>3</sub>	0.004214	173.9	31.16 <sup>d</sup>	8.84	0.55

<sup>a</sup> activation energy at  $\alpha = 0.5$  obtained by isoconversional analysis

<sup>b</sup> pre-exponential factor using a D2 kinetic model for  $\alpha = 0.5$

<sup>c</sup> pre-exponential factor using a n = 3 kinetic model for  $\alpha = 0.5$

<sup>d</sup> pre-exponential factor using a n = 4 kinetic model for  $\alpha = 0.5$

**Table 5.** Kinetic data of the thermal degradation of materials obtained from DGEBA and DGEBA/ $\gamma$ -VL formulations varying the proportion of Yb(OTf)<sub>3</sub> used as initiator in the curing

Formulation (mol/mol)	Proportion of initiator (phr)	mol init./eq. epoxy	$E_a^a$ (kJ/mol)	ln A (s <sup>-1</sup> )	$k_{350^\circ\text{C}} \cdot 10^2$ (s <sup>-1</sup> )	$v_{350^\circ\text{C}} \cdot 10^2$ (s <sup>-1</sup> )
DGEBA	1	0.002935	170.1	28.51 <sup>b</sup>	1.31	0.16
DGEBA/ $\gamma$ -VL 3:1	1	0.003207	166.0	28.04 <sup>b</sup>	1.81	0.23
DGEBA/ $\gamma$ -VL 2:1	0.5	0.001672	158.8	26.14 <sup>b</sup>	1.09	0.14
DGEBA/ $\gamma$ -VL 2:1	1	0.003344	154.6	26.00 <sup>b</sup>	2.12	0.26
DGEBA/ $\gamma$ -VL 2:1	3	0.010032	155.7	27.14 <sup>b</sup>	5.43	0.68
DGEBA/ $\gamma$ -VL 1:1	1	0.003751	169.4	29.74 <sup>c</sup>	5.19	0.32

<sup>a</sup> activation energy at  $\alpha = 0.5$  obtained by isoconversional analysis

<sup>b</sup> pre-exponential factor using a n = 3 kinetic model for  $\alpha = 0.5$

<sup>c</sup> pre-exponential factor using a n = 4 kinetic model for  $\alpha = 0.5$

Yb(OTf)<sub>3</sub>) we can conclude that the degradation rate is more dependent on the initiator. This indicates that the depolymerization process or the ether rupture should compete extensively with the  $\beta$ -elimination process. The important role of the rare earth triflates in the degradation mechanism is put into evidence when we compare the constants and reaction rates in **Table 4**, in which the values for BF<sub>3</sub>.MEA initiated materials are much lower than the others.

In order to confirm the goodness of the kinetic parameters calculated **Figure 8** represents three curves obtained for the system DGEBA/ $\gamma$ -VL 2:1 initiated by 1 phr of La(OTf)<sub>3</sub>: kinetic model data, isoconversional data obtained by the STAR software (KAS equation data) and the experimental data. It can be observed that the three curves show a similar trend. Only some few variations were found at low conversions. These small differences could be due to the exper-

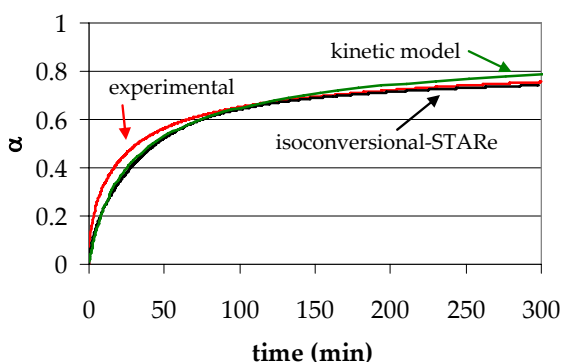


**Figure 8.** Conversion vs. time of data obtained experimentally (isothermally at 300 °C), isoconversionally with the STAR software (KAS equation data) and from the  $n=3$  kinetic model with the activation parameters (Table 3) for the degradation of the material obtained from a DGEBA/ $\gamma$ -VL 2:1 (mol/mol) formulation with 1 phr of La(OTf)<sub>3</sub> as initiator.

imental limits of the TGA device.

## Conclusions

The copolymerization of DGEBA and  $\gamma$ -lactones increases the thermal degradability of epoxy resins in which the cleavage of ester groups introduced in the polymeric chain plays an important role. The higher the proportion of lactone in the reactive mixture the more degradable the materials are.

Rare earth triflates lead to more degradable materials than the conventional BF<sub>3</sub>·MEA cationic initiator. The higher the Lewis acidity of the initiator or the higher its proportion the more thermally reworkable the materials are.

$E_a$  and  $\ln A$  values for the degradation of the materials obtained from  $\gamma$ -VL and  $\gamma$ -MBL show no dependence on the Lewis acidity of the rare earth triflates or its proportion, but both the constant and the degradation rate increase with the

acidity of the metal or its proportion.

The higher degradation rate at 350 °C is reached for the materials obtained from DGEBA/ $\gamma$ -VL 2:1 (mol/mol) mixtures initiated by 3 phr of Yb(OTf)<sub>3</sub>.

## Acknowledgements

The authors from the Universitat Politècnica de Catalunya would like to thank CICYT and FEDER (MAT2004-04165-C02-02) for their financial support. The authors from the Universitat Rovira i Virgili would like to thank the CICYT (Comisión Interministerial de Ciencia y Tecnología), FEDER (Fondo Europeo de Desarrollo Regional) (MAT2005-01806).

## References

- [1] Kobayashi S, Synlett 1994; 689-701.
- [2] Kobayashi S, Sugiura M, Kitagawa H, Lam WWL. Chem Rev 2002; 102: 2227-2302.
- [3] Castell P, Galià M, Serra A, Salla JM, Ramis X. Polymer 2000; 41: 8465-8474.
- [4] Mas C, Mantecón A, Serra A, Ramis X, Salla JM. J Polym Sci Part A: Polym Chem 2004; 42: 3782-3791.
- [5] Arasa M, Ramis X, Salla JM, Mantecón A, Serra A. J Polym Sci Part A: Polym Chem 2007; 45: 2129-2141.
- [6] Yang S, Chen JS, Corner H, Breiner T, Ober CK, Poliks MD. Chem Mater 1998; 10: 1475-1482.
- [7] Shirai M, Morishita S, Okamura H, Tsunnoka M. Chem Mater 2002; 14: 334-340.
- [8] Shirai M, Kawaue A, Okamura H, Tsunnoka M. Chem Mater 2003; 15: 4075-4081.
- [9] Wang L, Li H, Wong CP. J Polym Sci Part A Polym Chem 2000; 38: 3771-3782.



- [10] Wong CP, Wang L, Shi SH. *Mat Res Innovat* 1999; 2: 232-247.
- [11] Sadhir RK, Luck MR, Eds. *Expanding monomers: synthesis characterization and applications*. Boca Raton: CRC Press; 1992.
- [12] González L, Ramis X, Salla JM, Mantecón A, Serra A. *Polym Degrad Stab* 2007; 92: 596-604.
- [13] Paulik F. *Special trends in thermal analysis*. Chichester: Wiley & Sons; 1995 [chapter 10].
- [14] Friedman H. *J Polym Sci* 1964; C6: 183-195.
- [15] Coats AW, Redfern JP. *Nature* 1964; 201: 68-69.
- [16] Doyle DC. *Nature* 1965; 207: 290-291.
- [17] Ozawa T. *Bull Chem Soc Jpn* 1965; 38: 1881-1886.
- [18] Senum GI, Yang RT. *J Therm Anal* 1977; 11: 445-447.
- [19] Agrawal PK. *Thermochim Acta* 1992; 203: 93-110.
- [20] Kissinger HE. *Anal Chem* 1957; 29: 1702-1706.
- [21] Akahira T, Sunose T. *Res Report Chiba Inst Technol (Sci Technol)* 1971; 16: 22-31.
- [22] Flynn JH, Wall LA. *J Res Nat Bur Standards A Phys Chem* 1966; 70A: 487-523.
- [23] Cadenato A, Morancho JM, Fernández-Francos X, Salla JM, Ramis X. *J Thermal Anal Cal* 2007; 89: 233-244.
- [24] Gotor FJ, Criado JM, Malek J, Noga N. *J Phys Chem A* 2000; 104: 10777-10782.
- [25] Garcia SJ, Ramis X, Serra A, Suay JJ. *Therm Anal Cal* 2006; 83: 429-438.
- [26] Sivasamy P, Palaniandavar M, Vijayakumar CT, Ledered K. *Polym Degrad Stab* 1992; 38: 15-21.
- [27] Giménez R, Fernández-Francos X, Salla JM, Serra A, Mantecón A, Ramis X. *Polymer* 2005; 46: 10637-10647.
- [28] Salla JM, Fernández-Francos X, Ramis X, Mas C, Mantecón A, Serra A. *J Therm Anal Cal* 2008; 91: 385-393.
- [29] Morancho JM, Ramis X, Salla JM, Cadenato A. *Thermochim Acta* 2004; 419: 181-187.
- [30] Liu Y, Wei WL, Chen YJ, Wu CS, Tsai MH. *Polym Degrad Stab* 2004; 86: 135-145.
- [31] Vyazovkin S, Linert W. *Chem Phys* 1995; 193: 109-118.

2.4 KINETIC STUDY BY FTIR AND DSC ON THE CATIONIC  
CURING OF A DGEBA/ $\gamma$ -VALEROLACTONE MIXTURE  
WITH YTTERBIUM TRIFLATE AS INITIATOR

---

*Mercè Arasa, Xavier Ramis, Josep Maria Salla, Ana Mantecón, Àngels Serra; Thermochemica Acta 479 (2008) 37-44*

UNIVERSITAT ROVIRA I VIRGILI  
NOUS TERMOESTABLES EPOXÍDICS MODIFICATS AMB GAMMA-LACTONES I BIS-GAMMA-LACTONES CONDENSADAES  
M<sup>a</sup> Mercè Arasa Bertomeu  
ISBN:978-84-692-4157-8/DL:T-1171-2009



## KINETIC STUDY BY FTIR AND DSC ON THE CATIONIC CURING OF A DGEBA/ $\gamma$ -VALEROLACTONE MIXTURE WITH YTTERBIUM TRIFLATE AS AN INITIATOR

Mercè Arasa,<sup>1</sup> Xavier Ramis,<sup>2</sup> Josep Maria Salla,<sup>2</sup> Ana Mantecón,<sup>1</sup> Àngels Serra<sup>1</sup>

<sup>1</sup>Dpt. Q. Analítica i Q. Orgànica, URV. C/Marcel·lí Domingo s/n, 43007 Tarragona, Spain

<sup>2</sup>Lab. Termodinàmica, ETSEIB. UPC, Av. Diagonal 647, 08028 Barcelona, Spain

### Abstract

A mixture of diglycidylether of bisphenol A (DGEBA) and  $\gamma$ -valerolactone ( $\gamma$ -VL) was cured in the presence of ytterbium triflate as an initiator to obtain poly(ether-ester) thermosets. The kinetics of the various elemental reactions, which take place during the curing process, was studied by means of isothermal curing in the FTIR spectrometer. The kinetic parameters were calculated by means of the isoconversional procedure and the best-fit kinetic model was determined with the so-called compensation effect (isokinetic relationship). The isothermal kinetic analysis was compared with that obtained by dynamic curing in DSC.

*Keywords:* Epoxy resins, ytterbium triflate, kinetics, cationic polymerization, thermosets, lactones.

### Introduction

It is well known that internal stress usually occurs during the curing of epoxide resins and causes various defects, e.g., microcracks, microvoids, and delamination,<sup>1,2</sup> which reduce their durability and make worse their properties. Therefore, one of the main subjects in the field of epoxide resin technology is to prevent or reduce the internal stress generated in the thermoset. During the 1970s, Bailey et al.<sup>3-6</sup> described in various papers that some spiroorthoesters (SOEs) polymerize with

expansion in volume or with very low shrinkage. Therefore, they applied the term *expanding monomers* to these compounds. Among the expanding monomers, they also considered spiroortho-carbonates (SOCs) and bicycloorthoesters (BOEs), but SOEs were the most promising monomers of this type. The classical synthetic procedure applied in their synthesis consists of reacting epoxides and lactones in the presence of a Lewis acid.<sup>7</sup> The corresponding SOEs can polymerize in cationic medium to yield poly(ether-ester)s via a double-tandem ring opening process.



Conventionally,  $\text{BF}_3$  complexes are used as Lewis acid due to their latent character,<sup>8-10</sup> but as alternative we used lanthanide triflates in the polymerization of these compounds. Lanthanide triflates are stable in water, act as Lewis acid initiators, can be recovered,<sup>11,12</sup> and are capable of cross-linking pure glycidic and cycloaliphatic epoxy resins or their mixtures with lactones.<sup>13-15</sup> In a previous study,<sup>16</sup> we polymerized diglycidylether of bisphenol A (DGEBA) with  $\gamma$ -butyrolactone ( $\gamma$ -BL) using ytterbium triflate as an initiator. Although the global shrinkage was not reduced, by means of thermomechanical analysis (TMA) we proved that the addition of  $\gamma$ -BL to the DGEBA led to materials with lower contraction after gelation and therefore with lower internal stresses. The explanation to this behavior is based in the complex reaction mechanism. During the curing process four chemical processes coexist: (a) formation of SOE by reaction of DGEBA with  $\gamma$ -lactone, (b) homopolymerization of epoxy groups (c) homopolymerization of SOE, and (d) copolymerization of SOE with epoxy groups (**Scheme 1**). Because SOEs homopolymerize or copolymerize with some expansion in the final stages of the curing, the contraction after gelation is reduced. Thus, the main contraction is produced when the material is a viscous liquid and in this way the internal stresses are reduced. The knowledge of the kinetics of the elemental reactions that takes place during curing could allow estimating the times necessary to complete these processes. In this way it could be possible to relate these times with the shrinkage that occurs and also

with the stresses generated in the thermoset on curing.

FTIR-ATR can be applied to investigate the evolution of the different chemical reactions. By this technique detailed information can be obtained through the evolution of the absorption bands of the carbonyl and epoxy groups vs. time at several temperatures. From these conversion plots, by integral isoconversional analysis, activation energy and a second parameter (which is related to the pre-exponential factor and to the integral conversion function, which depends on the degree of conversion and represents the kinetic model that governs the process) can be calculated.

An alternative procedure to obtain kinetic parameters is by means of dynamic DSC experiments, which allows simulating the behavior during the isothermal curing.<sup>17</sup> However, DSC gives only information of the overall process but not on the elemental reactions that occur during curing and should be complemented with other techniques, such as FTIR.

The present study focuses on the kinetic analysis of the curing of mixtures of DGEBA with  $\gamma$ -VL using ytterbium triflate as an initiator. We studied the kinetics of the elemental reactions that are part of the curing by FTIR spectroscopy and the overall curing kinetics by DSC. Eventually, we propose a method that uses the isoconversional isothermal parameters determined by FTIR and the compensation effect<sup>18-20</sup> to calculate the complete kinetic triplet. The results were



compared with those obtained by non-isothermal procedures.

## Experimental Part

### Materials

Diglycidylether of bisphenol A (DGEBA) EPIKOTE RESIN 827 (epoxy equiv. = 182.08 g/equiv.) (Shell Chemicals),  $\gamma$ -valerolactone ( $\gamma$ -VL) and ytterbium (III) trifluoromethanesulfonate (Aldrich) were used as received.

### Preparation of the curing mixtures

The mixture was prepared by dissolving 1 phr (one part per hundred parts of mixture, w/w) of ytterbium triflate in 0.01 mol of  $\gamma$ -VL and adding 0.02 mols of DGEBA. The sample was kept at -18 °C before use.

### Characterization and measurements

**FTIR spectroscopy.** The isothermal curing process, between 120 and 160 °C, was monitored with a FTIR 680 Plus from Jasco with 4 cm<sup>-1</sup> of resolution in the absorbance mode. An attenuated total reflection accessory with thermal control and a diamond crystal (a Golden Gate heated single-reflection diamond ATR from Specac-Teknokroma) was used to determine FTIR spectra. The disappearance of the 910 and 1775 cm<sup>-1</sup> absorbance peak (epoxy bending and carbonyl C=O stretching of cyclic ester) was used to monitor the epoxy and  $\gamma$ -VL conversion respectively. The formation of the 1737 cm<sup>-1</sup> absorbance peak (carbonyl C=O stretching of aliphatic linear ester), which does not exist in the sample before curing, indicates that ring-

opening polymerization of SOE has occurred. Thus, this let us to evaluate the linear ester formation. The peak at 1605 cm<sup>-1</sup> (phenyl group) was chosen as an internal standard. Conversions of the different reactive groups, epoxy, lactone and linear ester, were determined by the Lambert-Beer law from the normalized changes of absorbance at 910, 1775, 1737 cm<sup>-1</sup>:<sup>10,16,21</sup>

$$\alpha_{\text{epoxy}} = 1 - \left( \frac{\bar{A}_{910}^t}{\bar{A}_{910}^0} \right) \alpha_{\gamma\text{-VL}} = 1 - \left( \frac{\bar{A}_{1775}^t}{\bar{A}_{1775}^0} \right)$$
$$\alpha_{\text{SOE}} = 1 - \left( \frac{\bar{A}_{1737}^t}{\bar{A}_{1737}^\infty} \right) \quad (1)$$

where  $\bar{A}^0$ ,  $\bar{A}^t$  and  $\bar{A}^\infty$  are the normalized absorbance of the reactive groups before curing, after reaction time  $t$ , and after complete curing, respectively.

$$\left( \bar{A}_{910}^0 = A_{910}^0 / A_{1605}^0 ; \bar{A}_{1775}^0 = A_{1775}^0 / A_{1605}^0 ; \bar{A}_{910}^t = A_{910}^t / A_{1605}^t ; \bar{A}_{1775}^t = A_{1775}^t / A_{1605}^t ; \bar{A}_{1737}^t = A_{1737}^t / A_{1605}^t ; \bar{A}_{1737}^\infty = A_{1737}^\infty / A_{1605}^\infty \right).$$

### Differential scanning calorimetry.

Calorimetric analyses were carried out on a Mettler DSC-821e thermal analyzer using N<sub>2</sub> as a purge gas in covered aluminium pans. The weight of the samples was approximately 5 mg. Nonisothermal curing was carried out at rates of 2, 5, 10 and 15 K/min and the degree of conversion was calculated as:

$$\alpha_{\text{DSC}} = \Delta H_T / \Delta H_{\text{dyn}} \quad (2)$$

where  $\Delta H_T$  is the heat released up to a temperature  $T$ , obtained by integrating the calorimetric signal up to that temperature, and  $\Delta H_{\text{dyn}}$  is the total reaction heat associated with complete



conversion of all reactive groups determined for each heating rate.

### Kinetic analysis

If we accept that the dependence of the rate constant on the temperature follows the Arrhenius equation, the kinetics of the reaction is usually described by the following rate equation:

$$\frac{d\alpha}{dt} = Af(\alpha)\exp\left(-\frac{E}{RT}\right) \quad (3)$$

where  $t$  is time,  $A$  is the pre-exponential factor,  $E$  is the activation energy,  $T$  is the absolute temperature,  $R$  is the gas constant, and  $f(\alpha)$  is the kinetic model.

In general, the kinetic analysis was carried out using an isoconversional method. The basic assumption of these methods is that the reaction rate at constant conversion is only function of the temperature.<sup>22,23</sup>

**Isothermal methods.** By integrating the rate equation [eq. (3)] in isothermal conditions we obtain:

$$\ln t = \ln\left[\frac{g(\alpha)}{A}\right] + \frac{E}{RT} \quad (4)$$

where  $g(\alpha)$  is the integral conversion function, defined as:

$$g(\alpha) = \int_0^\alpha \frac{d\alpha}{f(\alpha)} \quad (5)$$

According to eq. (4) the activation energy and the constant  $\ln[g(\alpha)/A]$  can be obtained, respectively, from the slope and the intercept of the linear relationship  $\ln t$  against  $1/T$  for  $\alpha = \text{constant}$ .

**Nonisothermal methods.** By integrating eq. (3) in nonisothermal conditions and reordering it, the so-called temperature integral can be expressed as:

$$g(\alpha) = \int_0^\alpha \frac{d\alpha}{f(\alpha)} = \frac{A}{\beta} \int_0^T e^{-(E/RT)} dT \quad (6)$$

where  $\beta$  is the heating rate.

By using the Coats-Redfern<sup>24</sup> approximation to solve eq. (6), and considering that  $2RT/E$  is much lower than 1, the term  $(1-2RT/E)$  can be neglected and the solution of the temperature integral may be expressed as:<sup>25</sup>

$$\ln \frac{g(\alpha)}{T^2} = \ln \left[ \frac{AR}{\beta E} \right] - \frac{E}{RT} \quad (7)$$

For a given kinetic model, linear representation of  $\ln[g(\alpha)/T^2]$  against  $1/T$  makes it possible to determine  $E$  and  $A$  from the slope and the ordinate at the origin. In this work, we selected the kinetic model that had the best linear correlation in the Coats-Redfern equation and that had an  $E$  value similar to that obtained isoconversionally (considered to be effective  $E$  value).

By reordering eq. (7) we can write the Kissinger-Akahira-Sunose (KAS) equation:<sup>26,27</sup>

$$\ln \frac{\beta}{T^2} = \ln \left[ \frac{AR}{g(\alpha)E} \right] - \frac{E}{RT} \quad (8)$$

For each conversion degree, the linear plot of  $\ln[\beta/T^2]$  against  $1/T$  enables  $E$  and the kinetic parameter  $\ln[AR/g(\alpha)E]$  to be determined from the slope and the intercept. If the model,  $g(\alpha)$ , is known,



the corresponding pre-exponential factor can be calculated from each conversion. This isoconversional procedure is similar to Flynn-Wall-Ozawa's method.<sup>28-30</sup>

The constant  $\ln[AR/g(\alpha)E]$  is directly related by  $R/E$  to the constant  $\ln[g(\alpha)/A]$  of the isothermal adjustment [eq. (4)]. Thus, taking the dynamic data  $\ln[AR/g(\alpha)E]$  and  $E$ , and applying eq. (8), we can determine the isoconversional lines [eq. (4)] and simulate isothermal curing.<sup>17,31</sup>

**Compensation effect (isokinetic relationship).** For complex processes (parallel reactions, successive reactions, physical changes, etc.) it is characteristic for the activation energy and the pre-exponential factor to depend on the degree of conversion. This generally reflects the existence of a compensation effect through the following equation:<sup>18,20,32,33</sup>

$$\ln A_{\alpha} = aE_{\alpha} + b = \frac{E_{\alpha}}{RT} + \ln \left[ \frac{(d\alpha/dt)_{\alpha}}{f(\alpha)} \right] \quad (9)$$

where  $a$  and  $b$  are constants, and subscript  $\alpha$  refers to degree of conversion, that is a factor producing a change in Arrhenius parameters in this study.

The slope  $a = 1/RT_{iso}$  is related to isokinetic temperature  $T_{iso}$  and the intercept  $b = \ln k_{iso}$  is related to the isokinetic rate constant. Eq. (9) represents an isokinetic relationship (IKR), which can be observed as a common point of intersection of the Arrhenius lines (i.e.,  $\ln k$  vs.  $1/T$ ) of a series of reactions (in this work the different degree of conversion). This intersection is characterized

by a  $k_{iso}$  and a  $T_{iso}$ . By reordering and applying logarithms to eq. (3), the eq. (9) can be deduced.

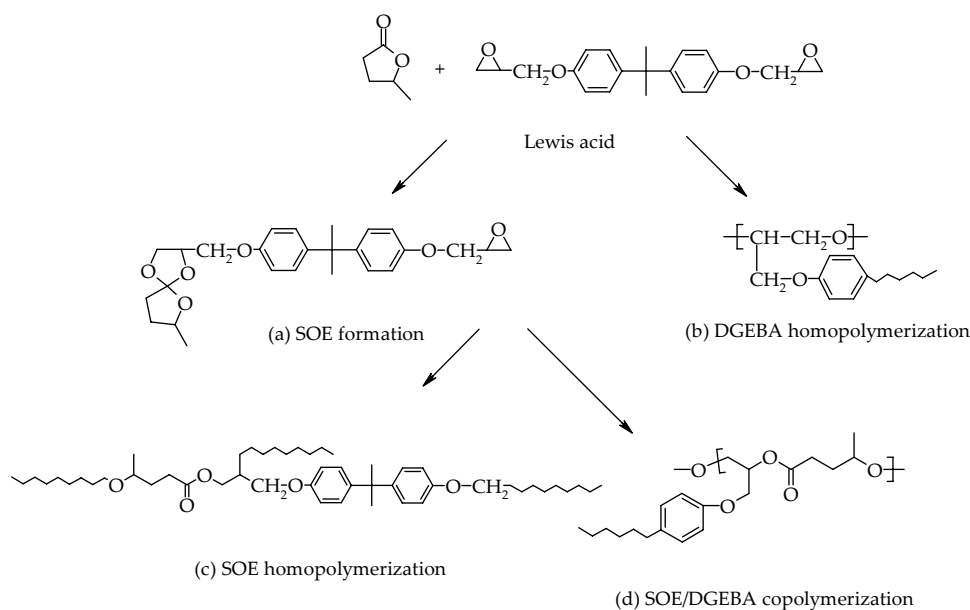
The appearance of the IKR shows that only one mechanism is present and that all reactions have analogous reaction profiles, whereas the existence of parameters that do not agree with the IKR implies that there are multiple reaction mechanisms.<sup>34,35</sup> According to certain authors, we selected the kinetic model whose IKR had the best linear correlation and in which the associated  $T_{iso}$  value was near the experimental temperature range.<sup>36</sup>

The aim of this study was to determine the complete kinetic triplet [ $E$ ,  $A$ ,  $g(\alpha)$ ] in complex systems with  $E = E(\alpha)$ , by using isoconversional kinetic parameters, the slope and intercept of eqs. (4) and (8), and the isokinetic relation, eq. (9). Eq. (9) was applied to the isothermal and nonisothermal isoconversional data when the conversion changes for different kinetic models. A similar procedure was proposed by Vyazovkin to obtain the kinetic triplet.<sup>36</sup>

## Results and discussion

The curing process of DGEBA with  $\gamma$ -lactones takes place by the complex reaction mechanism depicted in **Scheme 1**.

**Figure 1** shows the FTIR spectra of the mixture DGEBA/ $\gamma$ -VL 2:1 (mol/mol) with 1 phr of  $\text{Yb}(\text{TfO})_3$  before and after curing and at intermediate time of 7.5 min, performed at 160 °C. During the curing process there are changes mainly in three typical bands:



Scheme 1

1. The carbonyl stretching band of  $\gamma$ -VL at  $1775\text{ cm}^{-1}$ , which decreases because  $\gamma$ -VL reacts with the epoxide groups to form SOEs. In the final stages of the curing this absorption slightly increases again, due to the reversibility of the formation of SOE groups as previously reported.<sup>15</sup>

2. The peak at  $1737\text{ cm}^{-1}$ , attributable to the linear aliphatic ester, increases steadily and confirms that the ring-opening polymerization of SOE occurs by homo- or copolymerization with epoxide. In general, homopolymerization is less favourable and it is only important at the end of curing when there are few epoxide groups.<sup>16</sup>

3. The band at  $910\text{ cm}^{-1}$ , associated with the oxirane ring, disappears indicating that the epoxide completely polymerizes. Taking into account the stoichiometry of the formulation (4 equiv. epoxy per 1 equiv. of lactone), the epoxy group, in addition to the reaction with  $\gamma$ -VL, can

also homopolymerize and copolymerize with SOE.

After isothermal curing in the FTIR/ATR, the complete disappearance of the epoxy groups and the absence of residual enthalpy in a DSC scan allowed us to conclude that the material was completely cured. This result is coherent with the fact that all curing temperatures are higher than the glass transition temperature of the material completely cured ( $T_g^\infty = 93^\circ\text{C}$ , determined at  $10^\circ\text{C}/\text{min}$  after nonisothermal curing between 0 and  $250^\circ\text{C}$ ) so that vitrification during curing is not possible.

Due to the partial overlapping of carbonylic lactone and ester absorbances (between  $1825$  and  $1670\text{ cm}^{-1}$ ) we deconvoluted the spectroscopic signals in this zone to quantify the absorptions associated with each carbonyl group.<sup>37</sup> **Figure 2** shows an example of this deconvolution.

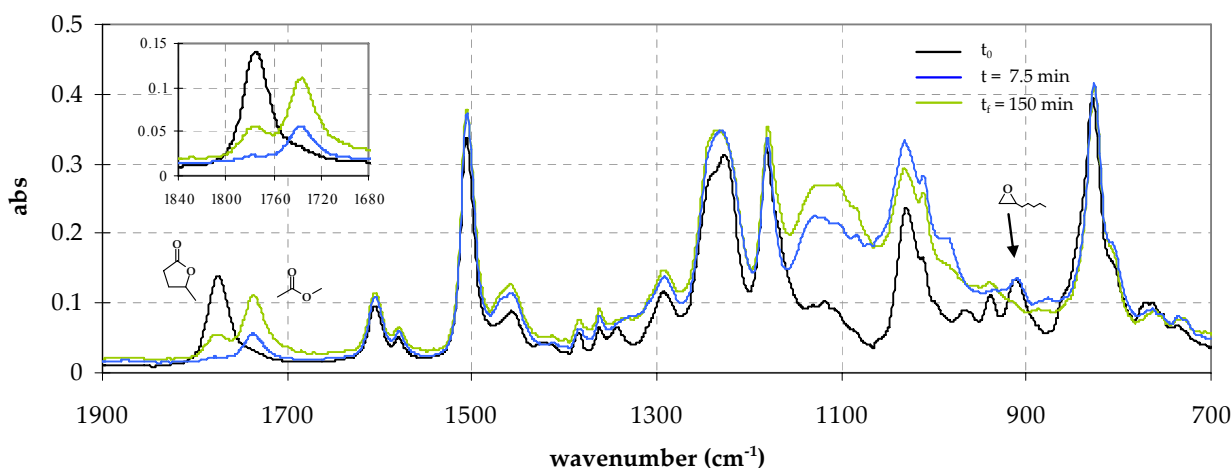


**Figure 1.** FTIR-ATR spectra of a mixture of DGEBA/ $\gamma$ -VL in a molar ratio of 2:1 with 1 phr of  $\text{Yb}(\text{OTf})_3$  registered at different curing times at 160 °C.

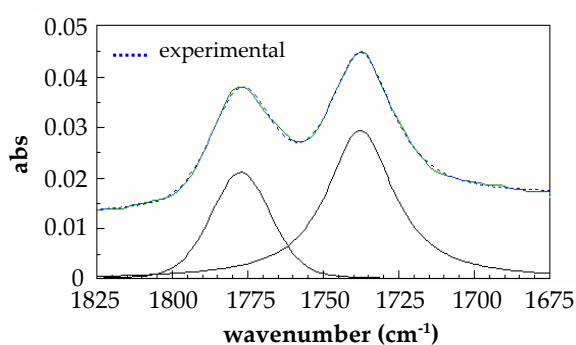


**Figure 2.** Cyclic and linear carbonyl ester absorption region of the FTIR-ATR spectra of the mixture DGEBA/ $\gamma$ -VL (2:1 molar) catalyzed by 1 phr of  $\text{Yb}(\text{OTf})_3$  cured at 160 °C. Dotted blue line corresponds to the experimental values and the other lines are obtained by deconvolution.

**Figure 3** shows the evolution of the conversions (corresponding to lactone and epoxide disappearance and to SOE appearance) vs. time. At first sight, it seems that the lactone reacts at short time more than epoxide, but we should consider that the proportion of epoxy groups to lactone is 4:1 and therefore that observation is not true. After 900 s at 140 °C, the lactone, which was run out, appears again. This appearance occurs when the epoxide has completely reacted and is due to the reversion of the SOEs.

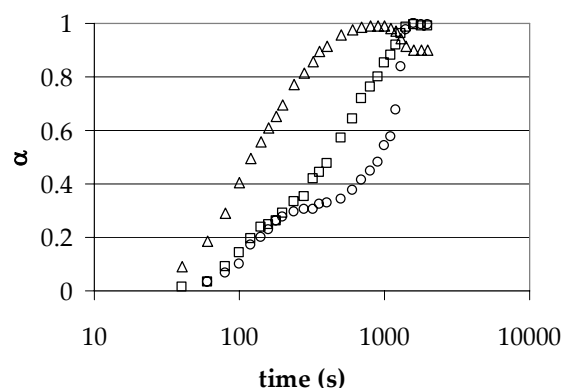


**Figure 3.** Plot of the experimental degrees of conversion ( $\square$ ) epoxy, ( $\Delta$ )  $\gamma$ -VL and ( $\circ$ ) SOE vs. curing time for the sample cured at 140 °C.

This process also leads to the formation of epoxide groups which immediately homopolymerize. After 1000 s of curing, SOEs disappear very quickly.

In **Figure 4** the conversion of  $\gamma$ -VL ( $\alpha_{\gamma\text{-VL}}$ ) is plotted against  $\alpha_{\text{epoxy}}$  and  $\alpha_{\text{SOE}}$ . The SOE conversion was evaluated by the formation of linear ester band, which appears on the SOE opening. Before looking at this figure, we should take into account that: (a) the molar ratio DGEBA/ $\gamma$ -VL is 2:1, (b) DGEBA has 2 equiv. of epoxide per mol, (c) each mol of  $\gamma$ -VL reacts with 1 equiv. of epoxide to produce one mole of SOE, and (d) the



homopolymerization of five-membered lactones is a thermodynamically unfavourable process. With these considerations, for  $\alpha_{\gamma\text{-VL}} \sim 0.4$  we can expect that the epoxy consumption ( $\alpha_{\text{epoxy}}$ ) should be 0.1, similar as it is found experimentally (0.125). Thus, we can conclude that until  $\alpha_{\gamma\text{-VL}} \sim 0.4$  the main reaction is the SOE formation.

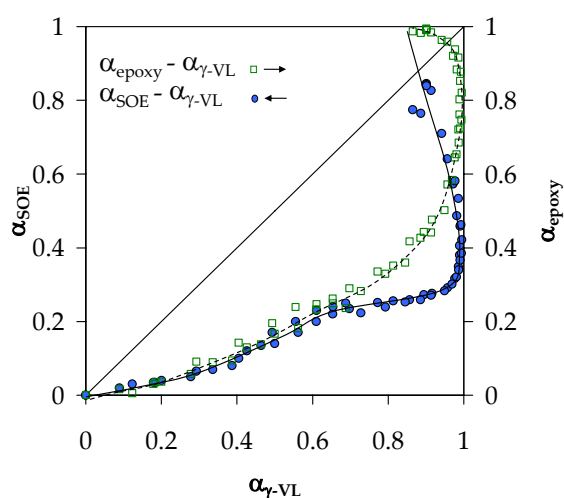


**Figure 4.** Plot of the experimental  $\alpha_{\gamma\text{-VL}}$  vs.  $\alpha_{\text{SOE}}$  and  $\alpha_{\gamma\text{-VL}}$  vs.  $\alpha_{\text{epoxy}}$  obtained at several temperatures.

In **Figure 4**, we can also see that when  $\alpha_{\gamma\text{-VL}} \sim 0.4$ , the SOE conversion is 0.1. If the copolymerisation of SOE and epoxide occurs, an additional consumption of  $\alpha_{\text{epoxy}} = 0.025$  should be expected. Because of the total consumption of epoxide ( $\alpha_{\text{epoxy}}$ ) is 0.125 at  $\alpha_{\gamma\text{-VL}} = 0.4$ , we can confirm that SOE preferentially copolymerizes with epoxide in the first stages of curing. After  $\alpha_{\gamma\text{-VL}} = 0.4$  the homopolymerization of epoxides can occur. The SOE polymerization takes mainly place when practically there is no lactone in the mixture  $\alpha_{\gamma\text{-VL}} \sim 1$ . That is because epoxy groups firstly prefer to react with lactones. When epoxy groups have almost disappeared, the band of  $\gamma\text{-VL}$

appears again. It seems that the remaining SOE groups prefer to revert to  $\gamma\text{-VL}$  and epoxy groups rather than homopolymerize, in contrast with what was observed in the curing of DGEBA/ $\gamma\text{-BL}$  mixtures<sup>16</sup>. In  $\gamma\text{-BL}$  mixtures, after the exhaustion of all epoxy groups, SOEs began to homopolymerize. The reversion of SOE in the present case can be attributed to the presence of the methyl group in the lactone.<sup>15</sup>

**Figures 5 - 7** show the plots of the degree of conversion of epoxide, lactone and SOE, respectively, against time, at several curing temperatures. These experimental curves were used to determine the isoconversional kinetics of each reactive process. By applying eq. (4) at different crosslinking degrees we obtained the kinetic parameters collected in **Table 1** for each reactive group. The precision of the applied isoconversional analyses is confirmed by the good regression of the isoconversional lines. As we can see, in general, both the activation energy and the pre-exponential factor increase along the curing process in all cases. The reactive processes associated to the epoxide and SOE groups present similar activation energies, whereas in the process in which lactone takes part the  $E$  value is substantially lower and it reacts at shorter times. In spite of the significance of the changes observed in the kinetic parameters, it is difficult to precisely know their meaning, because of the compensation effect between activation energy and pre-exponential factor. Thus, for a better comparison of the results it is necessary to know the rate constant,  $k$ , because it includes the effect of both parameters.

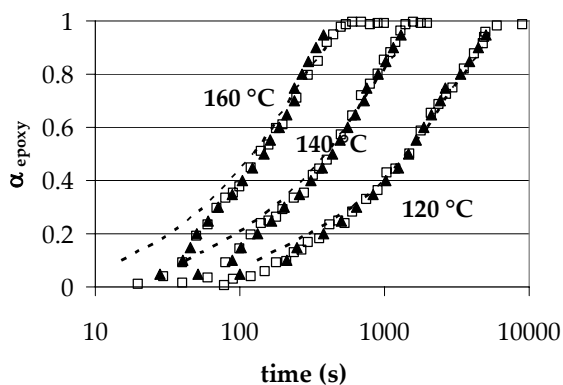


**Figure 5.** Plot of the experimental and simulated degrees of epoxy conversion vs. curing times for samples cured at different temperatures: (□) experimental isothermal curves; (▲) isoconversional isothermal data obtained by eq. (4) and isoconversional nonisothermal (---) data obtained by eq. (8).

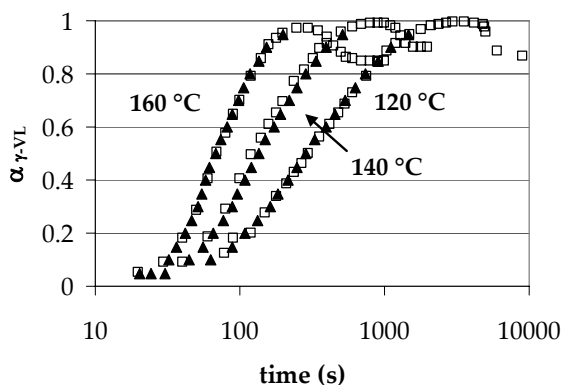


**Figure 6.** Plot of the experimental and simulated degrees of  $\gamma$ -VL conversion vs. curing time for samples cured at different temperatures: (□) experimental isothermal curves and (▲) isoconversional isothermal data obtained by eq. (4).

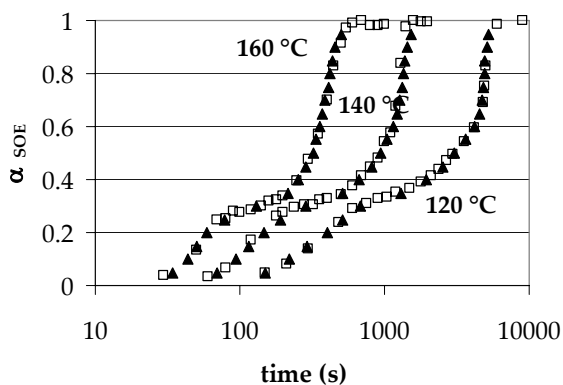


**Figure 7.** Plot of the experimental and simulated degrees of SOE conversion vs. curing time for samples cured at different temperatures: (□) experimental isothermal curves and (▲) isoconversional isothermal data obtained by eq. (4).

**Table 1.** Kinetic parameters of the curing obtained by FTIR for DGEGA/ $\gamma$ -VL reactive system catalyzed by ytterbium triflate

$\alpha$	epoxy (911 $\text{cm}^{-1}$ )			$\gamma$ -valerolactone (1776 $\text{cm}^{-1}$ )			SOE (1736 $\text{cm}^{-1}$ )		
	$E$ (kJ/mol)	$\ln A$ ( $\text{s}^{-1}$ )	$r$	$E$ (kJ/mol)	$\ln A$ ( $\text{s}^{-1}$ )	$r$	$E$ (kJ/mol)	$\ln A$ ( $\text{s}^{-1}$ )	$r$
0.1	58.6	-12.59	0.12	23.4	-3.02	0.77	57.0	-12.05	0.11
0.2	70.9	-15.78	0.17	34.1	-5.74	4.24	68.0	-14.82	0.15
0.3	78.0	-17.39	0.18	40.9	-7.42	6.39	59.1	-11.56	0.13
0.4	80.6	-17.74	0.16	46.6	-8.89	8.22	72.7	-14.66	0.08
0.5	81.4	-17.64	0.16	50.4	-9.76	9.39	79.2	-16.22	0.07
0.6	81.1	-17.31	0.16	55.7	-11.08	10.99	86.9	-18.28	0.08
0.7	82.1	-17.34	0.17	59.7	-11.99	12.18	88.2	-18.54	0.09
0.8	89.0	-19.13	0.18	65.1	-13.31	13.79	86.6	-18.02	0.12
0.9	91.0	-19.46	0.20	69.7	-14.34	15.18	85.6	-17.67	0.16

$\alpha$  refers to  $\alpha_{\text{epoxy}}$ ,  $\alpha_{\gamma\text{-VL}}$  and  $\alpha_{\text{SOE}}$  depending on the absorbance peak used

the intercept and the slope of the isoconversional relationship  $\ln t = \ln[g(\alpha)/A] + ER/T$  of the experimental data let us to obtain  $\ln[g(\alpha)/A]$  and  $E$ ;  $\ln A$  was calculated using kinetic model F1 and  $\ln[g(\alpha)/A]$



**Table 2.** Algebraic expressions for  $f(\alpha)$  and  $g(\alpha)$  for the kinetic model used

Model	$f(\alpha)$	$g(\alpha)$
A <sub>3/2</sub>	$(3/2)(1-\alpha)[- \ln(1-\alpha)]^{1/3}$	$[- \ln(1-\alpha)]^{2/3}$
A <sub>2</sub>	$2(1-\alpha)[- \ln(1-\alpha)]^{1/2}$	$[- \ln(1-\alpha)]^{1/2}$
A <sub>3</sub>	$3(1-\alpha)[- \ln(1-\alpha)]^{2/3}$	$[- \ln(1-\alpha)]^{1/3}$
A <sub>4</sub>	$4(1-\alpha)[- \ln(1-\alpha)]^{3/4}$	$[- \ln(1-\alpha)]^{1/4}$
R <sub>2</sub>	$2(1-\alpha)^{1/2}$	$1-(1-\alpha)^{1/2}$
R <sub>3</sub>	$3(1-\alpha)^{2/3}$	$1-(1-\alpha)^{1/3}$
D <sub>1</sub>	$1/2(1-\alpha)^{-1}$	$\alpha^2$
D <sub>2</sub>	$-\ln(1-\alpha)$	$(1-\alpha)\ln(1-\alpha)+\alpha$
D <sub>3</sub>	$3/2(1-\alpha)^{2/3}[-\alpha-(1-\alpha)^{-1/3}]$	$[1-(1-\alpha)^{1/3}]^2$
D <sub>4</sub>	$3/2(1-\alpha)^{1/3}[1-(1-\alpha)^{-1/3}]$	$(1-2/3\alpha)(1-\alpha)^{2/3}$
F <sub>1</sub>	$(1-\alpha)$	$-\ln(1-\alpha)$
Power	$2\alpha^{1/2}$	$\alpha^{1/2}$
n + m = 2; n = 1.5	$\alpha^{0.5}(1-\alpha)^{1.5}$	$[(1-\alpha)\alpha]^{-0.5}(0.5)^{-1}$
n = 2	$(1-\alpha)^2$	$-1+(1-\alpha)^{-1}$
n = 3	$(1-\alpha)^3$	$2^{-1}[-1+(1-\alpha)^{-2}]$
n = 2.4; m = 0.6	$\alpha^{0.6}(1-\alpha)^{2.4}$	$[((1-\alpha)/\alpha)^{-1.4}/1.4]+[((1-\alpha)/\alpha)^{-0.4}/0.4]$
n + m = 2; n = 1.7	$\alpha^{2.3}(1-\alpha)^{1.7}$	$[((1-\alpha)/\alpha)^{-0.7}/0.7]$
n = 1.5	$(1-\alpha)^{1.5}$	$[1-(1-\alpha)^{-0.5}/0.5]$

To determine  $k$  from the isoconversional parameters  $E$  and  $\ln[g(\alpha)/A]$ , first of all it is necessary to know the kinetic model that describes the reactive process, and then to evaluate the pre-exponential factor to finally calculate  $k$ , through the Arrhenius equation.

To determine the best-fit kinetic model  $g(\alpha)$ , which describes the reactive process during curing, we used the isoconversional parameters (**Table 1**) and the isokinetic relationships. From the parameter  $\ln[g(\alpha)/A]$  we obtained the pre-exponential factor for the different kinetic models used (**Table 2**). Then, we evaluated the isokinetic relationship, eq. (9), for all the models and processes studied. The results are collected in **Table 3** (the different  $T_{\text{iso}}$  were determined from the slopes of the IKRs). Although some models have good IKR, we considered that, in general, for all processes F1 model is the most suitable

because of its good regression and its  $T_{\text{iso}}$  lying on the experimental temperature range<sup>36</sup> (the  $T_{\text{iso}}$  obtained for epoxy groups is 124 °C, for  $\gamma$ -VL 115 °C and for SOE groups 147 °C). Although, there are other models with good regression, that could also be used to describe the curing, a model of  $n=1$  order (F1), of decelerative type, is consistent to describe the cationic curing of epoxy systems, in which the reaction rate decreases when the concentration of reactive species decreases. **Figure 8** shows the IKR plots of the reactive species for the F1 model. We can see that epoxy and SOE groups present similar IKR, whereas  $\gamma$ -VL has a slightly different value. These differences can be related with the different reactivity observed in **Figure 3**.

In isothermal curings, using the conventional kinetic methods, if the kinetic mechanism is unknown, it is not possible to determine the kinetic triplet.

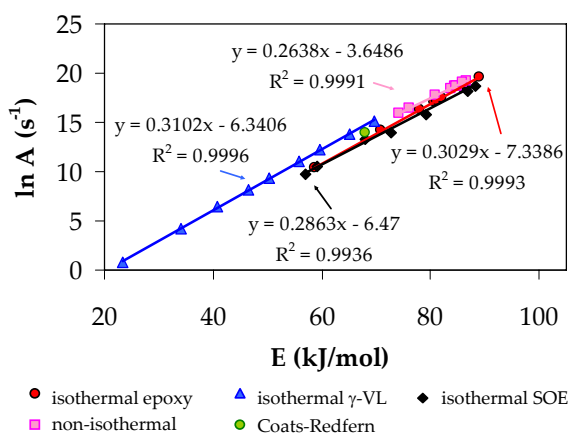


**Figure 8.** Isokinetic relationship (IKRs) deduced from isothermal data associated with each reactive group and for nonisothermal data for the F1 model. The plot includes the point (○) corresponding to the Coats-Redfern adjustment for the F1 model.

With the applied methodology we can determine the kinetic triplet by using the isoconversional parameters  $E$  and  $\ln[g(\alpha)/A]$ , taking into account that both parameters are related by means of the isokinetic relationships.

In **Table 1** we can see the pre-exponential factors and the  $k$  at 140 °C determined using the F1 model. We can observe as  $k_{\gamma\text{-VL}}$  values progressively increase due to the easiness in which the lactone reacts with the high quantity of epoxy groups that are in the mixture and to the formation of more active initiating species. In epoxy data, the values of  $k$  are in general constant but after conversion  $\alpha = 0.6$ , when there is not remaining lactone, these values slightly increase. This agrees with  $k_{\text{SOE}}$  values that increase, which seems to indicate that the copolymerization reaction becomes more important because the rest of the epoxy groups are available to react with SOE groups.

An alternative to isothermal curing is

the nonisothermal one made by DSC. One of the problems associated with this method is that the overall curing provides no kinetic information about the elemental processes.

In a previous study<sup>16</sup> using  $\gamma$ -BL, we determined that practically all the evolved heat in a dynamic experiment should be associated with the reactive processes in which epoxy groups participate, because the enthalpy per mol of epoxy group is about 95 kJ, whereas it is only 5 kJ by mol of lactone and 20 kJ per mol of SOE.<sup>16,38</sup> After complete curing all the epoxy and lactone groups have been opened and from the above mentioned enthalpies, the DGEBA/ $\gamma$ -VL 2:1 (mol/mol) formulation could evolve a theoretical enthalpy of 454 J/g, of which 448 J/g are associated to the opening of epoxides and 6 J/g to the lactone opening. Therefore, the kinetics obtained from nonisothermal experiments are expected to be similar to the kinetics obtained isothermally for the epoxy groups.

**Figure 9** shows the calorimetric curves of the nonisothermal curing of DGEBA with  $\gamma$ -VL at different heating rates. The shoulders that appear at low temperatures can be related with the contribution of the monomer activated mechanism (AM) that coexists with the activated chain end mechanism (ACE) associated to the main peak, as we described for similar DGEBA/ $\gamma$ -BL systems.<sup>13</sup> **Figure 10** shows the plot of conversion vs. curing temperature for the nonisothermal curing of DGEBA with  $\gamma$ -VL at different heating rates calculated by integration of the DSC curves (**Figure 9**). Using eq. (8) we determined the iso-



**Table 3.** Isokinetic parameters obtained from the compensation curves for the different models used

Model	epoxy (910cm <sup>-1</sup> )			γ-valerolactone (1775cm <sup>-1</sup> )			SOE (1737cm <sup>-1</sup> )					
	a (mol/kJ)	b (s <sup>-1</sup> )	T <sub>iso</sub> (°C)	r	a (mol/kJ)	b (s <sup>-1</sup> )	T <sub>iso</sub> (°C)	r	a (mol/kJ)	b (s <sup>-1</sup> )	T <sub>iso</sub> (°C)	r
<b>A3/2</b>	0.272	-4.686	170	0.9965	0.288	-5.094	144	0.9996	0.262	-4.476	186	0.9935
<b>A2</b>	0.256	-3.360	197	0.9933	0.277	-4.471	161	0.9997	0.250	-3.479	208	0.9919
<b>A3</b>	0.240	-2.033	228	0.9884	0.266	-3.847	178	0.9997	0.238	-2.482	232	0.9888
<b>A4</b>	0.232	-1.370	244	0.9851	0.261	-3.535	188	0.9997	0.232	-1.984	245	0.9866
<b>R2</b>	0.296	-7.980	134	0.9985	0.303	-7.237	124	0.9992	0.279	-7.161	158	0.9952
<b>R3</b>	0.292	-7.362	139	0.9980	0.300	-6.741	128	0.9989	0.276	-6.570	163	0.9957
<b>D1</b>	0.357	-12.803	64	0.9982	0.339	-9.040	82	0.9963	0.320	-10.288	103	0.9933
<b>D2</b>	0.368	-14.212	54	0.9983	0.349	-10.002	72	0.9974	0.331	-11.574	91	0.9913
<b>D3</b>	0.382	-16.580	42	0.9973	0.362	-11.873	59	0.9987	0.344	-13.833	76	0.9875
<b>D4</b>	0.373	-16.001	50	0.9981	0.353	-11.626	67	0.9979	0.335	-13.326	86	0.9902
<b>F1</b>	<b>0.303</b>	<b>-7.339</b>	<b>124</b>	<b>0.9993</b>	<b>0.310</b>	<b>-6.341</b>	<b>115</b>	<b>0.9996</b>	<b>0.286</b>	<b>-6.470</b>	<b>147</b>	<b>0.9936</b>
<b>Power</b>	0.246	-2.736	216	0.9881	0.268	-4.210	176	0.9990	0.240	-2.938	227	0.9909
<b>n+m=2 n=1.5</b>	0.269	-3.478	174	0.9970	0.290	-4.171	141	0.9999	0.263	-3.542	184	0.9897
<b>n=2</b>	0.329	-8.961	93	0.9975	0.336	-7.127	85	0.9996	0.313	-7.982	112	0.9820
<b>n=3</b>	0.360	-10.924	61	0.9881	0.368	-8.134	54	0.9960	0.345	-9.864	76	0.9596
<b>n=2.4 m=0.6</b>	0.278	-3.650	160	0.9963	0.304	-4.254	122	0.9979	0.277	-3.928	162	0.9775
<b>n+m=2 n=1.7</b>	0.293	-5.730	138	0.9988	0.309	-5.412	117	0.9998	0.283	-5.377	152	0.9879
<b>n=1.5</b>	0.315	-8.104	109	0.9993	0.322	-6.702	100	0.9999	0.299	-7.173	130	0.9892

T<sub>iso</sub> (°C) calculated using a = 1/RT<sub>iso</sub>



conversional parameters and then we calculated the isothermal parameters from eq.(4). From these parameters (**Table 4**) we simulated the conversion of epoxy groups, which are represented in **Figure 5**. The goodness of the simulation with the exception of a short deviation at low conversions, probably related with the contribution of AM mechanism in nonisothermal curing and the regressions obtained (**Table 4**) in addition to the fact that the nonisothermal kinetic parameters are similar to those of epoxy groups, confirm that our assumptions are correct.

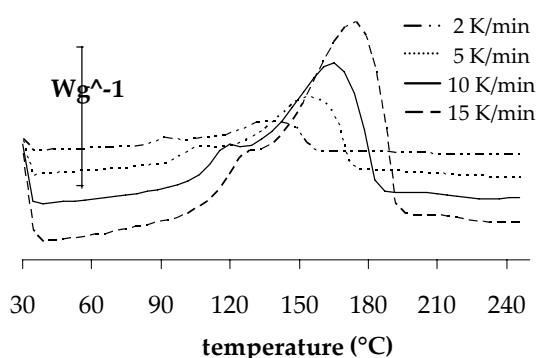


**Figure 9.** DSC scanning curves vs. temperature for nonisothermal curing at different heating rates.

To determine the kinetic best-fit model from nonisothermal parameters we used two different strategies. Coats-Redfern method allows, by applying eq.(7), to determine  $E$  and  $\ln A$  for the different models. **Table 5** shows all the results obtained at a heating rate of 15 K/min. We select F1 as the preferred model because it presents the best adjustment. Some other models also have good regressions, but we did not consider them because of  $E$  is quite different from that obtained isoconversionally (considered to be the true  $E$ ). If the variation in the activation energy

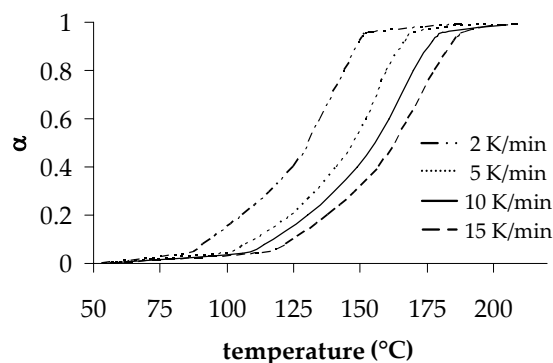


**Figure 10.** Conversion degree vs. temperature, calculated according eq.(2) for nonisothermal curing at different heating rates.

with the degree of conversion is taken into account, the kinetic model can be determined as in the isothermal case. From the nonisothermal values in **Table 4**, we calculated the IKRs for the different models. **Table 5** shows the results. Again the F1 model gives the best regression and the  $T_{iso}$  of 183 °C practically lies in the experimental range of curing temperatures. In **Table 4** we can see the pre-exponential factors determined from the isoconversional values by the F1 model and, in **Figure 8**, we can see the different IKR for the different reactive groups and processes. The kinetic parameters determined by the Coats-Redfern method practically lays on the extrapolated nonisothermal IKR. This result confirms that the nonisothermal methodology used is correct to determine the best-fit kinetic model.

## Conclusions

FTIR spectroscopy allows analyzing the individual elemental chemical reactions that take part in a complex curing process, such as the cationic cross-linking of DGEBA/ $\gamma$ -VL mixtures. In this reactive system we determined the con-



**Table 4.** Kinetic parameters of nonisothermal curing obtained by DSC

$\alpha$	$E$ (kJ/mol)	$\ln[AR/g(\alpha)E]$ (K/s)	$\ln[g(\alpha)/A]$ (s)	$\ln A$ (s <sup>-1</sup> )	$r$
0.1	74.2	0.15	-18.18	15.93	0.9960
0.2	76.0	0.15	-17.91	16.41	0.9845
0.3	80.9	0.16	-18.74	17.71	0.9906
0.4	84.4	0.17	-19.32	18.65	0.9950
0.5	83.7	0.16	-18.74	18.38	0.9936
0.6	84.9	0.16	-18.79	18.70	0.9953
0.7	84.7	0.15	-18.47	18.66	0.9959
0.8	86.6	0.16	-18.76	19.23	0.9985
0.9	85.8	0.15	-18.21	19.04	0.9994

the intercept and the slope of the isoconversional relationship  $\ln[\beta/T^2]=\ln[AR/g(\alpha)E]-E/RT$  from the nonisothermal data let us to obtain  $\ln[AR/g(\alpha)E]$  and  $E$   
 $\ln[g(\alpha)/A]$  was calculated on the basis of  $\ln[AR/g(\alpha)E]$  and  $E$   
 $\ln A$  was calculated using kinetic model F1 and  $\ln[g(\alpha)/A]$

**Table 5.** Arrhenius parameters determined by Coats-Redfern method and the isokinetic parameters [eq. (9)]

Model	Coats-Redfern			Isokinetic relationship			
	$E$ (kJ/mol)	$\ln A$ (s <sup>-1</sup> )	$r$	$a$ (mol/kJ)	$b$ (s <sup>-1</sup> )	$T_{iso}$ (°C)	$r$
A3/2	6.7	14.9	0.9961	0.194	2.226	345	0.9909
A2	2.9	11.1	0.9599	0.160	5.164	479	0.9714
A3	-1.0	7.2	0.9947	0.125	8.101	688	0.9238
A4	-3.1	5.1	0.9933	0.108	9.570	843	0.8796
R2	57.5	10.0	0.9995	0.245	-3.298	219	0.9980
R3	60.9	10.6	0.9990	0.236	-2.228	237	0.9956
D1	104.2	23.2	0.9982	0.368	-13.507	54	0.9967
D2	122.1	28.8	0.9996	0.397	-16.366	30	0.9968
D3	128.8	28.6	0.9991	0.433	-20.572	5	0.9933
D4	119.7	25.8	0.9996	0.409	-18.760	21	0.9961
<b>F1</b>	<b>68.1</b>	<b>14.0</b>	<b>0.9964</b>	<b>0.264</b>	<b>-3.649</b>	<b>183</b>	<b>0.9996</b>
Power	20.7	-0.4	0.9968	0.134	7.105	626	0.9189
n+m=2 n=1.5	43.7	7.9	0.9765	0.195	3.209	344	0.9933
n=2	94.4	22.1	0.9796	0.334	-8.943	87	0.9792
n=3	126.5	31.8	0.9586	0.420	-15.446	13	0.9380
n=2.4 m=0.6	56.2	12.2	0.9308	0.228	1.078	254	0.9646
n+m=2 n=1.7	63.9	13.6	0.9784	0.251	-1.711	207	0.9917
n=1.5	80.4	17.8	0.9893	0.297	-6.124	132	0.9937

isokinetic relationship obtained from eq. (9)

versions and kinetics of the different epoxy,  $\gamma$ -VL and SOE reactive groups. Calorimetric studies can not separate the elemental processes and only provided the global kinetics of the cross-linking. If the elemental reactions have different enthalpies, the obtained results are only

representative of the process with the highest enthalpy and extension.

Isoconversional methods make it possible the evaluation of the kinetic parameters on varying the degree of conversion, but they do not reveal the



complete kinetic triplet. Using these methods, in combination with the isokinetic relationships in the isothermal and non-isothermal curing, it has been possible to calculate the complete kinetic triplet [ $E$ ,  $A$ ,  $g(\alpha)$ ].

The kinetic parameters, in addition to the FTIR results, indicate that the reaction of  $\gamma$ -VL and epoxides is more favoured than the homopolymerization of epoxides or the ring-opening of SOE groups.

All the elemental reactions that participate in the curing of DGEBA epoxy resins with  $\gamma$ -VL catalyzed by ytterbium triflate followed an  $n$ th-order kinetic model, F1 type.

#### Acknowledgements

The authors from the Universitat Politècnica de Catalunya would like to thank CICYT and FEDER (MAT2004-04165-C02-02 and ENER2007-6784-C03-01) for their financial support. The authors from the Universitat Rovira i Virgili would like to thank the CICYT (Comisión Interministerial de Ciencia y Tecnología) and FEDER (Fondo Europeo de Desarrollo Regional) (MAT2005-01806).

#### References

- [1] SG. Croll, *J. Coat. Technol.*, 51 (1979) 49.
- [2] RK. Sadhir, MR. Luck, (Eds), *Expanding Monomers. Synthesis, Characterization and Applications*, CRC Press, Boca Raton, FL 1992.
- [3] WJ. Bailey, RL. Sun, *Polym. Prep. Am. Chem. Soc., Div. Polym. Chem.*, 13 (1972) 400.
- [4] WJ. Bailey, *Elastoplast*, 5 (1973) 142.
- [5] WJ. Bailey, *J. Polym. Sci. Polym. Chem. Ed.*, 14 (1976) 1735.
- [6] WJ. Bailey, RL. Sun, H. Katsuki, T. Endo, H. Iwana, R. Tsushima, K. Saigou, MM. Bitritto, *Am. Chem. Soc. Symp. Ser.* 59 (1977) 38.
- [7] K. Bodenbenner, *Justus Liebig Ann.*, 625 (1959) 183.
- [8] M. Tokizava, N. Okada, N. Wakabayashi, *J. Appl. Polym. Sci.* 50 (1993) 875.
- [9] K. Morio, H. Murase, H. Tsuchylla, T. Endo, *J. Appl. Polym. Sci.* 32 (1986) 5727.
- [10] L. Matějka, P. Chabanne, L. Tighzert, JP. Pascault, *J. Polym. Sci. Part A: Polym. Chem.*, 32 (1994) 1447.
- [11] S. Kobayashi (Ed), *Lanthanides: Chemistry and Use in Organic Synthesis, Topics in Organometallic Chemistry*, Springer Verlag, Berlin, 1999.
- [12] S. Kobayashi, M. Sugiura, H. Kitagawa, WWL. Lam, *Chem. Rev.* 102 (2002) 2227.
- [13] C. Mas, A. Mantecón, A. Serra, X. Ramis, JM. Salla, *J. Polym. Sci. Part A: Polym. Chem.* 42 (2004) 3782.
- [14] L. González, X. Ramis, JM. Salla, A. Mantecón, A. Serra, *J. Polym. Sci. Part A: Polym. Chem.* 44 (2006) 6869.
- [15] M. Arasa, X. Ramis, JM. Salla, A. Mantecón, A. Serra, *J. Polym. Sci. Part A: Polym. Chem.* 45 (2007) 2129.
- [16] C. Mas, X. Ramis, JM. Salla, A. Mantecón, A. Serra, *J. Polym. Sci. Part A: Polym. Chem.* 41 (2003) 2794.
- [17] X. Ramis, A. Cadenato, JM. Morancho, JM. Salla, *Polymer* 44 (2003) 2067.
- [18] S. Vyazovkin, W. Linert, *Int. Rev. Phys. Chem.*, 14 (1995) 355.
- [19] P. Budrugaec, D. Homentcovschi, E. Segal, *J. Therm. Anal. Cal.*, 63 (2001) 457.
- [20] JM. Salla, X. Ramis, JM. Morancho, A. Cadenato, *Thermochim. Acta*, 388 (2002) 355.



- [21] Z. Zhiqiang, J. Bangkun, H. Pingsheng, J. Appl. Polym. Sci. 84 (2002) 1457.
- [22] H. Fridman, J. Polym. Chem. C6 (1963) 183.
- [23] S. Vyazovkin, N. Sbirrazzuoli, Macromol. Chem. Phys. 200 (1999) 2294.
- [24] AW. Coats, JP. Redfern, Nature 207 (1964) 290.
- [25] S. Vyazovkin, D. Dollimore, J. Chem. Inform. Comput. Sci. 36 (1996) 42.
- [26] HE. Kissinger, Anal. Chem. 29 (1957) 1702.
- [27] A. Cadenato, JM. Morancho, X. Fernández-Francos, JM. Salla, X. Ramis, Therm. Anal. Cal. 89 (2007) 233.
- [28] JH. Flynn, LA. Wall, J. Res. Natl. Bur. Stad. A Phys. Chem. 70A (1996) 487.
- [29] T. Ozawa, Bull. Chem. Soc. Jpn. 38 (1965) 1881.
- [30] X. Ramis, JM. Salla, A. Cadenato, JM. Morancho, Therm. Anal. Cal. 72 (2003) 707.
- [31] X. Ramis, JM. Salla, J. Polym. Sci. Part B: Polym. Phys. 35 (1997) 371.
- [32] S. Vyazovkin, Int. J. Chem. Kinet. 28 (1996) 95.
- [33] S. Vyazovkin, CA. Wight, Annu. Rev. Phys. Chem. 48 (1997) 125.
- [34] S. Vyazovkin, W. Linert, J. Solid State Chem. 114 (1995) 392.
- [35] W. Linert, RF. Jameson, Chem. Soc. Rev. 18 (1989) 477.
- [36] S. Vyazovkin, W. Linert, Chem. Phys. 193 (1995) 109.
- [37] X. Ramis, JM. Salla, C. Mas, A. Mantecón, A. Serra, J. Appl. Polym. Sci. 92 (2004) 381.
- [38] AA. Yevstropov, BV. Lebedev, YG. Kipararisova, VA. Alekseyev, GA. Stashina, Vysokomol. Soedin. Ser. A22 (1980) 2450.

2.5 STUDY ON THE EFFECT OF RARE EARTH METAL  
TRIFLATES AS INITIATORS IN THE CATIONIC CURING OF  
THE DGEBA/ $\gamma$ -VALEROLACTONE MIXTURES AND  
CHARACTERIZATION OF THE THERMOSETS OBTAINED

---

*Mercè Arasa, Xavier Ramis, Josep Maria Salla, Francesc Ferrando, Àngels Serra, Ana Mantecón; European Polymer Journal, 45, 1282-1292 (2009)*

UNIVERSITAT ROVIRA I VIRGILI  
NOUS TERMOESTABLES EPOXÍDICS MODIFICATS AMB GAMMA-LACTONES I BIS-GAMMA-LACTONES CONDENSADES  
M<sup>a</sup> Mercè Arasa Bertomeu  
ISBN:978-84-692-4157-8/DL:T-1171-2009



# STUDY ON THE EFFECT OF RARE EARTH METAL TRIFLATES AS INITIATORS IN THE CATIONIC CURING OF DGEBA/ $\gamma$ - VALEROLACTONE MIXTURES AND CHARACTERIZATION OF THE THERMOSETS OBTAINED

Mercè Arasa,<sup>1</sup> Xavier Ramis,<sup>2</sup> Josep Maria Salla,<sup>2</sup> Francesc Ferrando,<sup>3</sup> Àngels  
Serra,<sup>1</sup> Ana Mantecón<sup>1</sup>

<sup>1</sup>Dpt. Q. Analítica i Q. Orgànica, URV. C/Marcel·lí Domingo s/n, 43007 Tarragona, Spain

<sup>2</sup> Lab. Termodinàmica, ETSEIB. UPC, Av. Diagonal 647, 08028 Barcelona, Spain

<sup>3</sup> Dpt. d'Engineria Mecànica, URV. C/Paisos Catalans 26, 43007 Tarragona, Spain

## Abstract

The thermal cationic curing of mixtures in different proportions of diglycidylether of bisphenol A (DGEBA) with  $\gamma$ -valerolactone ( $\gamma$ -VL) initiated by scandium, ytterbium and lanthanum triflates or a conventional  $\text{BF}_3\cdot\text{MEA}$  initiator was investigated. The non-isothermal differential scanning calorimetry (DSC) experiments at a controlled heating rate were used to evaluate the evolution of the reactive systems.  $\text{BF}_3\cdot\text{MEA}$  and rare earth metal triflates initiated curing systems follow a different evolution. Among rare earth metal triflates tested, the scandium was the most active initiator. The phenomenological changes that take place during curing were studied and represented in a time-temperature-transformation (TTT) diagram. Some characteristics of the materials were also evaluated.

*Keywords:* Epoxy resins, crosslinking, thermosets, cationic polymerization, calorimetry.

## Introduction

The processability of an epoxy resin critically depends on the rate and extent of polymerization under process conditions. Therefore, kinetic characterisation of the reactive system is not only important for a better understanding of structure-properties relationships but it is also fundamental in optimizing process conditions and product quality.

The choice of a particular curing initiator depends on the processing requirements, e.g. viscosity, pot-life, curing temperature, mixing ratio, etc. and the end-use requirements, e.g. thermal and chemical resistance or toughness of the cured material. Initiators also have a large influence on the molecular weight between crosslinks, long term stability



and reactivity in different chemical and physical environments and even in the total cost of the resulting material. Differential scanning calorimetry (DSC) is one of the most used experimental techniques to evaluate the kinetics of a reactive system. The results of the kinetic study can be used for various purposes, i.e. to analyze how an initiator or different proportions of a co-reactant can affect a reactive system or how the temperature can affect the evolution of the reaction.<sup>1</sup>

The cure reaction of thermosetting polymers has been investigated extensively.<sup>2,3</sup> Among them, epoxy resins studies are relevant because of their industrial applications.<sup>4-6</sup> However, they have been mainly performed on epoxy-amine traditional systems and few studies are based on cationic systems.<sup>7,8</sup> The catalytic curing of epoxy resins has been applied as an alternative to amine or anhydride agents. Generally, cationic initiators involve complexes such as  $\text{BF}_3 \cdot \text{amine}$  or  $\text{BF}_3 \cdot \text{ether}$ .<sup>9</sup> Although boron trifluoride complexes have been used for several decades, they are not only hygroscopic, but also at high temperature and high humidity the electrical properties of the thermosets obtained tend to deteriorate. Moreover,  $\text{BF}_3$  complexes are difficult to solve in DGEBA resins.

Rare earth triflates are commercially available Lewis acids that maintain their catalytic activity even in water and are regarded as environmentally friendly catalysts.<sup>10-12</sup> Generally, scandium triflate shows a higher catalytic effect than lanthanide triflates, due to its higher

Lewis acidity attributed to its small ionic radius.<sup>13</sup> We demonstrated that lanthanide triflates can effectively act as cationic initiators in the curing of epoxy resins.<sup>14</sup>

The ionic character of the rare earth metal triflates makes difficult to dissolve these initiators in DGEBA resins. To form a homogeneous mixture, Chabanne et al.<sup>15</sup> added a little proportion of a  $\gamma$ -lactone to a DGEBA/ $\text{BF}_3$ -amine complex. They observed that this lactone was incorporated into the network structure in spite of  $\gamma$ -lactones cannot homopolymerize in cationic systems. Their incorporation was explained by the formation of an intermediate spiroorthoester when reacting with DGEBA. This intermediate compound further homo- or copolymerize to produce poly(ether-ester) three-dimensional networks. The introduction of  $\gamma$ -lactone in the reactive system increases its reactivity and, when a larger proportion of lactone is added to the mixture, some characteristics of the materials can be improved. In previous studies we could demonstrate that thermal degradability, desirable to obtain reworkable thermosets, was highly increased.<sup>16</sup> Moreover, the incorporation of aliphatic structures between crosslinks improved the flexibility and in some cases the shrinkage after gelation was reduced. This fact diminishes the internal stress generated during curing.<sup>17</sup>

The present study deals with the curing of mixtures of diglycidylether of bisphenol A (DGEBA) with  $\gamma$ -valerolactone ( $\gamma$ -VL) in several proportions using scandium, ytterbium and lantha-



num triflates or  $\text{BF}_3 \cdot \text{MEA}$  as initiators and with the characterization of the materials obtained. The copolymerization of DGEBA with  $\gamma$ -valerolactone in the presence of rare earth triflates led, in addition to the four expected reactions (formation of SOE, homopolymerization of SOE and copolymerization with epoxide, and epoxide homopolymerization) to the reversion of SOE, producing different proportions of free lactone which remained entrapped in the thermoset (**Scheme 1**).

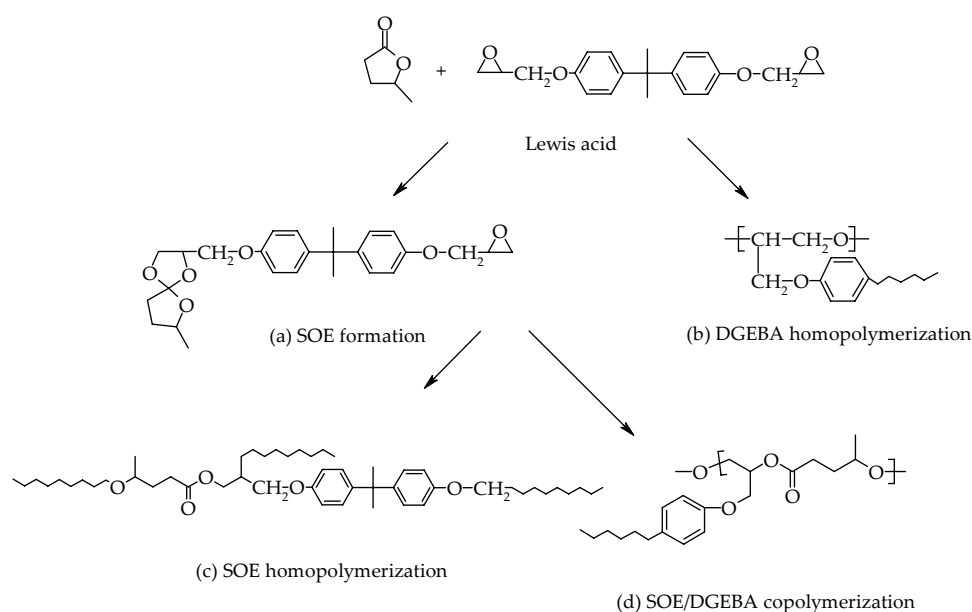
The cationic copolymerization between DGEBA and lactones are scarcely studied from the point of view of the kinetics.<sup>15,18-20</sup> As has been previously demonstrated, the copolymerization mechanism is rather complex and in the case of  $\gamma$ -valerolactone a depolymerization process that leads to the appearance of free lactone in the material has also been detected.<sup>21</sup> Moreover, cationic ring-opening polymerizations of cyclic monomers can occur by the activated chain

end (ACE) or by the activated monomer (AM) mechanisms and also back-biting processes can take place.<sup>22</sup> All these processes overlap during curing and therefore only a global study of curing can be made. At the same time, physical processes (gelation and vitrification) also take place and can affect not only the curing process but also the physical properties of the material.<sup>4</sup> The progress of the isothermal curing process and the state of the material has been summarized in a TTT diagram.

## Experimental Part

### Materials

Diglycidylether of bisphenol A (DGEBA) EPIKOTE RESIN 827 from Shell Chemicals (Epoxy Equiv. = 182.08 g/eq),  $\gamma$ -valerolactone ( $\gamma$ -VL), lanthanum (III), ytterbium (III) and scandium (III) trifluoromethanesulfonates and boron-trifluoride monoethylamine ( $\text{BF}_3 \cdot \text{MEA}$ ) (Aldrich) were used as received.



Scheme 1



### Preparation of the curing mixtures

The samples were prepared by the mixing the selected initiator in the corresponding amount of  $\gamma$ -VL and adding the required proportion of DGEBA with manual stirring. The amount of initiator is collected in **Table 1** and it is expressed in phr (1 part for 100 parts of lactone/resin mixture, w/w). The prepared mixtures were kept at  $-18\text{ }^{\circ}\text{C}$  before use.

### Characterization and measurements

**Calorimetric study.** Calorimetric studies were carried out on a Mettler DSC-821e thermal analyzer in covered Al pans under  $\text{N}_2$  at 2, 5, 10 and  $15\text{ }^{\circ}\text{C}/\text{min}$ . The calorimeter was calibrated using an indium standard (heat flow calibration) and an indium-lead-zinc standard (temperature calibration). The samples weighed approximately 7-9 mg. In the dynamic curing process the degree of conversion by DSC ( $\alpha_{\text{DSC}}$ ) was calculated as follows:

$$\alpha_{\text{DSC}} = \Delta H_T / \Delta H_{\text{dyn}} \quad (1)$$

where  $\Delta H_T$  is the heat released up to a temperature  $T$ , obtained by integration of the calorimetric signal up to this temperature, and  $\Delta H_{\text{dyn}}$  is the total reaction heat associated with the complete conversion of all reactive groups.

The  $T_g$  was measured as the half-way point of the jump in the heat capacity when the material changed from the glassy to the rubbery state at  $20\text{ }^{\circ}\text{C}/\text{min}$ .

The kinetics of the reaction is usually described by the following rate equation:

$$\frac{d\alpha}{dt} = Af(\alpha)\exp\left(-\frac{E}{RT}\right) \quad (2)$$

where  $t$  is time,  $A$  is the pre-exponential factor,  $E$  is the activation energy,  $T$  is the absolute temperature,  $R$  is the gas constant, and  $f(\alpha)$  is the differential conversion function.

By integrating the rate equation, eq. (2), under non-isothermal conditions and using the Coats and Redfern<sup>23</sup> approximation to solve the so-called temperature integral and considering that  $2RT/E$  is much lower than 1, the Kissinger-Akahira-Sunose (KAS) equation may be written:<sup>24</sup>

$$\ln\left(\frac{\beta_i}{T_{\alpha,i}^2}\right) = \ln\left[\frac{A_\alpha R}{g(\alpha)E_\alpha}\right] - \frac{E_\alpha}{RT_{\alpha,i}} \quad (3)$$

where  $\beta$  is the heating rate,  $g(\alpha)$  is the integral conversion function, the subscript  $\alpha$  refers to the value related to a considered conversion and  $i$  to a given heating rate.

For each conversion degree, the linear plot of  $\ln(\beta_i/T_{\alpha,i}^2)$  versus  $1/T_{\alpha,i}$  enables  $E_\alpha$  and  $\ln[A_\alpha R/g(\alpha)E_\alpha]$  to be determined from the slope and the intercept. These nonisothermal kinetic parameters are directly related for every value of  $\alpha$  with the isothermal integral kinetic parameter  $\ln[g(\alpha)/A_\alpha]$ . So we can simulate isothermal by using nonisothermal data curing without knowing  $g(\alpha)$ .

The kinetic analysis was carried out using an integral isoconversional method (eq. (3)). The basic assumption of this method is that the reaction rate at a given conversion is only a function of the temperature.<sup>25,26</sup> Isoconversional me-



thods make it possible to determine easily the dependence of  $E_{\alpha}$  on the degree of conversion in complex processes. Isoconversional STARE software from Mettler-Toledo was used in order to calculate conversion degrees and kinetics of the processes.

**Gelation point determination.** The gelation point was determined by solubility tests. Before gelation the material is completely soluble in dichloromethane and once past the gel point the solubility falls steeply. The conversion at the gelation was determined by the residual enthalpy in the DSC of the gelled sample.

**Thermomechanical analysis.** Thermal-dynamic-mechanical analyses (DMTAs) were carried out with a TA Instruments DMTA 2980 analyzer. The samples were cured isothermally in a mould at 150 °C for 1 h and were then subjected to a post-curing for 5 h at 160 °C. Three point bending of 10 mm was performed on cylindrical samples (10 × 4 mm, approximately). The apparatus operated dynamically at 5 °C/min from 35 to 200 °C at a frequency of 1 Hz.

The linear thermal expansion coefficients in the glassy and rubbery states were measured by thermal mechanical analysis using a Mettler-Toledo TMA40 heating at 10 °C/min as:

$$\alpha = \frac{1}{L_0} \frac{dL}{dT} = \frac{1}{L_0} \frac{dL/dt}{dT/dt} \quad (4)$$

where,  $L_0$  is the initial length. The gel conversion was determined by the residual enthalpy in the DSC of the sample gelled in TMA, as we explain in a

previous paper.<sup>27</sup>

**Mechanical tests.** Microhardness was measured with a Wilson Wolpert (Micro-Knoop 401MAV) device following the ASTM D1494-98(2002) standard procedure. The Knoop microhardness (HKN) was calculated from the following equation:

$$HKN = \frac{L}{A_p} = \frac{L}{I^2 C_p} \quad (5)$$

where,  $L$  is the load applied to the indenter (0.025 kg),  $A_p$  is the projected area of indentation in mm<sup>2</sup>,  $I$  is the measured length of long diagonal of indentation in mm,  $C_p$  is the indenter constant ( $7.028 \times 10^{-2}$ ) relating  $I^2$  to  $A_p$ .

Young modulus was measured with the Universal Testing Machine Hounsfield 10-KS. Tensile tests were performed on cylindrical samples of 4 mm of diameter. The gauge length was 50 mm and the test cross-head speed was 5 mm/min.

## Results and discussion

In a previous work<sup>21</sup> we studied the curing of mixtures of DGEBA/ $\gamma$ -VL 2:1(mol/mol) initiated by scandium, ytterbium and lanthanum triflates and BF<sub>3</sub>·MEA as Lewis acids by FTIR/ATR. When we used 1 phr of scandium triflate or 3 phr of ytterbium triflate as initiator, a depolymerization process was also observed. This process was related to the highest Lewis acidity of these catalysts. The homopolymerization of epoxide on changing the metal triflate was favoured in the order Sc > Yb > La, which is in accordance to the Pearson's hardness.<sup>28</sup>



The homopolymerization was also favoured when a higher proportion of  $\text{Yb}(\text{OTf})_3$  was used.

In the present work we studied the evolution of the curing process on changing the initiator and its proportion and the co-monomers ratio in the mixture. Previously,<sup>29,30</sup> we observed that the higher the Lewis acidity of the lanthanide triflates (from lanthanum to ytterbium) the higher the curing rate was. The  $\text{BF}_3$  complex need to be used in a higher proportion to reach the total curing and the materials obtained showed a higher  $T_g$ , which seems to indicate that the curing process present some differences.

In many exothermic polymerizations is difficult an accurate determination of the heat of reaction through isothermal experiments and the subsequent deduction of the kinetics from these values. When reactions are performed at high temperatures, some of the heat can be lost during the stabilization of the apparatus, whereas at low temperatures, the heat is released slowly and can fall below the sensitivity of the calorimeter. Another problem arises when a physical phenomenon (e.g. vitrification) takes place. One alternative in both cases is to simulate isothermal curing from non-isothermal data.<sup>31</sup> Thus, in this work we used the non-isothermal differential scanning calorimetry experiments at a controlled heating rate as the most suitable procedure for obtaining kinetic information of the reactive systems.

**Figure 1** shows the calorimetric curves of the curing process for the

formulation DGEBA/ $\gamma$ -VL 2:1 (mol/mol) with the four initiators tested. As we can see, the curves of the scandium and ytterbium triflates initiated curing show a main maximum and a shoulder, greater for scandium. The contribution of this shoulder to the total enthalpy released can be related to the extension of the homopolymerization of epoxide, as we previously saw by FTIR spectroscopy.<sup>21</sup>

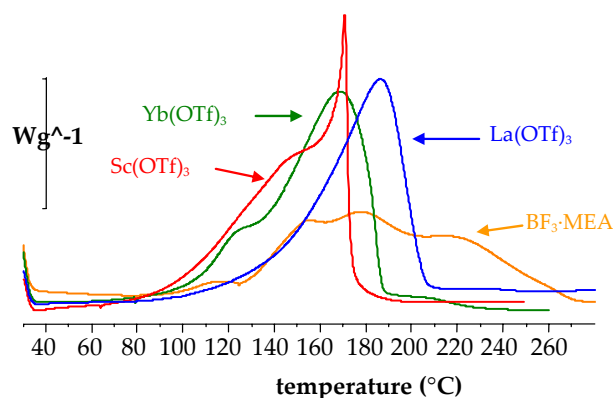


**Figure 1.** DSC scanning curves versus temperature of curing obtained through dynamic DSC experiments of DGEBA/lactone 2:1 (mol/mol) mixture initiated by 1 phr of Sc, Yb and La triflates and  $\text{BF}_3 \cdot \text{MEA}$  at a heating rate of  $10^\circ\text{C}/\text{min}$ .

In a previous work<sup>20</sup> on the curing of DGEBA/ $\gamma$ -butyrolactone ( $\gamma$ -BL) mixtures with ytterbium triflate we saw the appearance of two partially overlapped exotherms that change in shape depending on the competition between two propagation mechanisms related to the epoxy homopolymerization: monomer activated mechanism (AM) and activated chain end mechanism (ACE) and the exotherm at lower temperature could be assigned to the AM contribution (see **Scheme 2**). In that paper we could prove that the higher the acidity of the polymerization medium the higher the contribution of the AM mechanism.



Thus, the pattern of the curves in **Figure 1** seems to indicate a greater contribution of AM mechanism when we move from the lanthanum to scandium. AM mechanism requires the activation of epoxy monomer by the initiator and therefore the oxophilicity (related to Lewis acidity) of Sc, Yb and La, which are 2.37, 2.09 and 1.36, respectively,<sup>32</sup> can justify the behavior observed. **Figure 1** also shows the curve corresponding to the BF<sub>3</sub>·MEA initiated curing. For this initiator, the exotherm is very broad with final curing temperatures as high as 280 °C and the curing could overlap with the beginning of the degradation. The complex pattern can be attributed to the formation of the reactive species and to a complex reaction mechanism.<sup>33</sup> In **Figure 2** the influence of the proportion of ytterbium triflate on the shape of the calorimetric curves is shown. As the proportion increases the curves shift to lower temperatures and the shoulder rises, due to the higher contribution of the AM mechanism, as we described for similar DGEBA/γ-BL systems.<sup>20</sup>

Thermal data obtained from non-isothermal DSC for the curing of the samples studied are collected in **Table 1**. As can be seen, the T<sub>g</sub> of the materials

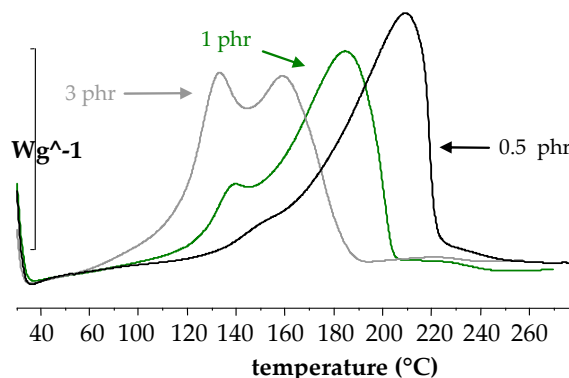
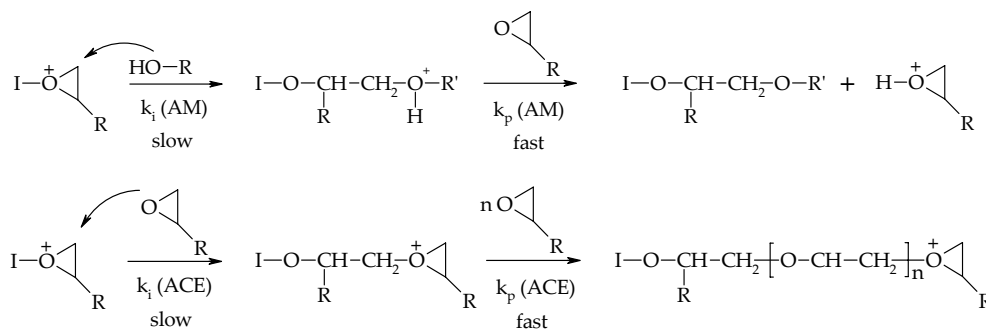


**Figure 2.** DSC scanning curves versus temperature of curing obtained through dynamic DSC experiments of DGEBA/lactone 2:1 (mol/mol) mixture initiated by 0.5, 1 and 3 phr of Yb(OTf)<sub>3</sub> at a heating rate of 10 °C/min.

decrease on increasing the proportion of lactone in the mixture as expected from the flexibility introduced by its aliphatic structure. On increasing the proportion of initiator a diminution of the T<sub>g</sub> is observed confirming the coexistence of the AM mechanism that leads to chain transfer reactions, which produces a higher proportion of hydroxylic dangling chains and therefore to a higher segmental mobility. However, dangling chains have a smaller plasticizing effect in networks than in linear polymers, because the free volume effect of the chain ends is counterbalanced by some physical crosslinking role of the branching point.<sup>34</sup> Among the initiators tested, BF<sub>3</sub> complex leads to materials with the



**Scheme 2**



Table 1. Calorimetric and thermomechanical data from the systems studied

Entry	Formulation <sup>a</sup>	Initiator	Proportion of initiator (phr)	mols init./ eq. epoxy	T <sub>g</sub> <sup>b</sup> (°C)	ΔH <sup>c</sup> (J/g)	ΔH <sup>d</sup> (kJ/ee)	E <sub>a</sub> (kJ/mol)	E' <sub>r</sub> (MPa)	tan δ
1	DGEBA	La(OTf) <sub>3</sub>	1	0.003106	127	531	97.6	78.41	9.36	144
2	DGEBA/γ-VL 3:1	La(OTf) <sub>3</sub>	1	0.003391	105	453	91.0	82.54	7.49	117
3	DGEBA/γ-VL 2:1	La(OTf) <sub>3</sub>	1	0.003534	95	412	89.4	87.49	6.65	107
4	DGEBA	Yb(OTf) <sub>3</sub>	1	0.002935	137	526	96.7	85.53	12.20	149
5	DGEBA/γ-VL 3:1	Yb(OTf) <sub>3</sub>	1	0.003205	100	453	91.1	82.47	11.46	117
6	DGEBA/γ-VL 2:1	Yb(OTf) <sub>3</sub>	0.5	0.001669	96	427	89.5	84.13	6.87	104
7	DGEBA/γ-VL 2:1	Yb(OTf) <sub>3</sub>	1	0.003339	93	430	90.1	85.23	7.40	102
8	DGEBA/γ-VL 2:1	Yb(OTf) <sub>3</sub>	3	0.010017	82	431	90.3	71.69	10.96	97
9	DGEBA/γ-VL 1:1	Yb(OTf) <sub>3</sub>	1	0.003743	65	378	88.8	89.75	4.89	80
10	DGEBA	Sc(OTf) <sub>3</sub>	1	0.003699	120	521	95.6	75.11	14.65	155
11	DGEBA/γ-VL 3:1	Sc(OTf) <sub>3</sub>	1	0.004039	93	455	91.4	75.32	10.32	103
12	DGEBA/γ-VL 2:1	Sc(OTf) <sub>3</sub>	1	0.004208	79	425	89.0	74.09	9.68	96
13	DGEBA/γ-VL 2:1	BF <sub>3</sub> ·MEA	3	0.058765	124	360	79.6	116.98	11.18	117

<sup>a</sup> the composition of the formulations are given in molar ratios

<sup>b</sup> T<sub>g</sub>s obtained by DSC in a second scan after dynamic curing

<sup>c</sup> enthalpies per gram of mixture

<sup>d</sup> enthalpies are expressed by the equivalent of epoxy groups



highest  $T_g$  value.

The total enthalpy per gram strongly decreases as the proportion of  $\gamma$ -VL increases. If we look at the enthalpy released per epoxy equivalent we can see a significant diminution on adding lactone, but on increasing its proportion only a low further diminution of the enthalpy can be observed. We should take into account that the heat released is mainly due to the opening of the strained epoxy ring. If we consider the heat evolved during curing for the DGEBA/ $\gamma$ -VL mixtures cured with the different metal triflates, we observed no great differences, indicating that the proportion of epoxide reacted is similar. The initiation with the boron trifluoride complex leads to a lower enthalpy release and a greater proportion (3 phr) of this initiator was necessary to reach the complete curing. The fact that this material has the highest  $T_g$  seems to be contradictory with the lower enthalpy released. The broadness of the exotherm and the high temperature reached should be the responsible of this unexpected result, which could be related to the occurrence of an endothermic process, as the evaporation of the lactone, which was proved by weighing the DSC pans after curing. This was also observed by FTIR experiments, which practically did not show any linear ester band in the materials obtained with  $\text{BF}_3$  complex.<sup>21</sup>

Although the change of the metal triflate or its proportion did not affect the total enthalpy released, the temperature of the maximum of the exotherm was influenced due to their different

catalytic activity. The addition of lactone reduces this temperature, which indicates an accelerative effect of the lactone, as we proved for other DGEBA/lactone systems.<sup>29</sup> **Figure 3** shows the variation of the conversion degree against temperature of the DGEBA/ $\gamma$ -VL 2:1 (mol/mol) formulation with all the initiators tested, where we can see that scandium triflate leads to the highest conversion for a prefixed temperature. The conversion evolution of the curing with  $\text{BF}_3\cdot\text{MEA}$  is quite different, especially after a 30 % of conversion, when the evolution become much slower. Moreover, higher temperatures are needed to reach the complete curing with this initiator.

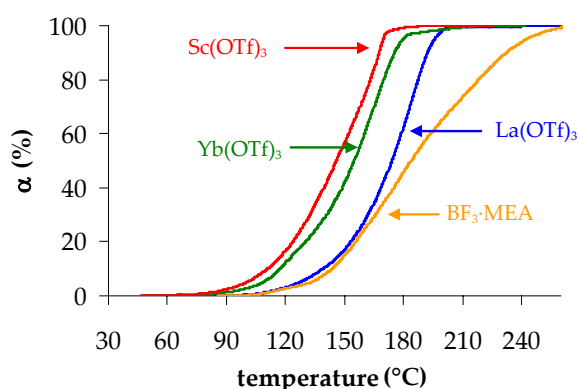


**Figure 3.** Conversion curves versus temperature of curing obtained through dynamic DSC experiments of DGEBA/lactone 2:1 (mol/mol) mixture initiated by Sc, Yb and La triflates and  $\text{BF}_3\cdot\text{MEA}$  at a heating rate of 10 °C/min.

The accelerative effect of the proportion of ytterbium triflate can be observed in **Figure 4**. The curves of 0.5 and 1 phr of initiator show similar shapes, whereas the corresponding to 3 phr seems to reflect the coexistence of a competitive mechanism. As can be seen, much higher conversions are reached at lower temperatures when the proportion of the initia-



tor increases, e.g. for 150 °C, the curing with 3 phr is practically complete, whereas with 0.5 phr is less than 20 %.

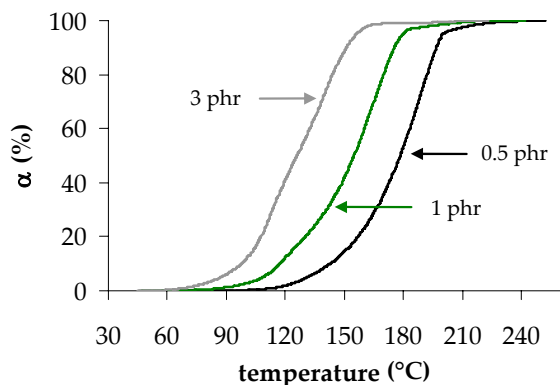


**Figure 4.** Conversion curves versus temperature of curing obtained through dynamic DSC experiments of DGEBA/lactone 2:1 (mol/mol) mixture initiated by 0.5, 1 and 3 phr of  $\text{Yb}(\text{OTf})_3$  at a heating rate of 10 °C/min.

In **Figure 5** we can see the effect of adding different proportions of lactone to DGEBA. The conversions increase with the proportion of  $\gamma$ -VL, although very little differences are observed at the highest proportion of lactone. The accelerative effect can be attributed to the formation of more reactive species as we saw in a similar system<sup>29</sup> but also to the lower viscosity of the mixture, which facilitates the reaction.

By the isoconversional method we calculated the evolution of the activation energy along the curing process. From the calorimetric curves at different heating rates and applying the eq. (3), we obtained the activation energy for each degree of conversion in all the formulations studied. **Figure 6** shows the plot of the apparent activation energy against the degree of conversion for the DGEBA/ $\gamma$ -VL 2:1 (mol/mol) formulation with the four initiators. The main dif-

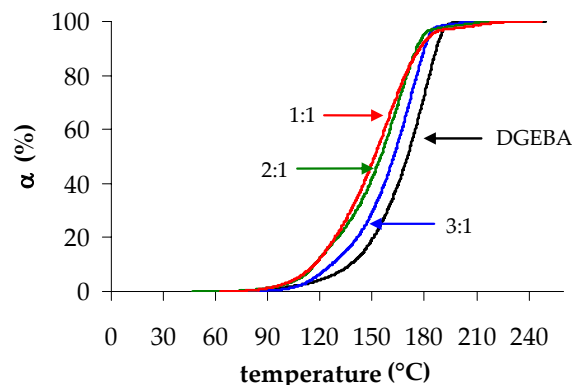


**Figure 5.** Conversion curves versus temperature of curing obtained through dynamic DSC experiments from pure DGEBA and mixtures DGEBA/lactone in different proportions initiated by 1 phr of  $\text{Yb}(\text{OTf})_3$  at a heating rate of 10 °C/min.

ference is observed in boron trifluoride, which leads to the highest activation energy in all the range, due to the formation of the true active initiating species,  $\text{HBF}_4$ . Among metal triflates, the differences are not as high. In the initial steps of the curing, activation energies follow the trend  $\text{Sc} < \text{Yb} < \text{La} < \text{BF}_3$ , related to the Pearson's theory hardness<sup>28</sup> and agree with the conversion evolutions represented in **Figure 3**.  $\text{La}(\text{OTf})_3$  shows a practically constant activation energy, which can be associated to an ACE propagation mechanism during all the curing process. On increasing the Lewis acidity of the metal triflate, the AM mechanism contributes in a higher extent. With scandium and ytterbium, especially with the former, the curing begins through the AM mechanism, which has lower activation energy, and then progressively the ACE mechanism, with higher activation energy becomes more important. Thus, the activation energy during curing steadily increases until it reaches a similar value to the lanthanum, for both scandium and ytterbium triflates.



The values of the activation energies calculated at 50 % of conversion, collected in **Table 1**, do not show any regular trend, but scandium leads to the lowest value and boron trifluoride complex to the highest.

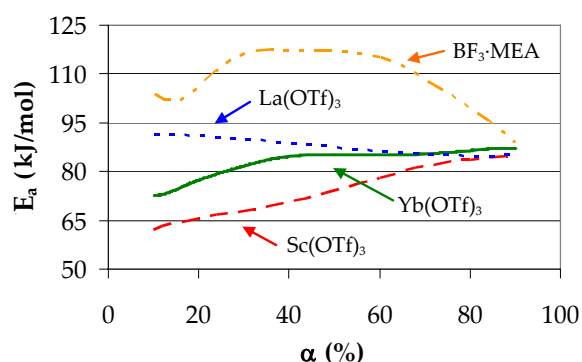


**Figure 6.** Dependence of the activation energy on the degree of conversion for DGEBA/lactone 2:1 (mol/mol) mixture initiated by 1 phr of Sc, Yb and La triflates and  $BF_3 \cdot MEA$ .

A useful framework for understanding and conceptualizing the changes that occur during curing of a thermosetting system is the isothermal time-temperature-transformation (TTT) diagram. Such a diagram displays the states of the material and characterizes the changes in the material during isothermal cure versus time. The various changes occurring in the material during isothermal cure are characterized by contours of the times to reach the events. Relevant contours could include molecular gelation, corresponding to the unique conversion at the molecular gel-point and vitrification, corresponding to the glass transition temperature. The basic parameter governing the state of the material is the chemical conversion. Therefore, the knowledge of how the rate changes with cure temperature is important and useful for predicting the

chemical conversion achieved after a cure schedule.

Three critical temperatures should be considered:  $T_g^0$ , the glass transition temperature of the uncured reactants,  $_{gel}T_g$ , the temperature at which molecular gelation and vitrification coincide, and  $T_g^\infty$ , the glass transition temperature of the fully cured material. **Figure 7** shows the TTT cure diagram of a DGEBA/ $\gamma$ -VL 2:1 (mol/mol) mixture with 1 phr of  $Yb(OTf)_3$ . The bold lines represent the time necessary to reach the gelation (red line) and vitrification (black line) in a selected curing temperature. This diagram was constructed using the experimental data determined previously (the isoconversional lines, the  $T_g$ - $\alpha$  relationship, the conversion at gelation, the  $T_g^0$  and the  $T_g^\infty$ ) following the methodology previously reported.<sup>35</sup>

The TTT diagram has a shape similar to other obtained by curing epoxy resins<sup>36,37</sup> and shows a value of 25 °C for the lowest temperature at which the material gels before vitrification ( $_{gel}T_g$ ), a value for  $T_g^0$  of -35 °C, below which the material does not crosslink at all, and a value for  $T_g^\infty$  of 93 °C, which is the lowest temperature at which complete curing can be achieved. If we compare this TTT diagram with the diagram of the pure DGEBA cured with ytterbium triflate ( $T_g^\infty = 137$  °C)<sup>35</sup> we can see that the addition of  $\gamma$ -VL makes it possible to reduce the curing temperature and consequently the thermal stresses. Moreover, performing the curing at low temperature implies an important energy saving.

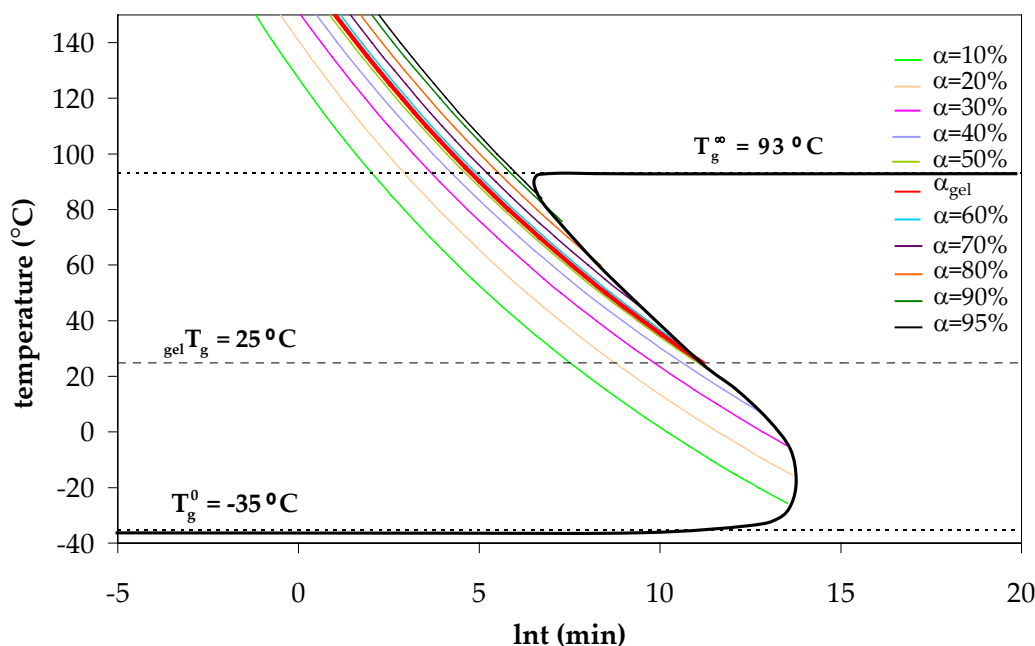


**Figure 7.** TTT diagram for the curing of the mixture DGEBA/ $\gamma$ -VL 2:1 (mol/mol) initiated by 1 phr of  $\text{Yb}(\text{OTf})_3$ . Vitrification curve (—), gelification curve (---). Isoconversional lines,  $T_g^0$ ,  $T_g^\infty$  and  $_{\text{gel}}T_g$  are also indicated.

**Figure 8** shows the mechanical relaxation spectra at 1 Hz and  $\tan \delta$  for the materials obtained from DGEBA/ $\gamma$ -VL 2:1 mol/mol formulations with all the initiators tested. The values of the modulus in the rubbery state and the  $\tan \delta$  are collected in **Table 1**. The practically unimodal shape of the curves of  $\tan \delta$  reflects the homogeneity of these materials. The relaxed modulus notably depends on the initiator used and increases in the order  $\text{La}(\text{OTf})_3 < \text{Yb}(\text{OTf})_3 < \text{Sc}(\text{OTf})_3 < \text{BF}_3 \cdot \text{MEA}$ . Moreover, there is a difference in the broadness of the relaxation of these materials, being the broadest that of  $\text{Sc}(\text{OTf})_3$ . The value of  $\tan \delta$  does not follow the above trend for materials obtained with rare earth triflates. However, the highest also corresponds to the material obtained with  $\text{BF}_3 \cdot \text{MEA}$ . These differences are based in two characteristics of the materials: the crosslinking density achieved, which is the highest for the boron complex, and the chemical

structure of the network that in turn depends on the initiator used. We showed in a previous paper<sup>21</sup> that the scandium salt induced a depolymerization process, which led to the presence of a great proportion of free lactone in the material that can act as a plasticizer, reducing the  $\tan \delta$  value. A similar behaviour was observed when the proportion of  $\text{Yb}(\text{OTf})_3$  was varied (entries 6-8 in **Table 1**). On increasing the proportion of initiator  $\tan \delta$  decreases whereas the relaxed modulus increases. A high proportion of initiator leads to a more densely crosslinked material because the depolymerization process allows a higher epoxide homopolymerization, but this process also leads to the formation of free lactone that remains entrapped in the network.

When the proportion of lactone increases both  $\tan \delta$  and relaxed modulus decreases. **Figure 9** shows the thermo-mechanical curves for ytterbium initiated



materials. When the proportion of lactone increases the materials seems to be less homogeneous. However, the materials are more homogeneous than those obtained from DGEBA/ $\gamma$ -caprolactone mixtures studied previously by us,<sup>17</sup> which showed bimodal  $\tan \delta$  curves.

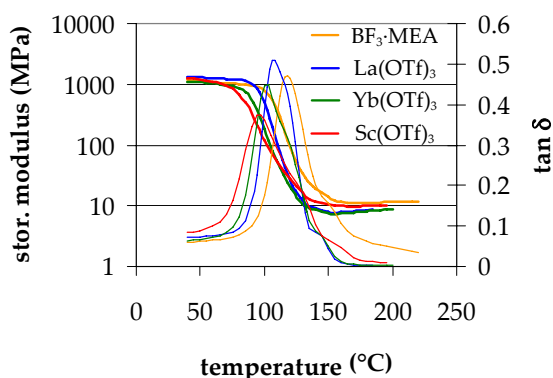


**Figure 8.** Storage modulus and loss tangent ( $\tan \delta$ ) versus temperature obtained by DMTA for the materials prepared from DGEBA/ $\gamma$ -VL 2:1(mol/mol) formulation initiated by all the initiators tested.

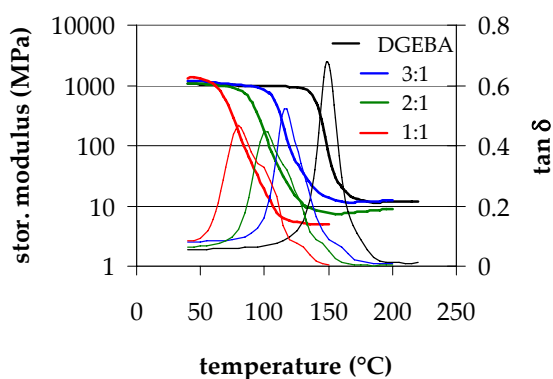


**Figure 9.** Storage modulus and loss tangent ( $\tan \delta$ ) versus temperature obtained by DMTA for the materials prepared from pure DGEBA and DGEBA/ $\gamma$ -VL formulations initiated by 1 phr of  $\text{Yb}(\text{OTf})_3$ .

The expansion of materials is characterized by the volumetric or lineal expansion coefficient, being the last one the most important in coatings applications. Polymers expand more than metals and ceramics and their linear thermal expansion coefficient is in the range of 20-100

ppm/ $^{\circ}\text{C}$ .<sup>38</sup> The high value of the thermal expansion coefficient (CTE) of polymers is caused by the low energy barrier for the chain conformation changes. Cross-linking decreases the thermal expansion coefficient whereas the introduction of aliphatic chains between crosslinks increases it. For these reason, it could be of interest to evaluate how the thermal expansion coefficient varies when different proportions of lactone are copolymerized with epoxy resins. **Table 2** collects the CTE values determined in the glassy and rubbery state for the samples obtained from mixtures of DGEBA with different proportions of  $\gamma$ -VL initiated by 1 phr of  $\text{Yb}(\text{OTf})_3$ . To compare the values, CTEs of pure DGEBA are also included. The  $T_g$ s collected in this table were determined by TMA, calculated as the cross of the tangents (**Figure 10**), and therefore they are slightly different from those determined by DSC and DMTA. As it was expected, on increasing the proportion of lactone in the mixtures, CTE values increase, but all these values lie in the usual range described for epoxy resins.

Microhardness measurements are very useful in rating coatings on rigid substrates for their resistance to mechanical abuse, such as that produced by blows, gouging and scratching. These measurements do not necessarily characterize the resistance to mechanical abuse of coatings that are required to remaining intact when deformed. This technique is used in the industry to characterize the mechanical properties related to resistance and hardness of materials and it measures their capability to resist static loads or applied at low rates.



**Table 2.**  $T_g$  values and thermal expansion coefficients in the glassy ( $\alpha_g$ ) and rubbery ( $\alpha_r$ ) status from materials obtained for different DGEBA/ $\gamma$ -VL formulations initiated by 1 phr of  $\text{Yb}(\text{OTf})_3$  determined by TMA

Formulation (mol/mol)	$T_g$ (°C)	$\alpha_g \times 10^6$ (K <sup>-1</sup> )	$\alpha_r \times 10^6$ (K <sup>-1</sup> )
DGEBA	137	54	182
DGEBA/ $\gamma$ -VL 3:1	107	60	193
DGEBA/ $\gamma$ -VL 2:1	90	67	202
DGEBA/ $\gamma$ -VL 1:1	73	74	246

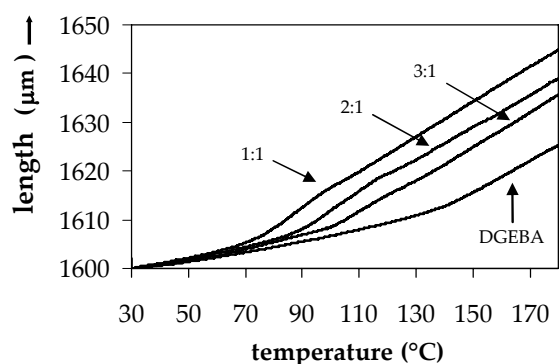


**Figure 10.** Plot of the TMA experiments for the materials prepared from pure DGEBA and DGEBA/ $\gamma$ -VL formulations initiated by 1 phr of  $\text{Yb}(\text{OTf})_3$ .

**Figure 11** collects the values obtained for all the materials prepared with the calculated precision, taken into account that we made six determinations for each material with a confidence level of 95 %. As we can see, the addition of lactone slightly reduces the microhardness in reference to pure cured DGEBA with all the cationic initiators tested and this reduction is more evident when the proportion of lactone increases. In general, a higher flexibility of the network is reflected in a lower microhardness value. In case of pure epoxy resin the change in the metal triflates scarcely influences the microhardness.  $\text{BF}_3 \cdot \text{MEA}$  leads to the

highest value when comparing all the materials obtained from DGEBA/ $\gamma$ -VL 2:1 mixtures. Among triflates, lanthanum led to the harder materials for all the composition studied. The highest the proportion of initiator the lowest the microhardness for the same composition is (samples 6, 7 and 8), which can be related to the extension of the depolymerization process.

**Figure 12** represents the values of Young modulus for all the materials prepared. For these measurements we also made six determinations for each material with a confidence level of 95 %. In general, the addition of lactone decreases this value. The addition of lactone to scandium triflate produces a greater variation, which can be attributed to the depolymerization process, more significant for this initiator. On increasing the proportion of ytterbium triflate as initiator the modulus also decrease, due to two different facts: the higher chemical incorporation of lactone in the network on increasing the initiator proportion and the depolymerization process that becomes evident when the proportion used is 3 phr.<sup>21</sup>

## Conclusions

The addition of  $\gamma$ -VL to the DGEBA accelerates the cationic curing and reduces the  $T_g$  of the materials obtained. Rare earth triflates are more active than  $\text{BF}_3 \cdot \text{MEA}$  as initiators and their activity increases from lanthanum to scandium. Moreover, the higher the acidity of the polymerization medium the higher is the contribution of the AM mechanism. As the proportion of initiator increases the

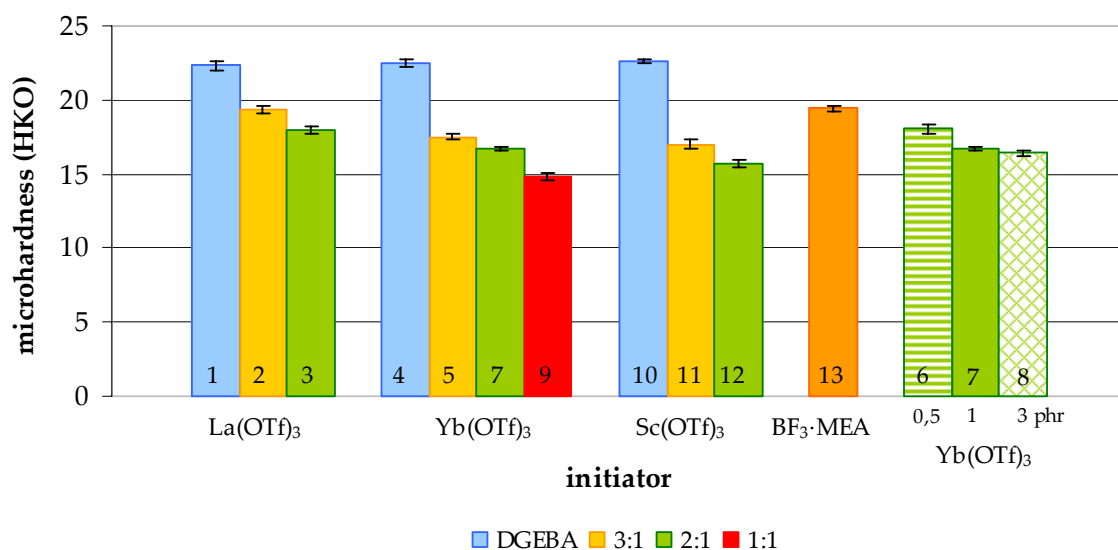


**Figure 11.** Knoop microhardness values in front of the composition for all the materials prepared. Numbers in the bars corresponds to the entries in **Table 1**. The colours indicate the composition of the initial.

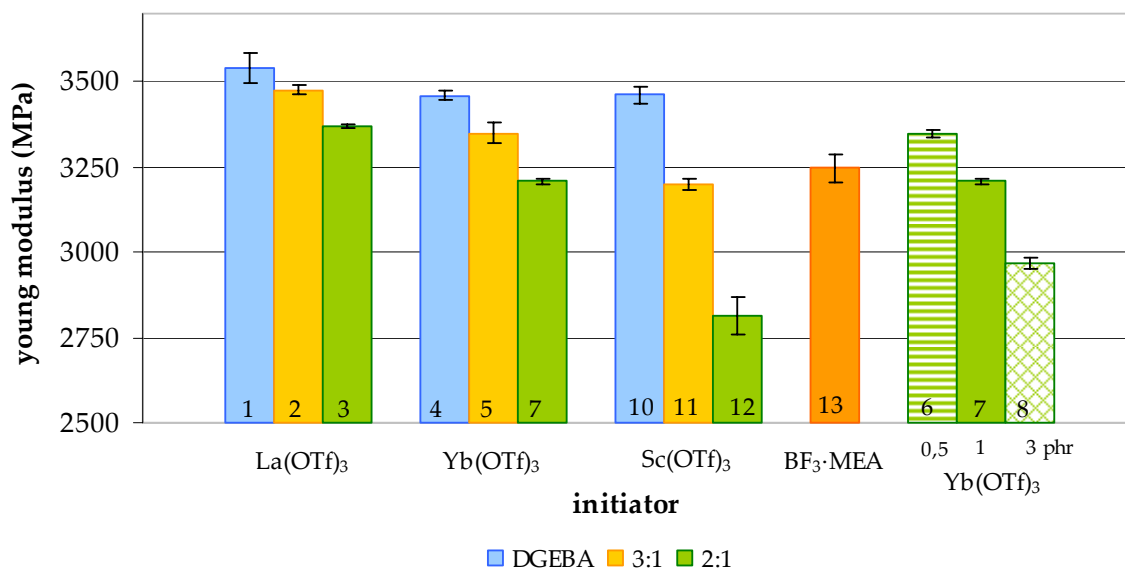


**Figure 12.** Young modulus in front of the composition for all the materials prepared. Numbers in the bars corresponds to the entries in **Table 1**. The colours indicate the composition of the initial mixtures.

curves shift to lower temperatures and the contribution of AM mechanism becomes more important.

The relaxed modulus of the materials obtained depends on the initiator used and increases in the order  $\text{La}(\text{OTf})_3 < \text{Yb}(\text{OTf})_3 < \text{Sc}(\text{OTf})_3 < \text{BF}_3 \cdot \text{MEA}$ . The materials obtained showed a practically unimodal  $\tan \delta$ , reflecting their homo-

geneous character.

The thermal expansion coefficient increase on adding lactone to DGEBA, but all the values lie in the usual range described for conventional epoxy resins.

The addition of lactone slightly reduces the microhardness and the Young modulus in reference to pure cured



DGEBA. On increasing the proportion of initiator used both parameters slightly decrease.

### Acknowledgements

The authors from the Universitat Politècnica de Catalunya would like to thank CICYT and FEDER (MAT2004-04165-C02-02) for their financial support. The authors from the Universitat Rovira i Virgili would like to thank the CICYT (Comisión Interministerial de Ciencia y Tecnología), FEDER (Fondo Europeo de Desarrollo Regional) (MAT2005-01806).

### References

- [1] Salla JM, Ramis X, Morancho JM, Cadenato A. *Thermochim Acta* 2002; 388: 355-370.
- [2] Leroy E, Dupuy J, Maazouz A. *Macromol Chem Phys* 2001; 202: 465-474.
- [3] Han JL, Hsieh KH, Chiu WY. *J Appl Polym Sci* 1993; 50: 1099-1106.
- [4] Sbirrazzuoli N, Vyazovkin S, Mititelu A, Sladic C, Vincent L. *Macromol Chem Phys* 2003; 204: 1815-1821.
- [5] Zvetkov VL. *Polymer* 2002; 43: 1069-1080.
- [6] Blanco M, Corcuera MA, Riccardi CC, Mondragón I. *Polymer* 2005; 46: 7989-8000.
- [7] Grazulevicius JV, Kublickas R, Kavaliunas RJ. *Macromol Sci Part A Pure Appl Chem* 1994; A31: 1303-1313.
- [8] García SJ, Ramis X, Serra A, Suay JJ. *Thermal Anal Cal* 2006; 83: 429-438.
- [9] May CA, editor. *Epoxy resins. Chemistry and technology*. New York: Marcel Dekker; 1988.
- [10] Kobayashi S, editor. *Lanthanides: chemistry and use in organic synthesis. Topics in organometallic chemistry, Vol. 2*. Berlin: Springer-Verlag; 1999.
- [11] Kobayashi S, Sugihura M, Kitagawa H, Lam WWL. *Chem Rev* 2002; 102: 2227-2302.
- [12] Kobayashi S, Manabe K. *Pure Appl Chem* 2000; 72: 1373-1380.
- [13] Kobayashi S. *Eur J Org Chem* 1999; 15-27.
- [14] Castell P, Galià M, Serra A, Salla JM, Ramis X. *Polymer* 2000; 41: 8465-8474.
- [15] Chabanne P, Tighzert L, Pascault JP. *J Appl Polym Sci* 1994; 53: 787-806.
- [16] Arasa M, Ramis X, Salla JM, Mantecón A, Serra A. *Polym Degrad Stab* 2007; 92: 2214-2222.
- [17] González S, Fernández-Francos X, Salla JM, Serra A, Mantecón A, Ramis X. *J Polym Sci Part A Polym Chem* 2007; 45: 1968-1979.
- [18] Matejka L, Dusek K, Chabanne P, Pascault JP. *J Polym Sci Part A Polym Chem* 1997; 35: 665-672.
- [19] Ramis X, Salla JM, Mas C, Mantecón A, Serra A. *J Appl Polym Sci* 2004; 92: 381-393.
- [20] Salla JM, Fernández-Francos X, Ramis X, Mas C, Mantecón A, Serra A. *J Therm Anal Calorim* 2007; 91: 385-393.
- [21] Arasa M, Ramis X, Salla JM, Mantecón A, Serra A. *J Polym Sci Part A Polym Chem* 2007; 45: 2129-2141.
- [22] Penczek S. *J Polym Sci Part A Polym Chem* 2000; 38: 1919-1933.
- [23] Coats AW, Redfern JP. *Nature* 1964; 201: 68-69.
- [24] Kissinger HE. *Anal Chem* 1957; 29: 1702-1706.
- [25] Vyazovkin S, Sbirrazzuoli N. *Macromol Chem Phys* 1999; 200: 2294-2303.
- [26] Vyazovkin S, Sbirrazzuoli N. *Macromol Rapid Commun* 2006; 27: 1515-1532.
- [27] Ramis X, Salla JM. *J Polym Sci Part B Polym Phys* 1997; 35: 371-388.
- [28] Pearson RG. *J Am Chem Soc* 1963; 85: 3533-3539.
- [29] Mas C, Mantecón A, Serra A, Ramis X, Salla JM. *J Polym Sci Part A Polym Chem* 2004; 42: 3782-3791.



- [30] Cervellera R, Ramis X, Salla JM, Mantecón A, Serra A. *J Polym Sci Part A Polym Chem* 2005; 43: 5799-5813.
- [31] Ramis X, Salla JM, Puiggalí J. *J Polym Sci Part A Polym Chem* 2005; 43: 1166-1176.
- [32] Luo S, Zhu L, Talukdar A, Zhang G, Mi X, Cheng JP, Wang PG. *Mini-Rev Org Chem* 2005; 2: 546-564.
- [33] Ghaemy M. *Eur Polym J* 1998; 34: 1151-1156.
- [34] Pascault JP, Sautereau H, Verdu J, Williams RJJ. *Thermosetting polymers*. New York: Marcel Dekker Inc.; 2002.
- [35] González S, Fernández-Francos X, Salla JM, Serra A, Mantecón A, Ramis X. *J Appl Polym Sci* 2007; 104: 3406-3416.
- [36] Wisanrakkit G, Gillham JK. *Polymer characterization*. In: Craver CD, Proveer T, editors. *ACS Adv Chem Ser*, Vol. 227. Washington: ACS; 1990; p. 143-166.
- [37] Barral L, Cano J, López AJ, López J, Nogueira P, Ramirez C. *J Appl Polym Sci* 1996; 61: 1553-1559.
- [38] Brandrup J, Immergut EH, Grulke EA, editors. *Polymer handbook*. New York: Wiley; 1999.

3. Preparació de *nanocomposites* per  
copolimerització catiónica de  
mescles DGEBA/ $\gamma$ -VL/argila  
iniciades amb tríflats de terres rares

UNIVERSITAT ROVIRA I VIRGILI  
NOUS TERMOESTABLES EPOXÍDICS MODIFICATS AMB GAMMA-LACTONES I BIS-GAMMA-LACTONES CONDENSADES  
M<sup>a</sup> Mercè Arasa Bertomeu  
ISBN:978-84-692-4157-8/DL:T-1171-2009

### 3.1 INTRODUCCIÓ

En els últims anys, la incorporació d'additius de mida nanomètrica ha esdevingut una estratègia important per millorar i diversificar les propietats dels materials polimèrics. Els *nanocomposites* són una nova classe de materials compostos que contenen partícules, on almenys una de les dimensions és de mida nanomètrica, en la matriu polimèrica. Es poden distingir tres tipus d'additius nanomètrics: (a) nanopartícules isodimensionals com les nanopartícules esfèriques de sílice on les tres dimensions són nanomètriques, (b) els nanotubs, on dues dimensions són nanomètriques i una tercera és més gran, donant lloc a una estructura allargada i (c) nanopartícules laminars, on només una dimensió és nanomètrica.

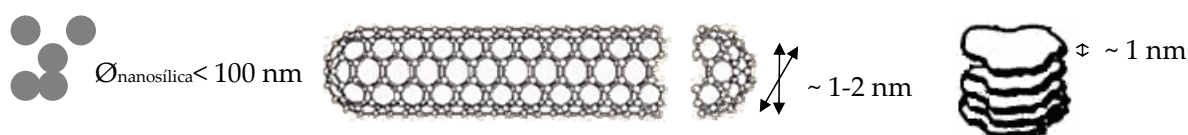


**Figura 3.1.** Diversos tipus de nanopartícules segons el nombre de dimensions de mida nanomètrica

Entre tots aquests tipus de partícules, les argiles (*clays*), han estat àmpliament estudiades, probablement degut a que són molt assequibles i perquè la seva química d'intercalació ha estat estudiada durant molt de temps<sup>1</sup>. La dispersió d'aquestes partícules en matrius polimèriques ha permès assolir millores notables en propietats mecàniques, tèrmiques, òptiques i físico-químiques quan es comparen amb la matriu pura o amb els *composites* convencionals (microescala) tal com van demostrar per primer cop les investigacions realitzades per Kojima i col.<sup>2</sup> en l'obtenció de *nanocomposites* de niló-argila. A més, com l'addició d'aquest additiu sol estar per sota d'un 10 %, els materials que s'obtenen són més lleugers que els *composites* convencionals.

Els silicats tradicionalment utilitzats en *nanocomposites* han estat els fil·losilicats o esmectites. La seva estructura cristal·lina consisteix en tres capes, dues capes externes tetraèdriques de sílice unides per els oxígens dels vèrtexs que formen una capa central octaèdrica que conté alumini o magnesi. El gruix de la làmina és al voltant de 1 nm, mentre que les dimensions laterals poden variar de 300 Å fins a varies micres. Aquestes làmines s'organitzen per formar apilaments regulars amb un espai entre elles anomenat espai interlaminar o galeria. La substitució isomòrfica entre cations, per exemple:  $\text{Al}^{3+}$  per  $\text{Mg}^{2+}$  o  $\text{Fe}^{2+}$  o  $\text{Mg}^{2+}$  per  $\text{Li}^+$ , genera una càrrega negativa que és contrarestada per cations alcalins o alcalinoterris situats a l'espai interlaminar, els quals mantenen unides les diferents làmines per interaccions de van der Waals. El nombre de substitucions isomòrfiques determina la densitat de càrrega superficial i a partir d'aquest valor es pot definir la capacitat d'intercanvi catiónic (CEC) com la concentració d'ions interlaminars (meq/100g argila) que poden ser intercanviats.

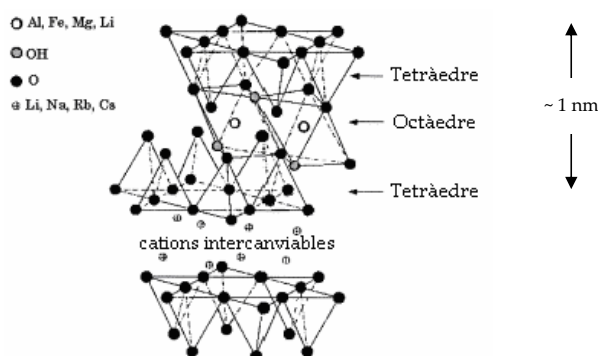


Figura 3.2. Estructura d'un fil·losilicat laminar

Els fil·losilicats són de naturalesa hidrofílica i, per tant, difícils de dispersar en matrius polimèriques. Ja que les forces que mantenen unides les làmines són relativament febles, una manera d'obtenir fil·losilicats més organofílics (organosilicats) seria intercanviar aquests cations interlaminars per surfactants catiónics com sals d'alquilamoni o d'alquilsfosfoni. Quan es produeix un intercanvi entre els cations hidratats interlaminars per cations orgànics voluminosos, l'espai interlaminar augmenta. El grau d'increment de la separació entre làmines depèn de l'estructura química dels ions intercalats i també de la densitat de càrrega del silicat<sup>3</sup>. Per tal d'optimitzar la seva compatibilitat amb un polímer donat es pot jugar amb diferents factors com són: la naturalesa de l'argila i l'estructura de l'agent modificant.

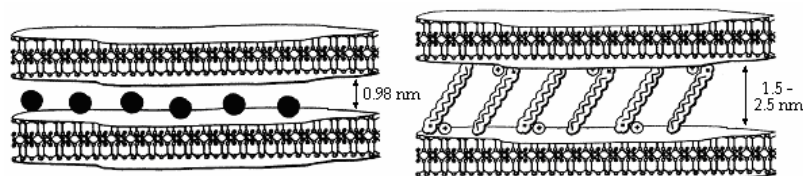
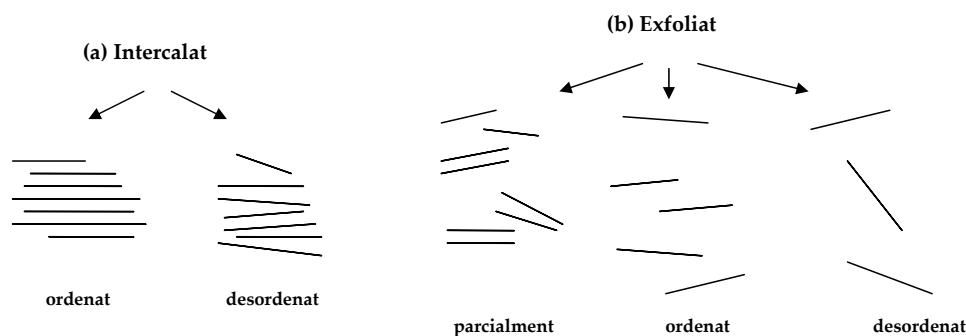


Figura 3.3. Distància interlaminar d'un silicat no modificat i modificat amb ions alquilamoni

Depenent de la naturalesa dels components utilitzats (silicat, modificant orgànic i matriu polimèrica) i del mètode de preparació, hi ha principalment tres tipus de *composites* que poden ser obtinguts quan un silicat es dispersa en un polímer: (a) *microcomposite* quan el polímer és incapaç d'intercalar-se entre les làmines del silicat, aquestes formen estructures micromètriques i les propietats del material final són similars a les dels *microcomposites* obtinguts de forma tradicional; (b) *nanocomposites* intercalats en els quals una cadena de polímer, i alguns cops més d'una, és intercalada entre les làmines del silicat donant lloc a una estructura ordenada construïda alternadament per una capa de polímer i una làmina de silicat i (c) *nanocomposites* exfoliats o deslaminats on les capes de silicat estan completament i uniformement dispersades en una matriu polimèrica. Val a dir que

aquestes categories esmentades (intercalat i exfoliat) descriuen només morfologies ideals mentre que la major part d'estructures reals es troben entre aquests extrems<sup>4</sup>. Vaia<sup>5</sup> va proposar un sistema de classificació més extens que ens donés una descripció més acurada de la morfologia d'un *nanocomposite*.



**Figura 3.4.** Nomenclatura detallada per a la caracterització d'estructures de *nanocomposites* de silicats laminars

De les diferents estructures que es poden obtenir, les exfoliades tenen especial interès degut a que en aquestes es maximitzen les interaccions entre el polímer i l'argila, cosa que hauria de portar a grans canvis en les propietats mecàniques i físiques<sup>6</sup>. De fet, està generalment establert que els sistemes exfoliats donen lloc a materials amb millors propietats mecàniques que els intercalats<sup>7</sup>. La completa dispersió de les làmines d'una argila en una matriu polimèrica optimitza el nombre d'elements reforçants facilitant la transferència de les tensions a la matriu, permetent així una millora en les propietats mecàniques<sup>6,8</sup>. Malgrat tot, no és fàcil aconseguir una completa exfoliació de les argiles i la majoria de polímers nanoreforçats descrits a la literatura són intercalats o parcialment intercalats/exfoliats<sup>7(b)</sup>. Això és degut a que les capes de silicats són altament anisotròpiques, amb unes dimensions laterals d'uns 100 a 1000 nm i inclús, quan es troben separades per grans distàncies, no poden distribuir-se completament en la matriu del polímer.

De totes les tècniques per determinar el tipus de *nanocomposite* obtingut, les més utilitzades són la difracció de raigs-X a angles alts (WAXD) i el microscopi de transmissió electrònica (TEM)<sup>4(c)</sup>. Estudis realitzats per Morgan i col.<sup>4(a)</sup> i Kornmann i col.<sup>9</sup> recomanen estudiar la microestructura, al igual que la nanoestructura, per aconseguir una completa descripció de la morfologia del *nanocomposite*. S'ha d'anar en compte al utilitzar el TEM de no oblidar que aquest treballa amb àrees de la mostra molt petites, cosa que pot ser problemàtica si el material no és homogeni. A més, és recomanable començar a treballar a augments petits i anar-los incrementant per tal de veure la distribució i la dispersió de les làmines. El WAXD pot presentar un inconvenient i és que a angles de difracció baixos, entre  $2\theta$  de 1 a  $6^\circ$ , és difícil detectar la distància entre capes ja que l'espaiat és massa gran i per tant es fa necessari la utilització del raigs X a angles baixos (SAXD)<sup>10</sup>. La informació

obtinguda de la tècnica de raigs X és altament depenent de l'ordre de l'argila, de la variabilitat en l'espaiat  $d$  i de qualsevol orientació desordenada, ja que aquests factors eixamplen i afebleixen els senyals a l'espectre de WAXD<sup>4(c)</sup>. També hi ha altres tècniques per caracteritzar aquests tipus de materials, com la microscòpia electrònica d'escombrat (SEM)<sup>11</sup>, tècnica que ens permet observar la distribució de les capes en el sí de la matriu a més de la superfície de fractura del material. D'altres tècniques que s'han aplicat són el microscopi de força atòmica (AFM)<sup>12</sup> i, en menor escala, la ressonància magnètica nuclear (RMN)<sup>13</sup>.

Hi ha diferents mètodes que ens permeten obtenir *nanocomposites*, d'entre els quals destaquen:

- Intercalació en solució: Les capes del silicat són prèviament exfoliades utilitzant un dissolvent adequat que, a més, permeti la solubilització del polímer o pre-polímer que es vol introduir. Un cop introduït el polímer, el dissolvent s'elimina i les làmines es reordenen deixant les cadenes del polímer en la zona interlaminar<sup>14</sup>.
- Polimerització *in situ*: es realitza un *swelling* o inflament del silicat mitjançant el monòmer líquid o una solució del monòmer. Després s'inicia la polimerització, que té lloc entre les làmines del silicat<sup>15</sup>.
- Intercalació en fusió: El silicat es mescla amb el polímer en estat fos. Si el silicat i el polímer són compatibles, el polímer pot introduir-se molt lentament entre les làmines del silicat, donant lloc a un *nanocomposite* intercalat o exfoliat. En aquesta tècnica no es requereix la utilització de cap dissolvent<sup>16</sup>.
- Síntesis en *template*: En aquesta tècnica, el silicat és format *in situ* en una solució aquosa que conté el polímer. El silicat es forma degut a forces d'autoacoblament. El polímer ajuda a la nucleació i al creixement dels cristalls inorgànics, els quals queden atrapats entre les cadenes del polímer<sup>17</sup>.

Dels diferents mètodes de preparació, la intercalació en fusió és molt important des del punt de vista industrial degut a que no es necessari la utilització de dissolvents. Tanmateix, per la preparació de *nanocomposites* termoestables cal utilitzar els mètodes de polimerització *in situ* o intercalació en dissolució, però el primer d'ells és més aconsellable des del punt de vista medioambiental.

Hi ha molts paràmetres que poden influir en la consecució de la morfologia desitjada del *nanocomposite* en materials termoestables. Entre aquests podem trobar:

- Mecanisme de dispersió de l'argila. Investigacions realitzades per Lan i col.<sup>18</sup> van constatar l'important paper del balanç entre les velocitats de reacció intra/extragaleries. Si la velocitat de reacció intragaleria és major que la extragaleria el grau d'exfoliació és més gran. A més, és important l'accessibilitat de la reïna o monòmers i l'iniciador a les galeries de l'argila durant el procés d'exfoliació<sup>4(c),9,19</sup>. A la figura 3.5 es representen els canvis de forces inter/extralaminars durant el procés d'intercalació/exfoliació originades durant el

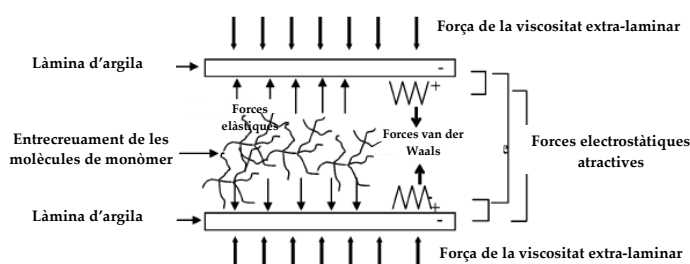


**Figura 3.5.** Il·lustració esquemàtica de les forces que actuen en un parell de làmines d'argila durant el procés d'intercalació i exfoliació

procés reactiu.

- Naturalesa del silicat i la seva capacitat d'intercanvi catiònic. La habilitat de l'espai interlaminar d'intercanviar ions, que actuen com a compatibilitzants i per tant converteixen l'espai interlaminar en organofíl, i l'efecte catalític dels ions intercanviats poden influir en la reacció de polimerització<sup>18,20</sup>.
- Agent de curat. L'elecció d'un agent de curat adequat també es relaciona en la literatura com un factor important en l'obtenció de *nanocomposites* deslaminats<sup>21</sup>. Kornmann i col.<sup>22</sup> van determinar que la mobilitat molecular i la reactivitat de l'agent de curat afectaven al balanç entre les reaccions intra i extragaleries. L'exfoliació depenia de la velocitat de difusió de l'iniciador dintre de les galeries i es veia millorada al augmentar la mobilitat molecular del iniciador.
- Condicions de curat. En molts casos s'ha observat que elevades temperatures de curat porten a una major exfoliació del organosilicat en la matriu polimèrica. Aquesta millora es creu que es deu a l'elevada mobilitat i velocitat de difusió dels monòmers o reïnes i de l'iniciador dintre de les galeries de l'argila<sup>4(a),9,22,23</sup>. Malgrat tot, hi ha d'altres investigadors que creuen que elevades temperatures afavoreixen les reaccions extragaleries. Per tant, depenent de la naturalesa dels monòmers i de l'agent de curat, cal dissenyar diferents cicles de curat per trobar un equilibri entre aquestes reaccions que permeti assolir una bona deslaminació<sup>18</sup>.
- Altres paràmetres que també poden influir són: l'ús de dissolvents per tal d'afavorir la dispersió de l'argila<sup>24</sup>, l'ús de l'agent modificant del silicat com a catalitzador<sup>25</sup>, el pre-acondicionament de la mescla<sup>26</sup>, la sonicació per tal d'augmentar la dispersió de l'argila en la matriu<sup>27</sup>, la irradiació amb microones<sup>28</sup>, la humitat<sup>29</sup> i la quantitat d'argila addicionada<sup>30</sup>. Normalment, baixes concentracions d'argila ja són suficients per tal d'aconseguir millores en les propietats. Tanmateix, un augment en la concentració d'argila implica un augment de la viscositat, dificultant la separació de les làmines. Una elevada quantitat d'argila pot comportar que no s'arribi a obtenir una morfologia exfoliada, senzillament pel fet de que les làmines no es puguin separar degut a la falta d'espai a la matriu.

Els *nanocomposites* d'epoxi-silicats han atret molt d'interès i se'n ha realitzat una recerca

exhaustiva, degut a que són aplicables a un ampli ventall d'àrees des d'adhesius i recobriments fins a aplicacions en microelectrònica. S'ha observat com l'addició de nanopartícules en baixes concentracions (3-5 % en pes) pot portar a l'obtenció de materials amb una major resistència front a dissolvents orgànics i aigua<sup>20(a),31</sup>, a una major estabilitat tèrmica<sup>32</sup> i de retardància a la flama<sup>33</sup>, a unes bones propietats òptiques<sup>24,34</sup>, a una reducció del coeficient d'expansió tèrmica, tant en l'estat vítri com en el cautxú<sup>35</sup> i a una millora en algunes propietats mecàniques. En concret, en alguns casos es va poder observar un increment del mòdul de Young<sup>12</sup> i del mòdul d'emmagatzematge en l'estat vítri i cautxú<sup>15(c)</sup> el qual depenia del grau d'exfoliació<sup>18,20(b),34</sup>, una millor resistència al trencament i a forces compressives<sup>7(c),35</sup>. Mitjançant l'observació de la superfície de fractura per SEM, es va comprovar com el camí de propagació d'una esquerda es veia molt dificultada al voltant de les àrees d'elevada concentració de silicat, en comparació amb el polímer pur<sup>31(a)</sup>, la qual cosa donava lloc en determinats casos a materials amb una elevada resistència a l'impacte<sup>36</sup>.

L'efecte d'un organosilicat en la temperatura de transició vítria ( $T_g$ ) també ha estat subjecte de molts estudis. En alguns d'ells s'ha arribat a observar un increment o un valor constant de la  $T_g$  al augmentar el contingut d'argila modificada<sup>15,24,34,37</sup>. Aquest augment el van associar a possibles interaccions a l'interfase entre el polímer i les làmines de silicat, on segments del polímer podien perdre la seva mobilitat, donant així un increment de la  $T_g$ <sup>38</sup>. D'altres investigadors van observar una disminució del valor de la  $T_g$ , que van associar a possibles reaccions laterals que produïen molècules petites que actuaven com a plastificants<sup>4(a),9</sup> o també a un possible efecte plastificant del modificant orgànic<sup>25</sup>. Tot això fa que la variació del valor de la  $T_g$  sigui difícil de preveure.

Estudis més recents realitzats per Wang i col.<sup>39</sup> proposen un nou mètode per aconseguir la major exfoliació possible en la preparació de *nanocomposites* de reïnes epoxi. En aquest cas, l'agent modificant queda unit covalentment a les làmines de silicat i degut a la presència de grups actius pot unir-se a la reïna. D'aquesta manera a la vegada que es redueixen les interaccions entre làmines es millora l'adhesió entre aquestes i el polímer.

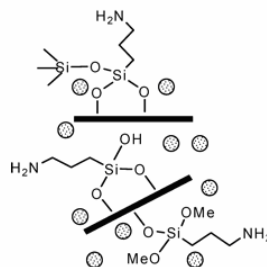


**Figura 3.6.** Representació de la modificació d'una argila realitzada per Wang i col.

En el treball sobre la preparació de *nanocomposites* que es presenta en aquesta memòria

s'ha estudiat l'efecte que causa la introducció de diverses argiles tipus montmorillonita en la copolimerització catiònica del diglicidilèter del bisfenol A (DGEBA) i la  $\gamma$ -valerolactona iniciada per triflats de terres rares.

A la literatura no es troben molts estudis relacionats amb la polimerització catiònica per obertura d'anell de reïnes epoxi iniciades tèrmicament, com és el nostre cas. Alguns treballs aprofiten les característiques àcides de la mateixa argila per iniciar la polimerització catiònica de DGEBA<sup>40</sup>. Sí s'han trobat més referències sobre el fotocurat catiònic de reïnes epoxi cicloalifàtiques, ancorades sobre partícules de sílice<sup>41</sup> o com a monòmer<sup>42</sup>. Entre aquests últims es troben els realitzats recentment per Sangermano i col.<sup>43</sup> on mitjançant un curat catiònic fotoinduit són capaços d'incorporar nanopartícules de plata a una matriu polimèrica aconseguint una bona distribució del metall i un augment de les propietats termodinamomecàniques del material o els realitzats per Bongiovanni i col.<sup>44</sup> on l'addició d'una argila produïa una influència negativa en la reacció de curat fotoquímic amb llum UV de reïnes epoxi degut a la presència d'aigua en l'argila i la naturalesa àcida o bàsica dels agents modificants d'aquesta. Aquests factors influïen en la velocitat de polimerització i conseqüentment en el grau d'intercalació/exfoliació.


## Referències

- [1] (a) Theng, BKG.; "The Chemistry of Clay-Organic Reactions" Wiley, New York (1974); (b) Ogawa, M.; Kuroda, K.; Bull. Chem. Soc. Jpn., 70, 2593-2618 (1997).
- [2] Kojima, Y.; Usuki, A.; Kawasumi, M.; Okada, A.; Fukushima, Y.; Karauchi, T.; Kamigaito, O.; J. Mater. Res., 6, 1185-1189 (1993).
- [3] (a) Lagaly, G.; Solid State Ionics, 22, 43-51 (1986); (b) Vaia, RA.; Teulkolsky, RK.; Giannelis, EP.; Chem. Mater., 6, 1017-1022 (1994); Hackett, E.; Manias, E.; Giannelis, EP.; J. Chem. Phys., 108, 7410-7415 (1998).
- [4] (a) Morgan, AB.; Gilman, JW.; Jackson, CL.; Macromolecules, 34, 2735-2738 (2001); (b) Becker, O.; Varley, RJ.; Simons, GP.; Polymer, 43, 4365-4373 (2002); (c) Becker, O.; Cheng, YB.; Varley, RJ.; Simons, GP.; Macromolecules, 36, 1616-1625 (2003).
- [5] Vaia, RA.; "Structural Characterization of Polymer-Layered Silicate Nanocomposite, in Polymer-clay nanocomposite", Pinnavia JT, Beall GW (eds), John Wiley & Sons, p. 229 (2000).
- [6] Beber, G.; Plast. Addit. Compound, 4, 22-27.
- [7] (a) Varlot, K.; Reynaud, E.; Kloppfer, MH.; Vigier, G.; Varlet, J.; J. Polym. Sci.: Part B: Polym. Phys., 39, 1360-1370 (2001); (b) Chin, IJ.; Thurn-Albrecht, T.; Kim, HC.; Russell, TP.; Wang, J.; Polymer, 42, 5947-5952 (2001); (c) Pluart, LL.; Duckett, J.; Santereau, H.; Polymer, 46, 12267-12278 (2005).
- [8] Wu, SH.; Wang, FY.; Ma, CCM.; Chang, WC.; Kuo, CT.; Kuan, HC.; Mater. Lett., 49, 327-333 (2001).

- [9] Kornmann, X.; Thomann, R.; Mühlaupt, R.; Finter, J.; Berlung, LA.; *Polym. Eng. Sci.*, **42**, 1815-1826 (2002).
- [10] Chen, C.; Curliss, D.; *Nanotechnology*, **14**, 643-648 (2003).
- [11] Kornmann, X.; Lindberg, H.; Berlung, LA.; *Polymer*, **42**, 1303-1310 (2001).
- [12] Zilg, C.; Mühlaupt, R.; Finter, J.; *Macromol. Chem. Phys.*, **200**, 661-670 (1999).
- [13] (a) VanderHart, DL.; Asano, A.; Gilman, JW.; *Macromolecules*, **34**, 3819-3822 (2001); (b) Devaux, E.; Bourbigot, S.; Achari, AE.; *J. Appl. Polym. Sci.*, **86**, 2416-2423 (2002).
- [14] (a) Lerner, M; Oriakhi, C.; "Handbook of Nanophase Materials", A. Goldstein (Ed.), Marcel Dekker, New York, 1997; (b) Lagaly, G.; *Appl. Clay Sci.*, **15**, 1-9 (1999); (c) Yano, K.; Usuki, A.; Okada, A.; Kurauchi, T.; Kamigaito, O.; *J. Polym. Sci.: Part A: Polym. Chem.*, **31**, 2493-2498 (1993); (d) Le, DC.; Jang, LW.; *J. Appl. Polym. Sci.*, **61**, 1117-1122 (1996).
- [15] (a) Fukushima, Y.; Okada, A.; Kawasumi, M.; Kurauchi, T.; Kamigaito, O.; *Clay Mineral*, **23**, 27-34 (1988); (b) Usuki, A.; Kojima, Y.; Kawasumi, M.; Okada, A.; Fukushima, Y.; Kurauchi, T.; Kamigaito, O.; *J. Mater. Res.*, **8**, 1179-1183 (1993); (c) Messersmith, PB.; Giannelis, EP.; *Chem. Mater.*, **6**, 1719-1725 (1994); (d) Lan, T.; Pinnavaia, TJ.; *Chem. Mater.*, **6**, 2216-2219 (1994).
- [16] (a) Vaia, RA.; Giannelis, EP.; *Macromolecules*, **30**, 7990-7999 (1997); (b) Vaia, RA.; Giannelis, EP.; *Macromolecules*, **30**, 8000-8009 (1997); (c) Vaia, RA.; Vasudevan, S.; Krawiec, W.; Wcanlon, LG.; Giannelis, EP.; *Adv. Mater.*, **7**, 154-156 (1995).
- [17] Carrado, KA.; Xu, LQ.; *Chem. Mater.*, **10**, 1440-1445 (1998).
- [18] Lan, T.; Kaviratna, PD.; Pinnavaia, TJ.; *Chem. Mater.*, **7**, 2144-2150 (1995).
- [19] Park, JH.; Jana, SC.; *Macromolecules*, **36**, 8391-8397 (2003).
- [20] (a) Wang, Z.; Massam, J.; Pinnavaia, TJ.; "Epoxy-Clay Nanocomposites, in Polymer-Clay Nanocomposites". Pinnavaia, TJ., Beall GW. (eds), Wiley, Chichester, p.127 (2000); (b) Wang, Z.; Pinnavaia, TJ.; *Chem. Mater.*, **10**, 1820-1826 (1998); (c) Chen, C.; Curliss, D.; *J. Appl. Polym. Sci.*, **90**, 2276-2287 (2003); (d) Román, F.; Montserrat, S.; Hutchinson, JM.; *J. Therm. Anal. Cal.*, **87**, 113-118 (2007).
- [21] (a) Jiankun, L.; Yucai, K.; Zongneng, Q.; Xiau-Su, Y.; *J. Polym. Sci.: Part B: Polym. Phys*, **39**, 115-120 (2001); (b) Wang, Q.; Song, C.; Lin, W.; *J. Appl. Polym. Sci.*, **90**, 511-517 (2003).
- [22] Kornmann, X.; Lindberg, H.; Berlung, LA.; *Polymer*, **42**, 4493-4499 (2001).
- [23] Tolle, TB.; Anderson, DP.; *Composite Science and Technology*, **62**, 1033-1041 (2002).
- [24] Brown, JM.; Curliss, D.; Vaia, RA.; *Chem. Mater.*, **12**, 3376-3384 (2000).
- [25] Triantafillidis, CS.; LeBaron, P.; Pinnavaia, TJ.; *Chem. Mater*, **14**, 4088-4095 (2002).
- [26] (a) Benson Tolle, T.; Anderson, DP.; *J. Appl. Polym. Sci*, **91**, 89-100 (2004); (b) Hutchinson, JM.; Montserrat, S.; Román, F.; Corté, P.; Campos, L.; *J. Appl. Polym. Sci.*, **102**, 3751-3763 (2006); (c) Montserrat, S.; Román, F.; Hutchinson, JM.; Campos, L.; *J. Appl. Polym. Sci.*, **108**, 923-938 (2008).
- [27] (a) Morgan AB.; Harries JD.; *Polymer*, **45**, 8695-8703 (2004); (b) Dean, K.; Krstina, J.; Tian, W.; Varley, RJ.; *Macromol. Mater. Eng.*, **292**, 415-427 (2007).
- [28] Yoo YJ.; Choi KY.; Lee JH.; *Macromol. Chem. Phys.*, **205**, 1863-1868 (2004).

- [29] Aranda P.; Mosqueda Y.; Perez-Cappe E.; Ruiz-Hitzky E.; *J. Polym. Sci.: Part B: Polym. Phys.*, **41**, 249-3263 (2003).
- [30] Zhong Y.; Wang S.; *J. Rheology*, **47**, 483-495 (2003).
- [31] (a) Zerda, AS.; Lesser, AJ.; *J. Polym. Sci.: Part B: Polym. Phys.*, **39**, 1137-1146 (2001); (b) Wang, K.; Chen, L.; Wu, J.; Toh, ML.; He, C.; Yee, AL.; *Macromolecules*, **38**, 788-800 (2005).
- [32] Gu, A.; Liang, G.; *Polym. Degrad. Stab.*, **80**, 383-391 (2003).
- [33] Hussain, M.; Varley, RJ.; Mathys, Z.; Cheng, YB.; Simon, GP.; *J. Appl. Polym. Sci.*, **90**, 3696-3707 (2003).
- [34] Wang, Z.; Lan, T.; Pinnavaia, TJ.; *Chem. Mater.*, **8**, 2200-2204 (1996).
- [35] Massam, J.; Pinnavaia, TJ.; *Mater. Res. Soc. Symp. Proc.*, **520**, 223-232 (1998).
- [36] Isik, I.; Yilmazer, U.; Bayram, G.; *Polymer*, **44**, 6371-6377 (2003).
- [37] (a) Lee, A.; Lichtenhan, JD.; *J. Appl. Polym. Sci.*, **73**, 1993-2001 (1999); (b) Kelly, P.; Akelah, A.; Qutubuddin, S.; Moet, A.; *J. Mat. Sci.*, **29**, 2274-2290 (1994); (c) Chen, KH.; Yang, SM.; *J. Appl. Polym. Sci.*, **86**, 414-421 (2002).
- [38] Okamoto M.; Morita S.; Taguchi H.; Kim YH.; Kotaka T.; Tateyama H.; *Polymer*, **41**, 3887-3890 (2000).
- [39] Wang, K.; Wang, L.; Wu, J.; Chen, L.; He, C.; *Langmuir*, **21**, 3613-3618 (2005).
- [40] (a) Wang, MS.; Pinnavaia, TJ.; *Chem. Mater.*, **6**, 468-474 (1994); (b) Lan, TL.; Kaviratna, PD.; Pinnavaia, TJ.; *J. Phys. Chem. Solids*, **57**, 1005-1010 (1996).
- [41] (a) Hartwig, A.; Sebald, M.; Kleemeier, M.; *Polymer*, **46**, 2029-2039 (2005); (b) Sangermano, M.; Acosta, R.; Garcia, AE.; Berlanga, L.; Amerio, E.; Priola, A.; Rizza, G.; *Polym. Bull.*, **59**, 865-872 (2008).
- [42] (a) Jiratumnukul, N.; Intarat, R.; *J. Appl. Polym. Sci.*, **110**, 2164-2167 (2008); (b) Esposito Corcione, C.; Frigione, M.; Maffezzoli, A.; Malucelli, G.; *Eur. Polym. J.*, **44**, 2010-2023 (2008).
- [43] Sangermano, M.; Yagci, Y.; Rizza, G.; *Macromolecules*, **40**, 8827-8829 (2007).
- [44] Bongiovanni, R.; Turcato, EA.; Di Gianni, A.; Ronchetti, S.; *Prog. Org. Coat.*, **62**, 336-343 (2008).

UNIVERSITAT ROVIRA I VIRGILI  
NOUS TERMOESTABLES EPOXÍDICS MODIFICATS AMB GAMMA-LACTONES I BIS-GAMMA-LACTONES CONDENSADAS  
M<sup>a</sup> Mercè Arasa Bertomeu  
ISBN:978-84-692-4157-8/DL:T-1171-2009

3.2.  NEW NANOCOMPOSITES PREPARED FROM DIGLYCYDIL  
ETHER OF BISPHENOL A AND  $\gamma$ -VALEROLACTONE  
INITIATED BY RARE EARTH METAL TRIFLATE INITIATORS



*Mercè Arasa, Richard Petrick, Ana Mantecón, Àngels Serra; to send*



## NEW NANOCOMPOSITES PREPARED FROM DIGLYCIDYL ETHER OF BISPHENOL AND $\gamma$ -VALEROLACTONE INITIATED BY RARE EARTH TRIFLATE INITIATORS

Mercè Arasa,<sup>1</sup> Richard Pethrick,<sup>2</sup> Ana Mantecón,<sup>1</sup> Àngels Serra<sup>1</sup>

<sup>1</sup>Dpt. Q. Analítica i Q. Orgànica, URV. C/Marcel·lí Domingo s/n, 43007 Tarragona, Spain

<sup>2</sup>Dpt. of Pure and Applied Chemistry, Thomas Graham Building, 295 Cathedral St., Glasgow G1 1XI

### Abstract

Mixtures of DGEBA with  $\gamma$ -valerolactone ( $\gamma$ -VL) 2:1 (mol/mol) with different clays were cationically copolymerized in the presence of scandium, ytterbium or lanthanum triflates as initiators. The evolution of the curing was followed by calorimetry and rheological techniques. The differences in the gelation time on adding clays were studied by rheologic measurements. These methods in addition to FTIR study of the materials allowed the selection of the best initiator and its proportion. The enhanced thermal stability of the nanocomposites was confirmed by thermogravimetry. The intercalated morphology of the nanocomposites obtained was confirmed by transmission electron microscopy. The nanocomposites prepared showed a more plastic fracture surface than the unfilled material. Thermomechanical characteristics were also studied.

*Keywords:* Epoxy resins, nanocomposites, lactones, shrinkage, thermosets, lanthanide triflates.

### Introduction

In the last years the incorporation of nanometric sized additives to epoxy resins has become one of the most used strategies to improve the properties of this type of thermosetting materials. The addition of nanometric fillers is much better than conventional fillers, because the latter impart drawbacks to the resulting materials, such as weight increase, brittleness and opacity.<sup>1</sup>

Among all the potential nanometric additives, those based on layered silicate

clays have been the most widely studied probably because the starting clay materials are easily available and the intercalation chemistry has been studied for a long time.<sup>2,3</sup>

The nanolayers are not easily dispersed in most polymers due to their preferred face-to-face stacking in agglomerated tactoids. Therefore, the layered silicates first need to be organically modified to produce polymer-compatible clays. The inorganic exchange cations in the galleries of the clay have been usually substituted by alkylammonium



cations to compatibilize the silicate with a hydrophobic polymer. The organic cations lower the surface energy of the silicate surface and improve wetting with the polymer matrix.<sup>4,5</sup> Moreover, the long organic chains increase the gallery distance facilitating the diffusion of the organic species into the galleries.<sup>6</sup>

Attending to the dispersion of a clay in a polymer matrix, three main types of composites can be distinguished: (a) microcomposites, when the polymer is unable to intercalate between the silicate sheets; (b) intercalated nanocomposites formed when polymer matrix is intercalated between the silicate layers and a well ordered multilayer structure of alternate polymeric and inorganic layers, with a repeat distance between them is formed; and (c) exfoliated or delaminated nanocomposites when the clay layers are well separated from one another and individually dispersed in the polymer matrix.<sup>7,8</sup>

Among the different methods for producing polymer-layered silicate nanocomposites, the *in situ* intercalative polymerization is the only possible when a nanocomposite thermoset is desired. The monomers and the crosslinking agent must migrate into the galleries, so that the crosslinking reactions can occur between the intercalated sheets. However, there is a competition between intra and extragalleries crosslinking and, if the polymerization rates are comparable, the curing heat produced is enough to overcome the attractive forces between the silicate layers and an exfoliated nanocomposite can be formed. If the extragallery crosslinking is quicker than

the intragallery diffusion and crosslinking, the extragallery resin will gel before the clay can be exfoliated.<sup>9</sup>

The choice of a suitable curing agent is reported to be a significant factor determining delamination of thermosetting nanocomposite systems. It has been shown that, using alkylammonium modified montmorillonites, low viscosity curing agents intercalate more easily into the clay than the higher viscosity curing agents.<sup>10</sup> Kornmann et al.<sup>11</sup> investigated the correlation of diffusion rate and reactivity of a DGEBA system and the subsequent degree of exfoliation and showed that the molecular mobility and reactivity of the curing agent are important factors affecting the balance between inter- and extragallery reactions. Moreover, the curing conditions can also affect the final nanocomposite structure. In most cases, it was observed that higher curing temperatures gave better exfoliations of the organosilicate in the epoxy matrix, which was mainly attributed to the higher molecular mobility and diffusion rate of the resin and hardener into the galleries.<sup>11-14</sup>

In the literature there are few papers on the formation of epoxy-clay nanocomposites by cationic curing and they are deboted to the photoinduced cationic crosslinking of cycloaliphatic epoxides.<sup>15,16</sup> However, it seems that catalytic systems could be advantageous to obtain exfoliated nanocomposites because in stoichiometric systems the intragallery diffusion of epoxide and curing agent can occur at different rate preventing the complete curing. This problem can be overcome by the use of catalytic curing



agents, since the ring opening polymerization of epoxide in the galleries occurs through attack of the epoxides to an active chain end. This makes unnecessary the presence of curing agent in the galleries.

In previous papers<sup>17,18</sup> we reported the copolymerization of DGEBA epoxy resin with  $\gamma$ -valerolactone ( $\gamma$ -VL) using rare earth metal triflates as cationic initiators. The interest in this copolymerization reaction was to improve some characteristics of the final thermosets by introducing ester and flexible aliphatic chains into the network structure. By copolymerizing  $\gamma$ -VL and DGEBA in cationic conditions networks with a poly(ether-ester) structure is obtained as depicted in **Scheme 1**. The addition of  $\gamma$ -VL to the reactive mixture notably decreased its viscosity, which can be advantageous to prepare epoxy nanocomposites as said above. Moreover, the lactone helps the metal triflate to dissolve by coordination. In the present paper we reported the preparation of new thermosetting nanocomposites by thermal cationic cure of DGEBA and  $\gamma$ -VL using rare earth metal triflates as initiators and the characterization of the materials obtained. As inorganic clay we used several types of commercially avail-

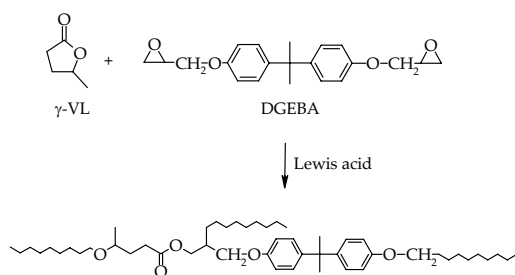
able montmorillonites Cloisite<sup>®</sup> Na<sup>+</sup>, 30B, 20A, 15A and 6A.

## Experimental Part

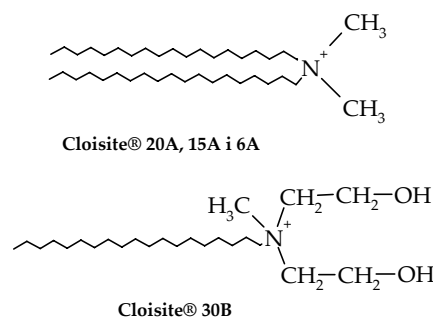
### Materials

Diglycidylether of bisphenol A (DGEBA) EPIKOTE RESIN 827 from Shell Chemicals (Epoxy Equiv. = 182.08 g/eq) was used as received.  $\gamma$ -Valerolactone ( $\gamma$ -VL) (Aldrich) was used as received. Lanthanum (III), ytterbium (III) and scandium (III) trifluoromethanesulfonates (Aldrich) were used without purification.

Cloisite<sup>®</sup> Na<sup>+</sup>, 30B, 20A, 15A and 6A were supplied by Southern Clay Products, a division of Rockwood Specialities. The structures of the quaternary ammonium modifiers of Cloisites<sup>®</sup> 20A, 15A and 6A are represented in **Scheme 2** (in which HT is a hydrogenated tallow composed of ~ 65% C18, ~ 30% C16, ~ 5% C14) with concentrations of 95, 125 and 140 meq of modifier per 100 g of clay, respectively. For Cloisite<sup>®</sup> 30B the modifier is also represented in the same Scheme with a concentration of 90 meq of modifier per 100 g of clay. The Cloisite<sup>®</sup> Na<sup>+</sup> is a natural montmorillonite with a concentration of ~ 92 meq of sodium per 100 g of clay.



Scheme 1



Scheme 2



### Preparation of the curing mixtures

Cloisites<sup>®</sup> were held in a 40 °C oven prior to sample preparation to ensure moisture homogeneity in all samples. The suspensions were prepared by adding Cloisites<sup>®</sup> to DGEBA and the mixture was stirred at 400 rpm whilst sonicated at amplitude of 40 % during 25 min until obtaining a visual homogeneous dispersion. The equipment used was a Eurostar Ika<sup>®</sup>-Werke stirrer and Cole Parmer Ultrasonic Processor. To produce the suspension, the samples were placed in a small water bath in a cooling jacket to dissipate the heat generated. The selected initiator was dissolved in the selected quantity of  $\gamma$ -VL and then the solution was added to the before prepared DGEBA-clay mixture. The final mixtures had a proportion DGEBA/ $\gamma$ -VL 2:1 (mol/mol) and contained the selected initiator expressed in phr (parts per hundred parts of reactive mixture in w/w) and 3 phr of the selected clay.

### Characterization and measurements

**Calorimetric study.** Calorimetric studies were carried out on a Mettler DSC-821e thermal analyzer in covered Al pans under N<sub>2</sub> at 2, 5, 10 and 15 °C/min. The calorimeter was calibrated using an indium standard (heat flow calibration) and an indium-lead-zinc standard (temperature calibration). The samples weighed approximately 7-9 mg. In the dynamic curing process the degree of conversion by DSC ( $\alpha_{DSC}$ ) was calculated as follows:

$$\alpha_{DSC} = \Delta H_T / \Delta H_{dyn} \quad (1)$$

where  $\Delta H_T$  is the heat released up to a temperature  $T$ , obtained by integration of the calorimetric signal up to this temperature, and  $\Delta H_{dyn}$  is the total reaction heat associated with the complete conversion of all reactive groups.

The  $T_g$  was measured as the half-way point of the jump in the heat capacity when the material changed from the glassy to the rubbery state at 20 °C/min.

The kinetics of the reaction is usually described by the following rate equation:

$$\frac{d\alpha}{dt} = Af(\alpha)\exp\left(-\frac{E}{RT}\right) \quad (2)$$

where  $t$  is time,  $A$  is the pre-exponential factor,  $E$  is the activation energy,  $T$  is the absolute temperature,  $R$  is the gas constant, and  $f(\alpha)$  is the differential conversion function.

By integrating the rate equation, eq. (2), under non-isothermal conditions and using the Coats-Redfern<sup>19</sup> approximation to solve the so-called temperature integral and considering that  $2RT/E$  is much lower than 1, the Kissinger-Akahira-Sunose (KAS) equation may be written:<sup>20</sup>

$$\ln\left(\frac{\beta_i}{T_{\alpha,i}^2}\right) = \ln\left[\frac{A_\alpha R}{g(\alpha)E_\alpha}\right] - \frac{E_\alpha}{RT_{\alpha,i}} \quad (3)$$

where  $\beta$  is the heating rate,  $g(\alpha)$  is the integral conversion function, the subscript  $\alpha$  refers to the value related to a considered conversion, and  $i$  to a given heating rate.

For each conversion degree, the linear plot of  $\ln(\beta_i/T_{\alpha,i}^2)$  versus  $1/T_{\alpha,i}$  enables  $E_\alpha$  and  $\ln[A_\alpha R/g(\alpha)E_\alpha]$  to be determined



from the slope and the intercept. These non-isothermal kinetic parameters are directly related for every value of  $\alpha$  with the isothermal integral kinetic parameter  $\ln[g(\alpha)/A_\alpha]$ . So, we can simulate isothermal by using non-isothermal data curing without knowing  $g(\alpha)$ .

The kinetic analysis was carried out using an integral isoconversional method (eq.(3)). The basic assumption of this method is that the reaction rate at a given conversion is only a function of the temperature.<sup>21,22</sup> Isoconversional methods make it possible to determine easily the dependence of  $E_\alpha$  on the degree of conversion in complex processes. Isoconversional STARE software from Mettler-Toledo was used in order to calculate conversion degrees and kinetics of the processes.

**Rheological study.** The evolution of the cure was also studied by means of rheological measurements using the Strathclyde Curemeter which let us to determine the gel point of the different studied samples. Gelation is the point at which the network has formed and the sample is no longer soluble. The viscosity at this point is approximately  $10^4$  Pa·s.<sup>23</sup> Glassy (fully cured) polymers have a shear modulus of approximately  $10^9$ – $10^{10}$  Pa·s, whereas in the rubbery state the modulus are approximately  $10^6$  Pa·s. Therefore, at the glass transition temperature, the modulus drops down from  $10^{10}$  to  $10^6$  Pa·s. The silicone oil bath used was set at the required temperature (110, 120, 130, 140 and 150 °C) and allowed to equilibrate, and the temperature checked using a thermocouple. The sample was poured into a small glass vial (10 mm diameter) to a depth of approximately

10 mm, and the vial secured into the oil bath by use of a clamp. The pin holding the paddle steadily was released to allow the paddle to oscillate, and it was then lowered so that it sat just above the bottom of the vial. This paddle is connected to constant amplitude of 0.5 mm and constant frequency linear motor of 2 Hz by a spring.<sup>24</sup> The software program PicoLog was used to record the change in the real and imaginary components over time. The results were converted to an ASCII file and then converted to a viscosity plots using Origin programme.

**Thermogravimetric analysis.** Thermogravimetric analyses (TGAs) were carried out with a Mettler TGA/SDTA 851e thermobalance. Cured samples with an approximate mass of 7 mg were degraded between 30 and 600 °C at a heating rate of 10 °C/min in N<sub>2</sub> (100 ml/min) measured in normal conditions.

**Thermomechanical analysis.** Thermal-dynamicmechanical analyses (DMTAs) were carried out with a TA Instruments DMTA 2980 analyzer. The samples were cured isothermally in a mould at 150 °C for 1 h and were then subjected to a post-curing for 5 h at 160 °C. Three point bending of 10 mm was performed on cylindrical samples (10 × 4 mm, approximately). The apparatus operated dynamically at 5 °C/min from 35 to 200 °C at a frequency of 1 Hz.

**Scanning Electron Microscope study.** A scanning electron microscope (SEM) Jeol JSM 6400 with a resolution of 3.5 nm was used to examine the fracture surface morphology of the samples which were previously coated with a conductive gold



layer.

**Transmission Electron Microscope study.** The morphology of the obtained nanocomposites has been observed by transmission electron microscopy (TEM) with a Jeol 1011 microscope. Samples have been prepared using an ultramicrotome at room temperature.

## Results and discussion

Rare earth metal triflates have not been studied until now in the preparation of epoxy nanocomposites and, therefore, we studied the effect of adding clay to a reactive mixture DGEBA/ $\gamma$ -VL 2:1 (mol/ mol) initiated by these cationic compounds. One reason to perform these studies is the novelty of the system and the use of cationic initiators in the preparation of epoxy nanocomposites. It should be taken in consideration that catalytic systems release more enthalpy per gram of mixture than stoichiometric ones and thus the curing heat produced could be enough to overcome the attractive forces between the silicate layers to get exfoliation. In addition, catalytic systems do not need stoichiometric ratios of resin and curing agent in the galleries to get completely cured materials but the only presence of monomer and an active chain end. The low viscosity of the mixture and the solubility of the initiator in the lactone should be advantageous for the diffusion of the reactive species into the galleries.

The samples were initially characterized by means of rheological measurements. The cure of a thermoset is characterized by an increase of the molar mass

until the development of an infinite molar mass network. The gelation process gives rise to an increase in viscosity and the development of elastic properties not existing in the initial reactive mixture. Generally, the gelation process is difficult to be directly determined using techniques only based in the chemical reaction as it is the calorimetry. Thus, the most suitable method to determine the gel time of the curing process is the use of rheologic techniques. The rheologic properties during curing were studied in isothermal conditions. **Figure 1** compares the isothermal complex viscosity at 110 °C as a function of the reaction time for a mixture of DGEBA/ $\gamma$ -VL 2:1 (mol/ mol) with a 3 phr of the corresponding clays initiated by 1 phr of Yb(OTf)<sub>3</sub>. Gelation time can be taken as the point in which the complex viscosity takes a value of approximately 10<sup>4</sup> Pa·s. We can observe that, when the clay is introduced, the increase of the viscosity begins later indicating a decelerative effect of the clay on the curing process. This observation contrast with what happens in some epoxy-clay nanocomposites, where the introduction of an organoclay has an accelerative effect on the reaction.<sup>25-27</sup> Thus, it seems that the clay can interact with the ytterbium triflate reducing its proportion or activity.

**Figure 2** shows the plot of gel time at different temperatures for the above mentioned formulation with different clays. All the clays tested increases the gel time in all the temperature range studied in reference to the neat mixture and this effect increases as the temperature decreases. The slight differences on changing the clay practically disappear

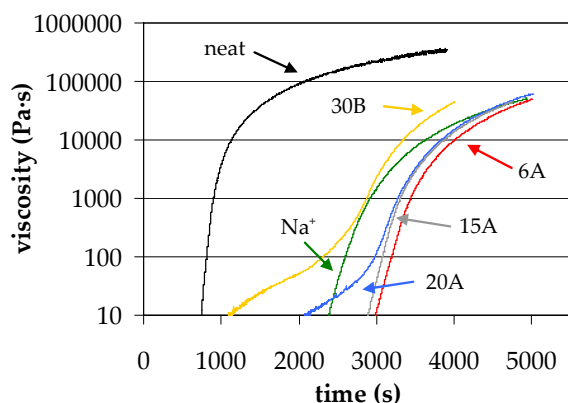


**Figure 1.** Plot of viscosity against curing time for a DGEBA/ $\gamma$ -VL 2:1 (mol/mol) mixture with 3 phr of the corresponding clay initiated by 1 phr of  $\text{Yb}(\text{OTf})_3$  at 110 °C.

at 150 °C.

Because of the clay seems to interact with the initiator we studied the possible influence of the cation exchange capacity (CEC) of the clays on the gel time at different temperatures. **Figure 3** shows that at high temperatures there is practically no influence of CEC in the gel time but at low temperatures the influence can be detected, and the higher the exchange capacity the longer the gel time is, which seems to support the interaction of the ytterbium cation with the interchangeable positions of the clay. The fact that the reaction was faster with the organo-clay Cloisite® 30B, could be due to the presence of hydroxylic groups in the am-

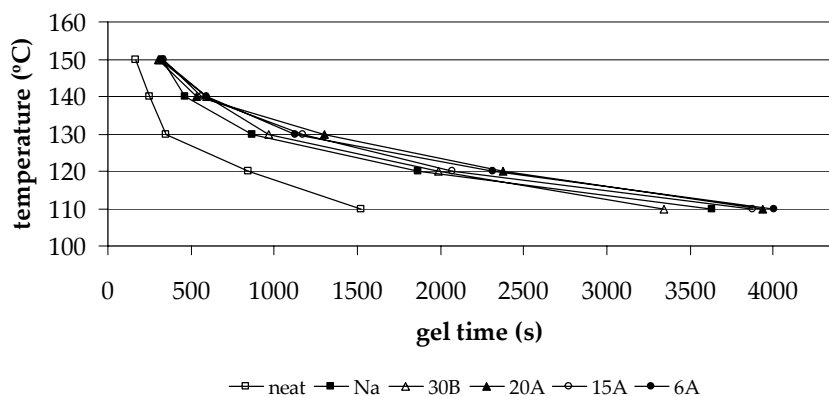


**Figure 2.** Temperature against gel time for DGEBA/ $\gamma$ -VL 2:1 (mol/mol) mixture with 3 phr of the corresponding clay initiated by 1 phr of  $\text{Yb}(\text{OTf})_3$  at 110 °C.

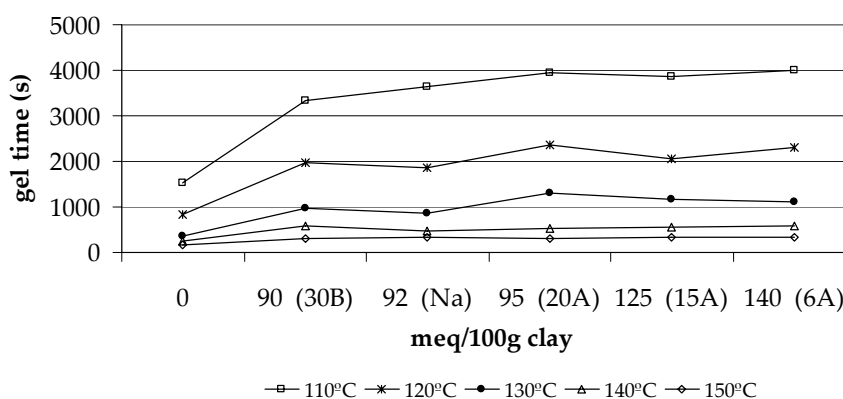


**Figure 3.** Gel time against cation exchange capacity for DGEBA/ $\gamma$ -VL 2:1 (mol/mol) mixture and 3 phr of the corresponding clay initiated by 1 phr of  $\text{Yb}(\text{OTf})_3$  at 110 °C.



monium salt, which generally improves the curing rate by the concurrence of the monomer activated mechanism (AM), which has been described to occur in the presence of hydroxyl groups.<sup>28</sup>

In a previous work,<sup>18</sup> we studied the influence of the rare earth metal triflates and their proportions in the evolution of the curing and we saw that on increasing the Lewis acidity of the cation the curing can be performed at lower temperature. The different Lewis acidity can also influence the interaction with the clay. Thus, it seemed interesting to study by rheological techniques the influence of the different initiators and their proportions on the gel time. For this study we selected Cloisite® Na<sup>+</sup> as the clay to eliminate the possible influence of the ammonium modifier. **Figure 4** shows the representation of the gel times against the proportions of La, Yb and Sc triflates. We have also included the gel times of the same mixtures without clay to compare. As we can see, on increasing the proportion of initiator the gel time decreases as expected. For all the initiators the presence of clay retards the gelation, but this delay decreases on increasing the proportion of initiator. The retarding effect is more evident for La(OTf)<sub>3</sub>, which is the less active initiator. Sc(OTf)<sub>3</sub> and Yb(OTf)<sub>3</sub> show a similar behaviour, but the former is slightly more active than the latter.

Although Sc(OTf)<sub>3</sub> resulted slightly more active than the other initiators, even in the presence of the clay, we can detect by FTIR that similarly to the observation made in a previous work<sup>17</sup> this initiator led to a depolymerization

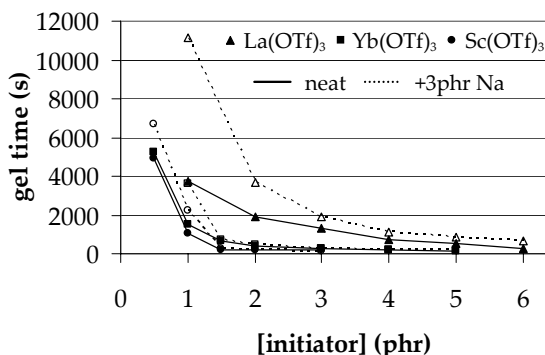


**Figure 4.** Gel time against initiator concentration for the mixture DGEBA/ $\gamma$ -VL 2:1 (mol/mol) with 3 phr of Cloisite® Na<sup>+</sup> initiated by different proportions of the rare earth metal triflates at 110 °C.

process. This depolymerization, which occurs during curing, led to a decrease in the linear ester band, initially formed in the copolymerization process, and to an increase of the band corresponding to the initial lactone. Thus, we consider that Yb(OTf)<sub>3</sub> is the most adequate initiator to cure these samples even in the presence of clay. In the same study we also saw that the use of a high proportion of the ytterbium salt (3 phr) led to the formation of free  $\gamma$ -VL that finally acted as a plasticizer. Thus, more than 1 phr of this initiator seems to be detrimental to the characteristics of the thermoset. In the basis of these results, 1 phr of Yb(OTf)<sub>3</sub> was selected as initiator to cure the mixtures and complete the study.

**Figure 5** shows the calorimetric curves obtained in the curing of a DGEBA/ $\gamma$ -VL 2:1 (mol/mol) mixture with 1 phr of Yb(OTf)<sub>3</sub> containing 3 phr of the different clays. To compare, we included the curve corresponding to the curing of the neat mixture without clay. As we can see, the addition of clays shifts the curves at higher temperatures, indicating that the clay retard the curing process. All the



**Table 1.** DSC, TGA and DMTA data of the materials prepared from a formulation DGEBA/ $\gamma$ -VL 2:1 (mol/mol) initiated by 1 phr of Yb(OTf)<sub>3</sub> and with 3 phr of the different clays

Samples	DSC data				TGA data			DMTA data	
	T <sub>g</sub> (°C)	$\Delta H$ (J/g)	T <sub>max</sub> (°C)	E <sub>a</sub> (kJ/mol)	T <sub>5%</sub> (°C)	T <sub>max</sub> (°C)	Char Yied (%)	E' (MPa)	Tan $\delta$ (°C)
neat polymer	93	430	165	85.2	258	340	19	7.4	102
Cloisite®Na	97	417	175	80.0	301	371	17	8.5	93
Cloisite®30B	93	410	174	79.3	291	357	19	8.8	87
Cloisite®A6	93	417	179	78.4	299	364	16	6.2	87

curves present an initial and small exotherm, which can be attributed to an activated monomer mechanism (AM).<sup>29</sup> This exotherm is less pronounced in the samples having clay and therefore the presence of clay seems to reduce the concurrence of this mechanism, which could influence in the network structure because the AM mechanism favours chain transfer processes.

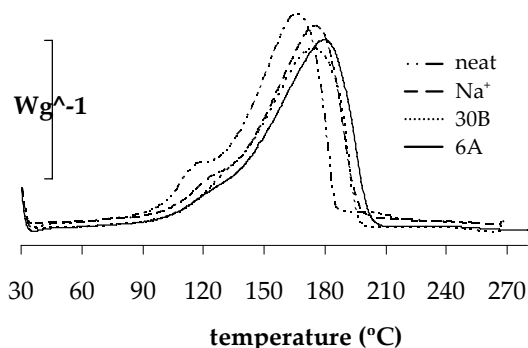


**Figure 5.** Differential calorimetric scanning curves against curing temperature of DGEBA/ $\gamma$ -VL 2:1 (mol/mol) formulation with 3 phr of the corresponding clay initiated by 1 phr of Yb(OTf)<sub>3</sub> at 10 °C/min in N<sub>2</sub> atmosphere.

The values obtained from the calorimetric curves are collected in **Table 1**. Total enthalpies are similar if we take into account that the samples with clays contain a lower proportion of epoxy groups, which release the main reaction heat. The T<sub>g</sub> values for the materials ob-

tained after dynamic cure are similar but the maximum of the exotherm has a higher value in the samples with clay. At the present, there is an uncertain situation about the effect of clay content on the glass transition temperature of nanocomposites based on DGEBA. The little effect of the clay on the T<sub>g</sub> is not surprising, since there are contradictory results in the literature; some authors<sup>30</sup> described a decrease in the T<sub>g</sub> on adding clay whereas others<sup>31,32</sup> reported an increase in this parameter.

Although the addition of clay did not influence the total enthalpy released, the addition of clay increases the temperature of the maximum of the exotherm, which indicates a decelerative effect of the clay. From the calorimetric parameters we can go to the conclusion that the presence of the tested clays does not influence the degree of crosslinking achieved but decreases the reactivity of the system.

From the calorimetric curves at different heating rates and applying the isoconversional method we calculated the evolution of the conversion and the activation energies along the curing processes. **Figure 6** shows the variation



of the conversion degree against temperature of the mixtures with  $\text{Yb}(\text{OTf})_3$  and the different clays, where we can see that there is not much difference for the evolution of the samples containing clay, but all of them are retarded in reference to the evolution of the uncharged sample.

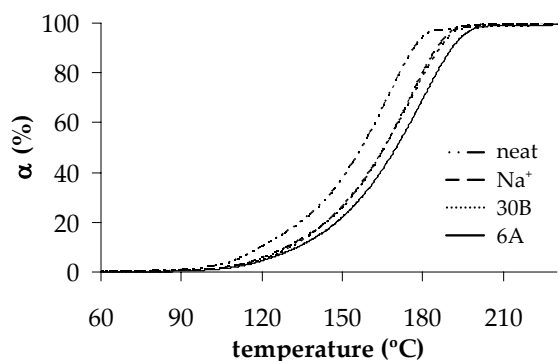


**Figure 6.** Conversion curves against curing temperature obtained through dynamic DSC experiments of DGEBA/ $\gamma$ -VL 2:1 (mol/mol) mixtures with 3 phr of the corresponding clay initiated by 1 phr of  $\text{Yb}(\text{OTf})_3$ .

In **Figure 7** is represented the evolution of the apparent activation energy along the curing process, which was obtained applying the eq (3). With this equation we obtained the activation energy for each degree of conversion in all the formulations studied. Although the shape of the curves is similar, the main difference is the higher value for the neat sample in all the range. The explanation to the higher reactivity of the neat system can be found in the compensatory effect between the activation energy and the pre-exponential factor.<sup>33,34</sup>

Although the final  $T_g$  of the materials obtained was similar despite of the presence of clay, we wanted to know if the formation of the network went for the same pathway than the neat resin.

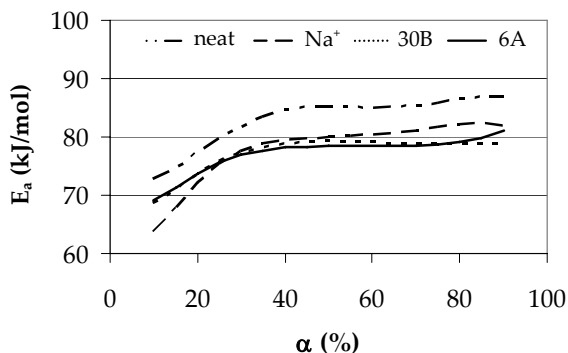


**Figure 7.** Dependence of the activation energy on the degree of conversion for DGEBA/ $\gamma$ -VL 2:1 (mol/mol) formulation with 3 phr of the corresponding clay initiated by 1 phr of  $\text{Yb}(\text{OTf})_3$ .

Thus, we followed the evolution of the  $T_g$  of the material on curing at  $110^\circ\text{C}$  up to curing completion. **Figure 8** represents the evolution of the  $T_g$  against degree of conversion for samples with or without clay. As can be seen, the evolution of this value is very similar, indicating that the presence of the clay does not influence the formation of the network. The final  $T_g$  reached was slightly higher than that obtained after dynamic experiments in the calorimeter. This difference can be explained by the complex reaction mechanism of the curing, which occurs through the formation of an intermediate spiroorthoester (SOE).<sup>17</sup> Spiroorthoesters form in the first stages of the curing but homopolymerize at the end of the curing or at higher temperature.<sup>35</sup> The temperature used in the present study could be enough to copolymerize SOE with epoxides but no to homopolymerize them. This fact can lead to a more rigid network structure by the presence of unreacted SOEs in the structure.

**Figure 9** shows the mechanical relaxation spectra at 1 Hz and  $\tan \delta$  for the materials obtained from DGEBA/

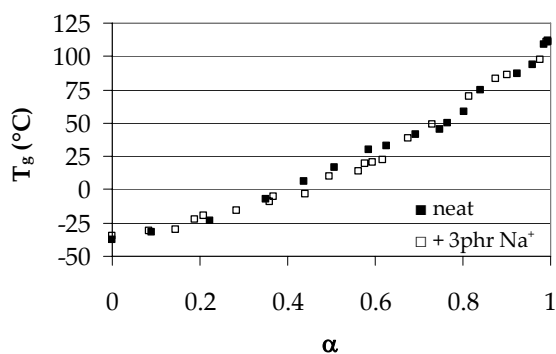


**Figure 8.** Evolution of  $T_g$  against conversion for a DGEBA/ $\gamma$ -VL 2:1 (mol/mol) mixture with 1 phr of  $\text{Yb}(\text{OTf})_3$  cured at 110 °C, with 3 phr of Cloisite<sup>®</sup> Na<sup>+</sup> or without clay.

$\gamma$ -VL 2:1 (mol/mol) mixture with 1 phr of  $\text{Yb}(\text{OTf})_3$  containing 3 phr of different clays cured isothermally at 150 °C for 1 h and then post-cured for 5 h at 160 °C. The values of the modulus in the rubbery state and the  $\tan \delta$  are collected in **Table 1**. The relaxed modulus notably depends on the clay added; being those with Cloisite<sup>®</sup> 30B and Cloisite<sup>®</sup> Na<sup>+</sup> which have a higher relaxed modulus, whereas Cloisite<sup>®</sup> 6A has the lowest. The addition of clay leads to more homogeneous materials, as can be seen from the shape of  $\tan \delta$ , but with lower temperatures of the maximum. The differences between the  $T_g$  of the materials and  $\tan \delta$  values can be explained by the determination technique, the complex reaction mechanism of the curing, and the different curing schedule applied.

The thermal stability of polymeric materials is usually studied by thermogravimetric analysis (TGA). It has been described that the incorporation of clay into the polymeric matrix was found to enhance thermal stability by acting as a superior insulator and mass transport barrier to the volatile products generated during the decomposition.<sup>2,3,36</sup> **Figure 10**

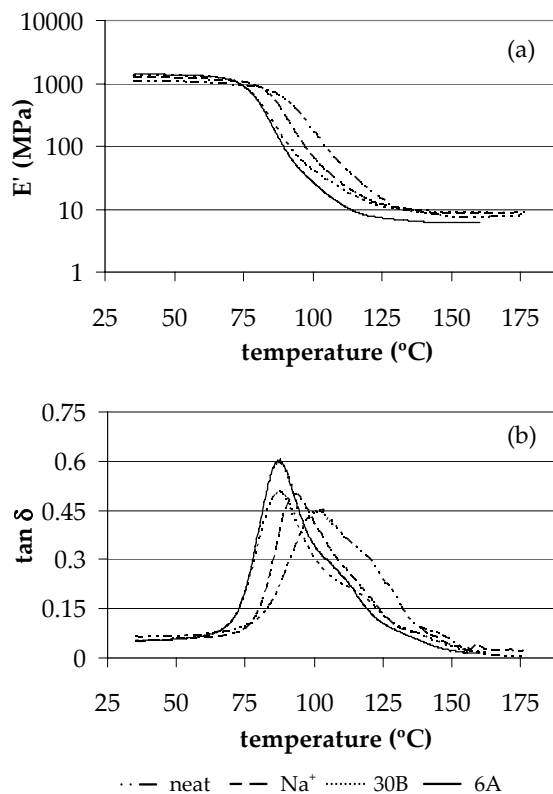


**Figure 9.** Storage modulus (a) and loss tangent ( $\tan \delta$ ) (b) against temperature obtained by DMTA for the thermosets prepared from DGEBA/ $\gamma$ -VL 2:1 (mol/mol) formulation with 3 phr of the corresponding clay initiated by 1 phr of  $\text{Yb}(\text{OTf})_3$ .

shows the plot of weight loss against temperature for the materials containing the different clays. To compare, the material without clay has been also included. As can be seen, the addition of all the clays increases the thermal stability. The effect of the clays is similar but Cloisite<sup>®</sup> Na<sup>+</sup> has a slightly higher temperature of the maximum degradation rate.

The fine distribution of the clay in the polymeric matrix was evidenced by TEM observation. **Figure 11** shows the TEM micrographs obtained for the Cloisite<sup>®</sup> 30B nanocomposite at different magnifications. The homogeneous distribution of the clay in the matrix and the intercalated character of the nanocomposite can

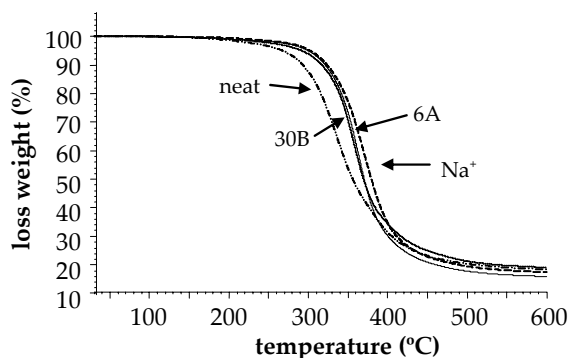


**Figure 10.** Thermogravimetric curves under N<sub>2</sub> atmosphere at 10 °C/min of the thermosets obtained from DGEBA/ $\gamma$ -VL 2:1 (mol/mol) formulation with 3 phr of the corresponding clay initiated by 1phr of Yb(OTf)<sub>3</sub>.

be observed. The interlayer distances were in the range 9-15 nm. Cloisite® 30B was the clay that allowed us to obtain the best dispersion in the matrix and the larger interlayer distances. However Cloisite® Na<sup>+</sup> was very difficult to disperse in the polymer matrix due to its hydrophilic character, which make difficult the polymer to be diffused into the galleries.

The enhanced toughness expected for the nanocomposites prepared was studied through the inspection of fracture surfaces, which were obtained by cracking the material in liquid nitrogen. **Figure 12** shows the SEM micrographs of the fractured surface for the neat resin and the nanocomposite obtained from Cloisite® 30B. As we can see, whereas the neat resin shows a typical fragile fracture morphology, the nanocomposite shows a ductile fracture evidenced by a more plastic deformation.

## Conclusions

Thermal cationic curing of DGEBA/ $\gamma$ -VL/clay mixtures initiated by rare earth

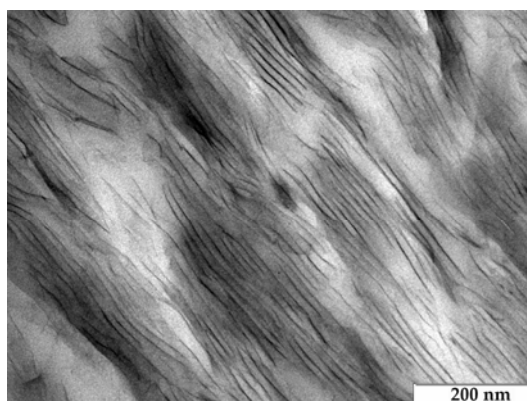
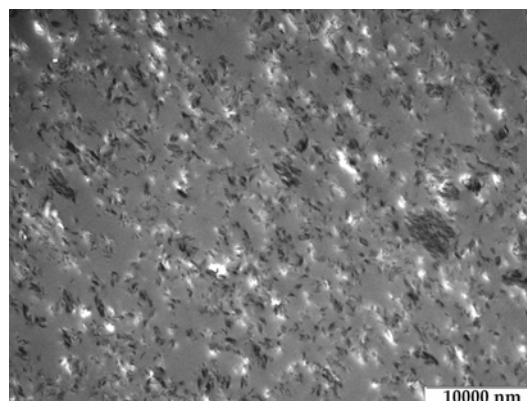


**Figure 11.** TEM micrographs of the intercalated nanocomposite obtained from a DGEBA/ $\gamma$ -VL 2:1 (mol/mol) formulation with 3 phr of the Cloisite® 30B initiated by 1 phr of Yb(OTf)<sub>3</sub>.

metal triflates allowed obtaining intercalated nanocomposites.

By rheological and FTIR studies we found that ytterbium triflate was the best initiator to prepare these nanocomposites and the proportion of 1 phr is the best proportion for this initiator to chemically incorporate the highest proportion of  $\gamma$ -valerolactone in the nanocomposite.

The addition of clay retarded the curing and the gelation, especially in the case of using the lanthanum initiator. The increase in the proportion of initiator reduced the retardant effect of adding clay. The reduction in the reactivity of the system has been attributed to an in-

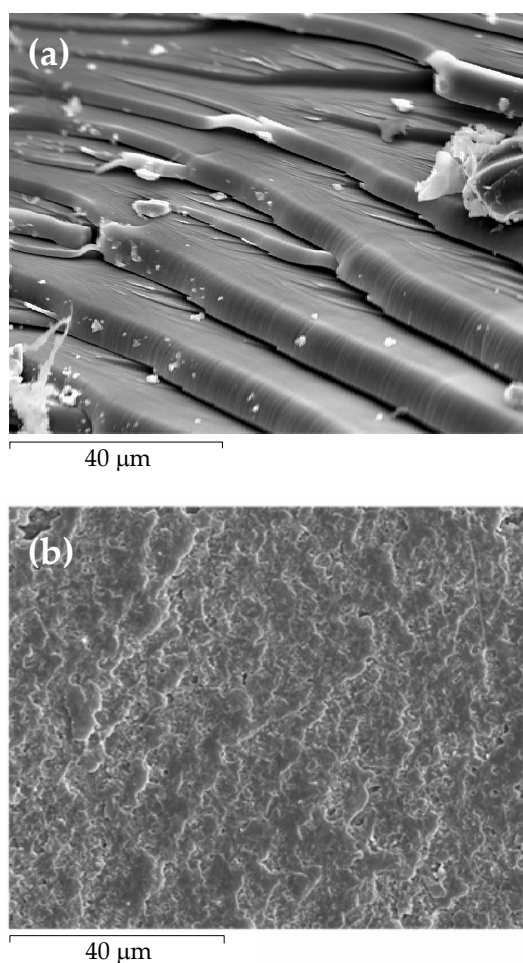


**Figure 12.** SEM micrographs of the fracture surfaces of the materials obtained from a DGEBA/ $\gamma$ -VL 2:1 (mol/mol) formulation initiated by 1 phr of  $\text{Yb}(\text{OTf})_3$  without clay (a) and with 3 phr of the Cloisite® 30B (b).

teraction of the cation with the clay.

The thermal stability of nanocomposites was higher than that of the unfilled thermoset.

By SEM microscopy we observed that the addition of clay converts the typical fragile fracture of epoxy materials to a more ductile one.

### Acknowledgements

Authors from the Universitat Rovira i

Virgili would like to thank the CICYT (Comisión Interministerial de Ciencia y Tecnología) and FEDER (Fondo Europeo de Desarrollo Regional) (MAT2008-06284-C03-01) for their financial support.

### References

- [1] Becker O, Simon GP. *Adv Polym Sci* 2005; 179: 29-82.
- [2] Pavlidou S, Papispyrides CD. *Prog Polym Sci* 2008; 33: 1119-1198.
- [3] Ray SS, Okamoto M. *Prog Polym Sci* 2003; 28: 1539-1641.
- [4] Giannelis EP. *Adv Mater* 1996; 8: 29-35.
- [5] Kornmann X, Lindberg H, Berglund LA. *Polymer* 2001; 42: 1303-1310.
- [6] Kim CM, Lee DH, Hoffmann B, Kressler J, Stoppelmann G. *Polymer* 2001; 42: 1095-1100.
- [7] Alexandre M, Dubois P. *Mater Sci Eng R* 2008; 28: 1-63.
- [8] Beyer G. *Plast Addit Compound* 2002; 4: 22-27.
- [9] Lan T, Kaviratna PD, Pinnavaia, TJ. *Chem Mater* 1995; 7: 2144-2150.
- [10] Jiankun L, Yucai K, Zongneng Q, Xiao-Su Y. *J Polym Sci Part B: Polym Phys* 2001; 39: 115-120.
- [11] Kornmann X, Lindberg H, Berglund LA. *Polymer* 2001; 42: 4493-4499.
- [12] Becker O, Cheng YB, Varley RJ, Simon GP. *Macromolecules* 2003; 36: 1616-1625.
- [13] Tolle TB, Anderson DP. *Compos Sci Technol* 2002; 62: 1033-1041.
- [14] Kornmann X, Thomann R, Mülhaupt R, Finter J, Berglund LA. *Polym Eng Sci* 2002; 42: 1815-1826.
- [15] Benfarhi S, Decker C, Keller L, Zahouily K. *Eur Polym J* 2004; 40: 493-501.
- [16] Bongiovanni R, Mazza D, Ronchetti S, Turcato EA. *J Colloid Interface Sci* 2006; 296: 515-519.



- [17] Arasa M, Ramis X, Salla JM, Mantecón A, Serra A. *J Polym Sci Part A: Polym Chem* 2007; 45: 2129-2141.
- [18] Arasa M, Ramis X, Salla JM, Ferrando F, Serra A, Mantecón A. *Eur Polym J* 2009 in press.
- [19] Coats AW, Redfern JP. *Nature* 1964; 201: 68-69.
- [20] Kissinger HE. *Anal Chem* 1957; 29: 1702-1706.
- [21] Vyazovkin S, Sbirrazzuoli N. *Macromol Chem Phys* 1999; 200: 2294-2303.
- [22] Vyazovkin S, Sbirrazzuoli N. *Macromol Rapid Commun* 2006; 27: 1515-1532.
- [23] Pethrick RA, "Chapter 3: Rheological Studies Using a Vibrating Probe, in *Rheological Measurement*", AA. Collyer and DW. Clegg, Editors. 1998, Chapman & Hall: London.
- [24] Affrossman S, Collins A, Hayward D, Trottier E, Pethrick RA. *J Oil & Colour Chem Assoc* 1989; 72: 452-453.
- [25] Le Pluart L, Duchet J, Sautereau H. *Polymer* 2005; 46: 12267-12278.
- [26] Brown JM, Curliss D, Vaia RA. *Chem Matter* 2000; 12: 3376-3384.
- [27] Chen D, Pingsheng H. *Compos Sci Technol* 2004; 64: 2501-257.
- [28] Kubisa P, Penczek S. *Prog Polym Sci* 1999; 24: 1409-1437.
- [29] Salla JM, Fernández-Francos X, Ramis X, Mas C, Mantecón A, Serra A. *J Therm Anal Calorim* 2008; 91:385-393.
- [30] Liu T, Tjiu WC, Tong Y, He C, Goh SS, Chung TS. *J Appl Polym Sci* 2004; 94:1236-1244.
- [31] Ratna D, Manoj NR, Varley R, Singh Raman RK, Simon GP. *Polym Int* 2003; 52: 1403-1407.
- [32] Hutchinson JM, Montserrat S, Román F, Cortés P, Campos L. *J Appl Polym Sci* 2006; 102: 3751-3763.
- [33] Vyazovkin S, Linert W. *Int Rev Phys Chem* 1995; 14: 355-369.
- [34] Budrugaec P, Homentcovschi D, Segal E. *J Therm Anal Calorim* 2001; 63: 457-463.
- [35] Mas C, Ramis X, Salla JM, Mantecón A, Serra A. *J Polym Sci Part A: Polym Chem* 2003; 41: 2794-2808.
- [36] Zhu J, Uhl FM, Morgan AB, Wilkie CA. *Chem Mater* 2001; 13: 4649-4654.

# Copolimerització aniónica i 4. catiónica del diglicidilèter de bisfenol A (DGEBA) amb bis( $\gamma$ - lactones) condensades

UNIVERSITAT ROVIRA I VIRGILI  
NOUS TERMOESTABLES EPOXÍDICS MODIFICATS AMB GAMMA-LACTONES I BIS-GAMMA-LACTONES CONDENSADAES  
M<sup>a</sup> Mercè Arasa Bertomeu  
ISBN:978-84-692-4157-8/DL:T-1171-2009

## 4.1 INTRODUCCIÓ

Una vegada finalitzats els estudis realitzats sobre la copolimerització catiònica entre el DGEBA i la  $\gamma$ -valerolactona, es va estudiar la copolimerització catiònica i aniónica del DGEBA amb dues bis( $\gamma$ -lactones) condensades: 1-metil-2,8-dioxabicyclo(3.3.0)-3,7-octandiona (bisMe) i la 1-fenil-2,8-dioxabicyclo(3.3.0)-3,7-octandiona (bisPhe).

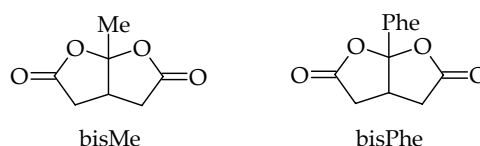


**Figura 4.1.** Estructura de les bis( $\gamma$ -lactones) emprades

Les bis( $\gamma$ -lactones) han estat sintetitzades en el laboratori seguint el procediment descrit per Tadokoro i col.<sup>1</sup>, introduint algunes modificacions com el canvi de base, utilitzant DMAP enlloc de piridina, i el mètode de separació del producte. Malgrat que el procediment experimental de preparació és senzill, el mecanisme de reacció és complex i s'inicia per una reacció tipus Dakin-West<sup>2</sup> que permet convertir grups carboxílics en grups cetona. Es va partir de l'àcid tricarbàl·lic i el corresponent anhídrid: acètic en el cas de la bisMe i benzoic per la bisPhe en presència de DMAP (figura 4.2). Mitjançant aquest procés s'obté el compost A que després evoluciona fins arribar a la bislactona.

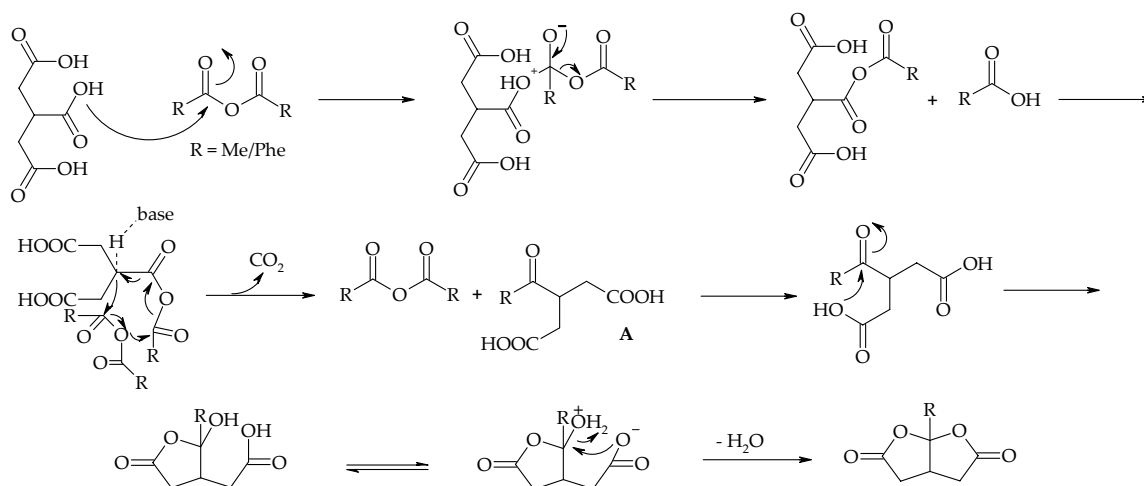


**Figura 4.2.** Mecanisme de reacció proposat per King i col.<sup>3</sup>

En la literatura no s'ha trobat descrita la copolimerització catiònica de bislactones condensades amb epòxids però si hi ha treballs de copolimerització amb mono i diepòxids en condicions anióniques utilitzant alcòxids (t-BuOK) com iniciadors<sup>4</sup>. En aquests treballs es va observar que tenia lloc una copolimerització alternada donant lloc al corresponent

poli(èter-ester-cetona), sense pràcticament canvi de volum<sup>5</sup>. El mecanisme de copolimerització proposat es mostra a continuació.

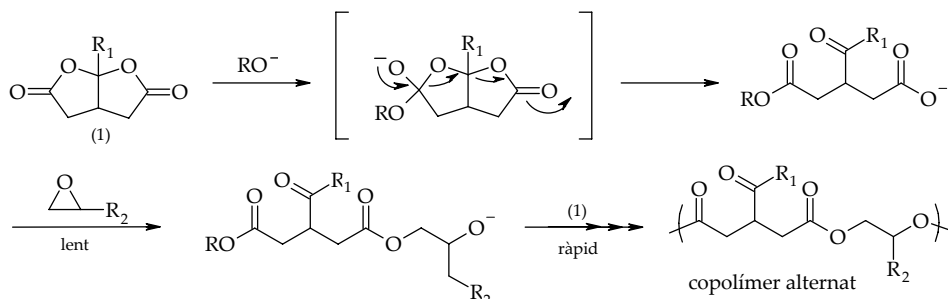


**Figura 4.4.** Mecanisme de copolimerització aniònica entre una bis( $\gamma$ -lactona) i un epòxid

En el treball que es presenta s'han dut a terme les copolimeritzacions entre el DGEBA i les bis( $\gamma$ -lactones), bisMe i bisPhe, en condicions aniòniques i catiòniques. En condicions aniòniques s'han emprant diverses amines terciàries: 1-metilimidazole (1MI), 1,8-diazabicyclo[5,4,0]undecen-7-è (DBU) i 4-(N,N-dimetilamino)piridina (DMAP). Aquesta última va ser descrita per primera vegada a la literatura com un iniciador eficaç en polimeritzacions d'obertura d'anell pel nostre grup de recerca<sup>6</sup>. Posteriorment, Dell'Erba i Williams<sup>7</sup> van realitzar un estudi sobre la homopolimerització de monòmers epoxídics com el DGEBA i el PGE iniciada per DMAP on es va observar com l'addició de DMAP donava lloc a un augment de la velocitat de polimerització respecte les típiques amines terciàries i que el valor de  $T_g$  obtingut era superior. Tot i així, la homopolimerització aniònica de grups epoxi iniciada per amines terciàries i imidazoles N-substituïdes és una reacció complexa i presenta dos inconvenients: (a) velocitats de reacció baixes i (b) formació de cadenes principals curtes degut a la elevada velocitat de les reaccions de transferència de cadena<sup>8</sup>.

En les copolimeritzacions catiòniques d'aquests bis( $\gamma$ -lactones) amb el DGEBA s'han utilitzat triflats de terres rares com iniciadors:  $La(OTf)_3$ ,  $Yb(OTf)_3$ ,  $Sc(OTf)_3$ , els quals ja havien estat estudiats prèviament amb les mono( $\gamma$ -lactones).

Els resultats d'aquest estudi es presenten en els següents treballs:

- Anionic copolymerization of DGEBA with two bicyclic bis( $\gamma$ -lactone) derivatives using tertiary amines as initiators.
- Cationic polymerization of DGEBA with two bicyclic bis( $\gamma$ -lactone) derivatives using rare earth metal triflates as initiators.
- Study of the copolymerization of DGEBA and two bicyclic bis( $\gamma$ -lactone)s using rare earth metal triflates as initiators by infrared spectroscopy.

## Referències

- [1] Tadokoro, A.; Takata, T.; Endo, T.; *Macromolecules*, 26, 4400-4406 (1993).
- [2] (a) Allinger, NL.; Wang, GL.; Dewhurst, BB.; *J. Org. Chem.*, 39, 1730-1735 (1974); (b) Buchanan, GL.; *Chem. Soc. Rev.*, 17, 91-109 (1988).
- [3] King, JA.; McMillan, FH.; *J. Amer. Chem. Soc.*, 73, 4451- 4453 (1951).
- [4] Takata, T.; Tadokoro, T.; Endo, T.; *Macromolecules*, 25, 2782-2783 (1992).
- [5] Takata, T.; Chung, K.; Tadokoro, A.; Endo, T.; *Macromolecules*, 26, 6686-6687 (1993).
- [6] (a) Galià, M.; Serra, A.; Mantecón, A.; Cádiz, V.; *J. Appl. Polym. Sci.*, 56, 193-200 (1995); (b) Ribera, D.; Mantecón, A.; Serra, A.; *J. Polym. Sci., Part A: Polym. Chem.*, 40, 3916-3929 (2007).
- [7] Dell'Ebra, IE.; Williams, RJJ.; *Polym. Eng. Sci.*, 46, 351-359 (2006).
- [8] (a) Mika, T.; Bauer, RS.; "Curing Agents and Modifier" in "Epoxy Resins Chemistry and Technology", C.A. May editor, 2nd edition, Marcel Dekker, New York, 465 (1988); (b) Pascault, JP.; Sautereau, H.; Verdu, J.; Williams, RJJ.; "Thermosetting Polymers", Marcel Dekker, New York 2002.

UNIVERSITAT ROVIRA I VIRGILI  
NOUS TERMOESTABLES EPOXÍDICS MODIFICATS AMB GAMMA-LACTONES I BIS-GAMMA-LACTONES CONDENSADES  
M<sup>a</sup> Mercè Arasa Bertomeu  
ISBN:978-84-692-4157-8/DL:T-1171-2009

4.2 ANIONIC COPOLYMERIZATION OF DGEBA WITH TWO  
DERIVATIVES OF BIS( $\gamma$ -LACTONES) USING TERTIARY  
AMINES AS INITIATORS

---

*Mercè Arasa, Xavier Ramis, Josep Maria Salla, Ana Mantecón, Àngels Serra; Polymer, 50, 2228-2236 (2009)*



## ANIONIC COPOLYMERIZATION OF DGEBA WITH TWO BICYCLIC BIS( $\gamma$ -LACTONE) DERIVATIVES USING TERTIARY AMINES AS INITIATORS

Mercè Arasa,<sup>1</sup> Xavier Ramis,<sup>2</sup> Josep Maria Salla,<sup>2</sup> Ana Mantecón,<sup>1</sup> Àngels Serra<sup>1</sup>

<sup>1</sup>Dpt. Q. Analítica i Q. Orgànica, URV. C/Marcel·lí Domingo s/n, 43007 Tarragona, Spain

<sup>2</sup>Lab. Termodinàmica, ETSEIB. UPC, Av. Diagonal 647, 08028 Barcelona, Spain

### Abstract

The anionic copolymerization, to form thermosets, of diglycidylether of bisphenol A (DGEBA) with two condensed bis( $\gamma$ -lactone)s (bisMe and bisPhe) using 4-(N,N-dimethylamino)pyridine (DMAP), 1,8-diazabicyclo[5.4.0]undec-7-ene (DBU), and 1-methylimidazole (1MI) as initiators was studied by differential scanning calorimetry (DSC). The kinetics was evaluated by isoconversional procedures. The evolution of the bands that form or disappear during curing was followed by Fourier Transform Infrared in the attenuated-total-reflection mode (FTIR/ATR) to clarify the reactive processes that take place. Unexpected processes, which lead to the formation of five-membered lactones, were detected when non-stoichiometric proportions of monomers were used. The stoichiometric DGEBA/bislactone ratio produces the expected alternate poly(ester-ketone) network. The thermal degradability of the materials obtained was evaluated by TGA, and their reworkable character was confirmed. Materials obtained from stoichiometric mixtures were completely soluble in ethanolic KOH.

*Keywords:* Anionic polymerization, thermosets, DSC, FTIR, tertiary amines.

### Introduction

Ring-opening is a polymerization mechanism that has the advantage of allowing the copolymerization of monomers with different reactive groups, such as lactones and epoxides. The polymerization of lactones leads to polyesters and the polymerization of epoxides leads to polyethers. Thus, the copolymerization of these two monomers can produce poly(ether-ester) structures with a relative proportion of structural units

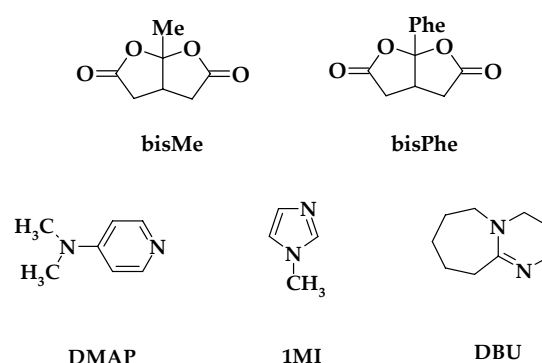
that depend on the feed ratio. This copolymerization can be initiated by both anionic and cationic species. Cationic initiators conduce to a rather complex mechanism, with four reactive processes, one of them being the formation of an intermediate spiroorthoester. On the other hand, anionic copolymerization takes place directly by the attack of the initiator to one of the monomers and the subsequent alternant addition of the others to the final reactive chain end.



Five membered lactones are difficult to homopolymerize or copolymerize with epoxides because their ring closing is much more favourable than their ring opening. Therefore, it is necessary to suppress ring closing by the accurate selection of the lactone structure. It has been described that bis( $\gamma$ -lactone)s copolymerize with epoxides to form the copolymer, which contains poly(ether-ester-ketone) moieties, being the ketone group produced by an isomerization of the bislactone, which takes place during their opening.<sup>1-4</sup>

Several authors reported the alternant character of the anionic copolymerization of epoxides with condensed<sup>3,5</sup> or spiranic<sup>6</sup> bis( $\gamma$ -lactone)s. Among anionic initiators, strong bases such as *t*-butoxide, methyl lithium and hydroxides have been used in the linear copolymerization of epoxides with bis( $\gamma$ -lactone)s.<sup>3</sup> However, from a technological point of view, these initiators are not suitable to obtain thermosets from diepoxides and bis( $\gamma$ -lactone)s because their use requires solvent and/or inert atmosphere. For this reason we propose the use of tertiary amines as initiators in the preparation of new thermosets from mixtures of diglycidylether of bisphenol A (DGEBA) and two different condensed bis( $\gamma$ -lactone)s, 1-methyl-2,8-dioxabicyclo[3.3.0]octane-3,7-dione (bisMe) and 1-phenyl-2,8-dioxabicyclo[3.3.0]octane-3,7-dione (bisPhe). As tertiary amines, we selected 4-(*N,N*-dimethylamino)pyridine (DMAP), 1,8-diazabicyclo[5.4.0]undec-7-ene (DBU) and 1-methylimidazole (1MI). Tertiary amines were previously reported to be active in the ring-opening homopolymerization of epoxides.<sup>7-9</sup>

The structure of monomers and initiators are represented in **Scheme 1**. The poly(ether-ester-ketone) three-dimensional structures obtained in this way should be more thermally degradable than the thermosets obtained from pure DGEBA, due to the presence of ester linkages. The introduction of ester groups in thermosetting materials has been used as one of the most fruitful strategies to improve the reworkability of the thermosets. The concept of reworkable thermoset is defined as the ability to break-down the network under controlled conditions to remove it from a substrate. However, this term does not mean that the polymeric material can be reused or recycled but only that the partially degraded material can be removed by solvents or by brushing from the surface where it is applied. Rework enables the straightforward repair, replacement or recycling of electronic devices assembled with such materials. Among the research groups that followed this strategy it should be considered the works reported by Ober,<sup>10,11</sup> Shirai<sup>12,13</sup> and Wong.<sup>14,15</sup>



**Scheme 1**

In addition to the thermal degradability, we expect to reach an improvement in the chemical degradation by saponifi-



cation of the ester groups, as we showed in a previous paper<sup>16</sup> based in the anionic copolymerization of DGEBA with spiranic bis( $\gamma$ -lactone)s, due to the alternant character of the copolymeric network that we obtained.

## Experimental Part

### Materials

Diglycidylether of bisphenol A (DGEBA) EPIKOTE RESIN 827 from Shell Chemicals (Epoxy Equiv. = 182.08 g/eq).

Tricarballic acid, acetic anhydride, benzoic anhydride, 4-(N,N-dimethylaminopyridine) (DMAP), 1,8-diazabicyclo[5.4.0]undec-7-ene (DBU), 1-methylimidazole (1MI) and phenylglycidylether (PGE) (from Aldrich) were used as received.

The solvents were purified by standard methods.

### Monomer synthesis

#### a) 1-Methyl-2,8-dioxabicyclo[3.3.0]octane-3,7-dione (bisMe). (Scheme 2)

A mixture of tricarballic acid (6 g, 33 mmol), acetic anhydride (50 ml, 508 mmol) and DMAP (0.9 g, 7.36 mmol) was

refluxed with stirring for 3 h under argon. After elimination of acetic acid in vacuum the product was precipitated in ethanol, being the remaining anhydride soluble in this solvent. After filtration, the solid product was dissolved in acetone and the solution was treated with active charcoal. After filtration and evaporation of the solvent a white solid was obtained. The product was recrystallized in ethanol affording a white crystalline solid. Yield: 40 %, m.p.: 101-2 °C. (lit.<sup>3</sup> 98-99 °C).

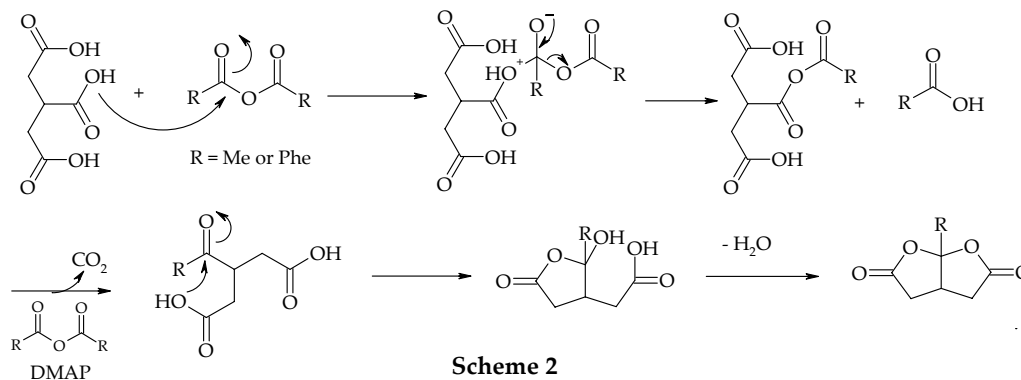
FTIR/ATR ( $\text{cm}^{-1}$ ): 1782, 1264, 1134, 1074, 1051, 922.

<sup>1</sup>H NMR (400 MHz  $\text{CDCl}_3$ ):  $\delta$  (ppm) 3.0-3.2 (m, 3H), 2.6 (dd, 2H), 1.8 (s, 3H). <sup>13</sup>C NMR (75.4 MHz  $\text{CDCl}_3$ ):  $\delta$  (ppm) 172.5, 113.2, 39.2, 35.6, 24.1.

#### b) 1-Phenyl-2,8-dioxabicyclo[3.3.0]octane-3,7-dione (bisPhe). (Scheme 2)

It was similarly synthesized using benzoic anhydride instead of acetic anhydride and using xylene as the solvent. Benzoic acid and anhydride were soluble in ethanol but the bislactone precipitated. Yield: 55 %, m.p.: 139-140 °C (lit.<sup>17</sup> 122 °C, lit.<sup>4</sup> 138-139 °C).

FTIR/ATR ( $\text{cm}^{-1}$ ): 1791, 1450, 1241, 1189, 1149, 1092, 992, 972, 859, 761.



Scheme 2



<sup>1</sup>H NMR (400 MHz CDCl<sub>3</sub>): δ (ppm) 7.5 (s, 5H), 3.4-3.3 (broad m, 1H), 3.2-3.1 (dd, 2H), 2.7-2.6 (dd, 2H). <sup>13</sup>C NMR (75.4 MHz CDCl<sub>3</sub>): δ (ppm) 172.9, 136.6, 130.8, 129.6, 125.4, 113.7, 42.0, 35.8.

### Preparation of the curing mixtures

The samples were prepared by mixing the selected quantity of initiator with the corresponding amount of bis-lactone and DGEBA with manual stirring in a mortar. The prepared mixtures were kept at -18 °C before use.

### Characterization and measurements

Calorimetric studies were carried out on a Mettler DSC-821e thermal analyzer in covered Al pans under N<sub>2</sub> at 10 °C/min. To determine kinetic parameters, the curves were registered at 2, 5, 10 and 15 °C/min. The calorimeter was calibrated using an indium standard (heat flow calibration) and an indium-lead-zinc standard (temperature calibration). The samples weighed approximately 7-9 mg.

In the dynamic curing process the degree of conversion by DSC ( $\alpha_{DSC}$ ) was calculated as follows:

$$\alpha_{DSC} = \Delta H_T / \Delta H_{dyn} \quad (1)$$

where  $\Delta H_T$  is the heat released up to a temperature  $T$ , obtained by integration of the calorimetric signal up to this temperature, and  $\Delta H_{dyn}$  is the total reaction heat associated with the complete conversion of all reactive groups.

The glass transition temperatures

( $T_{gs}$ ) were calculated, after complete curing by means of a second scan, as the temperature of the half-way point of the jump in the heat capacity when the material changed from the glassy to the rubbery state under N<sub>2</sub> atmosphere.

The isothermal curing process at 160 °C was monitored with a FTIR spectrophotometer FTIR-680PLUS from JASCO with a resolution of 4 cm<sup>-1</sup> in the absorbance mode. An attenuated-total-reflection accessory with thermal control and a diamond crystal (Golden Gate heated single-reflection diamond ATR, Specac-Teknokroma) was used to determine FTIR spectra.

Thermogravimetric analyses (TGAs) were carried out with a Mettler TGA/SDTA 851e thermobalance. Cured samples with an approximate mass of 7 mg were degraded between 30 and 600 °C at a heating rate of 10 °C/min in N<sub>2</sub> (100 cm<sup>3</sup> min<sup>-1</sup>) measured in normal conditions.

### Kinetic analysis

Integral isoconversional non-isothermal kinetic analysis named Kissinger-Akahira-Sunose procedure was used to determine the kinetic parameters of the curing process.<sup>18-20</sup>

### Chemical degradation

The chemical degradation via saponification was performed at reflux in 1 M ethanolic KOH (ethanol/water 90/10 v/v).

### Results and discussion

In a previous work<sup>6</sup> we studied the curing of mixtures of DGEBA epoxy



resin with 1,6-dioxaspiro[4.4]nonan-2,7-dione  $s(\gamma\text{-BL})$  using DMAP, 1MI and 1,5-diazabicyclo[4.3.0]non-5-ene (DBN), a homologous of DBU. The evolution of the reactive groups was monitored by FTIR. By this technique and DSC, it was proved that the pure bislactone cannot homopolymerize with none of the initiators tested and, therefore, the reactivity ratio of the spiranic bislactone tends to zero. Epoxy groups can homopolymerize in the presence of the anionic initiator when  $s(\gamma\text{-BL})$  is run out. To get a completely alternant copolymer a DGEBA/ $s(\gamma\text{-BL})$  1:2 (mol/mol) formulation is needed, since the functionality of DGEBA is four and the functionality of the bislactone is two. Thus, this formulation contains one bislactone per four epoxide groups. When epoxy groups were in excess in the formulation their homopolymerization also occurred. By DSC we saw that the addition of the spirobislactone to DGEBA produced an acceleration of the curing process and that DMAP, among the amines tested, was the most active. However, the efficiency of these initiators is related not only with the intrinsic activity of their tertiary nitrogens but also to the chance of undergoing termination reactions, which allow to refresh the initiator and keep a sufficient amount of active species<sup>8</sup> in the reaction medium. It was determined that a complete curing could be achieved with a small amount of any of the initiators tested, in contrast to the higher amount of initiator needed for the homopolymerization of pure DGEBA.

In the present study we copolymerized DGEBA with the condensed bis( $\gamma$ -lactone)s shown in **Scheme 1**. Similar

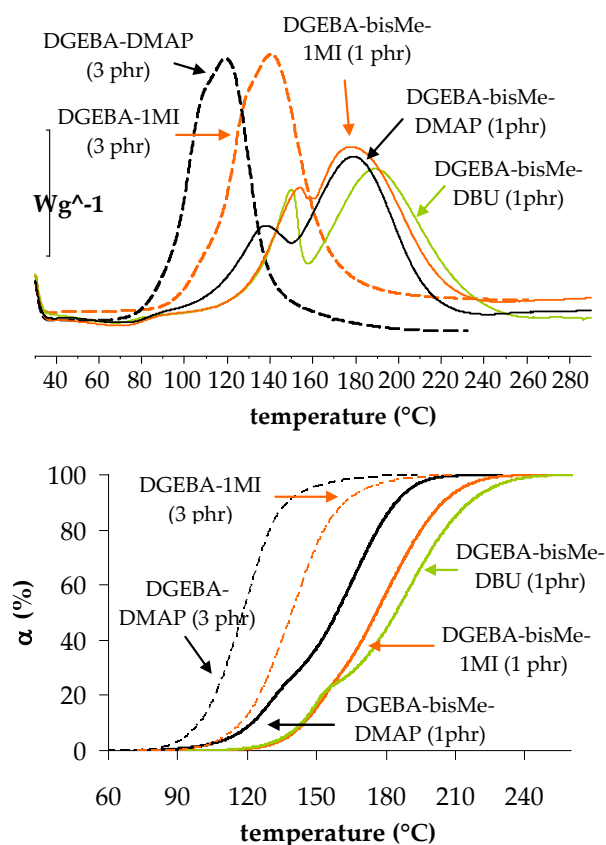


**Figure 1.** DSC scanning and conversion curves versus temperature of DGEBA initiated by 3 phr of 1MI and DMAP and DGEBA/bisMe 2:1 (mol/mol) mixture initiated by 1 phr of DMAP, MI and DBU at a heating rate of 10 °C/min.

systems were previously studied by other authors with mono or bifunctional epoxides using hydroxides, alkoxides or organometallics as initiators.<sup>3,5,21,22</sup> Because we used different initiators (DMAP, 1MI and DBU) we firstly studied by DSC the curing evolution of DGEBA/bisMe 2:1 (mol/mol) mixtures with 1-3 phr of each initiator. It should be said that in this reaction DGEBA acts as a tetrafunctional monomer and bis( $\gamma$ -lactone) as bifunctional and therefore homopolymerization of epoxide can be expected because it is in excess. The calorimetric curves are shown in **Figure 1**, which includes the curves for pure



**Table 1.** Calorimetric data of the formulations studied

Entry	Formulation (mol/mol)	Proportion of initiator (phr)	Initiator	mols initiator / eq. epoxy	T <sub>g</sub> (°C)	ΔH (J/g)	ΔH <sup>a</sup> (kJ/ee)	T <sub>max</sub> (°C)
1	DGEBA	3	DMAP	0.044711	145	473	86	119
2	DGEBA/bisMe 2:1	1	DMAP	0.018100	95	449	99	138/179
3	DGEBA/bisMe 2:1	2	DMAP	0.036201	106	473	105	129/165
4	DGEBA/bisMe 2:1	3	DMAP	0.054301	105	469	104	132/156
5	DGEBA/bisMe 1:1	1	DMAP	0.021297	80	361	94	152/186
6	DGEBA/bisMe 1:1	2	DMAP	0.042595	85	381	99	140/170
7	DGEBA/bisMe 1:2	1	DMAP	0.027682	69	272	92	160
8	DGEBA/bisMe 1:2	2	DMAP	0.055363	69	270	91	152
9	DGEBA/bisPhe	2	DMAP	0.038741	106	432	102	126/162
10	DGEBA/bisPhe	2	DMAP	0.047677	96	315	92	133/164
11	DGEBA/bisPhe	2	DMAP	0.065540	89	221	88	143
12	DGEBA	3	1MI	0.066533	141	490	89	141
13	DGEBA/bisMe 2:1	1	1MI	0.026934	94	446	99	154/178
14	DGEBA/bisMe 2:1	2	1MI	0.053869	105	474	105	145/164
15	DGEBA	3	DBU	0.035880	---	---	---	---
16	DGEBA/bisMe 2:1	1	DBU	0.014525	98	451	100	150/190
17	DGEBA/bisMe 2:1	2	DBU	0.029050	105	475	105	140/175

<sup>a</sup> enthalpy released by epoxy equivalent

DGEBA curing in order to compare. **Table 1** collects the main calorimetric data. In these studies we observed that 3 phr of DMAP or 1MI were necessary to completely cure pure DGEBA and that DBU was not able to cure DGEBA even in this proportion. The heat released per epoxy equivalent during DGEBA curing with 3 phr of DMAP or 1MI agrees with the values previously described.<sup>6</sup> In contrast, bislactone/DGEBA mixtures can cure with only 1-2 phr of initiator. As can be seen in the figure, DGEBA shows unimodal curves whereas the mixtures show bimodal shape, which indicates the occurrence of different reactive processes. To know the reaction responsible

of each exotherm, we registered the FTIR/ATR spectra of partially cured samples using DMAP at some selected curing temperatures: at the beginning of the first exotherm and in the maxima of the two exotherms (**Figure 2**). The most significant absorptions that indicate which process takes place during curing are the bands corresponding to the initial lactone at 1794 cm<sup>-1</sup>, the linear ester formed at 1738 cm<sup>-1</sup> and the epoxy absorption at 915 cm<sup>-1</sup>. In the first spectrum (a), registered at the beginning of the first exotherm, we can observe the lactone band and the expected linear ester and the ketone (at 1738 and 1716 cm<sup>-1</sup> respectively) that begin to form by open-

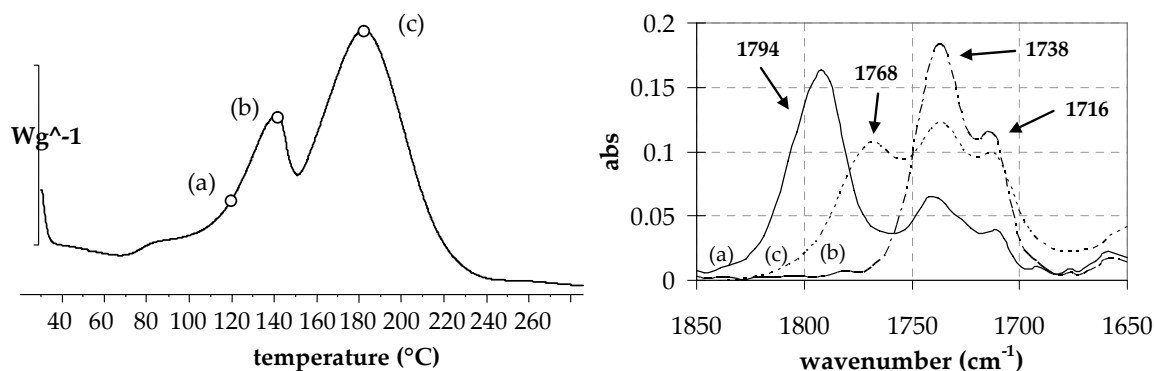
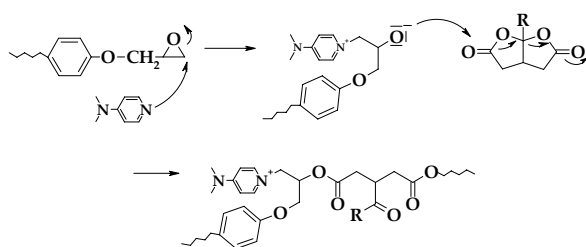


**Figure 2.** DSC curing exotherm with the detail of the thermal treatment of the samples investigated by FTIR and carbonylic region of the FTIR spectra of samples partially cured in the DSC from a DGEBA/bisMe 2:1 (mol/mol) formulation with 1 phr DMAP (a) before the 1st maximum, (b) in 1st maximum and (c) in the 2nd maximum.



**Scheme 3**

ing of the bislactone with isomerization (**Scheme 3**). In the spectrum registered in the first maximum (b), the band of the lactone has disappeared and the absorptions at 1738 and 1716  $\text{cm}^{-1}$  have increased. Moreover, the intensity of the epoxy band (not represented in the figure) has decreased. This indicates that the first exotherm corresponds to the copolymerization of epoxide and lactone. In the spectrum registered in the second maximum (c) the carbonyl bands previously formed have diminished and, surprisingly, a new absorption at 1768  $\text{cm}^{-1}$  appears. Moreover, the intensity of the epoxy band diminishes. These observations indicate that, in addition to the homopolymerization of epoxide, this second exotherm includes other reactive processes, which were not described before by Endo's group.<sup>3-5,21,22</sup> This second exotherm, corresponding to the

homopolymerization of epoxide, which includes these unexpected processes lead to a greater enthalpy than that observed in a previous work on the copolymerization of a spiranic bis( $\gamma$ -lactone), which did not experiment unexpected reactions.<sup>6</sup> With both spiranic and condensed bislactones the copolymerization occurs before the homopolymerization of epoxide. If we recall **Figure 1**, we can see that DMAP seems to be the most active initiator in both processes, while DBU is the less active. For this reason we selected DMAP to follow this study.

**Figure 3** shows the evolution of the activation energies during curing. As we can see, the curves reflect two different parts. The first one, up to a conversion of about 25 % corresponds to the copolymerization process of bislactone and epoxide. From this conversion, the predominant process is the homopolymerization of epoxide, which is accompanied by the unexpected processes before mentioned. The activation energy of the copolymerization is higher than that of the homopolymerization, as we reported previously.<sup>6</sup>

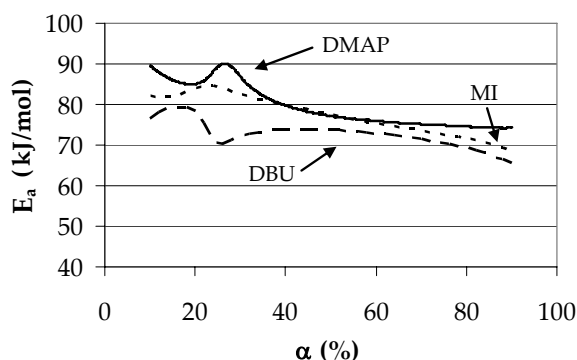


**Figure 3.** Dependence of the activation energy on the degree of conversion for the curing of DGEBA/bisMe 2:1 (mol/mol) mixture initiated by 1 phr of DMAP, 1MI and DBU.

**Figure 4** shows the calorimetric curves and conversions obtained in dynamic scans for the different DGEBA/bisMe formulations studied using 2 phr of DMAP as initiator. Before discussing these results, it should be commented that the main heat is released by the opening of the epoxide, because the enthalpy released in the opening of a  $\gamma$ -lactone is reported to be 5-10 kJ/mol.<sup>23</sup> The stoichiometric mixture 1:2 (mol/mol) shows an endotherm due to the melting of the solid bislactone and a unimodal exotherm, which seems to indicate that an only process occurs. In contrast, the other two formulations present a bimodal exotherm, the first one corresponding

to the ester formation and the second to the epoxide homopolymerization plus the unexpected processes, increasing the second one with the proportion of epoxide (2:1 formulation). The conversion curves against temperature show that until a conversion of 25 % the three formulations coincide and from this point formulation 2:1 slows down. Up to a conversion of about 50 % formulations 1:1 and 1:2 also coincide and then the former begins to delay, being from this conversion the stoichiometric formulation the fastest. This can be attributed to the fact that the copolymerization takes place at the beginning of the curing process, until the lactone is run out, and that it is faster than the homopolymerization of epoxide. These results are in accordance with those obtained for analogous anionic copolymerization of DGEBA/spirobislactones.<sup>6</sup>

If we look at the  $T_g$ s of the materials and the enthalpy per epoxy equivalent (**Table 1**) we can see that the use of 2 phr of each initiator allows the complete curing of the DGEBA/bislactone mixtures (entries 2-4) and even 1 phr was enough when the ratio epoxy/bislactone was

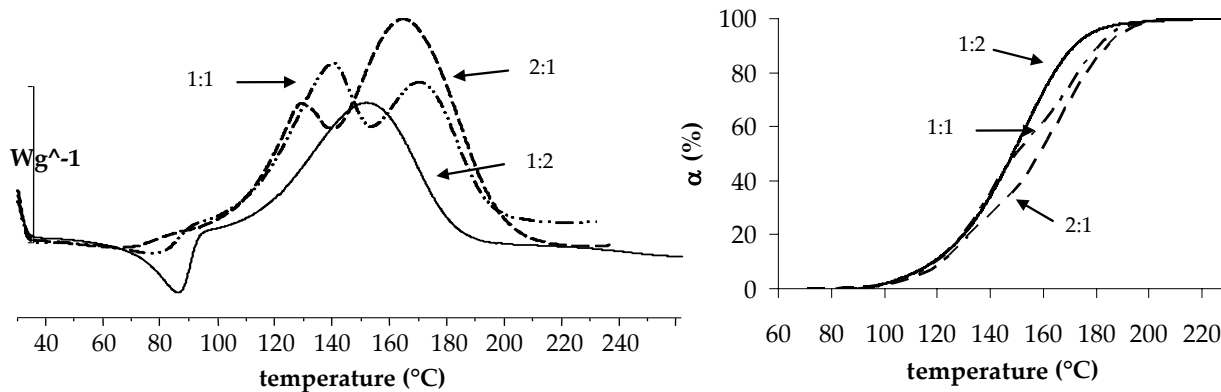


**Figure 4.** DSC scanning and conversion curves versus temperature of DGEBA/bisMe mixtures in molar ratios of 2:1, 1:1 and 1:2 (mol/mol) initiated by 2 phr of DMAP at a heating rate of 10 °C/min.

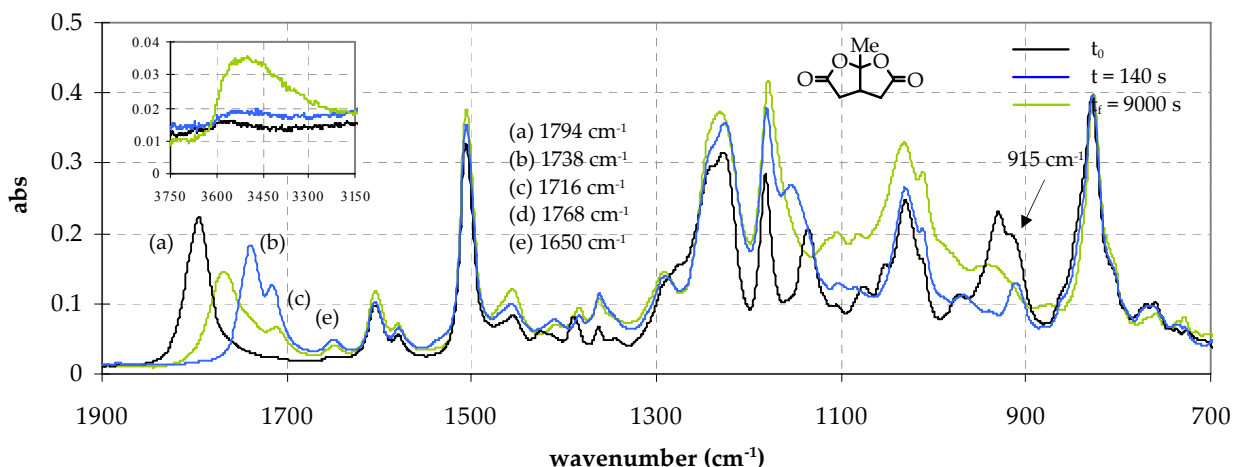


**Figure 5.** FTIR-ATR spectra taken at different curing times of a DGEBA/bisMe 2:1 (mol/mol) mixture with 2 phr of DMAP at 160 °C.

stoichiometric (entries 7 and 8). Due to the flexibility introduced by the copolymerization with the bislactone and the greater distance between crosslinks, the  $T_g$ s of the materials are reduced in comparison to pure DGEBA and their values decrease on increasing the proportion of lactone. The three initiators lead to similar  $T_g$ s and curing enthalpies but DMAP has a higher catalytic activity (entries 2, 3, 13, 14, 16 and 17).

We also studied the effect of changing methyl by phenyl group in the bislactone in the evolution of the curing process (entries 9, 10 and 11). It can be seen that when the proportion of bisPhe is low the  $T_g$ s are similar (entries 3 and 9), but when the proportion is high (entries 6 and 10, and 8 and 11) the values increase in reference to bisMe. The presence of the phenyl substituent slightly decreases the temperature of the maximum of the exotherms.

To go deeply in the reaction mechanism followed in the preparation of the thermosets, we registered the FTIR spectra during curing to see the evolu-

tion of the different absorptions. **Figure 5** collects the FTIR spectra of the curing of a DGEBA/bisMe 2:1 (mol/mol) formulation with 2 phr of DMAP obtained at 160 °C in the ATR before and after curing and at an intermediate stage. As we can see, the initial lactone band at 1794  $\text{cm}^{-1}$  has completely disappeared in the spectrum taken at 140 s, whereas the expected linear ester absorption at 1738  $\text{cm}^{-1}$  and the ketone absorption at 1716  $\text{cm}^{-1}$  can be clearly appreciated. At this curing time a little peak at 1650  $\text{cm}^{-1}$  can be also observed. This peak can be attributed to the formation of the pyridinium salt from the initiator, because it increases proportionally with the amount of DMAP added and it is not present when 1MI was used. As expected, the epoxy absorption at 915  $\text{cm}^{-1}$  decreases and the ether absorptions increase during curing indicating the homopolymerization of epoxide. In the spectrum of the final material the intensity of linear ester and the ketone bands decrease, and a new carbonyl absorption at 1768  $\text{cm}^{-1}$  appears. This seems to indicate that larger reaction times lead to unexpected processes in which linear ester and



ketone groups are involved. In the inset of the figure the hydroxylic absorption is also included, where we can see that this signal increases during curing.

To investigate if these unexpected processes take also place with other formulations, we registered their FTIR spectra during curing. **Figure 6** shows the carbonyl zone of the cured materials obtained from formulations DGEBA/bisMe 2:1, 1:1 and 1:2 (mol/mol) using 2 phr of DMAP as initiator at 160 °C. Whereas an excess of epoxide leads to the formation of the band at 1768 cm<sup>-1</sup>, the stoichiometric proportion (formulation 1:2) only produces the expected poly(ether-ester-ketone). Moreover, in the hydroxylic region (inset) we can see how the signal increases as the proportion of epoxide increases. From these results we can infer that the excess of epoxide and the subsequent formation of alkoxides could be the responsible of these unexpected processes. The substitution of DMAP by 1MI or DBU leads to similar results.

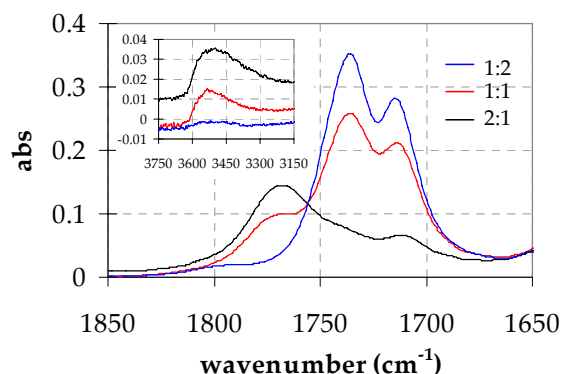


**Figure 6.** FTIR-ATR spectra taken of (a) hydroxylic and (b) carbonyl zone of DGEBA/bisMe 2:1, 1:1 and 1:2 (mol/mol) formulations initiated by 2 phr of DMAP after curing at 160 °C.

spectra of the DGEBA/bisPhe 2:1 (mol/mol) formulation (**Figure 7**), although the ketone appears at a different wavenumber (1685 cm<sup>-1</sup> for bisPhe and 1716 cm<sup>-1</sup> for bisMe) because of the conjugation with phenyl group in the former, the unexpected carbonyl band in both final materials appear at the same wavenumber (at 1768 cm<sup>-1</sup>). Again, in the spectrum of the material obtained from DGEBA/bisPhe 1:2 formulation, we could only observe the expected signals of poly(ether-ester-ketone).

In the carbonyl zone of the FTIR

Taking into account all these results, we can propose some plausible mech-

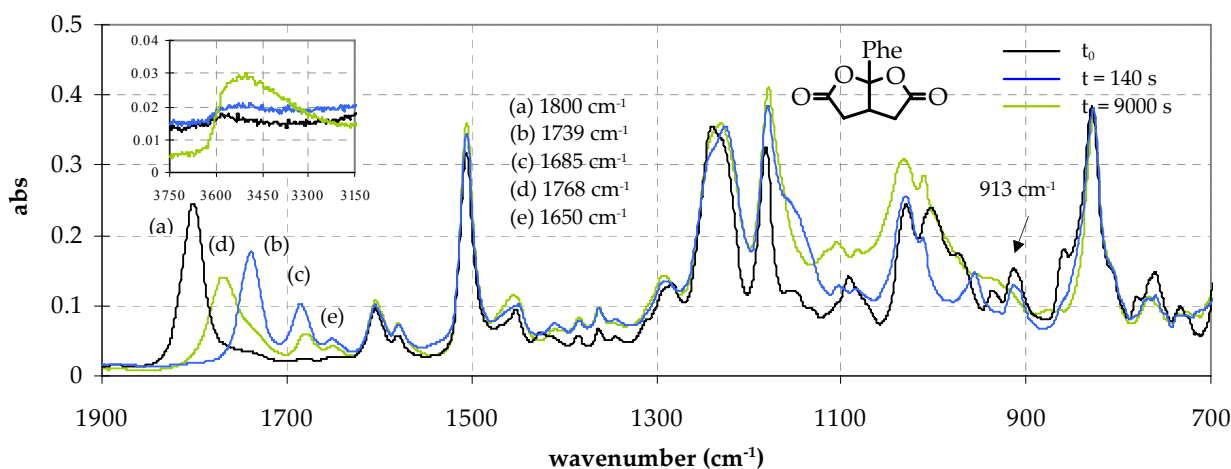


**Figure 7.** FTIR-ATR spectra taken at different curing times of a mixture of DGEBA/bisPhe in a molar ratio of 2:1 with 2 phr of DMAP at 160 °C.



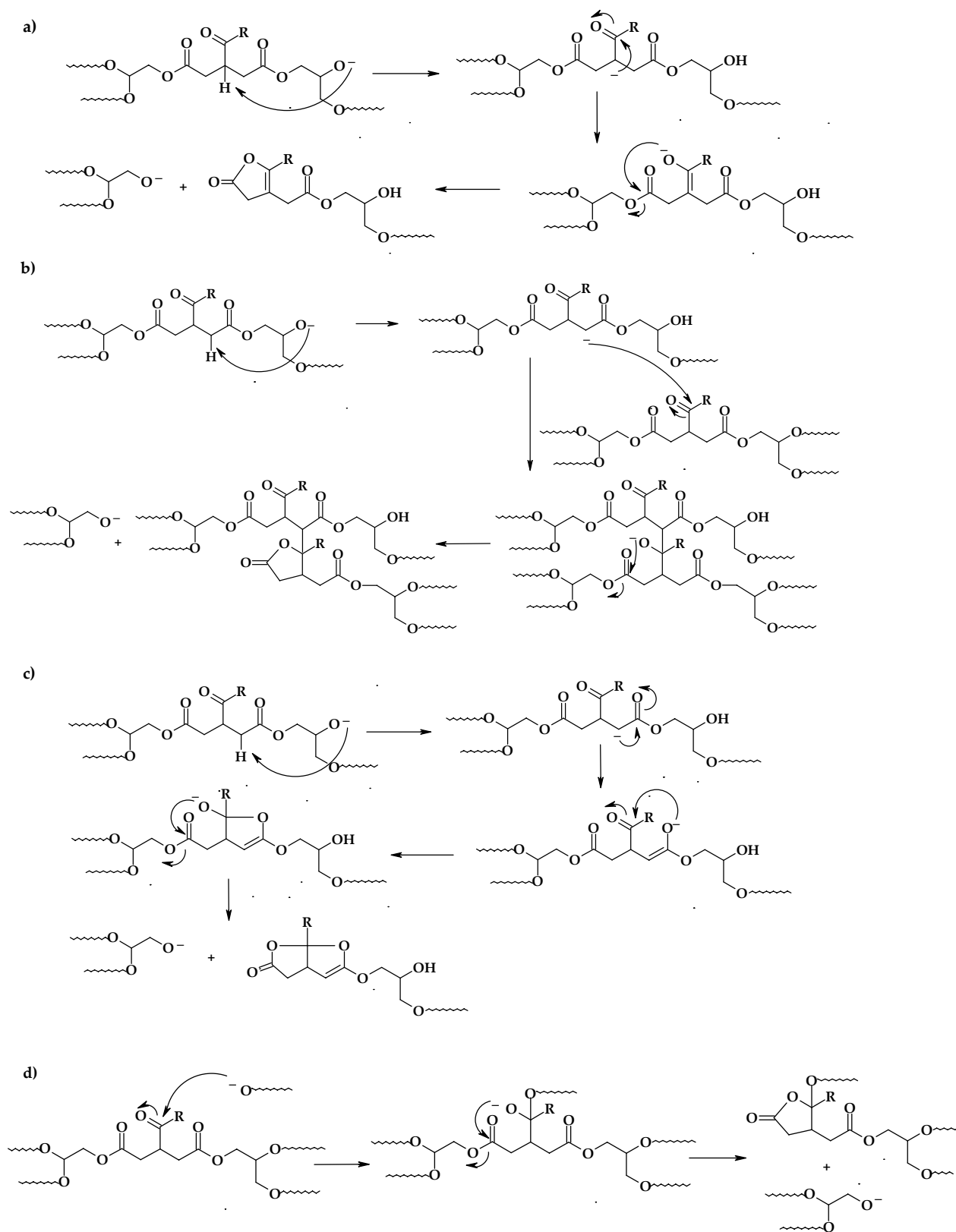
anisms, which are depicted in **Scheme 4**. At the first part of the curing, the alternant copolymerization takes place and, when the lactone is run out, the alkoxide groups can initiate the homopolymerization and other parallel reactions. At this point, the material has enough mobility because of the lactone moiety introduces flexibility and increases the distance between crosslinks.

The alkoxide, acting as a base, can extract the acidic  $\alpha$ -carbonyl protons (**Scheme 4 a, b** and **c**) or, as nucleophile, can directly attack the ketone (**Scheme 4 d**). In all these proposed reaction pathways, final thermodynamically stable five membered lactones are formed: in **a**, an unsaturated  $\gamma$ -lactone; in **b** and **d**, saturated  $\gamma$ -lactones and in **c**, a condensed lactone fused with an unsaturated five-membered ring. The first three processes are aldolic-like reactions and therefore there are equilibrium processes. The mechanism **d**, after the first attack of alkoxide to the ketone, consists in a transesterification. By mechanisms **a, b** and **c**, hydroxylic groups are formed, whereas none is formed by mechanism **d**. By FTIR we could see a significant increase of the hydroxylic absorption and therefore **a, b** and **c** mechanisms seem to be the most probable. Among these mechanisms, we can discard the mechanism **a** because we cannot observe in the FTIR spectra any difference in the wavenumber of the carbonyl absorption on changing methyl by phenyl in the final lactone; these absorptions should be different using bisPhe, because of the phenyl group is conjugated with the double bond. Moreover, the unsaturated lactone should produce a new absorption at about  $1680\text{ cm}^{-1}$  that

cannot be observed either.

The mechanism **b** can be an inter- or intramolecular process, being the latter highly improbable by entropic and steric reasons. However, Zhang and col.<sup>24</sup> observed by MALDI-TOF the formation of cyclic oligomers in the copolymerization of stoichiometric bisMe/PGE formulations using potassium t-butoxide as initiator. The formation of the analogous cyclic oligomers is more difficult in our case because of the three-dimensional character and the absence of solvent. The mechanism **c** is intramolecular and lead to a condensed structure with a certain similarity with the initial lactone.

In the mechanisms **a, b** and **d** when one alkoxide attacks, one ketone and one linear ester disappear but one linear ester remains unreacted. In these mechanisms one lactone ring is formed for each alkoxide that react. Therefore, it seems that these mechanisms should lead to similar absorption intensities for lactone and final ester groups. In mechanism **c** the attack of the alkoxide leads to the disappearance of one ketone and two linear ester groups at the same time and, therefore, the linear ester absorptions should be lower than that of the lactone formed. If we look at the intensities of the carbonyl signals in the final spectra (**Figures 5** and **7**) we can observe that a little proportion of ketone and ester groups remains unreacted, but the size of the lactone absorption is much bigger than that of linear ester. Pathway **c**, in which one ketone and two ester groups disappear, seems to be the mechanism that better explains the relative intensities of the carbonyl absorptions, and



Scheme 4

there



fore it could be the predominant pathway that follows this unexpected process.

The different evolution of the stoichiometric and non-stoichiometric DGEBA/bislactone formulations can be rationalized by the alternant character of the polymerization mechanism. In stoichiometric mixtures the initiators firstly attack to the epoxide and then the alkoxide formed opens the lactone, leading to final carboxylate groups. The lower basicity and nucleophilicity of these groups in comparison to alkoxides prevent the initial attack in the mechanism represented in **Scheme 4**. When epoxide is in excess in the formulation, the chain ends are mainly alkoxides, which are capable of initiating the unexpected processes.

Although the use of model compounds to investigate reaction mechanisms cannot always be applied to crosslinked materials, we studied the copolymerization in bulk of a monofunctional epoxide compound (PGE) with bisMe in different proportions using DMAP, to clarify the mechanisms implied. The stoichiometric proportion showed, by FTIR and <sup>13</sup>C NMR spectroscopy, the formation of the expected poly(ether-ester-ketone) as Endo et al. reported.<sup>3</sup> However, when epoxide was in excess in the initial mixture, the FTIR spectrum after reaction showed the band at 1768 cm<sup>-1</sup> of a five membered lactone, and the <sup>13</sup>C NMR spectrum showed a complex pattern with several carbonyl signals in the zone of 175-177 ppm and also a great number of signals in the aliphatic region. All the expected signals

of the condensed lactone formed by mechanism **c** were present in the <sup>13</sup>C NMR spectrum, but its complexity did not allow the total exclusion of the other structures formed by other side-reactions.

On the basis of these results, we can conclude that to obtain poly(ether-ester-ketone) networks the stoichiometric proportion DGEBA/condensed bis( $\gamma$ -lactone)s is required.

The thermosets, obtained using DMAP as initiator, were studied by thermogravimetry in order to test their thermal degradability. **Figure 8** shows the TGA and DTG curves of the materials obtained from bisPhe. We can see how, on increasing the proportion of lactone in the formulation, the temperature of the initial weight loss decreases and the rate of initial thermal degradation increases. However, the composition of the formulation has not a great influence on the temperature of the maximum rate of degradation. This fact can be rationalized by the ester rupture, which takes place at lower temperature, whereas the rupture of ether bonds occurs at higher temperature. It should be said, that the degradability of reworkable materials is usually associated to the temperature at which a low percentage of weight is lost (i.e. 5 %) because the loss of mechanical characteristics takes place at this low percentage, independently of the temperature at which the maximum weight loss occurs.

**Table 2** collects the thermogravimetric data of the materials prepared. In general, the introduction of ester groups



**Table 2.** Thermogravimetric data evaluated in N<sub>2</sub> atmosphere of the materials prepared

Entry	Formulation (mol/mol)	Prop. of initiator (phr)	Initiator	mol initiator/eq. epoxy	T (5%) <sup>a</sup> (°C)	T <sub>max</sub> <sup>b</sup> (°C)	Chair Yield (%)
1	DGEBA	3	DMAP	0.044711	396	435	13.2
3	DGEBA/bisMe 2:1	2	DMAP	0.036201	323	414	10.7
6	DGEBA/bisMe 1:1	2	DMAP	0.042595	278	405	8.7
8	DGEBA/bisMe 1:2	2	DMAP	0.055363	275	402	6.3
9	DGEBA/bisPhe 2:1	2	DMAP	0.038741	308	413	9.6
10	DGEBA/bisPhe 1:1	2	DMAP	0.047677	256	410	8.7
11	DGEBA/bisPhe 1:2	2	DMAP	0.065540	241	403	6.4

<sup>a</sup> temperature at which a 5% of weight loss occurs

<sup>b</sup> temperature of the maximum degradation rate

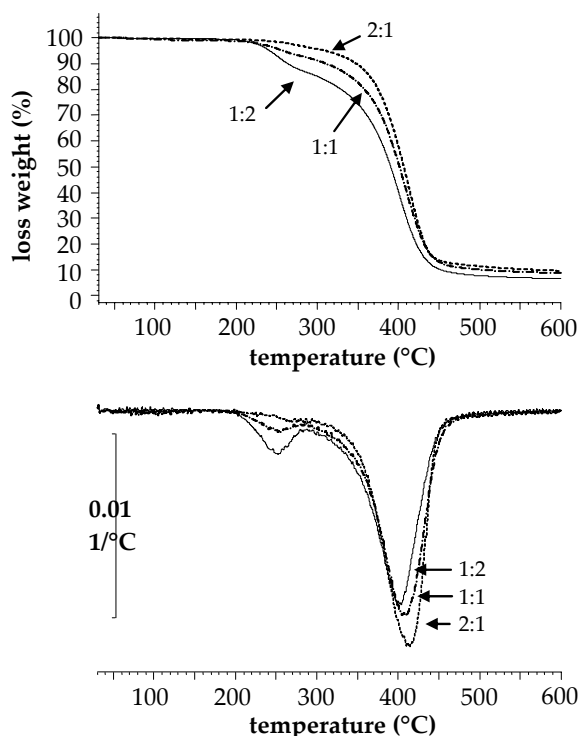


**Figure 8.** Thermogravimetric and DTG curves under N<sub>2</sub> atmosphere registered at 10 °C/min of the materials obtained from DGEBA/bisPhe (mol/mol) formulations initiated by 2 phr of DMAP varying the proportion of bislactone.

noteworthy increases the degradability in reference to pure DGEBA. The T<sub>max</sub> are similar for the materials obtained from both lactones but all of them are lower than the T<sub>max</sub> of the pure DGEBA. However, the nature of the substituent (Me or

Phe) affects the temperature of 5 % of weight loss, which can be explained by the higher weight of the lost fragment in the case of phenyl substituent. On increasing the proportion of bislactone in the formulation, the chair yield is reduced, as expected.

The breakage of the ester groups decreases the density of crosslinking and therefore the T<sub>g</sub> of the material will be reduced on heating. To confirm this, the material obtained from a stoichiometric mixture DGEBA/bisPhe, was maintained at 220 or 250 °C for several times and then the T<sub>g</sub> of the degraded material was determined and the FTIR spectrum was registered. **Figure 9a** shows the evolution of T<sub>g</sub> on heating for both temperatures. At both temperatures the T<sub>g</sub> strongly decreases until a plateau is reached, more quickly when the temperature is higher. The final T<sub>g</sub> achieved is slightly lower at 250 °C. A temperature in the range 230-250 °C has been described as optimal for safe rework operations in nitrogen atmosphere.<sup>25</sup> In **Figure 9b** is represented the carbonyl region of the FTIR spectra before and after heating,



where we can see the significant diminution of the ester and ketone groups. The lost of both groups not only implies the rupture of ester bonds, but the loss of ester-ketone fragments, which is responsible of the weight loss that occurs.

The thermosets obtained from stoichiometric mixtures were completely soluble in ethanolic KOH as a consequence of the presence of ester groups regularly distributed in the network structure, similarly to the observed for DGEBA/spiranic bis( $\gamma$ -lactones) formulations.<sup>16</sup>

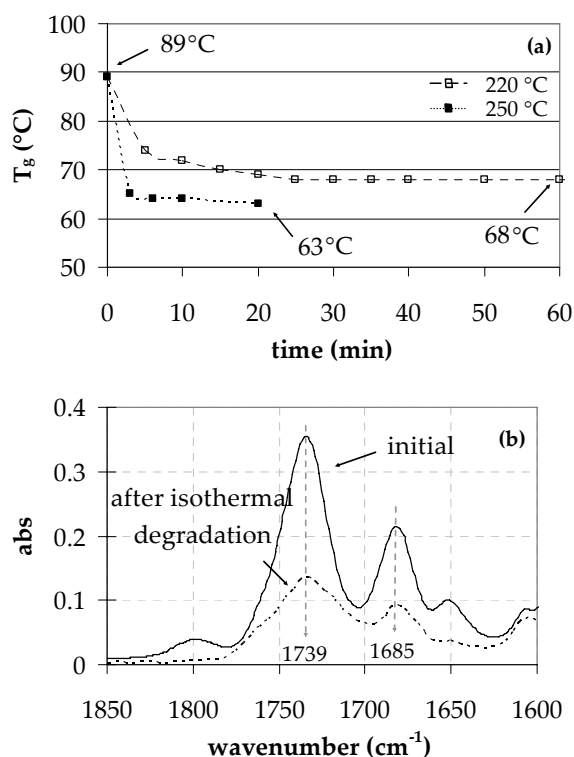


**Figure 9.** (a) Variation of the  $T_g$  on heating at 220 and 250 °C of a material obtained from a DGEBA/bisPhe 1:2 (mol/mol) formulation initiated by 2 phr of DMAP. (b) Carbonylic region of the FTIR spectra of the material before and after isothermal degradation at 250 °C.

## Conclusions

The anionic thermal curing of DGEBA

with condensed bis( $\gamma$ -lactone)s needs a lower proportion of tertiary amine as initiator than the curing of pure DGEBA. Among the initiators tested, DMAP is the most active and DBU is the least efficient. On increasing the proportion of bis-lactone in the reactive mixture, an apparent acceleration effect is observed.

Stoichiometric proportions of DGEBA/bis( $\gamma$ -lactone) lead to the expected alternate poly(ether-ester-ketone) structure and, in a dynamic scan, it produces a single exotherm in the DSC curves.

When DGEBA is in excess, the DSC curve shows two exotherms, being the first attributed to the copolymerization of epoxy and lactone, and the second to the homopolymerization of the epoxide and the unexpected processes. By FTIR we can see that these unexpected processes lead to the formation of five-membered lactones in the final material and to the practically total disappearance of the linear ester and ketone groups.

Thermogravimetric analysis allows confirming the reworkable character of the thermosets obtained. The higher proportion of bislactone in the formulation, the higher the thermal degradability is.

Thermosets obtained from stoichiometric formulations are completely soluble in ethanolic KOH.

## Acknowledgements

The authors from the Universitat Politècnica de Catalunya would like to thank CICYT and FEDER (MAT2008-06284-C03-02)



for their financial support. The authors from the Universitat Rovira i Virgili would like to thank the CICYT (Comisión Interministerial de Ciencia y Tecnología) and FEDER (Fondo Europeo de Desarrollo Regional) (MAT2008-06284-C03-01).

## References

- [1] Sikes, AM.; Brady, RF. *J Polym Sci Part A Polym Chem* 1990, 28, 2533-2546.
- [2] Brady, RF.; Sikes, AM. *Macromolecules* 1991, 24, 688-692.
- [3] Tadokoro, A.; Takata, T.; Endo, T. *Macromolecules* 1993, 26, 4400-4406.
- [4] Chung, K.; Takata, T.; Endo, T. *Macromolecules* 1995, 28, 1711-1713.
- [5] Takata, T.; Chung, K.; Tadokoro, A.; Endo, T. *Macromolecules* 1993, 26, 6686-6687.
- [6] Fernández-Francos, X.; Salla, JM.; Mantecón, A.; Serra, A.; Ramis, X. *J Appl Polym Sci* 2008, 109, 2304-2315.
- [7] Galià, M.; Serra, A.; Mantecón, A.; Cádiz, V. *J Appl Polym Sci* 1995, 56, 193-200.
- [8] Dell'Erba, IE.; Williams, RJJ. *Polym Eng Sci*, 2006, 46, 351-359.
- [9] Ooi SK.; Cook W.; Simon GP.; Such CH. *Polymer* 2000, 41, 3639-3649.
- [10] Yang, S.; Chen, JS.; Corner, H.; Breiner, T.; Ober, CK.; Poliks, MD. *Chem Mater* 1998, 10, 1475-1482.
- [11] Chen, JS.; Ober, CK.; Poliks, MD. *Polymer* 2002, 43, 131-139.
- [12] Shirai, M.; Morishita, S.; Okamura, H.; Tsunnoka, M. *Chem Mater* 2002, 14, 334-340.
- [13] Shirai, M.; Kawaue, A.; Okamura, H.; Tsunnoka M. *Chem Mater* 2003, 15, 4075-4081.
- [14] Wang, L.; H. Li.; Wong, CP. *J Polym Sci Part A Polym Chem* 2000, 38, 3771-3782.
- [15] Wong, CP.; Wang, L.; Shi, SH. *Mat Res Innovat* 1999, 2, 232-247.
- [16] Fernández-Francos, X.; Salla, JM.; Mantecón, A.; Serra, A.; Ramis, X. *Polym Degrad Stab* 2008, 93, 760-769.
- [17] Lawson, A. *J Chem Soc*, 1957, 144-150.
- [18] Cotas, AW.; Redfern, JP. *Nature*, 1964, 201, 68-69.
- [19] Kissinger, HE. *Anal. Chem.* 1957, 29, 1702-1706.
- [20] González, S.; Fernández-Francos, X.; Salla, JM.; Serra, A.; Mantecón, A.; Ramis, X. *J Appl Polym Sci* 2007, 104, 3406-3416.
- [21] Takata, T.; Tadokoro, A.; Chung, K.; Endo, T. *Macromolecules* 1995, 28, 1340-1345.
- [22] Chung, K.; Takata, T.; Endo, T. *Macromolecules* 1995, 28, 3048-3054.
- [23] Saiyasombat W.; Molloy R.; Nicholson TM.; Johnson AF.; Ward IM.; Poshyachinda S. *Polymer* 1998, 39, 5581-5585.
- [24] Zhang C.; Ochiai B.; Endo T. *J Polym Sci Part A Polym Chem* 2005, 43, 2643-2649.
- [25] Li H.; Wong CP. *IEEE Trans Adv Packaging* 2004, 27, 165-172.

UNIVERSITAT ROVIRA I VIRGILI  
NOUS TERMOESTABLES EPOXÍDICS MODIFICATS AMB GAMMA-LACTONES I BIS-GAMMA-LACTONES CONDENSADES  
M<sup>a</sup> Mercè Arasa Bertomeu  
ISBN:978-84-692-4157-8/DL:T-1171-2009

4.3 CATIONIC COPOLYMERIZATION OF DGEBA WITH TWO  
BICYCLIC BIS( $\gamma$ -LACTONE) DERIVATIVES USING RARE  
EARTH METAL TRIFLATES AS INITIATORS

---

*Mercè Arasa, Xavier Ramis, Josep Maria Salla, Ana Mantecón, Àngels Serra; Polymer, 50, 1838-1845 (2009)*



## CATIONIC POLYMERIZATION OF DGEBA WITH TWO BICYCLIC BIS( $\gamma$ -LACTONE) DERIVATIVES USING RARE EARTH METAL TRIFLATES AS INITIATORS

Mercè Arasa,<sup>1</sup> Xavier Ramis,<sup>2</sup> Josep Maria Salla,<sup>2</sup> Àngels Serra,<sup>1</sup> Ana Mantecón<sup>1</sup>

<sup>1</sup>Dpt. Q. Analítica i Q. Orgànica, URV. C/Marcel·lí Domingo s/n, 43007 Tarragona, Spain

<sup>2</sup>Lab. Termodinàmica, ETSEIB. UPC, Av. Diagonal 647, 08028 Barcelona, Spain

### Abstract

The thermal cationic curing of mixtures in different proportions of diglycidylether of bisphenol A (DGEBA) with two differently substituted condensed bis( $\gamma$ -lactone)s (BisMe and BisPhe) initiated by scandium, ytterbium and lanthanum triflates or a conventional BF<sub>3</sub>·MEA initiator was investigated. Non-isothermal differential scanning calorimetry (DSC) experiments at a controlled heating rate were used to evaluate the evolution of the reactive systems. BF<sub>3</sub>·MEA and rare earth metal triflates initiated curing systems follow a different evolution. Among rare earth metal triflates tested, the scandium was the most active initiator. The phenomenological changes that take place during curing were studied and represented in time-temperature-transformation (TTT) diagrams. The improvement in the reworkable character of the materials prepared was confirmed by thermogravimetry. The thermomechanical characteristics were also evaluated.

*Keywords:* Cationic polymerization, thermosets, DSC, kinetics, rare earth triflates.

### Introduction

The purpose of our research is not only the improvement of the characteristics of the cured epoxy resins to wide their application field, but to make easier and economically efficient their curing process. In previous publications we reported the copolymerization of commercially available epoxy resins with lactones,<sup>1</sup> spirobis lactones<sup>2</sup> or carbonates<sup>3</sup> modifying the network structure with the aim to improve some characteristics of the thermosets such as: (a) their "reworkable" character by introduction of

labile ester or carbonate groups that increase the thermal and chemical degradability;<sup>4,5</sup> (b) the reduction of the shrinkage during curing by adding or generating "in situ" expandable monomers to minimize the internal stresses generated in the process;<sup>6,7</sup> and (c) the toughness enhancement by increasing the flexibility of the network and increasing the distance between crosslinks.<sup>8</sup>

Because of condensed bis( $\gamma$ -lactone)s can copolymerize with epoxides introducing two ester groups per unit of lactone in the network and increasing in



six atoms the distance between cross-links, they has been selected as good candidates to improve the above mentioned characteristics of the epoxy thermosets. Due to the fact that these copolymerizations take place by a ring-opening mechanism it is necessary to select the most adequate initiator and its proportion.

It has been reported that spiranic or condensed bis( $\gamma$ -lactone)s copolymerize with epoxides in an alternating way by anionic mechanism via a tandem double ring-opening of bis( $\gamma$ -lactone)s and ring-opening of the epoxides.<sup>9-11</sup> However, when we cured rich-epoxy DGEBA/condensed bis( $\gamma$ -lactone) formulations unexpected reactions occurred. These reactions led to the practically total disappearance of the expected poly(ester-ketone) units in the network and to the formation of five-membered lactone rings. Thus, to obtain poly(ester-ketone) networks, which are the most degradable by the presence of ester groups in the network, stoichiometric DGEBA/condensed bis( $\gamma$ -lactone) mixtures are always required.<sup>12</sup>

One of the general advantages of the copolymerization strategy is the possibility to select the comonomer composition to tune the final properties of the thermosets obtained. Because anionic systems fail in the possibility to choose the proper formulation, we moved to cationic mechanisms to see if they are able to copolymerize the different formulations leading to poly(ester-ketone) structures and the conditions that should be applied to reach the complete curing in the selected times. Cationic copolymerization of these

bis( $\gamma$ -lactone)s with DGEBA has not been reported in the literature up to now.

As cationic initiators we chose rare earth metal triflates (Sc, La and Yb) because they were successfully used in the curing of DGEBA with several lactones<sup>1</sup> and bislactones,<sup>2</sup> leading to thermosets with ester moieties in the final materials. These initiators are active in very little proportions, even in humid environments, and have a low toxicity. These characteristics make them advisable in front of the conventional boron trifluoride complexes and those that contain transition metals.<sup>13,14</sup> The presence of rare earth triflates in the network structure facilitates the degradation of the thermosetting materials, decreasing the initial temperature of cleavage of the polymeric network, which enhances the reworkability of this type of materials when they are applied as coatings which needs to be removed from the substrate.<sup>15,16</sup>

As we saw in previous studies,<sup>1,2,6</sup> the cationic copolymerization of epoxides and lactones takes place by the formation of an intermediate spiroorthoester (SOE), which can homopolymerize or copolymerize with epoxide leading to poly(ether-ester) networks. If epoxide is in excess, polyetherification also occurs. Usually, the homopolymerization of SOE units takes place at the end of the curing and this fact is the responsible of the reduction of shrinkage after gelation observed by us.<sup>2,17</sup> The contribution of these four processes will depend on the composition of the mixture, on the initiator selected and its proportion, which influence the kinetics of each



process. During curing, different physical processes can also occur (gelation and vitrification), which affect not only the curing process but also the final characteristics of the thermosets.

The present work is devoted to the study of the curing kinetics by means of the isoconversional methodology and to the determination of gelation and vitrification of these systems. The results obtained will be collected and represented in TTT diagrams for a non-stoichiometric mixture of DGEBA with BisMe or BisPhe condensed bis( $\gamma$ -lactone)s. The thermal degradability and the thermomechanical characteristics of the materials prepared have been studied.

## Experimental Part

### Materials

Diglycidylether of bisphenol A (DGEBA) EPIKOTE RESIN 827 from Shell Chemicals (Epoxy Equiv. = 182.08 g/eq).

Tricarballic acid, acetic and benzoic anhydrides and 4-(N,N-dimethylamino-pyridine) (DMAP) (Aldrich) were used as received.

Lanthanum (III), ytterbium (III) and scandium (III) trifluoromethanesulfonates and borontrifluoride monoethylamine (BF<sub>3</sub>·MEA) (Aldrich) were used without purification.

The solvents were purified by standard method.

### Monomer synthesis

1-Methyl-2,8-dioxabicyclo[3.3.0]octane-3,

7-dione (bisMe) and 1-phenyl-2,8-dioxabicyclo[3.3.0]octane-3,7-dione (bisPhe) were synthesized from tricarballic acid and acetic anhydride or benzoic anhydride, respectively, in the presence of DMAP as previously described.<sup>12</sup>

### Preparation of the curing mixtures

The samples were prepared by mixing the selected quantity of initiator with the corresponding amount of bis-lactone and DGEBA with manual stirring in a mortar. The prepared mixtures were kept at -18 °C before use.

### Characterization and measurements

**Differential scanning calorimetry.** Calorimetric studies were carried out on a Mettler DSC-821e thermal analyzer in covered Al pans under N<sub>2</sub> at 2, 5, 10 and 15 °C/min. The calorimeter was calibrated using an indium standard (heat flow calibration) and an indium-lead-zinc standard (temperature calibration). The samples weighed approximately 7-9 mg. In the dynamic curing process the degree of conversion by DSC ( $\alpha_{DSC}$ ) was calculated as follows:

$$\alpha_{DSC} = \Delta H_T / \Delta H_{dyn} \quad (1)$$

where  $\Delta H_T$  is the heat released up to a temperature  $T$ , obtained by integration of the calorimetric signal up to this temperature, and  $\Delta H_{dyn}$  is the total reaction heat associated with the complete conversion of all reactive groups.

The  $T_g$  was measured as the half-way point of the jump in the heat capacity when the material changed from the



glassy to the rubbery state at 20 °C/min.

In order to establish the relations  $T_g$ - $\alpha$  we performed a series of non-isothermal scans from 20 °C to several temperatures, below 225 °C, at a heating rate of 10 °C/min. Then, the samples were immediately quenched and a second scan from -100 °C to 225 °C at a heating rate of 10 °C/min was registered to determine the  $T_g$  value and the residual heat. The degree of conversion was calculated on the basis of residual heat taking into account the total reaction heat.

The kinetic analysis was carried out using an integral isoconversional method as we will explain next. The basic assumption of this method is that the reaction rate at a given conversion is only a function of the temperature.<sup>18,19</sup> Isoconversional methods make it possible to easily determine the dependence of  $E$  on the degree of conversion in complex processes.

The kinetics of the reaction is usually described by the following rate equation:

$$\frac{d\alpha}{dt} = Af(\alpha)\exp\left(-\frac{E}{RT}\right) \quad (2)$$

where  $t$  is time,  $A$  is the pre-exponential factor,  $E$  is the activation energy,  $T$  is the absolute temperature,  $R$  is the gas constant, and  $f(\alpha)$  is the differential conversion function.

By integrating the rate equation, eq. (2), under non-isothermal conditions and using the Coats-Redfern<sup>20</sup> approximation to solve the so-called temperature integral and considering that  $2RT/E$  is much lower than 1, the Kissinger-Akahira-Sunose (KAS) equation may be written:<sup>21</sup>

$$\ln \frac{\beta}{T^2} = \ln \left[ \frac{AR}{g(\alpha)E} \right] - \frac{E}{RT} \quad (3)$$

where  $\beta$  is the heating rate and  $g(\alpha)$  is the integral conversion function.

For each conversion degree, the linear plot of  $\ln(\beta/T^2)$  versus  $1/T$  enables  $E$  and  $\ln[AR/g(\alpha)E]$  to be determined from the slope and the intercept.

If the reaction model,  $g(\alpha)$ , is known, for each conversion the corresponding pre-exponential factor can be calculated for every activation energy. In this study, we used the reduced master curves procedure of Criado,<sup>22</sup> described elsewhere, to assign a reaction model to the systems studied.<sup>23</sup> Different kinetic models have been studied: diffusion ( $D_1$ ,  $D_2$ ,  $D_3$  and  $D_4$ ), Avrami-Erofeev ( $A_2$ ,  $A_3$  and  $A_4$ ), power law, phase-boundary-controlled reaction ( $R_2$  and  $R_3$ ), autocatalytic ( $n+m=2$  and 3) and order  $n$  ( $n=1, 2$  and 3). We found that all systems studied follow a kinetic model of the surface-controlled reaction type,  $R_2$ , with  $g(\alpha)=[1-(1-\alpha)^{1/2}]$ . The rate constant,  $k$ , was calculated with  $E$  and  $A$  determined at conversion of 0.5, using the Arrhenius equation.

**Thermogravimetric analysis.** Thermogravimetric analyses (TGAs) were carried out with a Mettler TGA/SDTA 851e thermobalance. Cured samples with an approximate mass of 7 mg were degraded between 30 and 600 °C at a heating rate of 10 °C/min in  $N_2$  (100 cm<sup>3</sup>/min measured in normal conditions).

**Thermomechanical analysis.** Thermal-dynamic-mechanical analyses (DMTAs)

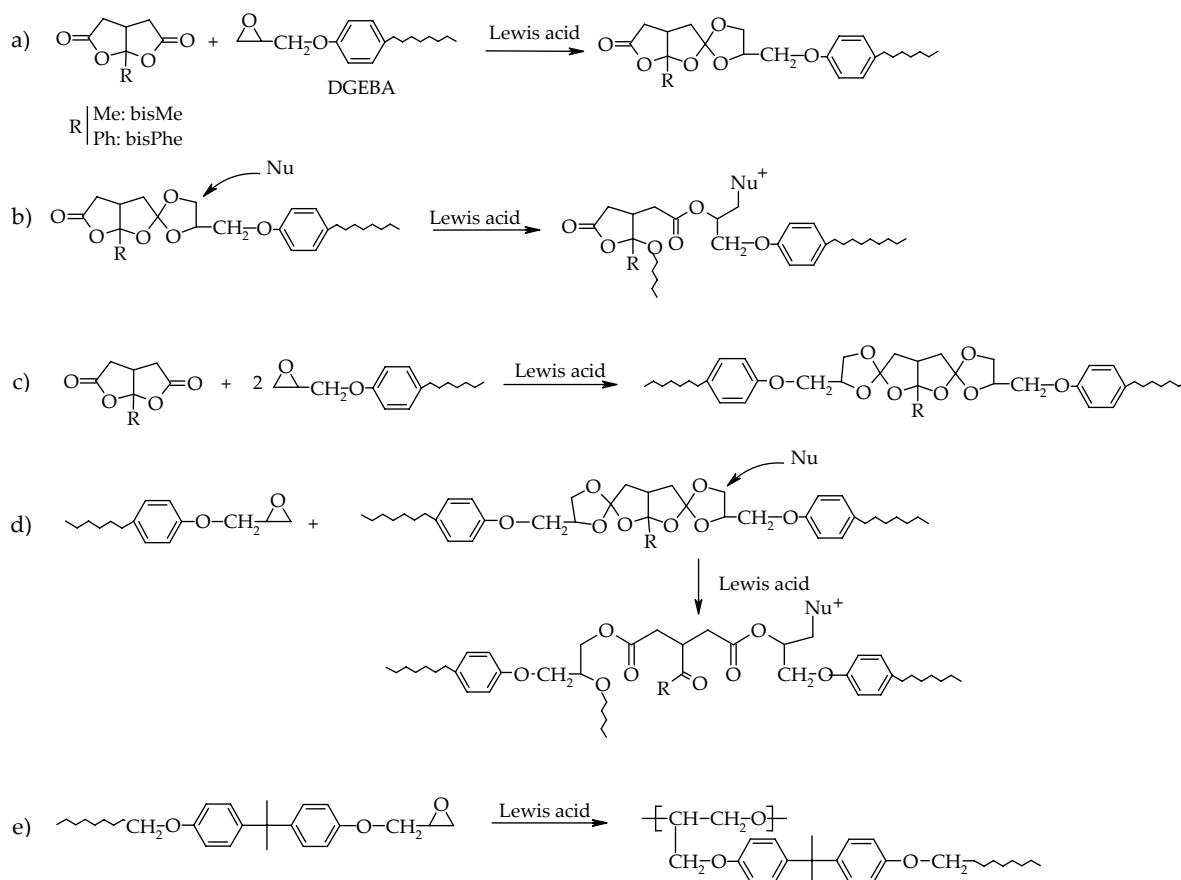


were carried out with a TA Instruments DMTA 2980 analyzer. The samples were cured isothermally in a mould at 140 °C for 3 h and were then subjected to a post-curing for 2 h at 160 °C. Three point bending of 10 mm was performed on cylindrical samples (10x4 mm, approximately). The apparatus operated dynamically at 5 °C/min from 35 to 200 °C at a frequency of 1 Hz.

**Gelation point determination.** The conversions at the gelation was determined by the residual enthalpy in the DSC of the gelled sample at different temperatures. The gel point was confirmed by solubility tests and the conversions at the gel point proved to be 0.58 for the mixture with bisMe and 0.56 for bisPhe.

## Results and discussion

The multistep reactive mechanism implied in the cationic curing of DGEBA/condensed bis( $\gamma$ -lactone)s (BisMe and BisPhe) is detailed in **Scheme 1**. Reaction (a) is the formation of the corresponding intermediate SOE catalyzed by the Lewis acid. The presence of two lactone groups in the monomer can lead to the formation of a bisSOE structure. This compound can copolymerize with epoxide (reaction b) or homopolymerize (reaction c) leading to a poly(ester-ether-ketone) structure. Epoxide groups can also homopolymerize (reaction d). It should be commented that, by reaction with epoxides,  $\gamma$ -lactones lead to poly-(ether-ester) units but condensed bis( $\gamma$ -lactone)s



**Scheme 1**



could experiment a tandem reaction that leads of ketone groups in the repetitive unit. In this reaction two ester groups could be formed, which are interesting from the point of view of the enhancement of the thermal and chemical degradability.

The formation of the expected chemical structure of poly(ether-ester-ketone), irrespective of the comonomer feed, was confirmed by FTIR. The concurrence among the different reactive processes, on changing the ratio between comonomers and the initiator selected, lead to some variations in the chemical structure of the network and therefore in the characteristics of the final material, which will be discussed in a forthcoming paper.

**Figure 1** shows the thermograms corresponding to the dynamic curing for the formulation DGEBA/bisMe 2:1 (mol/mol) with 1 phr of the rare earth triflates tested or 3 phr of  $\text{BF}_3\cdot\text{MEA}$ , which were the proportions required to reach the complete curing. As we can see, all the curves are unimodal but finish at different temperatures, being the lowest those of scandium and ytterbium triflates. From the conversion curves, we can clearly see that the highest active initiator is the scandium salt. The boron trifluoride complex needs a higher temperature to initiate the curing because of the formation of the true reactive specie,<sup>24</sup> but once initiated, it goes quicker than the curing with lanthanum triflate and at the end it slows down and higher temperatures are needed to reach the complete curing. This evolution is in accordance to the

complex reaction mechanism when boron complexes are used as initiators.<sup>24</sup> The order of reactivity of rare earth metal triflates follows the Lewis acidity trend, from lanthanum to scandium, as observed previously.<sup>1,3</sup>

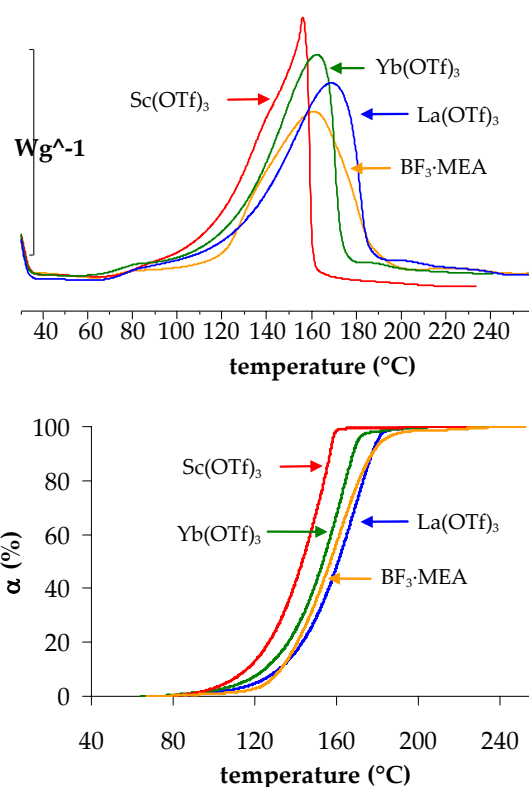


**Figure 1.** DSC scanning and conversion curves versus temperature of DGEBA/bisMe 2:1 (mol/mol) mixture initiated by 1 phr of the rare earth triflates tested or 3 phr of  $\text{BF}_3\cdot\text{MEA}$  at a heating rate of  $10\text{ }^\circ\text{C}/\text{min}$ .

The effect of the triflate salt and the structure of the lactone on the kinetics were also analyzed. **Figure 2** shows the conversion-temperature plots, which were obtained by the integration of the calorimetric signal for the formulations studied. It can be seen that the curves of both lactones have a similar shape, but bisMe reacts slightly faster than bisPhe when we used scandium or ytterbium salt as initiators.

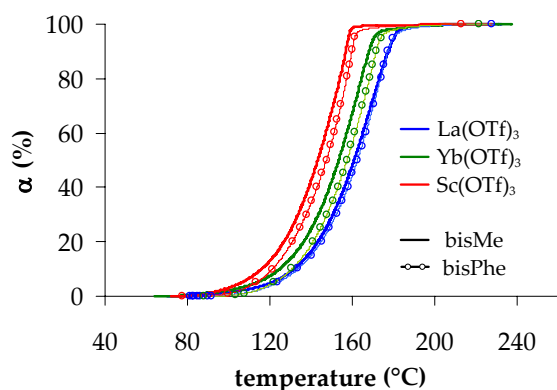


**Figure 2.** Conversion curves obtained by DSC from DGEBA/bisMe and bisPhe 2:1 (mol/mol) formulations with 1 phr of the rare earth triflates tested.

The accelerative effect of the proportion of initiator was studied with ytterbium triflate and is plotted in **Figure 3**. The curves of 0.5 and 1 phr of initiator show similar shapes. The curve corresponding to 3 phr has an initial broad exotherm that begins at about 60 °C before the main exothermic process, which finish before 160 °C. The broad initial exotherm can be attributed to the coexistence of a competitive mechanism. In a previous paper,<sup>25</sup> we could assign the exotherm at lower temperatures to the activated monomer mechanism (AM), which takes place in addition to the activated chain end mechanism (ACE) in the copolymerization of epoxides with lactones. AM mechanism becomes favored in the presence of a higher proportion of initiator. As can be seen in the  $\alpha$ -T curves, much higher conversions are reached at a selected temperature when the proportion of the initiator increases, e.g. for 160 °C, the curing with 3 phr is practically complete, whereas with 0.5 phr is less than 30 %.

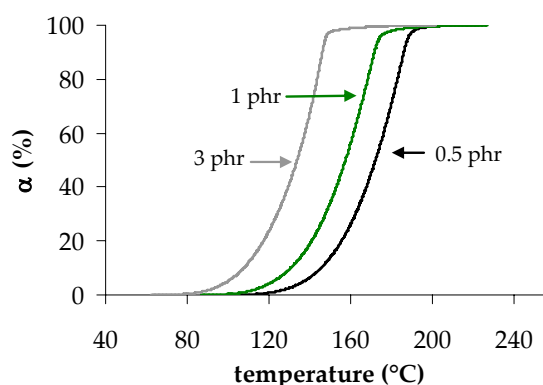
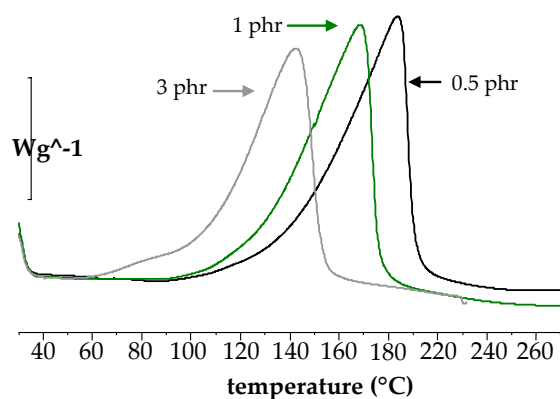


**Figure 3.** DSC scanning and conversion curves versus temperature of DGEBA/bisPhe 2:1 (mol/mol) mixture initiated by 0.5, 1 and 3 phr of Yb(OTf)<sub>3</sub> at a heating rate of 10 °C/min.

The effect of adding different proportion of lactone to DGEBA is represented in **Figure 4** for ytterbium triflate initiated systems containing bisMe. The shape of the exotherms is similar but on increasing the proportion of lactone there are little differences at the beginning and at the end of the exotherm. At the beginning there is a broad endotherm, which can only be seen in the 1:1 formulation, due to the melting of the lactone that is not totally dissolved in the DGEBA matrix. At the end of the curves of the formulations 2:1 and 1:1 we can see a broad exotherm, more important for the latter, which can be attributed to the homopolymerization of SOE that takes only place at high temperatures.<sup>17</sup> The conversions in-



crease, at a given temperature, on increasing the lactone proportion in the mixture. The accelerative effect can be attributed to the formation of more reactive species as we saw in similar system.<sup>2,17</sup>

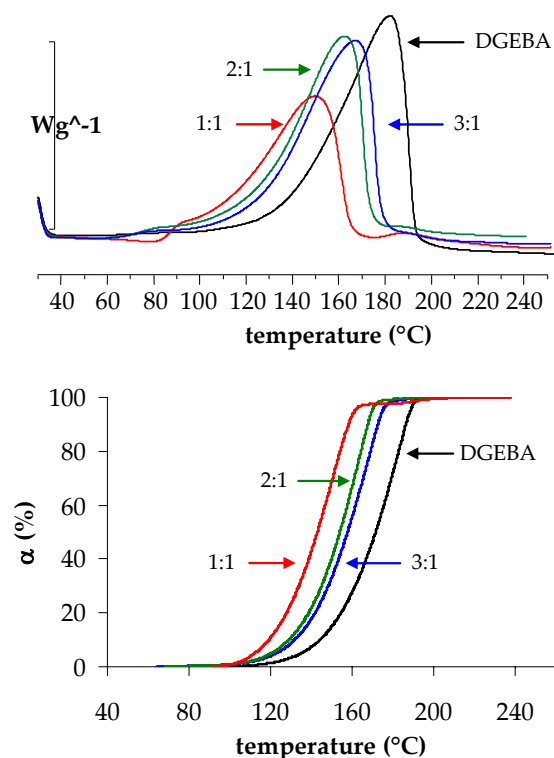


**Figure 4.** DSC scanning and conversion curves versus temperature of pure DGEBA and different DGEBA/bisMe formulations initiated by 1 phr of  $\text{Yb}(\text{OTf})_3$  at a heating rate of  $10\text{ }^\circ\text{C}/\text{min}$ .

In **Table 1** and **2** the calorimetric data of all the systems studied are collected. The  $T_g$ s of the materials decrease on increasing the proportion of bislactone in the formulation, because of the flexibility introduced in the network. The lower functionality of the lactone in comparison to the DGEBA enlarges the distance between crosslinks, which also reduces the crosslinking density. Whereas the materials obtained from pure DGEBA with all the initiators tested have a  $T_g$  over  $120\text{ }^\circ\text{C}$ , only  $\text{La}(\text{OTf})_3$  allows to

exceed  $100\text{ }^\circ\text{C}$  for a DGEBA/bisMe 2:1 (mol/mol) formulation. On changing methyl by phenyl in the lactone structure,  $T_g$ s slightly increase and are about  $100\text{ }^\circ\text{C}$  for the DGEBA/bisPhe 2:1 (mol/mol) formulations. For any selected formulation the  $T_g$  value depend on the rare earth metal triflate selected, being the highest for the materials obtained with La and the lowest those obtained with Sc.

In previous<sup>26</sup> works we saw how the Lewis acidity of the metal triflate influences the proportion in which ACE and AM propagation mechanisms occur. The latter and the transfer chain reactions associated to it are favoured on increasing the acidity of the initiator ( $\text{Sc} > \text{Yb} \gg \text{La}$ ). This can explain that the formulations initiated by Sc present the lowest  $T_g$ s, whereas those initiated by La have the highest  $T_g$ s.

Similarly, the proportion of initiator can also influence the final  $T_g$  of the materials because AM mechanism is favoured by high proportions of initiator. Because of we added 1 phr of each initiator, the lower molecular weight of scandium triflate makes its molar proportion greater, and this fact can also affect the  $T_g$ s of the materials.

The enthalpies released per gram of mixture or by epoxy equivalent decrease on increasing the proportion of bislactone because of the polymerization enthalpy of  $\gamma$ -lactones is far less than that of epoxy groups.<sup>27</sup> On changing the initiator, any significant difference can be observed in the enthalpy released, which can be explained in the basis of the same degree of epoxy reaction with all the



Table 1. Calorimetric data and calculated parameters of the DGEBA/bisMe formulations studied

Entry	Formulation (mol/mol)	Proportion of initiator (phr)	Initiator	mols initiator /eq. epoxy	T <sub>g</sub> (°C)	ΔH (J/g)	ΔH <sup>a</sup> (kJ/ee)	T <sub>max</sub> <sup>b</sup> (°C)	E <sub>a</sub> (kJ/mol)	ln A <sup>c</sup> (A in s <sup>-1</sup> )	k <sub>160°C</sub> ·10 <sup>3</sup> <sup>c</sup> (s <sup>-1</sup> )	T (5%) <sup>d</sup> (°C)	T <sub>max</sub> <sup>e</sup> (°C)
1	DGEBA	1	La(OTf) <sub>3</sub>	0.003106	127	531	97.6	192	78.4	13.8	0.79	314	360
2	DGEBA/bisMe 3:1	1	La(OTf) <sub>3</sub>	0.003550	113	442	92.0	175	74.8	14.5	1.93	297	358
3	DGEBA/bisMe 2:1	1	La(OTf) <sub>3</sub>	0.003773	108	401	88.7	169	71.8	13.9	2.47	289	345
4	DGEBA	1	Yb(OTf) <sub>3</sub>	0.002935	137	526	96.7	180	85.5	17.4	1.50	299	345
5	DGEBA/bisMe 3:1	1	Yb(OTf) <sub>3</sub>	0.003355	108	438	91.1	167	74.8	15.0	3.01	290	340
6	DGEBA/bisMe 2:1	0.5	Yb(OTf) <sub>3</sub>	0.000178	99	388	85.9	178	80.4	16.1	1.95	288	356
7	DGEBA/bisMe 2:1	1	Yb(OTf) <sub>3</sub>	0.003565	97	397	87.7	163	77.4	16.0	4.03	282	335
8	DGEBA/bisMe 2:1	3	Yb(OTf) <sub>3</sub>	0.010696	94	395	87.3	141	78.8	17.7	14.79	267	316
9	DGEBA/bisMe 1:1	1	Yb(OTf) <sub>3</sub>	0.004194	72	327	85.1	150	87.1	19.4	8.42	255	330
10	DGEBA	1	Sc(OTf) <sub>3</sub>	0.003699	120	521	95.6	183	75.1	15.0	1.04	296	338
11	DGEBA/bisMe 3:1	1	Sc(OTf) <sub>3</sub>	0.004228	103	439	91.3	164	72.4	14.6	4.10	277	328
12	DGEBA/bisMe 2:1	1	Sc(OTf) <sub>3</sub>	0.004493	94	400	88.4	156	79.9	17.2	6.97	268	326
13	DGEBA/bisMe 2:1	3	BF <sub>3</sub> ·MEA	0.058259	102	391	86.5	161	87.6	18.7	3.62	286	429

<sup>a</sup> enthalpies given by epoxy equivalent

<sup>b</sup> temperature of the maximum of the exotherm

<sup>c</sup> calculated using R2 as a model

<sup>d</sup> temperature of the maximum degradation rate



Table 2. Calorimetric data and calculated parameters of the DGEBA/bisPhe formulations studied

Entry	Formulation (mol/mol)	Proportion of initiator (phr)	Initiator	mols initiator /eq. epoxy	T <sub>g</sub> (°C)	ΔH (J/g)	ΔH <sup>a</sup> (kJ/ee)	T <sub>max</sub> <sup>b</sup> (°C)	E <sub>a</sub> (kJ/mol)	ln A <sup>c</sup> (A in s <sup>-1</sup> )	k <sub>100°C</sub> ·10 <sup>3</sup> <sup>c</sup> (s <sup>-1</sup> )	T (5%) <sup>d</sup> (°C)	T <sub>max</sub> <sup>e</sup> (°C)
1	DGEBA	1	La(OTf) <sub>3</sub>	0.003106	127	531	97.6	192	78.4	13.8	0.79	314	360
2	DGEBA/bisPhe 3:1	1	La(OTf) <sub>3</sub>	0.003727	116	426	93.0	178	80.9	16.2	1.93	300	359
3	DGEBA/bisPhe 2:1	1	La(OTf) <sub>3</sub>	0.004037	110	369	87.3	173	79.9	16.1	2.31	293	356
4	DGEBA	1	Yb(OTf) <sub>3</sub>	0.002935	137	526	96.7	180	85.5	17.4	1.50	299	345
5	DGEBA/bisPhe 3:1	1	Yb(OTf) <sub>3</sub>	0.003522	113	424	92.6	170	77.1	15.5	2.85	290	341
6	DGEBA/bisPhe 2:1	0.5	Yb(OTf) <sub>3</sub>	0.001908	100	364	86.1	184	79.4	15.5	1.45	289	358
7	DGEBA/bisPhe 2:1	1	Yb(OTf) <sub>3</sub>	0.003815	102	372	88.0	168	75.6	15.2	3.07	284	345
8	DGEBA/bisPhe 2:1	3	Yb(OTf) <sub>3</sub>	0.011446	98	371	87.7	150	73.9	16.1	11.35	265	322
9	DGEBA/bisPhe 1:1	1	Yb(OTf) <sub>3</sub>	0.002286	81	282	82.1	158	91.7	20.3	5.61	265	329
10	DGEBA	1	Sc(OTf) <sub>3</sub>	0.003699	120	521	95.6	183	75.1	15.0	1.04	296	338
11	DGEBA/bisPhe 3:1	1	Sc(OTf) <sub>3</sub>	0.004439	105	429	93.7	176	78.7	16.1	2.99	276	333
12	DGEBA/bisPhe 2:1	1	Sc(OTf) <sub>3</sub>	0.004808	94	376	89.0	159	74.9	15.6	5.14	269	330
13	DGEBA/bisPhe 2:1	3	BF <sub>3</sub> ·MEA	0.010391	109	387	91.6	153	-	-	-	288	428

<sup>a</sup> enthalpies given by epoxy equivalent

<sup>b</sup> temperature of the maximum of the exotherm

<sup>c</sup> calculated using R2 as a model

<sup>d</sup> temperature of the maximum degradation rate



initiators tested. However, if we take into account the differences in the  $T_g$ s, the networks should have some structural variations. This might be due to the above mentioned factors and to the different ability of each initiator to homopolymerize the SOE groups, as we saw in the study of other DGEBA/lactone systems.<sup>6</sup> The proportion of initiator practically does not influence the enthalpy released and only slightly influences the  $T_g$ s of the materials with bisMe (Table 1). It seems that 0.5 phr of the ytterbium salt is enough to complete the curing, but 1 phr is better from the point of view of the kinetics (see Figure 3). Higher proportions could initiate the curing during storage at room temperature and decrease the  $T_g$ .

By the isoconversional method we obtained the evolution of the activation energies during the curing process. From the calorimetric curves and applying the eq. 3, we obtained the activation energy for each degree of conversion in all the formulations studied. Figure 5 shows the plot of the apparent activation energy against the degree of conversion for the DGEBA/bisPhe 2:1 (mol/mol) formulation initiated by 1 phr of rare earth triflates or 3 phr of  $\text{BF}_3\cdot\text{MEA}$ . It can be seen that the activation energies are practically constant during the curing process and the boron trifluoride initiator leads to the highest activation energy. The high magnitude of the activation energy for  $\text{BF}_3\cdot\text{MEA}$  systems should be related with the formation of the true initiator species  $\text{HBF}_4$ .<sup>24,28</sup>

The values of the activation energies calculated at 50% of conversion, collected

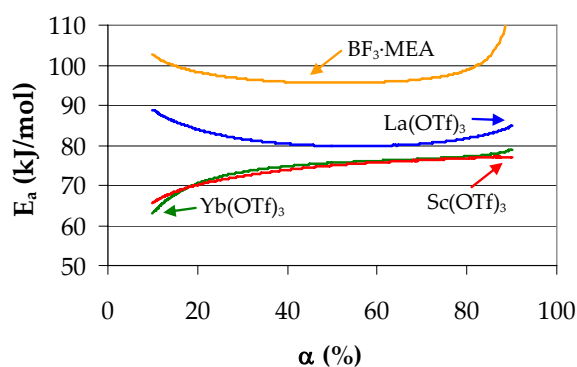
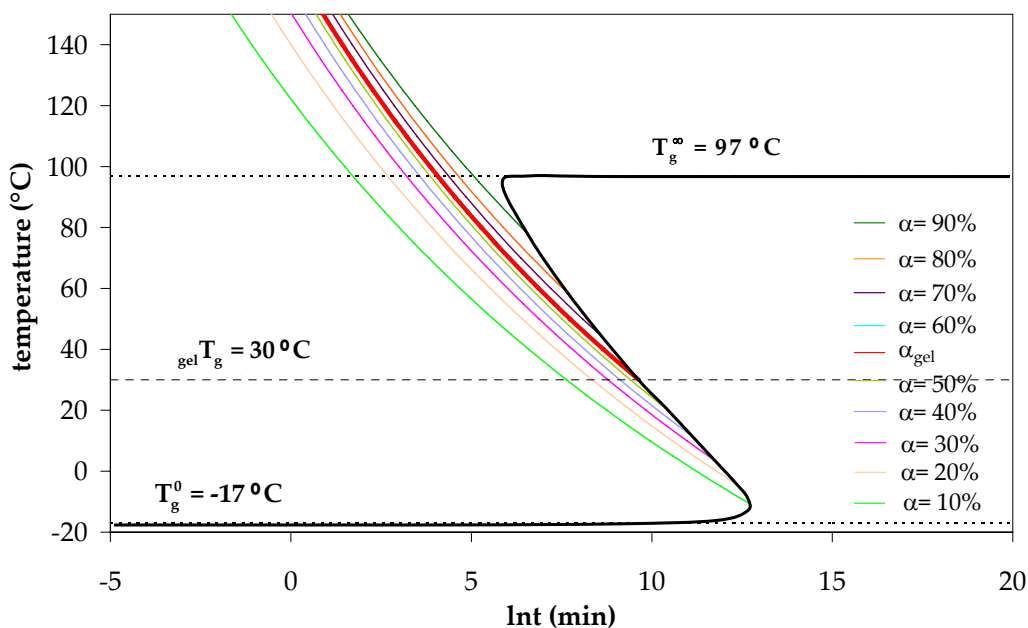


Figure 5. Dependence of the activation energy on the degree of conversion for the curing of DGEBA/bisPhe 2:1 (mol/mol) formulation initiated by 1 phr of the rare earth triflates or 3 phr of  $\text{BF}_3\cdot\text{MEA}$ .

in Tables 1 and 2, do not show any regular trend and they do not agree with the different curing rates, due to the compensation effect between activation energy and pre-exponential factor.<sup>25,29</sup> In this case we needed to determine the kinetic model and then estimate the pre-exponential factor and the kinetic constant by means of the Arrhenius equation. To establish the kinetic model for the systems studied we used the reduced master curves procedure<sup>22</sup> for all the models given in the experimental part. Among them,  $R_2$  model was considered as the best. Using this model we calculated the pre-exponential factors using the kinetic parameters obtained by applying eq. (3) and the constant rate at 160 °C. As we can see in Tables 1 and 2, the constant rate increases with the proportion of bislactone added to the curing mixture and with the proportion of initiator. Moreover, the rate constants are higher when scandium triflate is the initiator and lower for the lanthanum salt. BisMe mixtures have slightly higher constant rates than the analogous mixtures containing bisPhe. All these kinetic results agree with the kinetic effect



**Figure 6.** Time-temperature-transformation diagram for the curing of the DGEBA/bisMe 2:1 (mol/mol) mixture with 1 phr of Yb(OTf)<sub>3</sub>. Vitrification curve (—), gelification curve (—).

shown in **Figures 1, 2 and 3**.

We constructed the time-temperature-transformation (TTT) diagram to understand and conceptualize the changes occurring during curing. Such a diagram displays the states of the material and characterizes the evolution of the curing and the phenomenological changes in the material during isothermal cure versus time. The various changes occurring in the material during isothermal cure are characterized by contours of the times to reach the events as gelation, corresponding to the conversion at the gel-point and vitrification, corresponding to the glass transition temperature. The basic parameter governing the state of the material is the chemical conversion. Thus, to know how the rate changes with the curing temperature is basic for predicting the chemical conversion achieved after a cure schedule.

Three critical temperatures should be

considered:  $T_g^0$ , the glass transition temperature of the uncured mixture;  $_{gel}T_g$ , the temperature at which molecular gelation and vitrification coincide; and  $T_g^\infty$ , the glass transition temperature of the fully cured material. **Figure 6** shows the TTT cure diagram of a DGEBA/bisMe 2:1 (mol/mol) mixture with 1 phr of Yb(OTf)<sub>3</sub>. The bold lines represent the time necessary to reach the gelation (red line) and vitrification (black line) at a selected curing temperature. This diagram was constructed using the experimental data determined previously (the isoconversional lines, the  $T_g$ - $\alpha$  relationship, the conversion at gelation, and the  $T_g^0$  and the  $T_g^\infty$ ) following the methodology previously reported by us<sup>30</sup> and the use of the Di Benedetto equations.<sup>31,32</sup> We found a value of 30 °C for the lowest temperature at which the material gels before vitrification ( $_{gel}T_g$ ), a value for  $T_g^0$  of -17 °C, below which the material does not crosslink at all, and a value for  $T_g^\infty$  of 105 °C, which is the lowest temperature

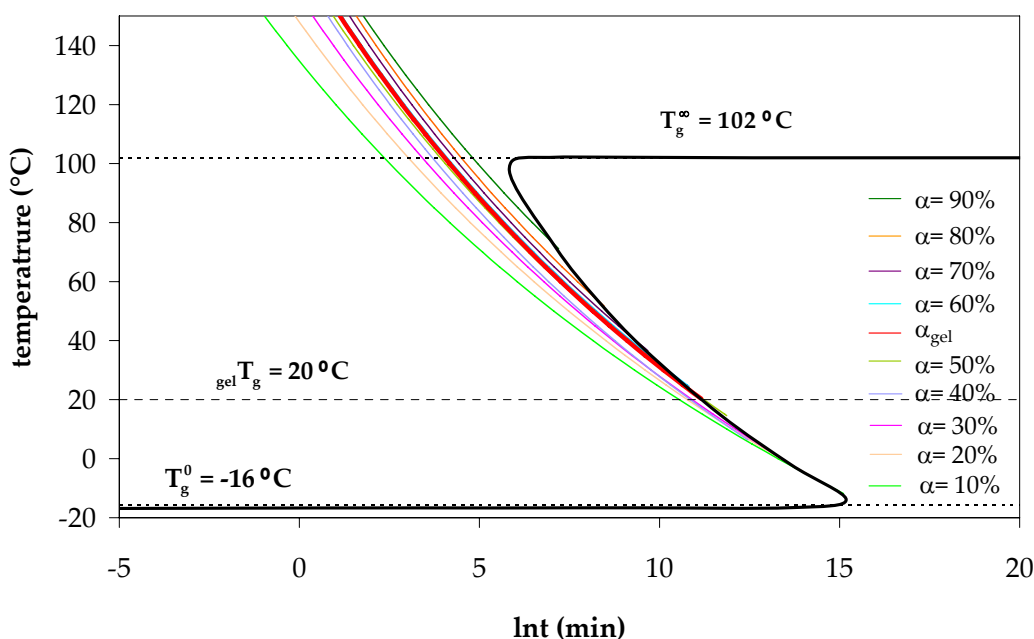


**Figure 7.** Time-temperature-transformation diagram for the curing of the DGEBA/bisPhe 2:1 (mol/mol) mixture with 1 phr of  $\text{Yb}(\text{OTf})_3$ . Vitrification curve (—), gelification curve (---).

at which the complete curing can be achieved. The TTT diagram has a shape similar to other obtained in the copolymerization of epoxy resins with lactones.<sup>27</sup>

**Figure 7** shows the TTT diagram for the curing process of a mixture DGEBA/bisPhe 2:1 (mol/mol) with 1 phr of  $\text{Yb}(\text{OTf})_3$ . There are not many differences in shape on changing the lactone but they have different parameters governing the state of the material. For bisPhe the  $\text{gel}T_g$  is 20 °C,  $T_g^0$  is -16 °C and  $T_g^\infty$  is 102 °C.

If we compare both TTT diagrams with the diagram of the cure of neat DGEBA with ytterbium triflate ( $T_g^\infty = 137$  °C)<sup>27</sup> we can say that the addition of bis( $\gamma$ -lactone)s makes possible to reduce the curing temperature and, consequently, the thermal stresses generated on cooling from the curing temperature.

In addition, the curing at lower temperature also implies an important energy saving.

The introduction of ester groups in the epoxy network has the purpose to facilitate the reworkability of the coated materials when their service life is over. Thermal degradation of the materials prepared was studied by thermogravimetry. The values obtained are collected in **Tables 1** and **2**. From the point of view of the reworkability, the most important parameter is the initial temperature of degradation, which we take as  $T_{5\%}$ , because at this temperature the main process is the breakage of labile ester bonds. When a 5 % of weight loss occurs, the mechanical properties go down and the coating can be eliminated by solvents or brushing.

The values of the tables make evident that on increasing the proportion of lac-



tone in the formulation the temperature of initial degradation decreases; however no differences are observed on changing the lactone.

In previous studies we observed that rare earth metal triflates play an important role in the degradation mechanism, facilitating it because of their Lewis acid characteristics. The effect on the degradation increases with the Lewis acidity of the cation.<sup>16</sup> In the tables we can see that the materials obtained with scandium triflate have the lowest  $T_{5\%}$  and those with lanthanum the highest.  $T_{5\%}$  also decreases on increasing the proportion of initiator, which supports the role of rare earth triflates in the degradation process. The different  $T_g$  values can also influence the thermal stability. In general, materials with low  $T_g$  (i.e., formulations with scandium triflate or with 3 phr of initiator) present lower stability. Analogous materials obtained anionically using *N,N*-dimethylamino-pyridine (DMAP)<sup>12</sup> as initiator showed higher  $T_{5\%}$ , and only stoichiometric DGEBA/lactone 1:2 (mol/mol) formulations led to more degradable materials than those obtained cationically in the present study. The materials obtained with DMAP showed a two step degradation curves with the main process, the rupture of ether bonds, at a temperature higher than 400 °C. Thermosets obtained in the present work present an only degradative process, due to the partial overlapping of the ester and ether ruptures. This overlapping can be explained because of rare earth triflates catalyze the ether rupture and lead to a lower  $T_{max}$  for the cationically obtained materials.

The materials prepared were also characterized by thermomechanical analysis. The effect of the proportion of lactone in the value of loss tangent can be observed in **Figure 8** for bisMe. The material obtained from pure DGEBA has been included to compare. As can be seen, the addition of lactone clearly reduces the temperature of the maximum of  $\tan \delta$ . The curve are unimodal, which indicates that the materials are homogeneous, but the curve becomes broader in the 1:1 (mol/mol) DGEBA/lactone formulation. As expected, the values of relaxed modulus decreased as the lactone content in the formulation increased, due to the flexibility introduced in the network structure, as is represented in **Figure 9** for DGEBA/bisPhe formulations.

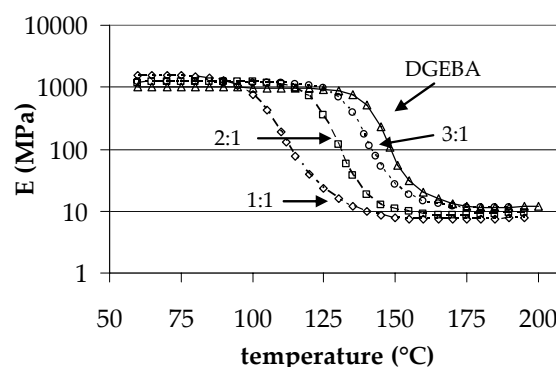


**Figure 9.** Dependence of storage modulus versus temperature for pure DGEBA and the materials obtained from different DGEBA/bisMe formulations initiated by 1 phr of  $\text{Yb}(\text{OTf})_3$  obtained by DMTA.

## Conclusions

The kinetic studies performed by calorimetry showed that, among rare earth metal triflates, the more active initiator was the scandium and the less the lanthanum triflate. This behaviour can be

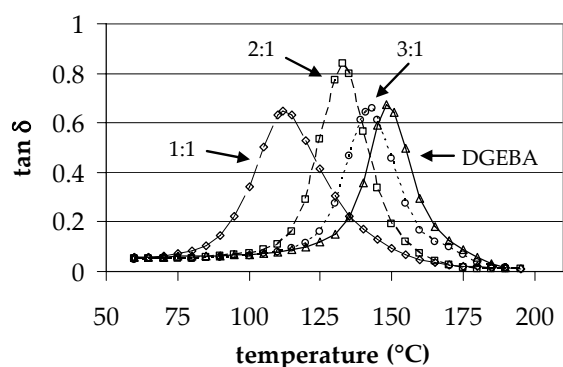


**Figure 8.** Dependence of  $\tan \delta$  versus temperature for pure DGEBA and the materials obtained from different DGEBA/bisMe formulations initiated by 1 phr of  $\text{Yb}(\text{OTf})_3$  obtained by DMTA.

correlated to their Lewis acidity. Moreover, on increasing the lactone proportion in the mixture the curing process accelerated. The acceleration was slightly higher with bisMe as the lactone.

The  $T_g$ s of the materials prepared decreased on increasing the proportion of bislactone in the formulation, because of the flexibility introduced in the network. The materials obtained from bisPhe showed a slightly higher  $T_g$  than those obtained from bisMe.

The use of calorimetric experiments and the determination of the gel point allowed us to construct the TTT diagrams for the curing of DGEBA/ bisMe and bisPhe 2:1 (mol/mol) mixtures initiated by  $\text{Yb}(\text{OTf})_3$  and the curing interval temperatures could be determined.

By thermogravimetry, the materials showed that the temperature of the 5% of weight loss went down on increasing the proportion of bislactone in the formulation. The materials prepared with  $\text{Sc}(\text{OTf})_3$  were the most degradable. The change in the lactone structure did not

produce any substantial difference.

By DMTA experiments we observed that the materials presented unimodal  $\tan \delta$  curves, irrespective to the initiator used, which account for the homogeneity of these materials. The  $\tan \delta$  curves shifted to lower temperatures and the relaxed moduli decreased on increasing the proportion of lactone in the formulation.

### Acknowledgements

The authors from the Universitat Rovira i Virgili would like to thank the CICYT (Comisión Interministerial de Ciencia y Tecnología) and FEDER (Fondo Europeo de Desarrollo Regional) (MAT2008-06284-C03-01) and the authors from the Universitat Politècnica de Catalunya to CICYT and FEDER (MAT2008-06284-C03-02) for their financial support.

### References

- [1] Arasa, M.; Ramis, X.; Salla JM., Mantecón, A.; Serra, A. *J Polym Sci Part A: Polym Chem* 2007, 45, 2129-2141.
- [2] Giménez, R.; Fernández-Francos, X.; Salla, JM.; Serra, A.; Mantecón, A.; Ramis, X. *J Polym Sci Part A: Polym Chem* 2005, 46, 10637-10647.
- [3] Cervellera, R.; Ramis, X.; Salla, JM.; Mantecón, A.; Serra, A. *J Polym Sci Part A: Polym Chem* 2005, 43, 5799-5813.
- [4] Fernández-Francos, X.; Salla, JM.; Mantecón, A.; Serra, A.; Ramis, X. *Polym Degrad Stab* 2008, 93, 760-769.
- [5] Chen, JS.; Ober, CK.; Poliks, MD. *Polymer* 2002, 43, 131-139.
- [6] González, L.; Ramis, X.; Salla, JM.; Mantecón, A.; Serra, A. *J Polym Sci Part A: Polym Chem* 2006, 44, 6869-6879.



- [7] Sadhir, RK.; Luck, MR. Ed. "Expanding Monomers. Synthesis, Characterization and Applications", Boca Raton: CRC Press, 1992.
- [8] García, SJ.; Serra, A.; Suay, J. J Polym Sci Part A: Polym Chem 2007, 45, 2316-2327.
- [9] Takata, T.; Tadokoro, A.; Chung, K.; Endo, T. Macromolecules 1995, 28, 1340-1345.
- [10] Chung, K.; Takata, T.; Endo, T. Macromolecules 1995, 28, 3048-3054.
- [11] Fernández-Francos, X.; Salla, JM.; Mantecón, A.; Serra, A.; Ramis, X. J Appl Polym Sci 2008, 109, 2304-2315.
- [12] Arasa, M.; Ramis, X.; Salla JM., Mantecón, A.; Serra, A. J Polym Sci Part A: Polym Chem send to revision
- [13] Kobayashi, S., Ed. "Lanthanides: Chemistry and Use in Organic Synthesis" Topics in Organometallic Chemistry, Berlin: Springer Verlag, 1999.
- [14] Kobayashi, S.; Sugiura, M.; Kitagawa, H.; Lam, WWL. Chem Rev 2002, 102, 2227-2302.
- [15] González, L.; Ramis, X.; Salla, JM.; Mantecón, A.; Serra, A. Polym Degrad Stab 2007, 92, 596-604.
- [16] Arasa, M.; Ramis, X.; Salla, JM.; Mantecón, A.; Serra, A. Polym Degrad Stab 2007, 92, 2214-2222.
- [17] Mas, C.; Ramis, X.; Salla, JM.; Mantecón, A.; Serra, A. J Polym Sci Part A: Polym Chem 2003, 41, 2794-2808.
- [18] Vyazovkin, S; Sbirrazzouli, N. Macromol Chem Phys 1999, 200, 2294-2303.
- [19] Vyazovkin, S; Sbirrazzouli, N. Macromol Rapid Commun 2006, 27, 1515-1532.
- [20] Coats, AW., Redfern, JP. Nature 1964, 201, 68-69.
- [21] Kissinger, HE. Anal Chem 1957, 29, 1702-1706.
- [22] Criado, JM. Thermochim Acta 1978, 24, 186-189.
- [23] Ramis, X.; Salla, JM.; Cadenato, A.; Morancho, JM. J Therm Anal Cal 2003, 72, 707-718.
- [24] Ghaemy M. Eur Polym J 1998, 34, 1151-1156.
- [25] Salla, JM.; Fernández-Francos, X.; Ramis, X.; Mas, C.; Mantecón, A.; Serra, A. J Thermal Anal Calorim 2008, 91, 385-393.
- [26] Mas C, Mantecón A, Serra A, Ramis X, Salla JM. J Polym Sci Part A: Polym Chem 2004, 42, 3782-3791.
- [27] Saiyasombat, W.; Molloy, R.; Nicholson, TM.; Johnson, AF.; Ward, IM.; Poshyachinda, S. Polymer 1998, 39, 5581-5585.
- [28] Tackie, M.; Martin GC. J Appl Polym Sci 1993, 48, 793-808.
- [29] Vyazovkin, S.; Wight CA. Annu Rev Phys Chem 1997, 48, 125-149.
- [30] González, S.; Fernández-Francos, X.; Salla, JM.; Serra, A.; Mantecón, A.; Ramis, X. J Appl Polym Sci 2007, 104, 3406-3416.
- [31] Nielsen, LE. J Macromol Sci Macromol Chem 1969, C3, 69-103.
- [32] Pascault, JP.; Williams, RJJ. J Polym Sci Part B: Polym Phys 1990, 28, 85-95.

UNIVERSITAT ROVIRA I VIRGILI  
NOUS TERMOESTABLES EPOXÍDICS MODIFICATS AMB GAMMA-LACTONES I BIS-GAMMA-LACTONES CONDENSADAES  
M<sup>a</sup> Mercè Arasa Bertomeu  
ISBN:978-84-692-4157-8/DL:T-1171-2009

4.4 | STUDY OF THE COPOLYMERIZATION OF DGEBA AND  
TWO BICYCLIC BIS( $\gamma$ -LACTONES) USING RARE EARTH  
TRIFLATES AS INITIATORS BY INFRARED SPECTROSCOPY

---

*Mercè Arasa, Xavier Ramis, Josep Maria Salla, Ana Mantecón, Àngels Serra; European Polymer Journal, send to revision*



## STUDY OF THE COPOLYMERIZATION OF DGEBA AND TWO BICYCLIC BIS( $\gamma$ -LACTONE)S USING RARE EARTH METAL TRIFLATES AS INITIATORS BY INFRARED SPECTROSCOPY

Mercè Arasa,<sup>1</sup> Xavier Ramis,<sup>2</sup> Josep Maria Salla,<sup>2</sup> Àngels Serra,<sup>1</sup> Ana Mantecón<sup>1</sup>

<sup>1</sup>Dpt. Q. Analítica i Q. Orgànica, URV. C/Marcel·lí Domingo s/n, 43007 Tarragona, Spain

<sup>2</sup>Lab. Termodinàmica, ETSEIB. UPC, Av. Diagonal 647, 08028 Barcelona, Spain

### Abstract

The thermal cationic curing of mixtures, in different proportions, of diglycidylether of bisphenol A (DGEBA) with two substituted condensed bis( $\gamma$ -lactone)s (BisMe and BisPhe) initiated by scandium, ytterbium and lanthanum triflates or a conventional  $\text{BF}_3\cdot\text{MEA}$  initiator was investigated. The evolution of the different reactive groups was followed by means of FTIR/ATR spectroscopy. The formation of mono spiroorthoesters (monoSOEs) and bis spiroorthoesters (bisSOEs) has been discussed. The polymerization of bisSOE structures led to the formation of ether-ester-ketone repetitive units, which implies the cationic polymerization taking place by a tandem reaction. The use of scandium triflate as an initiator led to the highest chemical incorporation of lactone in the network. Moreover, this initiator was the most active, incorporating a higher proportion of lactone in a shorter time. On the contrary, the conventional  $\text{BF}_3\cdot\text{MEA}$ , incorporated the lowest proportion of bislactone in the cured material. When the lactone was BisPhe a higher proportion of linear ester and ketone groups were incorporated in the material for all the initiators tested.

*Keywords:* Cationic polymerization, thermosets, FTIR, rare earth triflates, epoxy resins, bislactones.

### Introduction

One of the types of initiators that can be used to polymerize epoxy resins are Lewis acids. Among them, rare earth metal triflates have been widely used by us in homopolymerization of DGEBA<sup>1</sup> or in its copolymerization with several lactones.<sup>2-4</sup> These initiators are active in very little proportions, even in humid environments, and have a low toxicity. These characteristics make them advis-

able in front of the conventional boron trifluoride complexes and those that contain transition metals.<sup>5,6</sup> Moreover, the presence of rare earth triflates in the network structure facilitates the degradation of the thermosetting materials, decreasing the initial temperature of cleavage of the polymeric network,<sup>7,8</sup> which enhances the reworkability of this type of materials when they are applied as coatings and they need to be removed



from the substrate. The improvement of the reworkability of epoxy thermosets has been one of the aims of our research group. The introduction of labile linkages, such as ester groups, in the network structure by copolymerization of epoxy resins with lactones has been the strategy followed until now.<sup>9</sup>

By reaction of epoxides and lactones in the presence of a Lewis acid, spiro-orthoesters (SOEs) are formed, which can be cationically polymerized by a double ring-opening mechanism leading to poly(ether-ester) structures.<sup>10</sup> Because of condensed bis( $\gamma$ -lactone)s can copolymerize with epoxides introducing two ester groups in the network and increasing in six atoms the distance between crosslinks, they have been selected in the present study as good candidates to improve the thermodegradable character and the flexibility of the epoxy thermosets.

It is known that spiranic or condensed bis( $\gamma$ -lactone)s copolymerize with epoxides in an alternating way by anionic mechanism via a tandem double ring-opening of bis( $\gamma$ -lactone)s and ring-opening of the epoxides.<sup>11-13</sup> However, in systems with bis( $\gamma$ -lactone)s, when epoxide is in excess, unexpected reactions occurred.<sup>14</sup> These processes led to the practically disappearance of the desired poly(ester-ketone) units in the network with formation of new five-membered lactones. Thus, to obtain the most degradable poly(ether-ester-ketone) networks, stoichiometric DGEBA/condensed bis( $\gamma$ -lactone) mixtures were always required.

Because anionic systems fail in the possibility to choose the proper comonomer composition, we explored the cationic mechanisms. In previous work,<sup>15</sup> calorimetric studies, phenomenological behaviour and several characteristics of the materials such as thermodegradative and thermomechanical behaviour were reported. Because of FTIR allows following the evolution of the reactive species and determining the final structure of the epoxy network, we applied this technique to investigate the most adequate initiator and its proportion in the reactive mixture to get the higher proportion of linear ester in the network structure.

## Experimental Part

### Materials

Diglycidylether of bisphenol A (DGEBA) EPIKOTE RESIN 827 from Shell Chemicals (Epoxy Equiv. = 182.08 g/eq).

Tricarballic acid, acetic and benzoic anhydrides and 4-(*N,N*-dimethylamino)pyridine (DMAP) (Aldrich) were used as received.

Lanthanum (III), ytterbium (III) and scandium (III) trifluoromethanesulfonates and borontrifluoride monoethylamine ( $\text{BF}_3 \cdot \text{MEA}$ ) (Aldrich) were used without purification.

The solvents were purified by standard methods.

### Monomer synthesis

1-Methyl-2,8-dioxabicyclo[3.3.0]octane-3,7-dione (bisMe) and 1-phenyl-2,8-dioxabicyclo[3.3.0]octane-3,7-dione (bisPhe)



were synthesized from tricarballic acid and acetic anhydride or benzoic anhydride, respectively, in the presence of DMAP as previously described.<sup>14</sup>

### Preparation of the curing mixtures

The samples were prepared by mixing the selected quantity of initiator with the corresponding amount of bis-lactone and DGEBA with manual stirring in a mortar. The prepared mixtures were kept at -18 °C before use.

### Characterization and measurements

The isothermal curing process, at 160 °C, was monitored with a Fourier transform infrared spectrophotometer (FTIR) 680 Plus from Jasco with resolution of 4 cm<sup>-1</sup> in the absorbance mode. An attenuated total reflection accessory (ATR) with thermal control and a diamond crystal (a Golden Gate heated single-reflection diamond ATR from Specac-Teknokroma) was used to determine FTIR spectra. The consumption of the reactive carbonyl group in the lactone was evaluated by measuring the changes in absorbance at 1800 (bisPhe) and 1795 cm<sup>-1</sup> (bisMe) (carbonyl C=O stretching of cyclic ester). The appearance of the peak at 1737 cm<sup>-1</sup> (carbonyl C=O stretching of aliphatic linear ester), which does not exist in the sample before curing, indicates that ring-opening polymerization has occurred in SOE. Ketone bands for bisMe and bisPhe appear at 1716 and 1685 cm<sup>-1</sup> respectively. Because of the partial overlapping of linear ester and ketone bands we used the total area of both to follow the evolution of the curing. The peak at 1605 cm<sup>-1</sup> (phenyl

group) was chosen as an internal standard. Conversions of the different reactive groups: lactone and linear ester and ketone were determined by the Lambert-Beer law from the normalized changes of absorbance as follows:

$$\alpha_{bisMe} = 1 - \left( \frac{\overline{A}_{1795}^t}{\overline{A}_{1795}^0} \right) \quad \alpha_{bisPhe} = 1 - \left( \frac{\overline{A}_{1800}^t}{\overline{A}_{1800}^0} \right)$$
$$\alpha_{ester+ketone(Me)} = \left( \frac{\overline{A}_{1737-1716}^t}{\overline{A}_{1737-1716}^\infty} \right)$$
$$\alpha_{ester+ketone(Phe)} = \left( \frac{\overline{A}_{1737-1685}^t}{\overline{A}_{1737-1685}^\infty} \right)$$

where  $\overline{A}^0$ ,  $\overline{A}^t$  and  $\overline{A}^\infty$  are the normalized absorbance of the reactive group before curing, after reaction time  $t$  and after complete curing.

### Results and discussion

As we saw in previous studies,<sup>2,3,16</sup> the cationic copolymerization of epoxides and mono( $\gamma$ -lactone)s initiated by rare earth metal triflates takes place by the formation of an intermediate spiroorthoester (SOE), which can homopolymerize or copolymerize with epoxide leading to poly(ether-ester) networks. If epoxide is in excess, polyetherification also occurs. Usually, the homopolymerization of SOE moieties takes place at the end of the curing.<sup>3</sup> The contribution of these four processes depends on the composition of the mixture and on the initiator selected and its proportion. All these variables influence the kinetics and extension of each process and therefore the chemical structure of the final network. In mixtures of DGEBA with  $\gamma$ -





ear esters and one ketone are formed.

The tandem double ring-opening mechanism of bisSOE were not reported until now but a similar process, which leads to a similar structure, was reported in the anionic copolymerization of epoxide and condensed bis( $\gamma$ -lactone)s.<sup>11,12,17,18</sup>

Simple  $\gamma$ -lactones cannot homopolymerize by thermodynamic reasons, but there are no studies on the homopolymerization of condensed bis( $\gamma$ -lactone)s. Thus, the possible homopolymerization of these compounds by the cationic initiators tested was studied by FTIR. In these studies we did not observe any evolution after 3 h at 160 °C. Thus, the homopolymerization of the bis( $\gamma$ -lactone)s must not be considered in the global reactive process.

The formation of the poly(ether-ester-ketone) in the curing of DGEBA/bis( $\gamma$ -lactone) mixtures was observed by FTIR, confirming the formation of bisSOE and its posterior opening (reactions **c** and **d**). However, the concurrence among the different reactive processes on changing

the ratio between comonomers and the initiator selected leads to some variations in the chemical structure of the network. **Figures 1** and **2** show the FTIR spectra before and after isothermal curing at 160 °C in the ATR for the formulations DGEBA/bisMe and DGEBA/bisPhe 2:1 (mol/mol) with 1 phr of lanthanum triflate respectively. In these figures we can see the initial lactone bands at 1795 (bisMe) and 1800 cm<sup>-1</sup> (bisPhe), which decrease without total disappearance in the final spectra. In the spectra of the cured materials, the bands corresponding to the linear ester at 1737 cm<sup>-1</sup> and to the ketone at 1716 (bisMe) or 1685 cm<sup>-1</sup> (bisPhe) can be observed, which are partially overlapped in the case of bisMe. In both mixtures, the epoxide band at 916 cm<sup>-1</sup> is partially overlapped with a band attributed to the lactone structure, which hinders to follow accurately its evolution during curing. Moreover, the reaction mechanism converts two carbonyl groups of the initial lactone to one ester and one lactone when reaction **b** takes place or to two linear ester and one ketone carbonyls when reaction **d** occurs. Because of both processes occur in a dif-

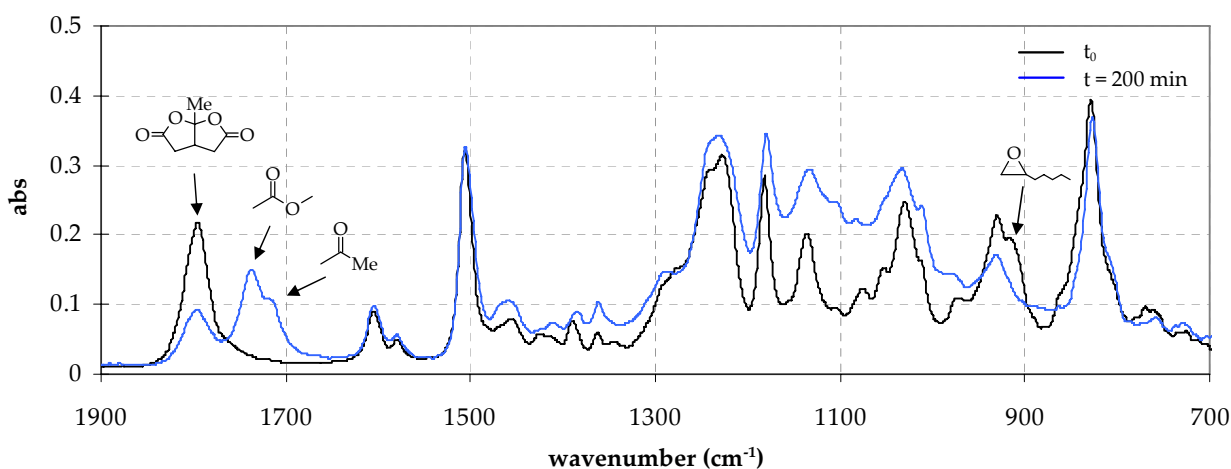


**Figure 1.** FTIR spectra before and after curing of a DGEBA/bisMe 2:1 (mol/mol) mixture initiated by 1 phr of La(OTf)<sub>3</sub> in the ATR at 160 °C.

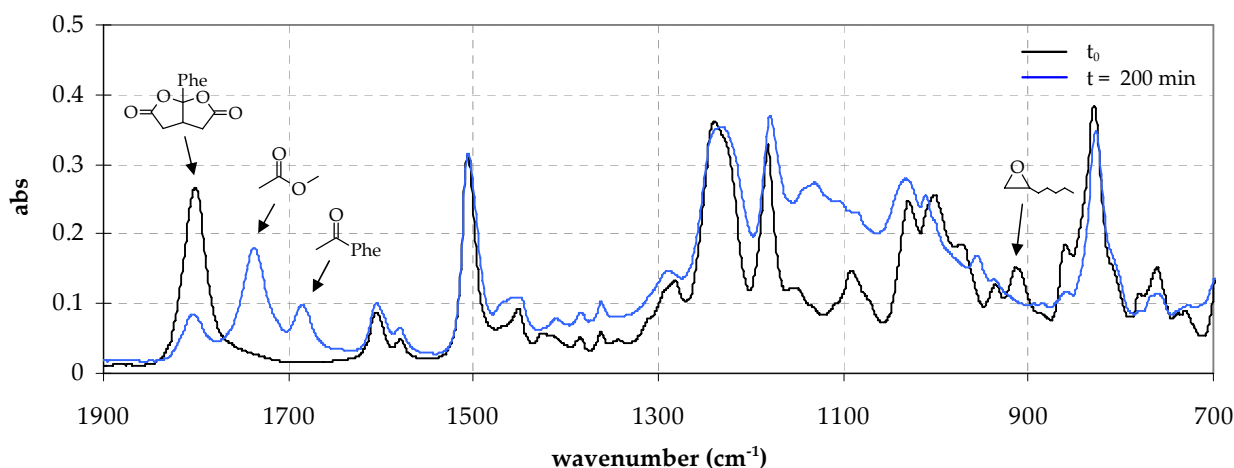


**Figure 2.** FTIR spectra before and after curing of a DGEBA/bisPhe 2:1 (mol/mol) mixture initiated by 1 phr of  $\text{La}(\text{OTf})_3$  in the ATR at  $160^\circ\text{C}$ .

ferent extent but simultaneously, the quantitative evaluation of the extent of each reactive process from the areas is not suitable. However, from the intensity of the ketone group it seems that the opening of bisSOE by the tandem reaction is the most important process.

The lactone band in the spectra of the cured materials could be due to the presence of unreacted bisMe or bisPhe or to the formation of a monolactone structure by polymerization of monoSOEs (reaction **b**). To elucidate if initial lactone is the origin of this absorption we extracted the cured material during 24 h with methylene chloride at reflux temperature. In the solution, oligomers with a similar spectrum to the cured material could be separated but a little proportion of initial lactone was also detected. In the insoluble fraction after extraction we could also detect a lactone band by FTIR. This indicates that the initial lactone reacts to produce mono-SOE (reaction **b**) as intermediate, which can further polymerize but some lactone can remain unreacted in the cured material, in a proportion that depends on

the initiator and its proportion. The presence of a little amount of unreacted lactone in the material could be attributed to the difficulty of the SOE formation by the steric hindrance, produced by the rigid structure of the condensed bislactone, or to a reversion of SOE groups to form epoxide and lactone, which was previously observed in  $\gamma$ -substituted mono( $\gamma$ -lactone)s.<sup>8</sup> Reactions **b** and **d** must coexist during curing because of the formation of ketone bands (reaction **d**) and the presence of a lactone band (reaction **b**). Experiments with phenylglycidylether as a model compound and these lactones with cationic initiators performed by FTIR and NMR spectroscopy did not give any conclusive information to distinguish the origin of the lactone band.

In a previous article,<sup>15</sup> we described the kinetic effect of the different initiators on the curing process of these systems. We saw that the curing rate increased from lanthanum to scandium triflates, in accordance to their Lewis acidity. In the present work, we studied the influence of the rare earth triflates on the evolution



of the species that participate in the overall curing process. This influence is due to the different coordination ability of the initiators with the oxygens in the monomers and reaction intermediates. Because boron trifluoride is the most commercially used cationic initiator, we also studied its influence on our complex curing system.

**Figure 3** shows the carbonyl region of the recorded FTIR spectra for the materials obtained from a DGEBA/bisMe 2:1 (mol/mol) mixture with all the initiators tested. As we can see, the proportion of linear ester and ketone groups increases and the proportion of lactone decreases from lanthanum to scandium.  $\text{BF}_3 \cdot \text{MEA}$  incorporates the lowest proportion of linear ester to the network structure and leads to the highest proportion of lactone in the material, although 3 phr of this initiator were necessary to complete the curing. **Table 1** collects the proportion of lactone in the final spectra for bisMe and bisPhe. For the same comonomer ratio, the proportion of remaining lactone decreases from lanthanum to scandium triflate (entries 1, 3 and 8 or 2, 5 and 9). The highest proportion of remaining lactone corresponds to the material obtained with boron trifluoride (entry 10). If we compare the values for both lactones, we can observe that the materials obtained from bisPhe have a lower proportion of lactone and, therefore, it seems that bisPhe facilitates the copolymerization with DGEBA. In the same table we have also collected the normalized global area of ester and ketone bands referred to the  $1605 \text{ cm}^{-1}$  absorption ( $\text{Abs}_{\text{ester+ketone}}$ ), and the ratio of this absorption to the

absorption of the initial lactone ( $\text{Abs}_{\text{ester+ketone}}/\text{Abs}_0$ ). As we can see, these values increase from lanthanum to scandium (entries 1, 3 and 8 or 2, 5 and 9) whereas the boron initiator leads to the lowest (entry 10). It can be also observed that the use of bisPhe gives higher values than bisMe. It should be taken into account that the fact that two ester groups of the bislactone converts into three carbonyl groups by reaction **d** justifies obtaining values higher than 1 for the ratio  $\text{Abs}_{\text{ester+ketone}}/\text{Abs}_0$ .

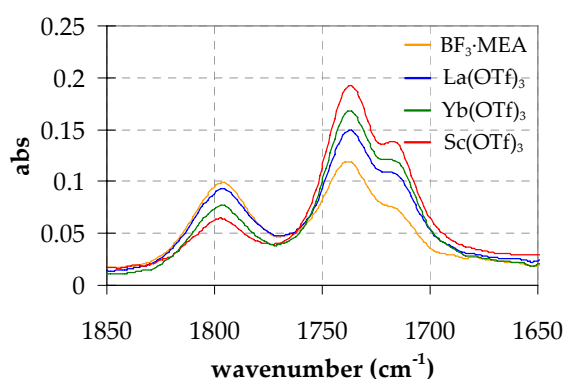


**Figure 3.** Carbonyl region of the FTIR spectra of the cured materials obtained from a DGEBA/bisMe 2:1 (mol/mol) mixture initiated by 1 phr of the different rare earth metal triflates or 3 phr of  $\text{BF}_3 \cdot \text{MEA}$ .

We also studied the effect of the proportion of initiator on the lactone incorporation. In **Table 1** we can see how the increase in the proportion of ytterbium triflate (entries 4, 5 and 6) increases the linear ester and ketone absorption and reduces the proportion of remaining lactone in the cured material. Moreover, higher proportions of bislactone in the reactive mixture lead to higher proportions of linear ester in the cured material (entries 3, 5 and 7). This means that cationic copolymerization allows varying the proportion of linear ester in the network, which was not possible in ani-



**Table 1.** Composition of the initial curing mixture and relative quantifications by FTIR of lactone and linear ester+ketone groups after curing at 160 °C in the ATR

Entry	Formulation (mol/mol)	Proportion of initiator	Initiator	γ-lactone remaining (%)		Abs <sup>a</sup> <sub>ester+ket</sub>		Abs <sup>a</sup> <sub>ester+ket</sub> /Abs <sub>0</sub> <sup>a</sup>	
				bisMe	bisPhe	bisMe	bisPhe	bisMe	bisPhe
1	DGEBA/bislac 3:1	1	La(OTf) <sub>3</sub>	28.33	19.99	2.008	3.085	0.681	0.846
2	DGEBA/bislac 2:1	1	La(OTf) <sub>3</sub>	27.71	18.02	2.820	4.735	0.662	0.912
3	DGEBA/bislac 3:1	1	Yb(OTf) <sub>3</sub>	18.84	11.18	2.550	3.620	0.902	0.969
4	DGEBA/bislac 2:1	0.5	Yb(OTf) <sub>3</sub>	24.02	21.23	2.599	4.331	0.627	0.904
5	DGEBA/bislac 2:1	1	Yb(OTf) <sub>3</sub>	22.95	15.24	3.572	5.155	0.859	0.997
6	DGEBA/bislac 2:1	3	Yb(OTf) <sub>3</sub>	18.00	13.01	3.953	5.395	1.029	1.199
7	DGEBA/bislac 1:1	1	Yb(OTf) <sub>3</sub>	30.53	25.84	5.555	7.572	0.811	0.900
8	DGEBA/bislac 3:1	1	Sc(OTf) <sub>3</sub>	8.76	8.02	2.879	3.684	1.004	1.056
9	DGEBA/bislac 2:1	1	Sc(OTf) <sub>3</sub>	14.64	11.97	4.239	5.700	0.964	1.019
10	DGEBA/bislac 2:1	3	BF <sub>3</sub> ·MEA	31.92	20.24	1.882	3.691	0.456	0.782

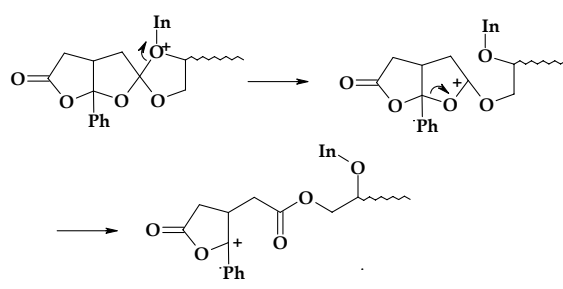
<sup>a</sup> all absorbance data are normalized taking the 1605 cm<sup>-1</sup> band as a reference



onic initiated systems due to unexpected reactions when DGEBA was in excess.

It is known that in the copolymerization of epoxide and lactones some proportion of SOE remains unreacted in the cured material.<sup>2,3</sup> Thus, to know the influence of the initiator in the reaction in which SOE opens, we integrated the carbonyl region in **Figure 3** and then the area was normalized taking the band at 1605 cm<sup>-1</sup> as a reference. The lowest the proportion of total carbonyl absorption, the higher the proportion of unreacted SOE is. These values are collected in **Table 2**. The normalized areas of carbonyl absorptions slightly increase from lanthanum to scandium triflates and the boron initiator gives the lowest proportion. This indicates that scandium triflate has the highest ability to polymerize SOE and the boron initiator the lowest. In a previous study<sup>3,19</sup> in the copolymerization of DGEBA with  $\gamma$ -valerolactone we also observed that, among rare earth metal triflates, scandium had the highest ability to polymerize SOE, but its highest activity also led to an appreciable depolymerization process, which has not been observed in the present study with condensed bis( $\gamma$ -lactone)s. On comparing the values of the normalized total carbonyl region obtained for both lactones we can see that SOEs formed from bisPhe are more reactive than those formed from bisMe. The higher reactivity of bisPhe in the cationic copolymerization could be related to the better stabilization of an intermediate benzylic cation formed in the ring-opening mechanism, such as is exemplified in **Scheme 2** for monoSOE polymerization. In previous papers, we reported the copolymer-

ization of DGEBA/ $\gamma$ -butyrolactone<sup>2,20</sup> and DGEBA/1,6-dioxaspiro [4.4]nonane-2,7-dione mixtures,<sup>4</sup> where we observed the complete disappearance of the lactone, differently that occurs in DGEBA/ $\gamma$ -valerolactone mixtures.<sup>3</sup> Thus, as is observed in the present study, it seems that the presence of substituents in  $\gamma$ -position makes difficult the SOE formation and also its polymerization, which leads to a lower formation of linear ester in the network.



Scheme 2

If we compare the effect of the proportion of initiator we can see that the total carbonyl absorption has a maximum value for 1 phr of ytterbium triflate (entries 3, 4 and 5 in Table 2) although there is no much difference between 1 and 3 phr. This result can be explained because of a greater proportion of initiator favors the SOE formation, but also accelerates the homopolymerization of epoxide by the monomer activated mechanism,<sup>20</sup> leading to a quick reduction of the epoxide able to copolymerize with SOE, leaving some unreacted SOEs. On the other hand, a low proportion of initiator is capable to form SOE but not to open all the SOE units, which remains unreacted in the material. In a previous article<sup>15</sup> we proved that 0.5 phr of Yb(OTf)<sub>3</sub> was enough to obtain a completely cured thermoset from this mix-



**Table 2.** Relative quantifications by FTIR of carbonylic zone after curing at 160 °C in the ATR for DGEBA/lactone 2:1 (mol/mol) mixtures

Entry	Initiator	Proportion of initiator (phr)	Abs <sup>a</sup> <sub>carbonylic zone</sub>	
			bisMe	bisPhe
1	BF <sub>3</sub> ·MEA	1	4.883	6.098
2	La(OTf) <sub>3</sub>	1	5.690	7.096
3	Yb(OTf) <sub>3</sub>	0.5	4.953	6.731
4	Yb(OTf) <sub>3</sub>	1	5.892	7.233
5	Yb(OTf) <sub>3</sub>	3	5.757	7.010
6	Sc(OTf) <sub>3</sub>	1	5.915	7.461

<sup>a</sup> all absorbance data are referred to the 1605 cm<sup>-1</sup> band

ture, but 1 phr is better from the point of view of the kinetics. Higher proportions of initiator led to lower  $T_g$  values and could initiate the curing during storage. Taking all these results into account, 1 phr seems to be the best proportion of ytterbium triflate to obtain thermosets with a high proportion of linear ester.

**Figure 4** shows the evolution of lactone (a) and linear ester and ketone groups (b) against curing time for the DGEBA/bisPhe 2:1 (mol/mol) formulation initiated by 1 phr of the different rare earth triflates or 3 phr of BF<sub>3</sub>·MEA, calculated from the FTIR spectra and normalized to the band at 1605 cm<sup>-1</sup>. If we look at the plot of lactone conversions, we can see that the reaction rate increases from lanthanum to scandium following the Lewis acidity trend. Boron initiator leads to the slowest reaction. Similar information can be extracted from the ester and ketone conversion against time, related to SOE polymerization. The values of the curves (b) have been referred to the maximum reached, regardless of the initiator used. Thus, scandium leads to the quickest and max-

imum degree of SOE polymerization, whereas BF<sub>3</sub>·MEA to the slowest and to the minimum degree of SOE polymerization. The evolution of the disappearance of lactone and the formation of linear ester and ketone are parallel for

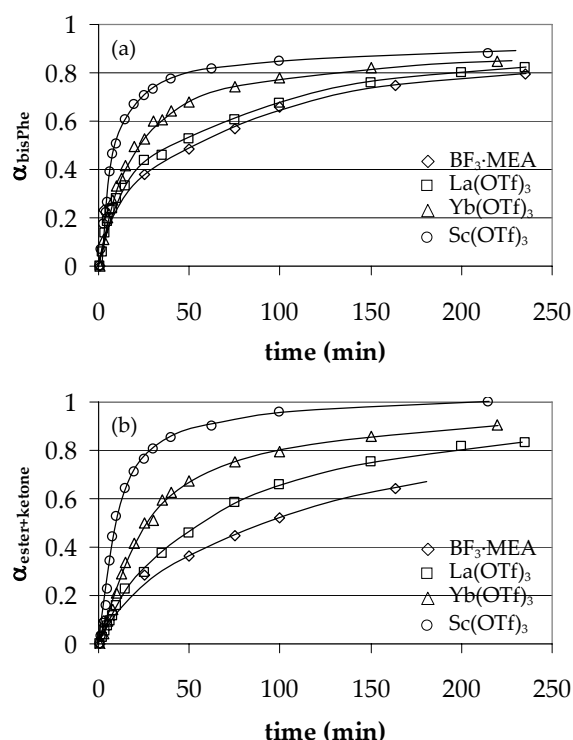


**Figure 4.** Conversion of bisPhe (a) and formation of linear ester and ketone groups (b) against time for a DGEBA/bisPhe 2:1 (mol/mol) mixture initiated by 1 phr of the different rare earth metal triflates or 3 phr of BF<sub>3</sub>·MEA from FTIR data.



the rare earth metal triflates, which indicates that the kinetics of the SOE formation and its polymerization should be similar. When  $\text{BF}_3\cdot\text{MEA}$  is the initiator the evolution of the formation of SOE moieties (a) goes similarly to that of the lanthanum salt, but the SOE polymerization (b) is much slower and reach a lower formation of linear ester and ketone. This seems to indicate that  $\text{BF}_3\cdot\text{MEA}$  is a better catalyst to form SOEs than initiator to polymerize them.

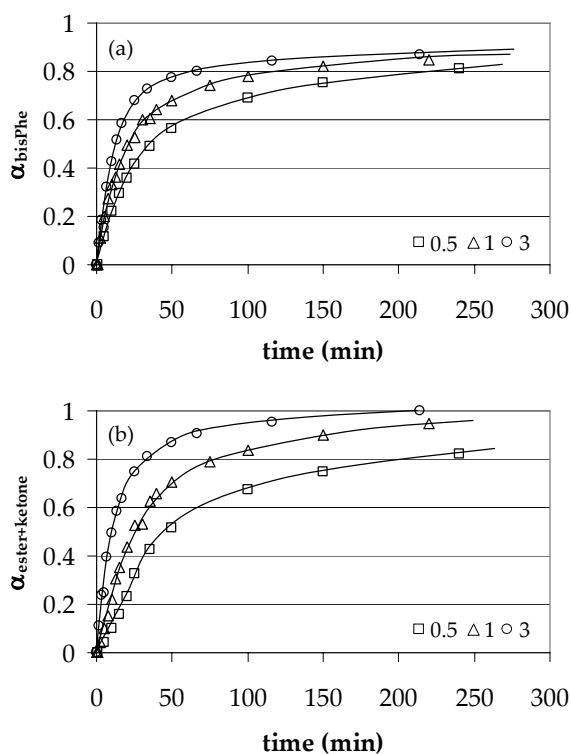


**Figure 5.** Conversion of bisPhe (a) and formation of linear ester and ketone groups (b) against time for a DGEBA/bisPhe 2:1 (mol/mol) mixture initiated by 0.5, 1 and 3 phr of ytterbium triflate from FTIR data.

Lactone disappearance and opening of SOE moieties to produce linear ester and ketone go faster on increasing the proportion of initiator in the reactive mixture, as expected (**Figure 5**, (a) and (b)). In the initial steps of curing the

disappearance of lactone (a), related to the formation of SOE, is similar for all the proportions of initiator. However, this does not occur in the opening of SOE. This implies that the proportion of initiator mainly affect the polymerization of SOE groups. In agreement to this, a higher proportion of initiator favors the formation of linear ester.

When we compare the evolutions on changing the lactone (**Figure 6**, (a) and (b)) we can see that there is no much differences in the formation of SOEs (a), although until 0.7 of conversion bisMe reacts slightly faster than bisPhe. From this conversion, the behavior is the opposite and a lower conversion is achieved for bisMe. Higher differences are observed in the SOE polymerization (b), in all the conversions range the SOE derived from bisPhe converts into linear and ketone groups at much higher rate and reaches a higher extension.

## Conclusions

Cationic initiated curing of DGEBA/bisMe or bisPhe mixtures allowed to vary the proportion of linear ester in the network by changing the feed ratio of comonomers in the reactive mixture. This is advantageous in comparison to analogous anionic initiated systems, in which non stoichiometric proportions led to unexpected reactions.

The formation of linear ester and ketone groups during curing implies the formation of bis(spiroorthoester) moieties and their opening by a tandem reaction. However, mono spiroorthoesters were formed and some proportion

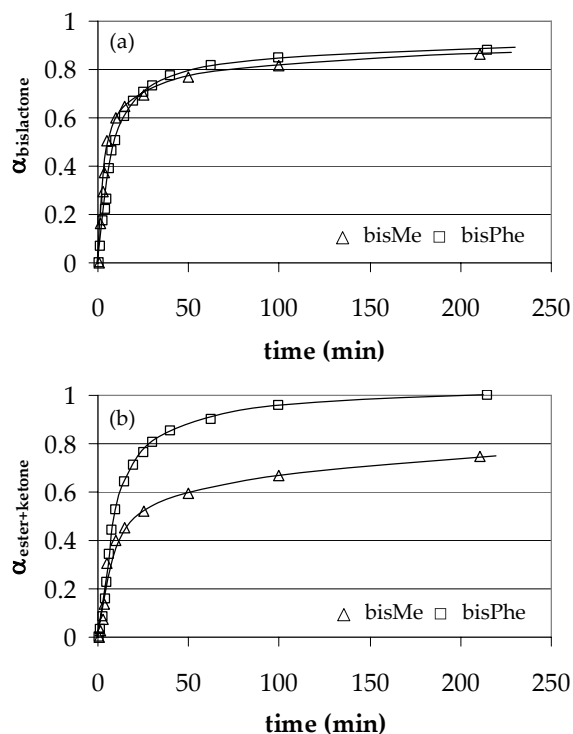


**Figure 6.** Conversion of lactone (a) and formation of linear ester and ketone groups (b) against time for DGEBA/bisPhe and DGEBA/bisMe 2:1 (mol/mol) mixtures initiated by 1 phr of ytterbium triflate from FTIR data.

of  $\gamma$ -lactone remained unreacted in the cured material. The chemical incorporation of bis( $\gamma$ -lactone)s in the network was favored by the acidity of the cation in the rare earth triflates, following the order  $Sc > Yb > La$ . Rare earth metal triflates were better than the conventional  $BF_3 \cdot MEA$  in the polymerization processes in which SOE participates.

The rate of polymerization of mono or bis(spirorthoesters) followed the increasing Lewis acidity of the rare earth metal triflates.  $BF_3 \cdot MEA$  produced the lowest reaction rates.

The chemical incorporation of bis-lactone and the opening of SOE moieties to produce linear ester and ketone accelerated on increasing the proportion

of initiator in the reactive mixture. The proportion of initiator mainly affected the rate of polymerization of SOEs and a higher proportion of initiator also increased the proportion of linear ester in the final material.

BisPhe led to a higher chemical incorporation in the thermoset than bisMe. Although there was not much difference in the rate of SOE formation, its polymerization was quicker in case of bisPhe. This fact can be explained by the stabilization of cationic intermediate species produced by the phenyl ring.

#### Acknowledgements

The authors from the Universitat Rovira i Virgili would like to thank the CICYT (Comisión Interministerial de Ciencia y Tecnología) and FEDER (Fondo Europeo de Desarrollo Regional) (MAT2008-06284-C03-01) and the authors from the Universitat Politècnica de Catalunya to CICYT and FEDER (MAT2008-06284-C03-02) for their financial support.

#### References

- [1] Castell, P.; Galià, M.; Serra, A.; Salla, JM.; Ramis, X. *Polymer* 2000, 41, 8465-8474.
- [2] Mas, C.; Ramis, X.; Salla, JM.; Mantecón, A.; Serra, A. *J Polym Sci Part A: Polym Chem* 2003, 41, 2794-2808.
- [3] Arasa, M.; Ramis, X.; Salla JM., Mantecón, A.; Serra, A. *J Polym Sci Part A: Polym Chem* 2007, 45, 2129-2141.
- [4] Giménez, R.; Fernández-Francos, X.; Salla, JM.; Serra, A.; Mantecón, A.; Ramis, X. *J Polym Sci Part A: Polym Chem* 2005, 46, 10637-10647.
- [5] Kobayashi, S., Ed. "Lanthanides: Chemis-



- try and Use in Organic Synthesis" Topics in Organometallic Chemistry, Springer Verlag, Berlin, 1999.
- [6] Kobayashi, S.; Sugiura, M.; Kitagawa, H.; Lam, WWL. Chem Rev 2002, 102, 2227-2302.
- [7] González, L.; Ramis, X.; Salla, JM.; Mantecón, A.; Serra, A. Polym Degrad Stab 2007, 92, 596-604.
- [8] Arasa, M.; Ramis, X.; Salla, JM.; Mantecón, A.; Serra, A. Polym Degrad Stab 2007, 92, 2214-2222.
- [9] González, L.; Ramis, X.; Salla, JM.; Mantecón, A.; Serra, A. J Polym Sci Part A: Polym Chem 2006, 44, 6869-6879.
- [10] Sadhir, RK.; Luck, M.R. Eds. "Expanding Monomers. Synthesis, Characterization and Applications" CRC Press, Boca Raton, 1992.
- [11] Takata, T.; Tadokoro, A.; Chung, K.; Endo, T. Macromolecules 1995, 28, 1340-1345.
- [12] Chung, K.; Takata, T.; Endo, T. Macromolecules 1995, 28, 3048-3054.
- [13] Fernández-Francos, X.; Salla, JM.; Mantecón, A.; Serra, A.; Ramis, X. J Appl Polym Sci 2008, 109, 2304-2315.
- [14] Arasa, M.; Ramis, X.; Salla JM., Mantecón, A.; Serra, A. Polymer, send to revision.
- [15] Arasa, M.; Ramis, X.; Salla JM., Serra, A.; Mantecón, A. Polymer, in press.
- [16] González, S.; Fernández-Francos, X.; Salla, JM.; Serra, A.; Mantecón, A.; Ramis, X. J Polym Sci Part A Polym Chem 2007, 45, 1968-1979.
- [17] Chung, K.; Takata, T.; Endo, T. Macromolecules 1995, 28, 4044-4046.
- [18] Takata, T.; Chung, K.; Endo, T. Macromolecules 1995, 28, 1711-1713.
- [19] Mas, C.; Mantecón, A.; Serra, A.; Ramis, X.; Salla, JM. J Polym Sci Part A: Polym Chem 2004, 42, 3782-3791.
- [20] Salla, JM.; Fernández-Francos, X.; Ramis, X.; Mas, C.; Mantecón, A.; Serra, A. J Thermal Anal Calorim 2008, 91, 385-393.

UNIVERSITAT ROVIRA I VIRGILI  
NOUS TERMOESTABLES EPOXÍDICS MODIFICATS AMB GAMMA-LACTONES I BIS-GAMMA-LACTONES CONDENSADAES  
M<sup>a</sup> Mercè Arasa Bertomeu  
ISBN:978-84-692-4157-8/DL:T-1171-2009

## 5. Conclusions

---

## 5. CONCLUSIONS

1. The copolymerization of DGEBA with  $\gamma$ -VL or  $\gamma$ -MBL in the presence of rare earth metal triflates led to the formation of poly(ether-ester) networks. In addition to the expected reactions: formation of intermediate SOE, SOE polymerization and homopolymerization of epoxide, the reversion of SOE was observed. Moreover, in the case of using  $\gamma$ -VL with 1 phr of Sc(OTf)<sub>3</sub> or 3 phr of Yb(OTf)<sub>3</sub>, a depolymerization process was also observed. These processes led to different proportions of unreacted lactone, which remained entrapped in the thermoset. The use of 1 phr of Yb(OTf)<sub>3</sub> led to the highest proportion of linear ester.  $\gamma$ -MBL was incorporated in a less extent than  $\gamma$ -VL.
2. Cationic and anionic copolymerization of DGEBA/bis( $\gamma$ -lactone)s led to poly(ether-ester-ketone) networks. In cationic conditions some ( $\gamma$ -lactone) remained unopened in the final material. The chemical incorporation of bis( $\gamma$ -lactone)s in the network was favoured by the acidity of the cation in the rare earth metal triflates, following the order Sc > Yb > La. BF<sub>3</sub>·MEA led to the lowest incorporation.
3. The anionic copolymerization of DGEBA/bis( $\gamma$ -lactone)s had an alternating character but, when epoxide was in excess, unexpected processes took place leading to the formation of five-membered lactones and to the practically total disappearance of linear ester and ketone groups in the final material.
4. The addition of lactones to DGEBA accelerated the cationic curing and reduced the T<sub>g</sub> of the materials obtained. The kinetic parameters indicated that the reaction of lactones with epoxides was more favoured than the homopolymerization of epoxides or the ring-opening of SOE groups. Rare earth metal triflates were more active than BF<sub>3</sub>·MEA as initiators and their activity increased from lanthanum to scandium. On increasing the lactone or the initiator proportion the curing process accelerated.
5. The anionic curing of DGEBA with condensed bis( $\gamma$ -lactone)s required a lower proportion of tertiary amine as initiator than the curing of pure DGEBA. Among the initiators tested, DMAP was the most active and DBU was the least efficient. On increasing the proportion of bislactone in the reactive mixture, an apparent acceleration effect was observed, being slightly higher for bisPhe.
6. Thermogravimetric analysis allowed confirming the reworkable character of the thermosets obtained cationically from DGEBA and mono or bis( $\gamma$ -lactone)s. The higher the proportion of lactone or the Lewis acidity of the initiator and its proportion was the more thermally degradable the materials were. Thermosets obtained anionically from stoichiometric proportions were chemically reworkable and completely soluble in ethanolic KOH.
7. The relaxed modulus of the materials prepared from DGEBA and  $\gamma$ -VL varied with the initiator used and increased in the order La(OTf)<sub>3</sub> < Yb(OTf)<sub>3</sub> < Sc(OTf)<sub>3</sub> < BF<sub>3</sub>·MEA but no

tendency was established for materials with bis( $\gamma$ -lactone)s. All the materials prepared showed a practically unimodal  $\tan \delta$ , reflecting their homogeneous character. The higher the proportion of lactone in the reactive mixture the lower the temperature of the relaxation was.

8. The addition of  $\gamma$ -VL to DGEBA led to materials with a higher thermal expansion coefficient, which increased with the proportion of lactone, but all the values laid in the usual range of conventional epoxy resins. Moreover, the microhardness and the Young modulus were reduced in reference to pure cured DGEBA.

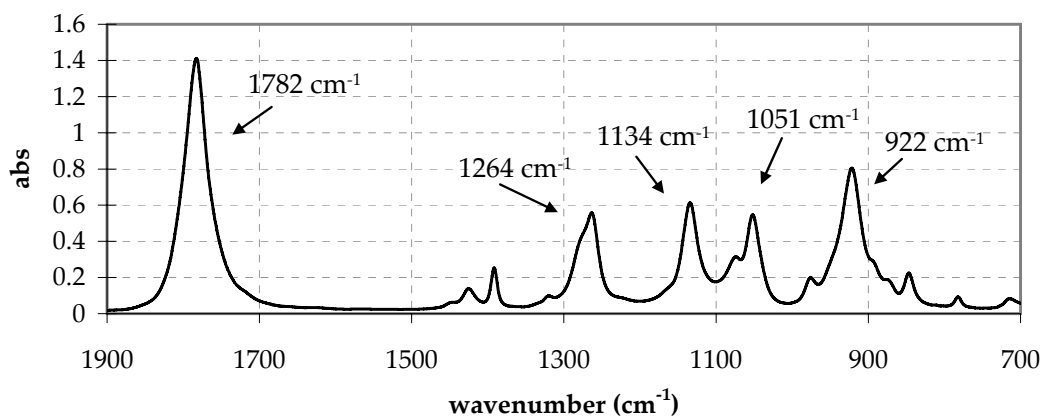
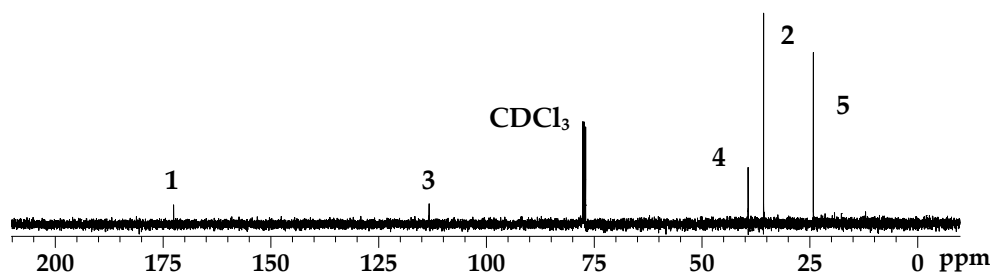
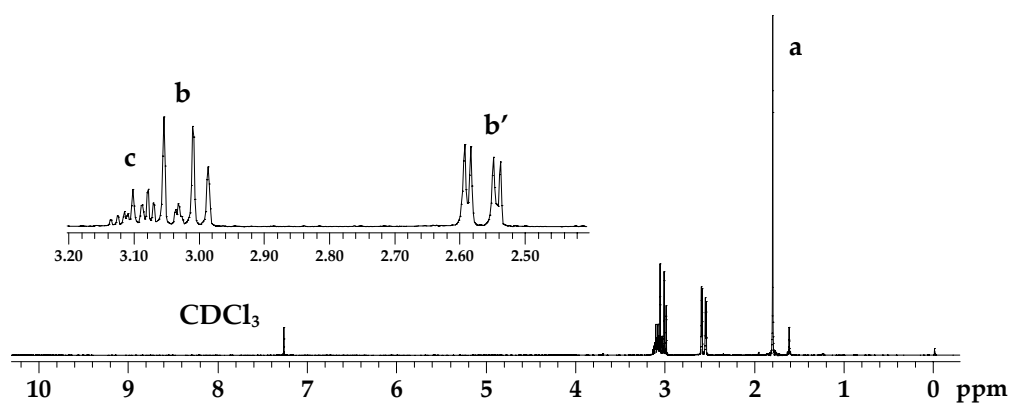
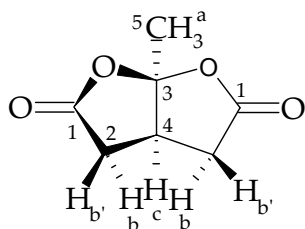
9. Cationic curing of DGEBA/ $\gamma$ -VL/clay mixtures initiated by rare earth metal triflates allowed obtaining intercalated nanocomposites.  $\text{Yb}(\text{OTf})_3$  (1 phr) was the best initiator to prepare these nanocomposites and to incorporate the higher proportion of linear ester groups in the network. The addition of clay retarded the curing and the gelation, but the effect was lower on increasing the proportion of initiator. This addition led to increase the thermal stability.

## 6. Annex i acrònims

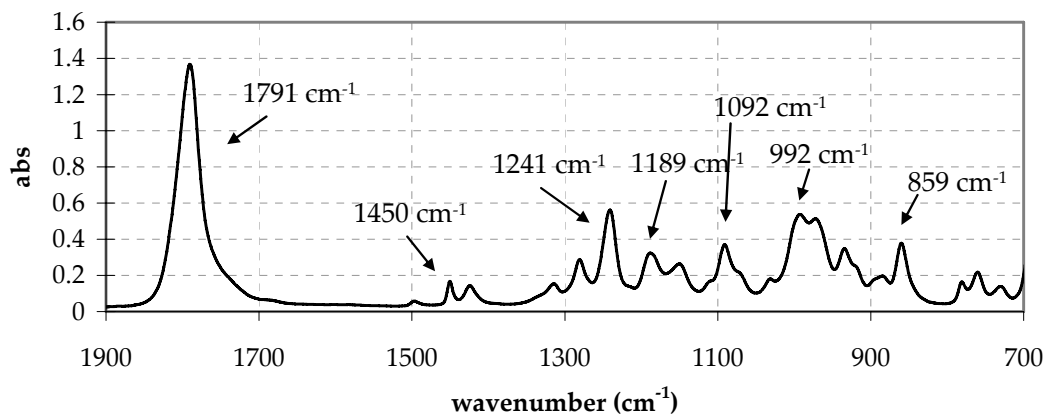
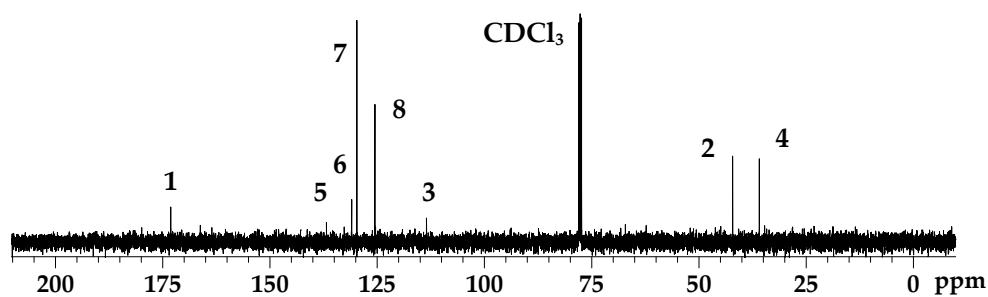
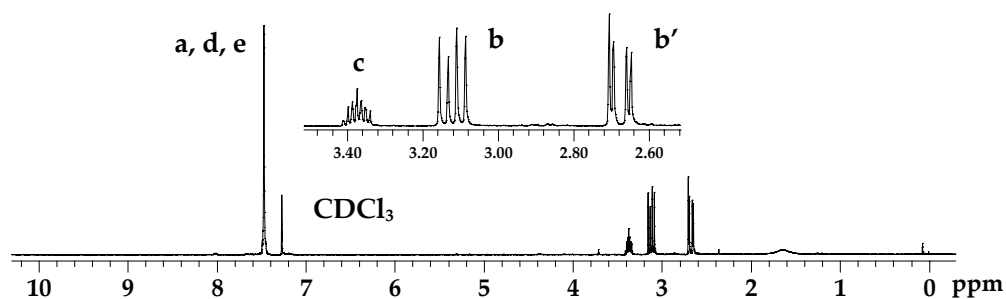
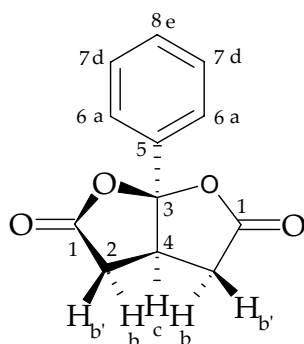
UNIVERSITAT ROVIRA I VIRGILI  
NOUS TERMOESTABLES EPOXÍDICS MODIFICATS AMB GAMMA-LACTONES I BIS-GAMMA-LACTONES CONDENSADAES  
M<sup>a</sup> Mercè Arasa Bertomeu  
ISBN:978-84-692-4157-8/DL:T-1171-2009

## 6.1. CARACTERITZACIÓ DE LES BIS( $\gamma$ -LACTONES)

### ■ 1-Metil-2,8-dioxabicyclo(3.3.0)-3,7-octandiona (bisMe)



### ► 1-Fenil-2,8-dioxabicyclo(3.3.0)-3,7-octandiona (bisPhe)



## 6.2. ACRÒNIMS

<b>bisMe</b>	1-metil-2,8-dioxabicyclo(3.3.0)-3,7-octandiona
<b>bisPhe</b>	1-fenil-2,8-dioxabicyclo(3.3.0)-3,7-octandiona
<b><math>\gamma</math>-BL</b>	$\gamma$ -butirolactona
<b>BOE</b>	bicicloortoester
<b>DBU</b>	1,8-diazabicyclo(5.4.0) -7-undecè
<b>DGEBA</b>	diglicidilèter del bisfenol A
<b>DMAP</b>	4-(N,N-dimetilamino)piridina
<b>DMTA</b>	anàlisi termodinamomecànica
<b>DSC</b>	calorimetria diferencial d'escombrat
<b>FTIR-ATR</b>	infraroig amb transformada de Fourier- reflectança atenuada total
<b>KHN</b>	número de duresa Knoop
<b><math>\gamma</math>-MBL</b>	$\alpha$ -metil- $\gamma$ -butirolactona
<b>MEA</b>	monoetilamina
<b>1MI</b>	1-metilimidazole
<b>NMR</b>	ressonància magnètica nuclear
<b>PGE</b>	fenilglicidilèter
<b>phr</b>	parts d'iniciador per cent parts de mescla de monòmers
<b>SOE</b>	espiroortoester
<b>SOC</b>	espiroortocarbonat
<b>TGA</b>	anàlisi termogravimètrica
<b>T<sub>g</sub></b>	temperatura de transició vítria
<b>TTT</b>	diagrama temps-temperatura-transformació
<b><math>\gamma</math>-VL</b>	$\gamma$ -valerolactona

UNIVERSITAT ROVIRA I VIRGILI  
NOUS TERMOESTABLES EPOXÍDICS MODIFICATS AMB GAMMA-LACTONES I BIS-GAMMA-LACTONES CONDENSADAS  
M<sup>a</sup> Mercè Arasa Bertomeu  
ISBN:978-84-692-4157-8/DL:T-1171-2009

7.  Contribucions  
científiques

## 7.1 PUBLICACIONS

“FTIR-ATR study of the copolymerization of diglycidyl ether of bisphenol A with methyl-substituted  $\gamma$ -lactones catalyzed by rare earth triflates initiators”. Arasa, M.; Ramis, X.; Salla, JM.; Mantecón, A.; Serra, A.; *Journal of Polymer Science: Part A: Polymer Chemistry*, 45 (2007) 2129-2141.

“Study on the degradation of ester modified epoxy resins obtained by cationic copolymerization of DGEBA with  $\gamma$ -lactone initiated by rare earth triflates”. Arasa, M.; Ramis, X.; Salla, JM.; Mantecón, A.; Serra, A.; *Polymer Degradation and Stability*, 92 (2007) 2214-2222.

“Kinetic study by FTIR and DSC on the cationic curing of a DGEBA/ $\gamma$ -valerolactone mixture with ytterbium triflate as initiator”. Arasa, M.; Ramis, X.; Salla, JM.; Mantecón, A.; Serra, A.; *Termochimica Acta*, 479 (2008) 37-44.

“Study on the effect of rare earth metal triflates as initiators in the cationic curing of DGEBA/ $\gamma$ -valerolactone mixtures and characterization of the thermosets obtained”. Arasa, M.; Ramis, X.; Salla, JM.; Ferrando, F.; Serra, A.; Mantecón, A.; *European Polymer Journal*, 45 (2009) 1282-1292.

“Anionic copolymerization of DGEBA with two derivatives of a bicyclic bis( $\gamma$ -lactone)s using tertiary amines as initiators”. Arasa, M.; Ramis, X.; Salla, JM.; Mantecón, A.; Serra, A.; *Polymer*, in press.

“Cationic copolymerization of DGEBA with two bicyclic bis( $\gamma$ -lactone) derivatives using rare earth metal triflates as initiators”. Arasa, M.; Ramis, X.; Salla, JM.; Mantecón, A.; Serra, A.; *Polymer*, in press.

“Study of the copolymerization of DGEBA and two bicyclic bis( $\gamma$ -lactone)s using rare earth metal triflates as initiators by infrared spectroscopy”. Arasa, M.; Ramis, X.; Salla, JM.; Mantecón, A.; Serra, A.; *European Polymer Journal*, send to revision.

“New nanocomposites prepared from diglycidyl ether of bisphenol and  $\gamma$ -valerolactone initiated by rare earth triflate initiators”. Arasa, M.; Pethrich, R.; Mantecón, A.; Serra, A.; to send.

## 7.2 CONFERÈNCIES

IX Reunión del Grupo Especializado en Polímeros (GEP) el qual va tenir lloc a Jaca (Espanya) des del 11 fins el 15 de Setembre del 2005.

Pòster: "Nuevos materiales termoestables obtenidos por copolimerización de DGEBA y  $\gamma$ -valerolactona".

4th International Conference on Polymer Modification, Degradation and Stabilization (MoDeSt) el qual va tenir lloc a San Sebastián (Espanya) des del 10 fins el 14 de Setembre del 2006.

Pòster: "Study on the influence of the rare earth triflate initiators in the preparation and degradation of ester modified epoxy resins".

IUPAC International Symposium on Ionic Polymerization, el qual va tenir lloc a Bayreuth (Alemanya) des del 9 fins el 11 de Setembre del 2007.

Pòster: "Crosslinking study of DGEBA/ $\gamma$ -bislactones initiated by rare earth triflates".

X Reunión del Grupo Especializado en Polímeros (GEP) el qual va tenir lloc a Sevilla (Espanya) des del 16 fins el 20 de Setembre del 2007.

Pòster: "Copolimerización de resinas epoxy con  $\gamma$ -bislactonas. Evolución del curado en condiciones catiónicas y aniónicas".

4<sup>th</sup> International Symposium on Nanostructured and functional polymer-based materials and nanocomposites, el qual va tenir lloc a Roma (Itàlia) des del 16 fins al 18 d'Abril del 2008.

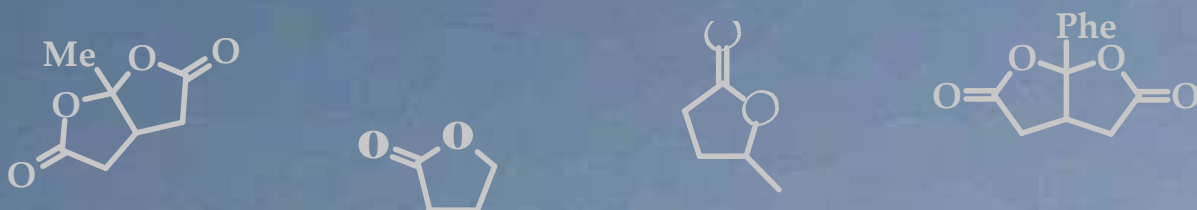
Pòster: Preparation of nanocomposites by copolymerization reaction of DGEBA/ $\gamma$ -VL initiated by ytterbium triflate using several clays.

Jornades de química sostenible, organitzades per la facultat de Química de la URV i patrocinades per la Càtedra de Desenvolupament Sostenible URV-DOW, les quals van tenir lloc a Tarragona (Espanya) des del 11 fins el 13 de Març del 2008.

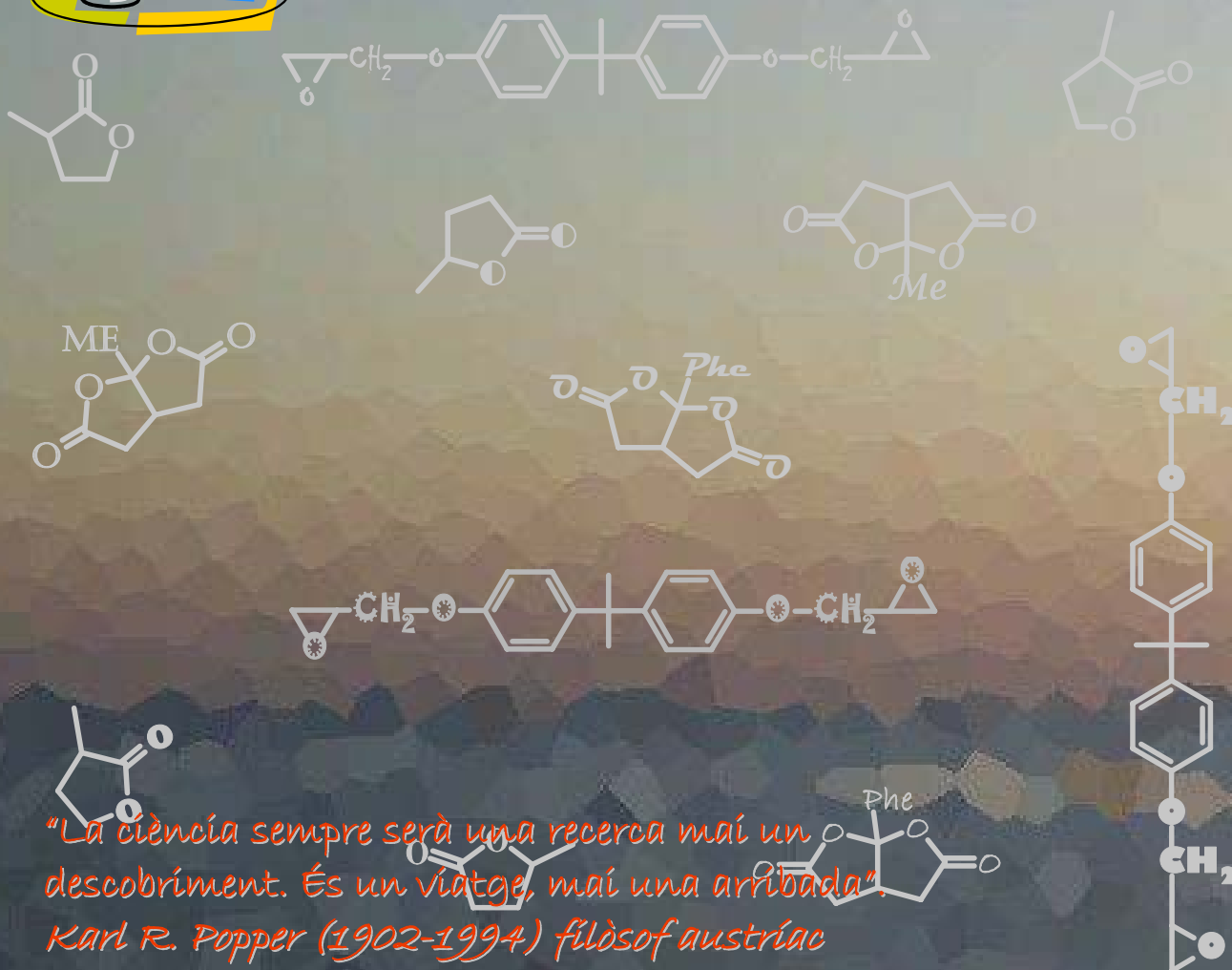
Pòster: "Nous materials termoestables obtinguts per copolimerizació de DGEBA i  $\gamma$ -valerolactona".

IV Congreso de Jovenes Investigadores en Polímeros (JIP) el qual va tenir lloc a Penyíscola (Espanya) des del 15 fins al 19 de Juny del 2008.

Comunicació oral: Preparación de nanocomposites por reacción de copolimerización de DGEBA/ $\gamma$ -VL iniciada por triflato de iterbio usando diferentes clays.



**Copolimerització del DGEBA amb mono i bis( $\gamma$ -lactones).** Estudi de la polimerització catiònica del diglicidilèter de bisfenol A (DGEBA) en presència de mono( $\gamma$ -lactones) com la  $\gamma$ -valerolactona ( $\gamma$ -VL) i la  $\alpha$ -metil- $\gamma$ -butirolactona ( $\gamma$ -MBL) i bis( $\gamma$ -lactones) com la 1-metil-2,8-dioxabicyclo(3.3.0)-3,7-octandiona (bisMe) i la 1-fenil-2,8-dioxabicyclo(3.3.0)-3,7-octandiona (bisPhe) emprant triflats de terres rares com iniciadors. Preparació de nanocomposites per copolimerització catiònica de mesclades DGEBA/ $\gamma$ -VL/argila iniciades per triflats de terres rares. Estudi final de la polimerització aniònica del DGEBA amb les bis( $\gamma$ -lactones) utilitzant diferents amines terciàries com iniciadors.



*"La ciència sempre serà una recerca mai un descobriment. És un viatge, mai una arribada".  
Karl R. Popper (1902-1994) filòsof austríac*